Universidade de Aveiro Departamento de Química
2019

NUNO FILIPE MARTINS BRANCO

ESTUDO DA ESTABILIDADE OXIDATIVA E DO COMPORTAMENTO A BAIXAS TEMPERATURAS DE MISTURAS DE GASÓLEO COM BIODIESEL

Universidade de Aveiro Departamento de Química
2019

NUNO FILIPE MARTINS BRANCO

ESTUDO DA ESTABILIDADE OXIDATIVA E DO COMPORTAMENTO A BAIXAS TEMPERATURAS DE MISTURAS DE GASÓLEO COM BIODIESEL

Tese apresentada à Universidade de Aveiro para cumprimento dos requisitos necessários à obtenção do grau de Doutor em Engenharia da Refinação, Petroquímica e Química, realizada sob a orientação científica do Professor Dr. João Manuel da Costa Araújo Pereira Coutinho, Professor Catedrático do Departamento de Química da Universidade de Aveiro, do Professor Dr. Luís Manuel das Neves Belchior Faia dos Santos, Professor Associado com Agregação do Departamento de Química e Bioquímica da Universidade do Porto e o orientador empresarial Mestre Jorge Correia Ribeiro responsável do Laboratório da refinaria de Matosinhos e do Centro de Desenvolvimento Ramôa Ribeiro

Apoio financeiro da FCT e da Galp Energia, SGPS, S. A. ao abrigo do Programa Doutoral EngIQ (PD/BDE/113540/2015)

Dedico este trabalho à minha família pelo apoio incansável ao longo de toda a minha vida académica.

o júri

presidente

Prof. Doutor Victor Miguel Carneiro de Sousa Ferreira
professor catedrático da Universidade de Aveiro

Prof. Doutor Carlos Manuel Santos da Silva
professor associado da Universidade de Aveiro

Prof. Doutora Nídia de Sá Caetano
professora Coordenadora do Instituto Superior de Engenharia do Porto

Prof. Doutor Maria Isabel da Silva Nunes
Professora Auxiliar da Universidade de Aveiro

Prof. Doutor Cristina Borges Correia
Diretora de Investigação, Desenvolvimento e Inovação da PRIO Energy Aveiro

Prof. Doutor Luís Manuel das Neves Belchior Faia dos Santos
professor Associado com Agregação na Faculdade de Ciências da Universidade do Porto

agradecimentos

Gostaria de expressar aqui a minha gratidão e apreço a todas as pessoas que de alguma forma me ajudaram e acompanharam durante esta etapa da minha vida. Foram quatro anos de grandes desenvolvimentos e mudanças na minha vida nas quais todas as pessoas aqui referidas tiveram um papel muito importante.

Começo por agradecer aos meus orientadores, Professor João Coutinho e Dr. Jorge Ribeiro pela oportunidade e confiança que me deram para desenvolver este trabalho. Gostaria de deixar um agradecimento especial ao meu coorientador professor Luís Belchior por me receber no seu grupo e me acompanhar e ensinar muitas das capacidades pessoais e materiais necessárias para desenvolver este projeto.

A todos os trabalhadores dos laboratórios da refinaria de Matosinhos que me receberam para desenvolver parte deste trabalho e sempre estiveram disponíveis para me ajudar em tudo o que precisei especialmente à Eng. Ana Luísa Monteiro.

Aos meus colegas da FCUP que receberam de braços abertos um estudante de engenharia num grupo de química. Muito obrigado por todos os bons momentos passados ao longo destes anos. Dentro destes um agradecimento especial ao Carlos, Zé Carlos, Inês, Filipe e Bruno por toda a amizade ao longo destes anos, com eles desenvolvi para além de conhecimento científico, fortes relações de amizade, companheirismo e passamos bons momentos. Espero que consigam encontrar na ciência e na vida tudo o que procuram.

Um agradecimento muito especial a todos os meus amigos do curso de engenharia química e do ENGIQ que me acompanharam ao longo dos cinco anos de mestrado integrado no IST ou no programa doutoral e que ficaram até aos dias de hoje. Muito obrigado Casinhas, Serineu, Magui, Sofia, Carmen, Jacinto e Sérgio com vocês passei dos melhores momentos da minha vida espero que consigamos manter a nossa amizade por muitos mais anos.

Um obrigado a todos os meus amigos, com eles aprendi muito mais que em qualquer curso pode ensinar. Para além dos já mencionados um obrigado especial ao André e ao Cenoura por todos os bons momentos.

Aos meus familiares um grande obrigado. Ao meu irmão André por toda a compreensão, amor e paciência ao longo da minha vida. Ao meu sobrinho Marco por todos os bons momentos passados, espero que consigamos manter sempre esta empatia e que nos consigamos sempre fazer rir. Aos meus pais, Emília e João, e Avós, Porfírio e Luísa, que desde sempre me deram todo o apoio, compreensão, paciência e sobretudo amor, muito obrigado por tudo, vocês foram sempre a grande força para conseguir chegar aqui. Espero que consiga manter sempre os bons valores por vocês passados.

Por fim o agradecimento final para as pessoas que nos últimos anos me acrescentaram novas visões e tornaram a minha vida muito mais especial. Magda muito obrigado por todo o amor, sentido de humor, motivação, carinho e apoio. Contigo passo os melhores momentos da minha vida. A Inês é a maior prova do nosso amor. Muito obrigado Magda e Inês por darem um novo sentido à vida e mostrarem que todos os problemas podem ser minimizados com um sorriso.

palavras-chave

Gasóleo, Biodiesel, Alcanos; FAME; Diagramas de fase; DSC; co-cristalização; Soluções sólidas; Estabilidade oxidativa; Estabilidade em armazenamento;

resumo

O uso de misturas de biodiesel com diesel mineral é comum no mercado europeu. Esta mistura, embora melhore muitas características do combustível e reduza seu impacte ambiental, prejudica outras características do combustível, como as propriedades de fluxo a frio (pontos de turvação, escoamento e temperatura limite de filterabilidade) e a estabilidade oxidativa. Este trabalho visa compreender as propriedades de fluxo a frio e da estabilidade oxidativa das misturas de biodiesel com o diesel mineral procurando compreender o impacte do uso do biodiesel em misturas com diesel mineral ou como substituto dele.

As propriedades a frio foram investigadas com o estudo do comportamento de fase de misturas binárias entre esteres metílicos de ácidos gordos (biodiesel) e alcanos (diesel mineral) como modelo para o entendimento do comportamento das misturas diesel mineral / biodiesel. Neste trabalho o comportamento de fase de seis misturas binárias do éster metílico saturado (estearato de metilo ou palmitato de metilo) com um alcano saturado (hexadecano, octadecano ou eicosano) foram avaliadas por calorimetria diferencial de varrimento (DSC), difração de raios-X (XRD) e microscopia ótica. As misturas binárias estudadas mostram um comportamento de fase mais complexo do que o relatado anteriormente, e que é dependente da diferença de tamanho entre o comprimento da cadeia alquílica dos ésteres e dos alcanos. Os resultados aqui descritos mostram, pela primeira vez, que em misturas com o mesmo comprimento de cadeia alquílica é formado um co-cristal e em misturas com um alcano com uma cadeia dois metilenos maior que o FAME leva à formação de uma solução sólida aumentando a estabilidade da sua fase sólida. Estes resultados são um bom modelo para a interpretação do aumento do ponto de turvação e fluxão em misturas de biodiesel com uma fração rica de palmitato de metilo ou estearato de metilo quando combinados com diesel mineral rico em octadecano ou eicosano, respetivamente.

O estudo da estabilidade oxidativa aborda o efeito da concentração e da presença de antioxidantes em misturas de biodiesel com o diesel mineral. Nestes testes foram usados diferentes tipos de biodiesel, diesel mineral e antioxidantes. Foi também estudado a estabilidade oxidativa do biodiesel puro e a influência de metais, água e ar na evolução da estabilidade oxidativa das misturas de biodiesel com diesel mineral. Este teste mostra que a estabilidade oxidativa do biodiesel tem um forte efeito na estabilidade oxidativa das misturas com diesel mineral sendo estas também afetadas pela capacidade de proteção do diesel mineral. Esta capacidade de proteção tem um efeito sinergético quando um antioxidante está presente. A presença de uma liga metálica carbono ferrosa (Aço NP-Fe360-2), água e/ou oxigênio não influencia significativamente a estabilidade das misturas de biodiesel e diesel mineral quando armazenados.

keywords

Diesel, Biodiesel, Alkanes; FAME; phase diagram; DSC; co-crystallization; Solid solutions; Oxidative Stability; Storage stability; Rancimat.

abstract

Biodiesel blends with mineral diesel are common nowadays in the European market. This blending, although improving many characteristics of the fuel and lowering its environmental impact, detriments for some characteristics of the fuel as its cold flow properties (increasing the cloud, pour points and the cold filter plugging point) and the oxidation stability. This work aims to understand the cold flow properties and the oxidative stability of the blends of biodiesel with diesel looking to comprehend the impact of biodiesel and its use in blends with mineral diesel.

The cold flow properties are studied with the understanding of the phase behaviour of binary mixtures between fatty acid methyl esters (biodiesel) and alkanes (mineral diesel) as model for understanding the behaviour of the mineral diesel/biodiesel blends. In this work the phase behaviour of six binary mixtures of the most common saturated methyl ester (methyl stearate or methyl palmitate) with a saturated alkane (hexadecane, octadecane or eicosane) were evaluated by differential scanning calorimetry (DSC), X-ray diffraction (XRD) and optical microscopy. The studied binary mixtures of saturated methyl esters and alkanes show a more complex phase behaviour than previously reported, which is dependent of the size difference between the alkyl chain length in the esters and the alkanes. The results here reported show, for the first time, that in mixtures with equal alkyl chain length a co-crystal is formed and in mixtures with an alkane with a chain larger than the FAME by two methylenes leads to the formation of a solid solution increasing their solid phase stability. These results can be used as a model for the interpretation of the cloud and pour points increase in biodiesel blends.

The oxidative stability (OS) is explored by the study of the effect of concentration of biodiesel and antioxidants in blends of biodiesel with mineral diesel. Different types of biodiesel, antioxidants and mineral diesel were studied. Moreover, the study of the evolution in the storage stability of pure biodiesel and the influence of metals, water and air in the storage stability of blends was also carried out. The main effect in the OS of the blends is the OS of the biodiesel. However, the protective capacity of mineral diesel plays also an important role. The tests also show a synergistic effect between the mineral diesel and the antioxidants added to the biodiesel. The storage stability shows that the presence of an alloy (Steel NP-Fe360-2), water or/and oxygen don't influence significantly the storage stability of blends.

Contents

List of Abbreviations

AO	Antioxidant;
ASTM	American Society for Testing and Materials;
BHA	Butylated hydroxyanisole;
BHT	Butylated hydroxytoluene;
B_{xx}	xx is the %(v/v) of biodiesel in a blend with mineral diesel;
C16	Hexadecane;
C18	Octadecane;
C20	Eicosane;
CFPP	Cold filter plugging point;
CI	Compression ignition;
CP	Cloud point;
CSO	Cottonseed oil;
DPD	Diphenyl-p-phenylenediamine;
DSC	Differential scanning calorimetry;
DTBHQ	Di-*tert*-butylhydroquinone;
EIA	Energy Information Administration;
EN	European normative;
EQ	Ethoxyquin;
FAEE	Fatty acid ethyl esters;
FAME	Fatty acid methyl esters;
FFA	Free Fatty acids;
GC	Gas chromatography;
GHG	Greenhouse gases;
ha	Hectare;
IB	Ionol BF200;
IP	Induction period;
ISO	International Organization for Standardization;
IUPAC	International union of pure and applied chemistry;
MBEBP	2,2'-methylenebis (4-methyl-6-*tert*-butyphenol);
MeC16	Methyl palmitate;
MeC18	Methyl stearate;
MO	Methyl oleate;
OBPA	Octylated butylated diphenyl amine;
OECD	Organisation for Economic Co-operation and Development:
OG	Octyl gallate;
OPEC	Organization of the petroleum Exporting Countries;
OS	Oxidative stability;
PF	Poultry fat;
PG	Propyl gallate;
PO	Palm oil;
PoO	Pongamia oil;
PP	Pour point;
PY	Pyrogallol;
RO	Rapeseed oil;
RTD	Resistance Temperature detector;
SEM	Scanning electron microscope;
SO	Soybean oil;

SSR	Solid-state relay;
TBHQ	*tert*-butylhydroquinone;
TBP	*tert*-butylated phenol;
UCOME	Used cooking oil;
UCO	Used cooking oil;
XRD	X-ray diffraction;
YG	Yellow grease.

List of Tables

List of Figures

1. Introduction

The use and availability of energy are essential for the humanity. The energy resources, and their sustainability, are nowadays a key factor of progress. The main sources of energy that have been used during the last decades are non-renewable, and thus finite. The needs have been increasing every year. If the society wants to continue to have energy at relatively low cost and abundance, alternative sources and types of energy must be explored.

Among biofuels, biodiesel is an important alternative to mineral sources energy, but some challenges must be overcome to optimize their production, usability, sustainability and to decrease their environmental impact. In the next chapters, some challenges, disadvantages, advantages and new results concerning the use of biodiesel/diesel blends will be presented.

Global Energy Demand and Perspectives.

In 2010, the world consumption of energy was 1.54×10^8 GW·h. The non-OECD countries contributed to 54 % for this consume. The consumption of energy in the world is increasing each year. In 2040 the world consumption of energy will increase to 2.41×10^8 GW·h as predicted by U.S. Energy Information Administration (EIA). The non-OECD countries will be responsible for 66 % of this energy consumption, being the main responsibles for the increase of energy consumption.[1,2] Figure 1.1 and Figure 1.2 shows the predicted evolution of energy consumption by type of fuel and by region (OECD or non-OECD).

In these two figures it is possible to see that the increase of energy consumption will be mainly in the non-OECD countries. The world energy consumption is expected to increase 41 % between 2015 and 2050. In the OECD countries, the energy consumption should increase only 9 %. The non-OECD Asia countries should be responsible for the main increase in the energy consume being responsible for more than the half of this increase, in particular in China and India, where the economic growth will lead to an increased access to marketed energy, and the grow of population will increase the demand for energy. Nevertheless, this is a much slower increase when compared with the 300 % increase in the energy use from 1990 to 2015.[1–3]

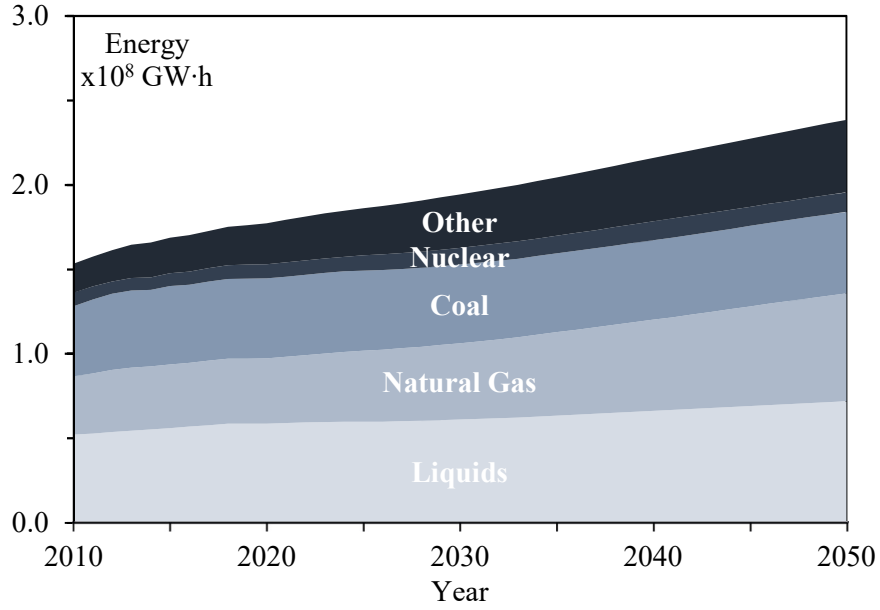

Figure 1.1 - World energy consumption by fuel source.[1]

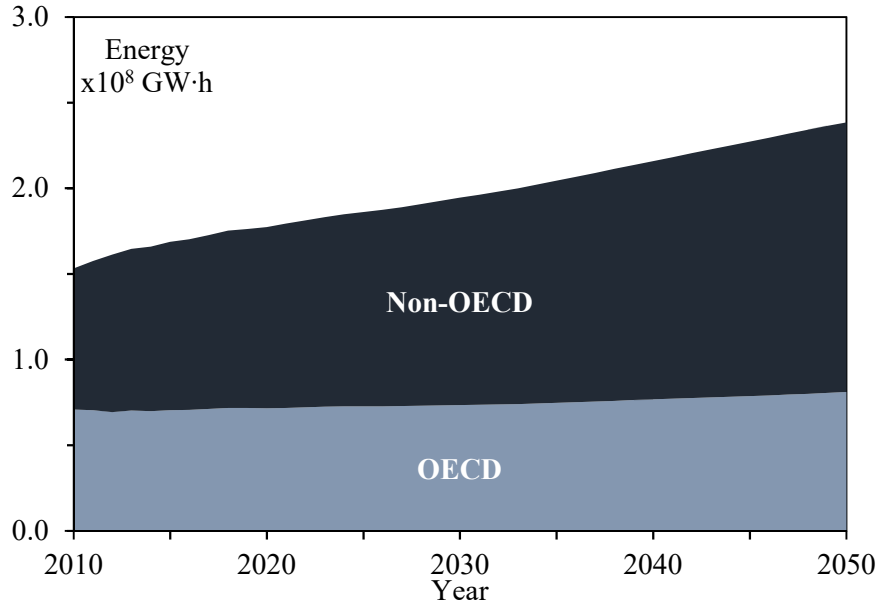

Figure 1.2 - World energy consumption of OECD and non-OECD countries. [1]

The lowest regional growth in non-OECD countries will be in Europe and Euroasia. This low growth is related to the decline over the projection of the population in Russia, and the gains in the energy efficiency.[1]

The availability of the energy resource will play a critical role in the physical future of our planet and the progress of the societies. In Figure 1.1, it is possible to see that most of the world energy needs are met using nuclear energy and fossil fuels like coal, natural gas and oil, but the use of these fossil fuels has environmental consequences and will be soon exhausted

which should contribute to the increase in the fossil fuel prices. In Figure 1.3, it is depicted the consumption by end-use sector of the energy produced in 2010 and 2050. The industrial sector is the largest energy consumer in 2010, but the energy demand in others sector will grow faster than in the industrial sector. [1,2]

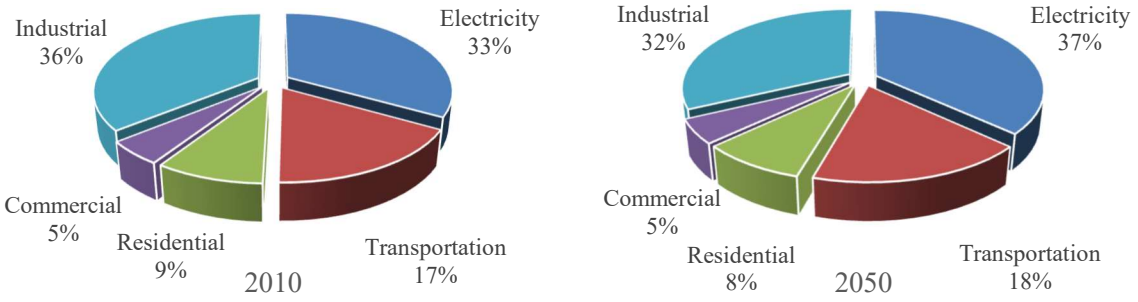

Figure 1.3 - Energy consumes by sector. [1]

In 2025, the sector of electricity should surpass the industrial sector demand of energy becoming the biggest energy consumer. [1,2] If the electricity sector is neglected, the industrial sector will be responsible for more than 50 % of the energy demand increasing 42 % between 2010 and 2050 being, as said before, the lowest increase comparing with other sectors. [1]

The world demand for liquid fuels will continue increasing between 2015 and 2040, mainly in non-OECD countries where strong economic and population growth increase the demand for these fuels by 39 %, while in OECD it should decrease by 3 %. The main countries responsible for this growth are countries with a rapid industrial growth and increased demand for transportation, as China, where the liquid fuels for transportation should increase by 36 %, and India, where an increase of 142 % is expected in this period.

The transportation sector consumes more than 50 % of the total energy from liquid sources (Figure 1.4). In 2015, it is estimated that were 1040 million passenger cars, with 1/3 in developing countries, and 218 million commercial vehicles with half of them in developing countries. By 2040, the total number of passenger cars should be 2030 million and 463 million of commercial cars. This increase should come mainly from developing countries like China and India. [1,3]

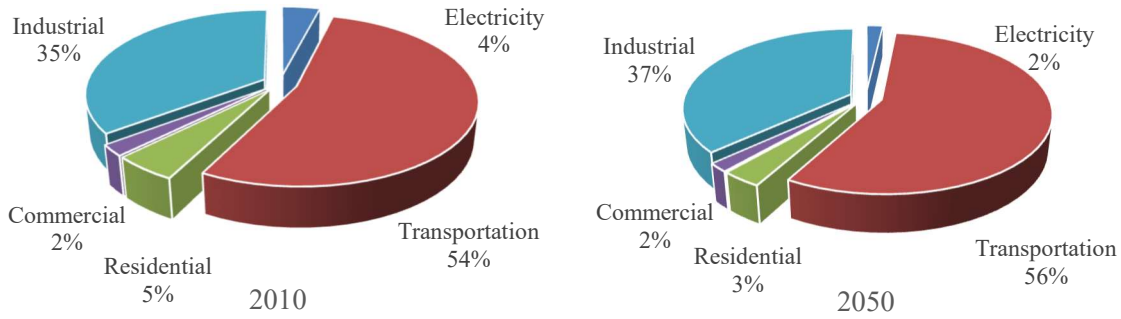

Figure 1.4 - Energy consumes from liquid sources by sector. [1]

The petrol fuels have adverse environmental effects like the emission of CO_2, SO_2, and NO_x. The petrol fuels will not always be available and with reliable prices, mainly in the non-OPEC countries. The society have seen the necessity to start to think about sustainability and renewable sources of energy.[4]

The yearly CO_2 emissions should increase from 31.2 Gt in 2010 to 42.7 Gt by 2050. The main increase will be in the non-OECD countries with an average annual percent change, between 2015-2050, of 0.9 %. In the OECD countries the increase will be of 0.2 % and the global average increase of 0.7 %.[1] This evolution can be explained by the increase of the world population to 9.5 billion in 2050 and the growth of world gross domestic product with an increase of 2.8 % *per* year from 2010 to 2050. [1,4]

The environmental impact will also play a critical role in the progress of the world's societies, this impact produced already some international regulations such as the Kyoto and Montreal Protocols, that have the objective of reducing the emission of greenhouse gases (GHG) (Kyoto: CO_2, CH_4, N_2O, SF_6, HFCs and PFCs; Montreal: CFCs, HCFCs, HFCs).[5,6]

This evolution stimulates the countries governments and industries looking for new sources of energy, with particular attention for clean, and commercially feasible energy. One of the alternatives explored are the biofuels. The biofuel has a leading role on the alternatives for petrol fuel. The biofuels are clean, can be produced from agricultural or domestic products and are renewables. They can be indigenous reducing the dependency on oil imports. Besides, the biofuel can be used in conventional diesel engines without any modification in the engine, is energetically efficient and renewable. In Table 1.1, is shown the availability of some fuels and it is possible to see that biofuels is one of the best substitutes for diesel showing an excellent future availability with a moderate current availability.[7]

Table 1.1 - Availability of the alternative fuels for transportation. [7]

Type of fuel	Current availability	Future availability
Gasoline	Excellent	Moderate/poor
Compressed natural gas	Excellent	Moderate
Hydrogen fuel cell	Poor	Excellent
Biofuel	Moderate	Excellent

The biofuels supply should increase in the non-OPEC countries from 2.2 $mb \cdot d^{-1}$ in 2016 to 3.8 $mb \cdot d^{-1}$ in 2040. This growth will be led by Brazil followed by the European countries like Germany and France. The ethanol accounts for approximately 2.6 $mb \cdot d^{-1}$ in 2040 and biodiesel with 1.2 $mb \cdot d^{-1}$.[3,8] European Union, Brazil, EUA and China will be responsible for 80 % of biofuels demand. [9]

1.1. Biodiesel

The use of fuels from vegetable oils in engines was first described in a Belgium patent in 1937. [7] However, its use date back to the first Rudolf Diesel experiment, when he tested his engine with peanut oil. The competency of vegetable oils in a compression ignition (CI) engine as fuel comes from the good heating value and releases almost no sulphur or aromatic polycyclic compounds. Even though the vegetable oils can be used as a substitute of the mineral diesel, the use of these oils induce problems associated with its use due to its high viscosities (21-400 $mm^2 \cdot s^{-1}$). The high viscosities of biofuels can lead to problems such as injector coking, polymerization in the piston ring belt area, making stuck or broken piston rings, and a tendency to thicken lubricating oil causing sudden and catastrophic failure of the rod and crankshaft bearings caused by reduction of the fuel atomization and increase in the penetration that the high kinematic viscosities can cause. [7] The normal injection, as used in diesel engine, cannot be used with vegetable oils due to their different atomization characteristics, leading to the necessity of modifications in engine and preheating arrangement. To minimize some of these problems, in 1970 scientists discovered that the viscosity of the vegetable oils and animal fat could be decreased by a simple chemical process. This allow that the new fuel could be used in the modern engines, this fuel is Biodiesel. [10,11]

Biodiesel is a fuel comprised of monoalkyl esters of long-chain fatty acids made from natural and renewable sources such as new/used vegetable oils or animal fats. The main characteristics of the biodiesel are similar to conventional mineral diesel. Although biodiesel contains no petroleum products, it can be blended with conventional mineral diesel because it has a high compatibility with it.

For pure biodiesel it is used the reference B100, while fuels with blends of biodiesel with mineral diesel is common being referred as B_{xx}, where xx represent the volumetric fraction of biodiesel in the blend. This blends can be used in CI engine without any significant changes in the engine hardware.[10]

The composition of the biodiesel depends mainly of the triglyceride fatty acid composition of the main oils/fats, Table 1.2. The oil can contain many substances depending of the origin such as antioxidants, free fatty acids (FFA), triglycerides, etc. but the major composition of the oil is triglycerides (Figure 1.5) that are composed by three fatty acids and one glycerol.

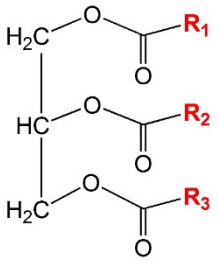

Figure 1.5 - Generic representation of triglyceride. R1, R2 or R3 are the different alkyl chain of the fatty acid.

The triglycerides can contain numerous types of fatty acids but is generally dominated by only few species, as palmitic, stearic, oleic, linoleic, and linolenic acids, as it is possible to verify in the composition of each oil or animal fat in Table 1.2. For this reason, the biodiesel produced by transesterification also has a composition dominated by the correspondent alkyl esters of these species.

To represent the fatty acids, a simple convention is used, this consists of two numbers, separated by a colon symbol. The first number refers to the number of carbon atoms in the fatty acid chain, and the second number refers to the number of carbon-carbon double bonds. In the Figure 1.6, is represented the oleic acid (C18:1), this fatty acid has 18 carbons in the chain and 1 carbon-carbon double bond in the fatty acid chain as shown in Figure 1.6.

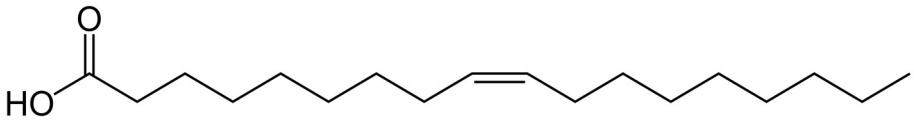

Figure 1.6 - Simplified representation of a fatty acid chain (Oleic acid C18:1).

Table 1.2 - Typical triglyceride fatty acid composition of various oils/fats feedstocks / %(m/m).

Fatty Acid	Abb.	Brown grease	Canola	Coconut	Corn	Jatropha	Olive	Palm	Peanut	Rapeseed	Safflower	Soy	Sunflower	Tallow	Used Frying oil	Yellow grease
Capriotic	6:0			0.6										0.1		
Caprylic	8:0			6.8				0.8								
Capric	10:0		0.1	5.4				0.6		0.6				0.1		
Lauric	12:0			47.7		0.1		0.3	0	0.1		0.1	0.1	0.2		0.2
Myristic	14:0	1.66		18.5		0.3		1.1	0	0	0.1	0.1	0.1	2.6		0.8
Myristoleic	14:1													0.3		
Pentadanoic	15:0													0.6		0.1
Palmitic	16:0	22.83	4.2	9.1	11.5	14.9	12.2	42.5	11.2	4.2	8.2	11.6	6.4	24.3	12	16.5
Palmitoleic	16:1	3.13	0.3	0.1	0.2	1		0.2		0.1	0.1	0.2	0.1	2.6		0.9
Heptadecanoic	17:0		0.1			0.1		0.1		0.1		0.1	0.1	1.4		0.1
Heptadecenoic	17:1		0.1		0.1								0.1	0.6		0.1
Stearic	18:0	12.54	2	2.7	1.9	6.1	2.5	4.2	3.2	1.6	2.5	3.9	3.6	18.2		7.1
Oleic	18:1	42.36	60.4	6.8	26.6	40.4	71.9	41.3	45.5	59.5	14.2	23.7	21.7	42.2	53	44.6
Linoleic	18:2	12.09	21.2	2.1	58.7	36.2	10.5	9.5	31.7	21.5	74.3	53.8	66.3	4.4	33	25.1
Linolenic	18:3	0.82	9.6	0.1	0.6	0.3	0.6	0.3	0.4	8.4	0.1	5.9	1.5	0.9	1	1.1
Stearidonic	18:4													0.4		0.5
Arachidic	20:0		0.7	0.1	0.3	0.3		0.3		0.4	0.1	0.3	0.3	0.2		0.3
Gondoic	20:1		1.5		0.1	0.1		0.3		2.1		0.3	0.2	0.6		0.5
Eicosadiensic	20:2		0.1							0.1						
Behenic	22:0		0.3		0.1	0.1		0.1		0.3		0.3	0.6	0.1		0.4
Erucic	22:1		0.5		0.1	0.1		0.1		0.5		0.1	0.1	0.1		0.1
Lignoceric	24:0		0.2		0.1	2.6		0.1		0.1		0.1	0.2			0.2
Nervonic	24:1		0.2	1		0.1				0.1		0.3				4.4
Others			2.2		0.3	1.2	2.3	0.9	8	4.3	0.8	4.1	0.1	2		
References		[11]	[12]	[12]	[12]	[12]	[13]	[12]	[13]	[12]	[12]	[12]	[12]	[12]	[11]	[12]

Biodiesel is an excellent alternative to fossil fuels like mineral diesel. It has many advantages comparing with mineral diesel or other renewable fuels, but it still exists some problems with its use. In the next paragraphs, will be enounced some of the biodiesel characteristics, advantages and disadvantages of the use and production of biodiesel.

As mentioned before, biodiesel is one of the most promising alternatives to the conventional mineral diesel because it can be used in most conventional diesel engines with no, or only small, modifications, but it has other advantages as well. From the environmental point of view the biodiesel is renewable, energy efficient, portable, biodegradable and presents a positive energy balance. [7,14,15] The feedstocks used to make biodiesel are agricultural or recycled resources. Besides, biodiesel has a clean burning when compared with mineral diesel. It is environmentally friendly because CO_2 emissions are the same that the plants absorbed in the production of oil. Biodiesel usually does not contain sulphur, and also decreases significantly the emissions of other compounds like polycyclic aromatic hydrocarbons and nitric polycyclic aromatic hydrocarbons, thus, reducing many of the GHGs exhausted by the use of conventional mineral diesel.[7,14,16] Biodiesel can not only be used in conventional diesel engines as it improves its lubricity, has a better ignition quality and has a higher cetane number compared with mineral diesel. As said before, it can be blended with mineral diesel at any proportion because it has a significant molecular similarity with paraffinic diesel compounds.[7,14,15]

Comparing with the mineral diesel, the biodiesel also has properties that make it a safer product with a nontoxic character. It has a flash point around 423 K, that is much higher than mineral diesel, 337 K, making the biodiesel non-flammable, non-explosive and with lower vapour pressures, leading to safer storage and handling.[14,17]

For the society, biodiesel can also leave a mark reducing the dependency on foreign oil bringing economic, environmental and technical benefits to the countries without oil reserves. It creates employment by bringing these countries to the fuel market and giving them the possibility to became energetically self-sustainable.[7,14] For this reason, biodiesel does not only prevent a direct impact on the ecosystem, but can also provide new jobs and market opportunities with the new domestic crops and their further processing to biodiesel.

Although it has a lot of positive effects, biodiesel has also some disadvantages when compared with other fuels. These disadvantages are mainly related with the fuel quality and the environment paradox.

The quality of biodiesel as fuel has some disadvantages as a lower energy content leading to lower calorific value, higher reactivity of unsaturated hydrocarbons chains, higher viscosity,

higher pour point, higher cloud point, higher hygroscopicity, lower oxidative stability and a lower engine power and speed. The reactivity of unsaturated hydrocarbons makes the biodiesel degrade four times faster than the mineral diesel, when pure. These characteristics can bring some problems to the engine and fuel lines. [14,15,17,18]

The use of biodiesel has also some problems and controversial opinions regarding the environmentally friendly aspect. In the production of biodiesel there are processes and compounds that are not environmentally friendly. The catalyst for the transesterification process is sometimes a synthetic catalyst with sulphuric acid, sodium or potassium hydroxide which are caustic and toxic. The process, to produce biodiesel, use in most of the cases methanol derived from petroleum. So, biodiesel production is not completely renewable using some petroleum products in the production process. The production process will be explored in more detail in subchapter 1.2. Above, it was mentioned that biodiesel reduces the emissions of many gases, but biodiesel have 10-11 % of oxygen and for that reason the emissions of NO_x increase 10 to 15 % when compared to mineral diesel.[14,15,17] Some studies also report that the biodiesel blends up to B10 does not show significant differences in the gas emissions. [19]

The society can also suffer some consequences from the production of biodiesel, mainly due to the feedstocks used. Some people defend that the use of agricultural crops to produce vegetable oil for biodiesel increase the food price. This problem occurs mainly in the third world countries. The fuels vs. food problem appears when arable soil or farmland is used to produce edible oils for biodiesel in detriment of the food production, this makes the price of the biodiesel feedstock increase and may turn the production economically not-viable comparing with the mineral diesel. The production of oil for biodiesel is controversial, when the crops are converted for the production of oil to biodiesel and are used for a longer time, it also creates other ecological problems, converting habitats into monocultures and with that reducing the biodiversity and the natural carbon sink capacity of the land, inverting the role of biodiesel and increasing the GHGs emission, when compared with mineral diesel. Some authors suggested that cultivation of biofuel crops in rainforests, peatlands, savannas, or grasslands like in Brazil, Southeast Asia, and the USA creates a carbon debt by releasing 17 to 420 times more CO_2 than the annual GHGs reductions that these biofuels would provide by displacing fossil fuels, what does not happen when biofuel is made from waste biomass or biomass grown on degraded and abandoned agricultural lands.[20] It was also suggested that biofuels derived from low-input high diversity mixtures of grassland perennials have more energy, greater GHG reductions and less agricultural pollution per hectare than corn ethanol or soybean biodiesel.[21]

For all these reasons (economical and environmental) the feedstock is one of the greatest bottlenecks in the expansion of biodiesel production, corresponding to 85 % of the production costs. These problems demand looking for cheaper feedstock types such as non-edible oil plants, waste cooking oil and animal fats.[14,15,22]

The Table 1.3 shows some of the values of biodiesel based on feedstock price showing that the profitable biodiesel has to be produced from low-cost feedstocks such as used cooking oil, animal fats or greases.[7,11,14,15,17]

Table 1.3 - Example of values of biodiesel base on the feedstock compared with diesel price. [11]

Feedstock type	**Year**	**Biodiesel price** /US$·L^{-1}	**Diesel price** /US$·L^{-1}
Soybean, canola, sunflower, rapeseed	1999	0.54 – 0.62	0.38
Waste grease	1999	0.34 – 0.42	0.38
Soybean	2001	0.428	0.435
Yellow grease	2001	0.324	0.435
Brown grease	2001	0.246	0.435
Canola	2003	0.72	0.48
Waste cooking oil	2003	0.54 – 0.74	0.48
Soybean	2005	0.53	0.63
Edible and inedible beef tallow	2006	0.22-0.63	0.69

The use of non-edible oils, animal fats and other low-cost feedstocks bring other components to the mixture that should be removed of biodiesel or feedstock, for this reason the choice of the correct method of production of biodiesel regarding the feedstock is essential for obtain the desirable quality of the final biodiesel fuel.

1.2. Production of biodiesel

The production and demand of biodiesel is increasing in the last years and should continue in the next few years. [23] This increase should be led by the European Union as shown in Figure 1.7.[14] In Portugal, the Biodiesel is industrially produced and commercialized since 2006. Since 1 January of 2010, the diesel commercialized in Portugal have around 7 % of biodiesel (B7).[24] In this subchapter will be discussed how this biodiesel is produced, the influence of the process of production in the final product, the influence of the feedstock and some alternatives to the most common production process.

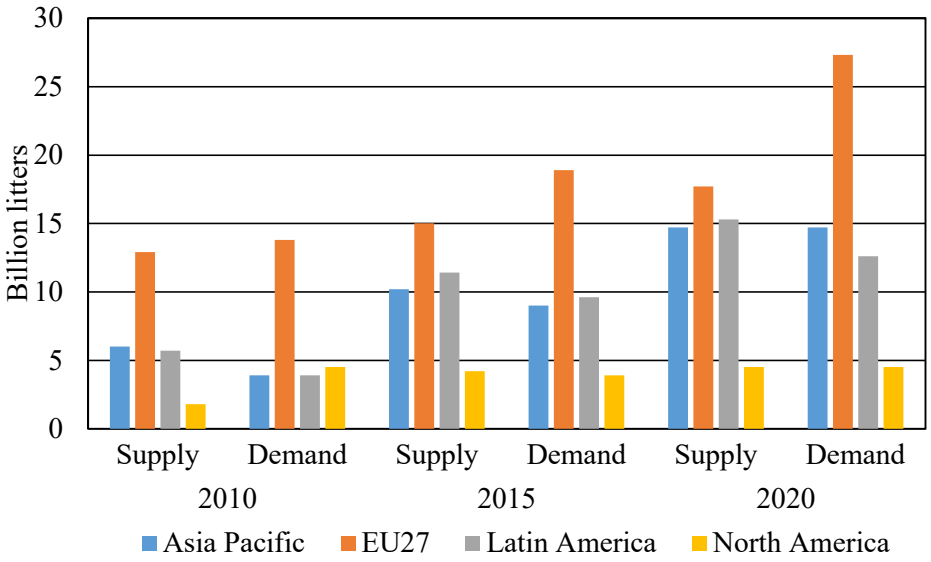

Figure 1.7 - Global biodiesel supply and demand. Adapted from [14]

1.2.1. Biodiesel feedstock influence

The feedstock, as said before, has a great influence in the characteristics of the final biodiesel. The main feedstocks for the production of biodiesel is the alcohol and the oil or fat used. [25]

The **Oil or fat** used is an important parameter to control. Understand the influence of its composition on the final biodiesel has a major importance. Depending on the type of oil used, biodiesel can have some problems like the lower oxidative stability (OS) and the poor temperature behaviour. Some authors suggest that these problems can be controlled using biotechnological tools to modify the fatty acid profile for enhancing the characteristics of performance of biodiesel.[26] However it should be kept in mind that while reducing the unsaturation of the oils would improve its oxidative stability, it would lead to worst cold flow performances.

Despite the use of virgin edible oils to produce biodiesel be easier and cleaner, it is expensive and competes with food supply, it is important to explore the use of low-cost oils and other alternatives sources like non-edible oil, animal fats, waste cooking oils (yellow grease), microbial oils or oils produced in non-arable lands to increase the economic viability of biodiesel. The problem of the use of these low cost feedstocks is that they have relatively higher amounts of FFA and water content being necessary additional steps to remove the water and FFA or soaps from the reaction mixture.[14,17] Other oils have been already tested like rice

bran, safflower, palm kernel, Jatropha curcas, Ethiopian mustard.[27] USA researchers suggest that even the use of these oils will not be enough to meet the future demand of biodiesel and have been exploring algae as a raw material for biodiesel.[28] Table 1.4 compares the yield of oil production per hectare and shows that algae can produce larger volumes of biodiesel per hectare than other crops.

Table 1.4 - Potencial biodiesel yield from different sources. [12]

Source	Potential annual yield /L·ha^{-1}
Corn	168-187
Cottonseed	327-421
Soybean	374-514
Mustard	561-1310
Camelina	561-608
Safflower	748-795
Sunflower	702-982
Canola	1029-1356
Rapeseed	1029-1216
Jatropha	1310-1871
Coconut	2338-2806
Palm oil	3742-6080
Algae	>46770

The choice of the oil used will be a compromise between the oil availability and cost, and the properties required for the biodiesel that will depend of the region and time of the year. The European Union and USA are self-sufficient in the production of edible oils and even have surpluses to export, so in these countries edible oils can be used to produce biodiesel. In the European Union are used rapeseed and sunflower oil and, in the USA, the most typical feedstocks are soybean oil and animal fats. Other tropical countries such as Indonesia and Malaysia use coconut or palm oil to produce biodiesel, but Africa and India have to import edible oils to meet the food requirements so the emphasis of biodiesel is on non-edible oils from plants like Jatropha or karanja.[28,29]

The biodiesel oils can be classified on their FFA (free fatty acid) content or by generation.

Classification on their FFA:

- Refined Oils (FFA <1.5 %) - soybean or refined canola oil; [17]
- Low FFA (FFA <4.0 %) - like yellow greases and animal fats; [17]
- High FFA (FFA > 20 %) - like greases and animal fats. [17]

Classification by generation:

- 1st generation – Edible oils that are normally obtained from food crops and vegetable oils (soybean, sunflower, corn, palm, etc.);
- 2nd generation - Non-edible oils that are derived from variety of feedstocks including lignocellulosic feedstocks and non-food crops (Karanja, Jatropha curcas, etc.);
- 3rd generation – From other sources include microalgae biomass, animal fats, waste cooking oil etc..[29]

The **Alcohol** is another important component in biodiesel production and take a big influence in the properties of the final product. It can influence properties like cetane number, cold flow, OS, lubricity, and viscosity. [25] To produce biodiesel alcohols such as methanol, ethanol, propanol, butanol, 2-butanol, isopropanol can be used. The influence in the biodiesel properties of these alcohols have already been study and reported.[25]

The influence in the kinetics of the reaction of butanol, methanol, *tert*-butanol, ethanol, or isopropanol was studied and methanol, ethanol, and butanol show a decreasing in the initial conversion rate. This study report that the conversion to alkyl esters is negatively influenced by the length of the chain in alcohol.[30] However, the yield of the reaction after 100 min show a conversion above 99 %(mol/mol) not showing significant variations between the use of methanol or ethanol.[31] Sanchez *et al*. compared properties of the biodiesel prepared with different alcohols and conclude that methanol gave the highest yield.[32] The Figure 1.8 shows a comparation of the yields in the production of biodiesel with various alcohols which shows, in most of the cases, a declining trend in yield with the increased of the number of carbon atoms.

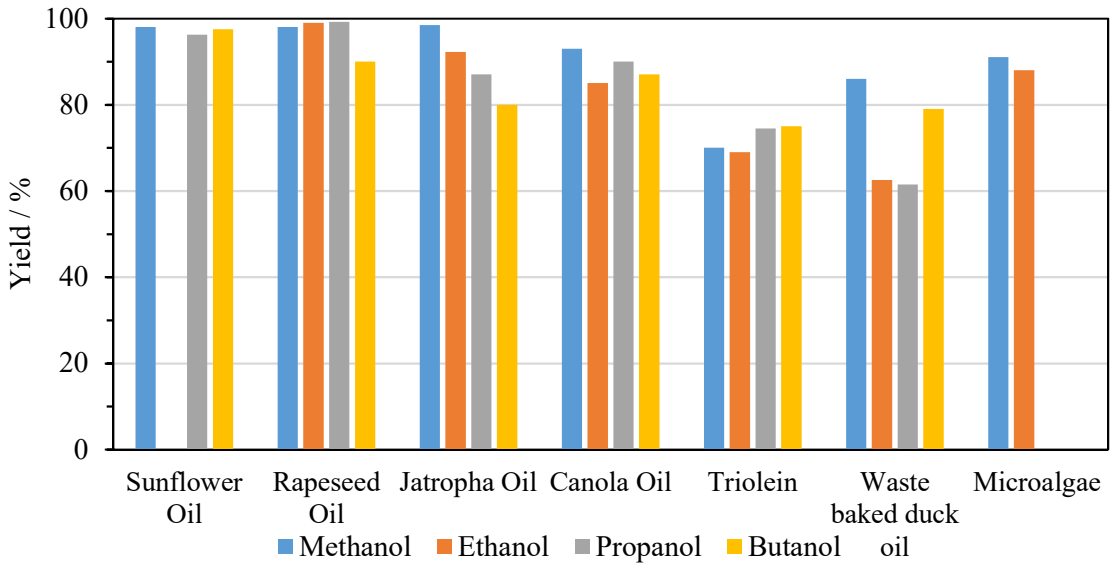

Figure 1.8 - Yield for biodiesel produced with different alcohols. Adapted from [29]

The use of branched esters is of interest because they show improvements in the low-temperature properties. The choice of the branched esters could influence the properties of the final biodiesel but can also increase the price of production. Studies with propanol, butanol, 2-butanol, isopropanol show improvement in the cold flow properties.[25,33,34] The branched esters produced using iso-propanol were studied by Knothe *et al*. [33] It was verified that these esters had cetane numbers competitive with methyl esters or other straight-chain alkyl esters. Despite the use of branched esters leads in biodiesel improves the cold flow properties, the yield in the production is lower compared with the methanol or other lower alcohols (Figure 1.8). Another major disadvantage of the use of branched esters is their higher price when compared with methanol.[25,33,34]

Ethanol is an important alternative to other alcohols because has the advantage of being obtained from biomass, it is renewable, whereas other alcohols as methanol is obtained from fossil sources.[31] Despite that, the alcohol most commonly used in all world to produce biodiesel is the methanol: The principal reason for this is because it is the least expensive alcohol, reacts fast, and the separation of the esters from the reaction media is easier.

1.2.2. Biodiesel synthesis process

To produce biodiesel there is a big range of processes as micro-emulsification, blending, use of nanocatalyst, pyrolysis and transesterification. [7,35] Was also reported that the biodiesel from an oil with superior acid charge can be produce in ionic liquids and observed a maximum yield of 99.7 %.[16,36] Despite all of these processes to produce biodiesel the main and most important production process to reduce the viscosity of the oils and fats is the transesterification.

In Figure 1.9 is represented a simplified scheme for the production of biodiesel from vegetable oils. The vegetable oils react (transesterification reaction) with an alcohol (normally methanol) and a catalyst to produce biodiesel and glycerine.[7,14]

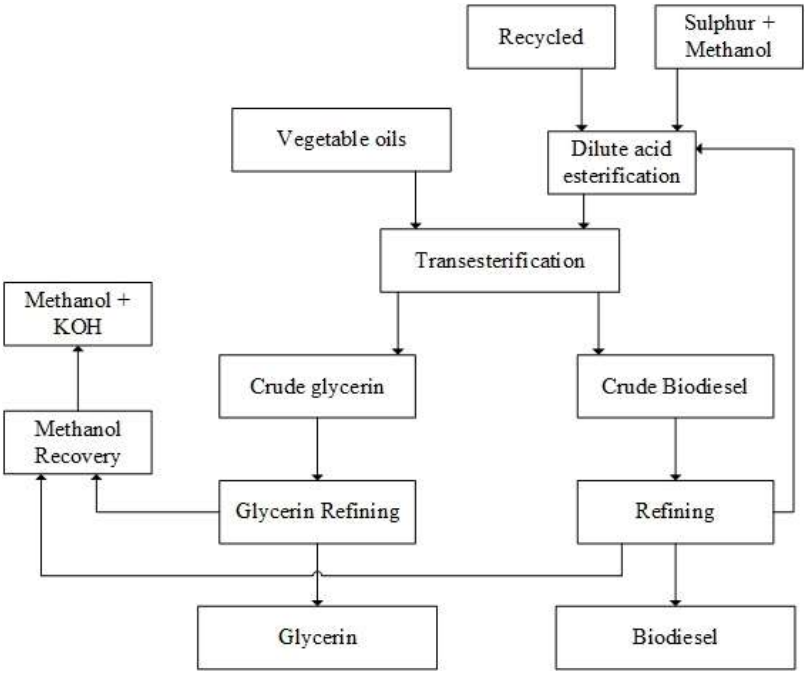

Figure 1.9 - Biodiesel production scheme. Adapted from ref. [7]

The commercial biodiesel technologies can be grouped as: base catalysed transesterification with refined oils; base catalysed transesterification with low FFA greases, and fats or acid esterification followed by transesterification of low or high FFA greases and fats. These technologies can occur in batch or in continuous processes. In the domestic market of USA, most firms use batch technology. In Europe and in industrial processes in USA (producing methyl esters for other uses) the firms use continuous processes. The great advantage of batch processes is that they provide higher productions and excellent opportunities for quality control if the variation of feedstock is common. Typical values of input and output stream are shown in the Table 1.5.[17]

Table 1.5 - Typical input and output stream in a biodiesel production process.[17]

Input Streams		**Output Streams**	
Refined oil /kg	1000	Biodiesel /kg	1000
Methanol /kg	107	Glycerine 88 % /kg	125
KOH 88 % /kg	10	Fertilizer /kg	23
Acid /kg	8	By-product chemicals /kg	≈0
Water /kg	17		
Electricity /kW·h	20		

1.2.2.1. Pre-treatments

As discussed before the biodiesel can be made from different feedstocks and some of them have properties that reduce the yield of reaction or the quality of the final product. The raw materials could have water or other contaminants in various proportions. The use of raw material with lower costs as non-edible oil plants, wasted cooking oil and animal fats, bring the problem of high amount of impurities, and the higher FFA and water content in these feedstocks demands the use of additional pre-treatment, product separation, purification units and other process steps to produce biodiesel with quality.[22]

Some crude vegetable oil contains phospholipids that need to be removed in a degumming step. The degumming can be performed by membrane filtration, hydration, acid micelles degumming, or supercritical extraction, depending on the raw oil.[15] The supercritical extraction is not commercially attractive although the oil extracted with supercritical CO_2 is of much higher quality. [37]

Other problems with the feedstock are commonly related with the FFA content. Higher values of FFA during the transesterification, cause the formation of soap.[29] Sometimes is necessary a pre-treatment step to reduce the FFA content of the feedstock. The reduction of FFA content could be made by a process of steam distillation, extraction by alcohol, deodorization step and esterification by acid catalysis. [15,38] The deodorization step would remove also the aldehydes, unsaturated hydrocarbons, and ketones, that are compounds that cause undesirable odours and flavours in the oil. This step is performed using steam pressurized injected into the oil to a temperature between 490 to 550 K.[15,38] In the esterification by acid catalysis the FFA are esterify before the transesterification of the triglycerides with an alkaline catalyst, this is the best use of the FFA in the oil.[15]

The use of an alkali catalyst has a maximum amount of FFA permitted in the feedstock of 2.5 %, being necessary a pre-treatment before the transesterification when the feedstock presents higher values of FFA. For these reasons the oils are normally subjected to a pre-treatment process. An example of a case for biodiesel production using alkali catalyst and a feedstock with more than 2.5 % of FFA is represented in Figure 1.10. [15,39]

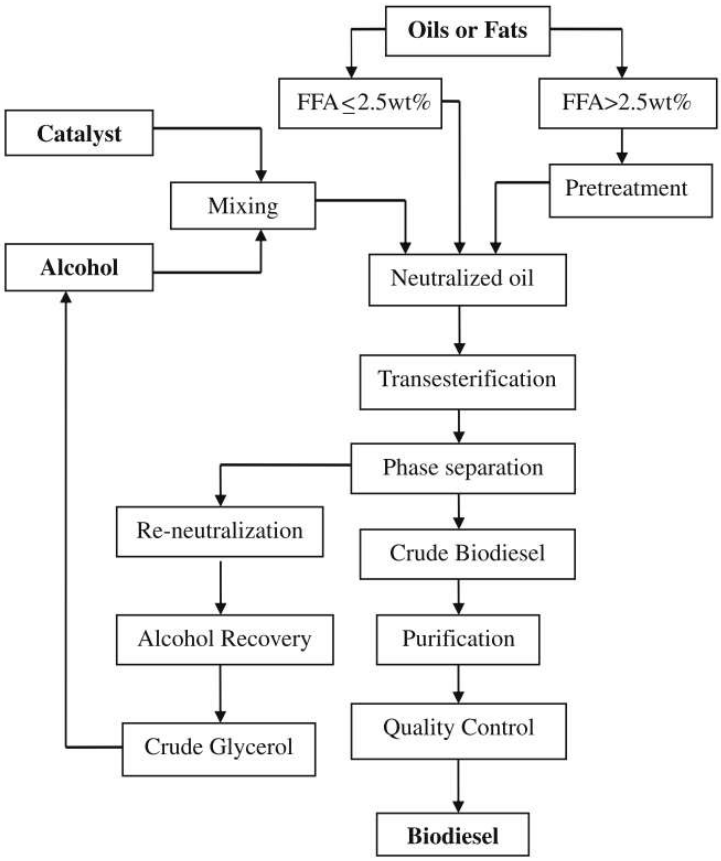

Figure 1.10 - Process flow chart for biodiesel production with high or low FFA feedstock.[15]

1.2.2.2. Reaction

There are different ways to produce biodiesel such as the BIOX Co-Solvent Method, the Non-Catalytic Supercritical Alcohol Transesterification, the Catalytic Supercritical Methanol transesterification, the Ultrasound and Radio-Frequency-Assisted Transesterification and *in situ* Biodiesel Techniques.[7,15,29] However as said before the transesterification is still the most common and it is this reaction that is industrially used to produce Biodiesel.[7,40]

Transesterification is a reaction of an oil or fat with an alcohol in the presence of a catalyst to form esters and glycerol. In this reaction a triglyceride is converted first to diglyceride, this diglyceride is converted to a monoglyceride, and this is converted to a fatty acid ester releasing the glycerol. In each step is produced a fatty acid ester, so in the complete reaction three fatty acid esters are produced from a molecule of triglyceride. In Figure 1.11 is represented the transesterification reaction. The R_1, R_2, R_3 are alkyl chains that can be different or equal in the same triglyceride.[7]

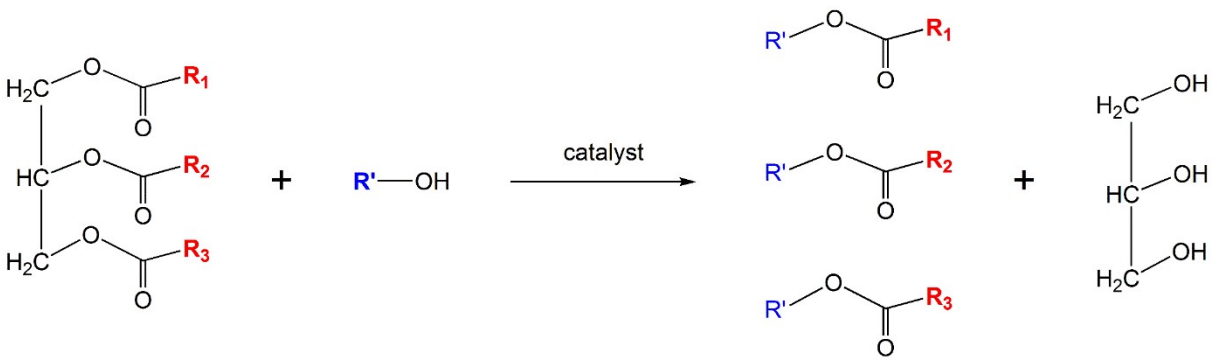

Figure 1.11 - Transesterification of triglycerides with an alcohol.

This reaction is affected by various parameters such as the molar ratio alcohol/oil. The presence of a sufficient amount of alcohol is essential during the transesterification reaction to break the glycerine fatty acid linkages, this ratio depends on the oil used, but the alcohol should always be in stoichiometric excess; Other constituents of the raw material should be removed or treated in a previous step as shown above. The water and moisture content affect the yield of biodiesel, and could create a negative effect so the feedstock should be water free; The FFA content is another factor affecting this reaction mainly in alkaline transesterification, the FFA reacts with the alkaline catalyst to produce soaps; The mixing, the specific gravity and temperature should also be taken in consideration.[15,40]

When the transesterification reaction is completed two major products are present: the biodiesel and the glycerol. The glycerol has a higher density than the biodiesel and settles at the bottom of the reaction vessel.

Catalysis

As catalyst is normally used an acid or alkali catalyst depending on the nature of the oil, other catalysts like lipase are being studied. Although lipase have advantage over acid and alkali catalysts its cost is a limiting factor for its use in large scale production. [15,40]

The choice between acid and alkali catalyst depends mainly on the FFA content in the oil. Various authors favoured acid esterification using H_2SO_4, prior to alkaline transesterification to reduce the acid value.[40] For oils with less than 2 % of FFA the alkaline transesterification is preferred over the acid catalysed transesterification because is reported to proceed about 4000 times faster. In cases of feedstocks with high FFA was verified by Canakci and Gerpen that a process with two steps, first an acid catalysed pre-treatment followed by an alkali catalysed transesterification, made the reaction to be completed in much less time than would be possible with only acid-catalysed transesterification.[41]

The most used catalysts at industrial level are the sodium hydroxide, and potassium hydroxide.[40] This last catalyst is preferred to speed up the reaction at lower temperature and pressure, achieving a higher yield in less time, is cheaper, and more abundant.[29]

In Table 1.6 is made a comparation of the different transesterifications processes

Table 1.6 - Comparation of the different catalyst for transesterification.[42]

Variable	Alkali catalysis	Acid catalysis	Lipase catalysis
Reaction time	Short	Long (9 h)	Very long (36 h)
Reaction temperatures /ºC	60-70	55-80	30-40
Production cost of catalyst	Inexpensive	Inexpensive	Expensive
FFA in raw materials	Saponified products	Esters	Methyl esters
Water in raw materials	Interference with reaction	Interference with reaction	No influence
Yields of methyl esters	Normal	Normal	Higher
Recovery of glycerol	Difficult	Difficult	Easy
Purification of methyl esters	Repeated washing	Repeated washing	None

The use of these types of catalysts has been successful, however the biodiesel and glycerine produced must be purified to remove the catalyst by washing with hot distilled water, which leads to a high consumption of water. Some studies were made to avoid this neutralization and separation steps from the reaction mixture in homogeneous catalysis using heterogeneous catalysis where separation is possible without using solvent and shows an easy regeneration. This makes the nature of the final product less corrosive and the whole process safer, cheaper and more environment friendly. This includes catalysts like alkaline-earth oxides, zeolites, MgO, CaO and hydrotalcites. This process would prevent the most complicated separation step, the large volume of water and the regeneration is easy.[40] A list of advantages or disadvantages of heterogeneous or homogeneous base transesterifications are listed in Table 1.7.

Table 1.7 - Advantages and disadvantages of Heterogeneous and homogeneous base transesterification.[29]

Type of catalyst	Advantages	Disadvantages
Heterogeneous	• Relatively easier separation of catalyst • Rapid completion • Reusability of catalyst that make the process cheaper. • Esterification and transesterification occur in simultaneous	• Complex catalyst synthesis that increase the cost. • Normally, high reaction temperature, high alcohol to oil molar ratio and long reaction time are required. • Energy intensive.
Homogeneous	• Can be used with oil having higher FFA content. • Use of oil with inferior quality	• Catalyst has to be stored away from air. • Emergence of soap lowers down the yield and makes purification difficult. • Formation of soap with oils that have FFA >2 %(m/m).

The type of feedstock is one more time crucial for the determination of the best reaction scheme. In Table 1.8 are shown some optimized values used in biodiesel production of the most common biodiesels feedstocks.[40]

Table 1.8 - Biodiesel production from different feedstocks. [40]

Feedstock	Transesterification stages	Alcohol	Molar ratio (methanol:oil)	Catalyst	Temperature /K	Duration	Conversion
Sunflower oil	Single step	Supercritical methanol	40:1	No catalyst	473-673 (200 bar)	10-40 min	78-96 % with increase in temperature
				CO_2 + Lipase 30 %(m/m) of oil		6 h	23-27 %
		ethanol	5:1		318		
Canola oil	Single step	Methanol	6:1	NaOH 1.0 %(m/m)	318	15 min	98 % ester content
Used Frying oil	Single step	Methanol	7:1	NaOH 1.1 %(m/m)	333	20 min	94.6 % ester content
Soybean oil	Single step	Methanol	6:1	NaOH	318	10-20 min	100 %
Jatropha, Pongamia, Sunflower, Soybean, Palm	Single step	Methanol	3:1	NaOH/KOH (1 %(m/m) of oil)		2-4 h	
Sunflower oil	Single step	Methanol	13:1	Activated CaO (1 %(m/m))	333	100min	
Jatropha oil	Two step acid catalysed	Methanol	0.28 v/v	H_2SO_4 1.43 %(v/v)	333	88min	>99 %

1.2.3. Biodiesel post-treatment and refining

The glycerol and biodiesel separated in the reaction vessel are both contaminated with unreacted catalyst, alcohol, and oil. Some soap could be also formed on the transesterification step, which is also a contaminant to biodiesel and glycerol. So after the transesterification there should be a refining of biodiesel and glycerol.[43]

The refining of the glycerol is also important. Glycerol is not the main product but is also valuable due to its numerous applications in industrial products such as soaps, medicines, cosmetics, etc. The glycerol produced is about 50 % glycerol or less in composition and contains water, salts, unreacted alcohol, and unused catalyst. This solution is neutralized using acid to neutralize the catalyst remaining, the water is removed in a distillation column and alcohol is removed in a vacuum flash process or other processes producing an 80 – 88 % pure glycerol sold as crude glycerol. This glycerol could, after other separation processes, be used to produce 99 % pure glycerol.[15,44]

The crude biodiesel, produced after the separation of glycerol in the transesterification step, contains contaminants like residual catalyst, water, unreacted alcohol, free glycerol and soaps. The crude biodiesel normally passes first through a neutralization step and then an alcohol stripper followed by a washing step. In the neutralization step, acid is added to the biodiesel to neutralize any remaining catalyst and split any soap. After this step, the alcohol remaining is removed with distillation equipment before the washing step to prevent excess of alcohol in the wastewater effluent. [15,43–45] In the end is carried a washing step to remove the remaining catalyst, soaps, salts, residual alcohol and free glycerol.[15]

After all these steps of purification are carried, the biodiesel should be analysed to ensure that meets the international standards. These parameters will be described briefly in the next subchapter.

1.3. Biodiesel and Biodiesel blends properties

Several properties of the biodiesel are required to meet international standards for commercialization. The main standard in European Union for biodiesel is the European normative EN 14214. This standard define limits and methods to follow to test the different properties of biodiesel, the limits can depend of the region or the season. In this subchapter are discussed some of the properties enounced in this standard as well as other properties also

important to characterize the Biodiesel. For the blends of diesel up to B7 the EN 590 should be applied.

The properties related to the oxidative stability and cold temperatures like cloud point, pour point, and cold filter plugging point will be discussed in the subchapters 1.4 and 1.5 in more detail and thus will not be mentioned below.

– Ester content

The ester content is important to ensure that the fuel is mainly composed by esters and no other type of fuels as for example mineral Diesel. This biodiesel can subsequently be used to blend with diesel.

The minimum limit for ester content is 96.5 %(m/m) determined by gas chromatography according to a procedure using internal calibration (nonadecanoic acid methyl ester) described in the method EN 14103.

– Density

The fuel density is a key property that affects engine performance. The densities in biodiesel are generally higher than those of mineral diesel. The density changes with the fatty acid composition as well as with their purity. It increases with the decreasing chain length and the increasing number of double bonds or decrease with the presence of contaminants with low-density. The fuel injection pumps meter fuel by volume, so a greater or lesser mass fuel is injected depending upon its density affecting the mass of fuel injected into the combustion chamber and thus, the air-fuel ratio. It can also affect the efficiency of atomization of fuel, the higher the density makes the fuel spray narrow and its penetration deeper.[46–48]

The density at 15 ºC should be in the range of 860 to 900 $kg \cdot m^{-3}$ and is analysed introducing a small portion of the test sample into a temperature-controlled sample cell, the oscillation frequency is noted, and the density of the sample calculated using cell constants as described in EN ISO 12185 or by the hydrometer method like described in EN ISO 3675

– Viscosity

Viscosity is the measurement of resistance to flow of a liquid due to internal friction. A high viscosity affects the atomization of the fuel in the injection to the combustion chamber, causing larger droplet sizes, poorer vaporization, a narrower injection spray angle, a greater in-cylinder penetration on the fuel spray and also increase, with the increase of the viscosity, the potential for the formation of engine deposits. Other problems like the excessive pump

resistance, filter blockage, high pressure, and delivery of low fuel rates could also be caused by a high viscosity. A low viscosity results in an excessive wear in injection pumps and power loss due to pump leakage. The viscosity increases with the chain length and with increasing degree of saturation and is greatly affected by temperature. [7,12,27,46,49,50]

The viscosity at 40 ºC must be in the interval between 3.50 e 5.00 $mm^2 \cdot s^{-1}$ and the standard method to analyse it is the EN ISO 3104 that obtain the viscosity measuring the time for a fixed volume of liquid to flow under gravity through the capillary of a calibrated viscometer under a reproducible driving head and at a known and closely controlled temperature.

– Flash Point

The flash point is the lowest temperature at which there is enough concentration of evaporated fuel in the air for the flame to propagate after an ignition source has been introduced. It is related to fuel volatility and is specifications in biodiesel are meant to guard against contamination by highly volatile impurities like the alcohol remaining in the finished fuel. The flash point is also important for safety precautions in the fuel handling and storage. The flash point increases with the increasing chain length and also decreases significantly with increase of alcohol content in the fuel.[7,12,48,49]

The flash point must be higher than 120 ºC and measured by introducing a specified volume into a test vessel that is set and maintained at the required test temperature, and after a specific time, an ignition source is applied, and a determination is made as to whether a flash occurred. To determine the actual flash point further tests at different test vessel temperatures and with fresh test portions are carried out until the flash point is determined like defined in EN ISO 3679.

– Cetane number

The cetane number gives a measurement of the ignition characteristics of diesel fuel in a CI engine. The ignition performance is related to the ignition delay of the fuel as determined when the standard test engine is operated under controlled conditions of fuel flow rate, injection timing and compression rate.[48,51]

A high cetane number is associated with a smooth combustion, and rapid engine start so a better ignition quality. The biodiesel in general has a higher cetane number than mineral diesel.[48]

The cetane number is determined at constant speed in a pre-combustion chamber type of a CI test engine. It is obtained comparing its combustion characteristics with those for blends

of reference fuels of know cetane number. The minimum value for this is 51.0 measured by EN ISO 5165. [51]

- Copper strip corrosion

This measured the tendency of a fuel to cause corrosion to copper, zinc and bronze parts of the engine or storage tank. The corrosion made by biodiesel can be induced by some sulphur compounds and by acids.[48]

The copper strip corrosion is measured immersing a polished copper strip in a specified volume of sample and heated under specific conditions of temperature and time to the class of material being tested. At the end of the heating period, the strip is removed, washed, and the colour assessed against corrosion standards and should be rating as class 1 as defined by the EN ISO 2160.

- Acid Value

The acid value is a measure of the FFA in a fresh fuel sample and of FFA and acids from degradation in aged samples. It is influenced by the type of feedstock used for fuel production and its degree of refinement. The acid can also be generated during the production process. The value increases gradually due to degradation in the fuel storage.[7,48]

It is expressed as the mass (mg) of KOH required to neutralize 1 g of biodiesel and it is determined by titration using phenolphthalein as an indicator. It has a maximum value of 0.50 mg KOH·g^{-1} measured following the EN 14104.

- Iodine Value

It is a measure of the total unsaturation within a mixture of fatty acids. Engine manufacturers said that fuels with higher iodine number tend to polymerize and form deposits on injector nozzles, piston ring grooves and piston rings when heated. The unsaturated esters can form high-molecular compounds that will impair the lubrication. [48]

The method used to measure the iodine value is defined by the EN 14111 and EN 16300 with a restriction for maximum value of 120 g iodine·100 g^{-1}. In the method EN 14111 the value is measured dissolving a test portion in a mixed solvent and then Wijs reagent is added. After a specified time, potassium iodide and water are added to the sample and the liberated iodine is titrated using a sodium thiosulphate standardized solution.

– Linolenic acid methyl ester

These parameters have consequences similar to the Iodine Value whereas analyses one of the unsaturated compounds in the biodiesel.

It is measure by the same method that the ester content, EN 14103, and have a limit of 12.0 %(m/m).

– Polyunsaturated

The excess in this parameter has the same prejudicial effects that the described for the iodine value.

It is measure by the same method that the ester content, EN 14103, and have a limit of 1.00 %(m/m)

– Methanol and Ethanol Content

These compounds have high volatilities so the high content in methanol or ethanol can cause corrosion in the fuel system, low lubricity, adverse effects on injectors and affect the flash point of esters.[48]

The amount of ethanol or methanol is limited to 0.20 %(m/m) and should be measure following the described in the EN 14110.

– Mono-, di-, and try-Glycerides content

The content of glycerides in the biodiesel is dependent on the production process, and high values of glycerides are prone to deposit formation on injection nozzles, pistons and valves.[48]

The limits for content of these compounds are specified in separated, for mono-glycerides the limit is 0.70 %(m/m) and for di- and tri-glycerides the limit is 0.20 %(m/m). All the compounds should be analysed following the EN 14105 that measured this value by gas chromatography on a short capillary column with thin film thickness, with an on-column or equivalent device, and flame ionization detection.

– Free glycerol

As for the glycerides the free glycerol is also dependent of the production process, and high values can result from an inefficient separation or washing of the biodiesel. Excess glycerol can damage the fuel injection system and high levels can cause injector coking.

It is limited to 0.02 %(m/m) and is also measured following the de same principle of glycerides content and the same method, EN 14105 or EN 14106.

– Total glycerol

The Total glycerol is basically the sum of the two previous parameters. It depends basically of the same factors and has the consequences previously reported for the system.

It is measured also by the EN 14105 and limited to 0.25 %(m/m).

– Water

The water is introduced in the system during the washing step of the production process and must be reduced by drying. The water promotes the biological growth, sludge and slime formation causing blockage in the fuel filters and fuel lines. It is also associated with hydrolysis reactions, partly converting biodiesel to FFA. In blends lower water concentrations, which pose no difficulties in pure biodiesel fuels, may become problematic when this biodiesel is blended with mineral diesel. [7,48]

The water content is limited to a maximum of 500 $mg \cdot kg^{-1}$ and it is measured introducing a weighed portion into the titration vessel of a coulometric Karl Fischer apparatus in which iodine for the Karl Fischer reaction is generated coulometrically at the anode. When all the water has been titrated, excess iodine is detected by an electrometric end-point detector and the titration is terminated. Based on the stoichiometry of the reaction, one mole of iodine reacts with one mole of water, thus the quantity of water is proportional to the total integrated current according to Faraday's Law. This is described in the method described in the EN ISO 12937.

– Total contamination

The total contamination is the insoluble material retained after filtration of a fuel sample under standardized conditions. High values of total contamination can lead to blockage of fuel filters and injection pumps, can be related to the high concentrations of soaps and sediments.[48]

The total contamination is limited to a maximum of 24 $mg \cdot kg^{-1}$. This value is obtained weighed a sample portion and filtered under vacuum through a pre-weighed filter. The filter with the residue is washed, dried and weighed as defined by EN 12662.

– Sulphated ash

The sulphated ash content is the number of inorganic contaminants, such as abrasive solids and catalyst residues, and the concentration of soluble metal soaps contained in the fuel. The ash content is correlated with the formation of engine deposits and filter plugging. [7,48]

The amount of sulphated ash is measured by the ISO 3987 and have a maximum value of 0.02 %(m/m). In this method a sample is ignited and burned until only ash and carbon remain. After cooling, the residue is treated with sulphuric acid and heated at 775 ºC until oxidation of carbon is complete. The ash is then cooled, retreated with sulphuric acid, and heated at 775 ºC to constant mass, and finally the sulphated ash obtained is calculated.

– Sulphur Content

As said before the biodiesel is sulphur free, this parameter has been imposed mainly for environmental reasons. The sulphur content affects the emission control system performance and can cause some engine wear and deposits. The maximum value for the sulphur content is 10.0 $mg \cdot kg^{-1}$ measured injecting a sample into a UV fluorescence detector and enter in a high temperature combustion tube, where the sulphur is oxidized. The water produced is removed and the sample combustion gases are exposed to the UV light. The fluorescence emitted from the excited sulphur dioxide is detected by a photomultiplier tube and the resulting signal is a measure of the sulphur contained in the sample as defined by the EN ISO 20846, EN ISO 20884 or EN ISO 13032, the last one measure the sulphur content using X-ray. [7,48]

– Group I and II metals

Alkali and alkaline earth metals are introduced into the biodiesel fuel during the production process. They can be originated by the catalyst residues and hard washing water. Some of this metals are related with the formation of ashes within the engine and the calcium soaps are responsible for injection pump sticking. [48]

These compounds are limited to 5.0 $mg \cdot kg^{-1}$ and are measured by the EN 14108 and EN 14109 where the sample is diluted with a xylene solution. The Group I metals content is determined by atomic absorption spectrometry with a specific wavelength for the measure of sodium or potassium content. This parameter can also be measured following the method described by the EN 14538 for metals of both groups.

– Phosphorus content

Phosphorus appear in biodiesel from phospholipids of animal, vegetable material and inorganic salts of used frying oil contained in the feedstock. It has a strong impact on the long--term activity of exhaust emission catalytic systems. [7,48]

The phosphorus content is measured diluting a weighed sample in xylene. The solution is introduced in aerosol form into an inductively coupled argon plasma where the phosphorus content is determined by comparing the emission of the element in the solution of the sample with the emission of the standards at the same wavelength as defined in the EN 14107. This value is limited to a maximum of 4.0 $mg \cdot kg^{-1}$.

1.4. Cold Flow Behaviour

The cold flow behaviour is an important factor to define and understand to achieve a better use of biodiesel. It is related to one of the main problems of the use of biodiesel when compared to mineral diesel, since it has higher crystallization points than mineral diesel, and this is particularly important in cold regions during winter months [6,7]. The low temperature properties of biodiesel are controlled by several specifications, such as pour point (PP) (ASTM D-97, ASTM D-5949), cold filter plugging point (CFPP) (EN 116, IP-309, ASTM D-6371) and cloud point (CP) (EN 23015, ASTM D-2500)[14–17]. These three essays are defined as:

- **Pour Point:** The lowest temperature at which movement of the test specimen is observed under prescribed condition of test;[52,53]
- **Cold Filter Plugging Point:** Lowest temperature at which a given volume of fuel fails to pass through a standardized filtration device in a specified time, when cooled under standardized conditions;[54,55]
- **Cloud Point:** Temperature at which a cloud of wax crystals first appears in a liquid when it is cooled under specified conditions.[53,56]

The formation of solids residues leads to the formation of solid deposits that clog fuel filters in vehicles or cause blockage in fuel lines, leading to the fuel starvation in engine operation. [8–13] The cold flow behaviour can be influenced by the fuel composition and the presence of other components. A reduce quality in cold flow properties can have consequences in the performance and durability of the fuel system.

The problem is particular to the biodiesel used since every biodiesel has a different composition, so different length of the hydrocarbon chains and presence of saturated fatty acids in different concentrations. In Table 1.9 are specified some effects on the engine when the CP, CFPP and PP are higher than the biodiesel temperature.[54] In this table it is also possible to observe that the effects are similar for all the properties that characterize the behaviour of the biodiesel at low temperature.

Table 1.9 - Effects on engine by higher CP, PP and CFPP.[54]

Property	Effect on engine
Cloud Point	• Starting problems in cold conditions; • Plugging and gumming of filters and wax formation; • Fuel Starvation and operation problem; • Solidification of fuel lines; • Fuel cannot be pumped; • Poor ignition;
Cold filter plugging point	• Plugging and gumming of filter, lines and injector; • Driving problem in cold conditions; • Wax formation; • Clogging of fuel lines and filters
Pour point	• Plugging and gumming of filters and wax formation; • Pumping problem in engine; • Fuel ceases to flow; • Fuel starvation

1.4.1. Influence of feedstock, fuel composition and additives

The cold flow properties of biodiesel are influenced by different factors. The main factors that define these properties are the feedstock used, the composition of the final fuel and the presence of additives. In the next topics will be explained how these factors could influence positively and negatively the low temperature behaviour of the biodiesel.

1.4.1.1. Feedstock

The feedstock has a great importance on the final composition of biodiesel and can be improved to present better cold flow properties. The biodiesel fuels with significant amounts of saturated fatty compounds show a higher CP and PP due to the high melting point of the saturated fatty compounds.[33] Improvements in the feedstock can be made for example by using a genetically modified feedstock more unsaturated [57] or by crystallization fractionation that is the separation of the components of lipids based on differences in crystallization

temperature. This last process can be divided into two processes: dry and solvent fractionation.[27]

The dry fractionation, defined as crystallization from a melt without dilution in solvent, is the simplest and least expensive process for separating high and low melting point fatty derivatives. The principle of this fractionation process is based on the cooling of oil under controlled conditions without the addition of chemicals or solvents, being the liquid and solid phases separated by filtration[27,58]

The solvent fractionation consists in the separation of triglycerides components that differ in solubility and is accomplished by fractional crystallization of a solution of oil in an organic solvent, followed by separation of the solids from the liquid by filtration and removal of the solvent by steam stripping. This is the most versatile technique. Is the most expensive process because of solvent loss, equipment, lower temperature requirement, and stringent safety features.[58]

Comparing both techniques, solvent fractionation has the advantages that it reduces the viscosity, makes the separation easier, reduces crystallization times, have high separation efficiencies, and improves yield. As disadvantages, as enounced before, are the high operation costs.[27,58]

The use of branched alcohols is also of interest to improve the cold flow behaviour. The alcoholic moiety of the ester can influence the cold flow properties. Studies with propanol, butanol, 2-butanol, isopropanol show improvement in the cold flow properties.[25,33,34] The branched esters produced using iso-propanol were studied by Knothe *et al*. [33] It was verified that these esters had cetane numbers competitive with methyl esters or other straight-chain alkyl esters. The use of long normal alcohols or branched alcohols to biodiesel manufacture reduces the CP.[59] The use of ethyl and other largest alkyl esters including non-polar head-groups make the alignment in a head-to-tail arrangement with larger molecular spacing. The bulky head-groups disrupt the spacing between individual molecules causing rotational disorder in the tail-group. The esters with branched head groups have a CP of around 3 ºC for canola oil and 9 ºC for soybean oil that is lower than the normal methyl head-group.[27] Malins *et al*, show that the increase of the free fatty alkyl ester hydrocarbon chain length in alcohol moiety and branched alcohols significantly helps to improve the cold flow properties. [34]

1.4.1.2. Fuel composition

As explained in the subchapter 1.2 the composition of the biodiesel is an important factor in the study of the properties of the biodiesel and this is particularly true for the cold flow properties. The fuel composition is strictly related to the feedstock but can be modified to improve the cold flow properties. This can be made by similar processes used in the feedstock as for example by winterization.

The process of winterization of the fuel, is similar to the dry fractionation, involves equilibrating a quiescent mixture of methyl esters at a temperature between its CP and PP. In this operation the saturated fatty acids precipitate and form a suspension in a liquid-phase. After that the solid fuel is filtered and remain a liquid richer in unsaturated fatty acid methyl esters (FAMEs) that should result in better cold-flow properties for that fuel, with lower CP and PP.[57] Some studies shown that the winterization is a process that improve the cold-flow properties but reduces drastically the yield of the separated liquid fraction.[60,61] As expected some of the improvements in the low temperature properties of the winterised fuel resulted from a reduction of the saturated FAME, this reduction can have consequences in other parameters like the OS[27,61,62] Alternatively to the winterization could also be in used another processes of crystallization fractionation as dry fractionation, dewaxing and solvent fractionation. [27] These processes are similar to the process described previously for the vegetable oils.

The size of the chain is also important for the value of CP and PP, this significantly increases with saturated methyl esters longer than C_{12} even when blended with conventional diesel. The longer the carbon chain the poorer the low-temperatures properties.[33,63,64]

The amount of saturated FAME is related with the cold flow properties as the CP. There are studies showing that the cloud point of biodiesel could be determined by the amount of saturated FAME regardless the composition of unsaturated esters [13]

Sarin *et al.* verified a dependence of the cold flow properties using for the experiments blends of biodiesel from Pongamia oil (PoO), jatropha oil (JO), and palm oil (PO). The equations [1.1],[1.2] show a correlation between the CP and PP with methyl palmitate fraction (X_{MeC16}) in %(m/m), respectively.[65]

$$CP(°C) = 0.526 \cdot X_{MeC16} - 4.992 \qquad (0 < X_{MeC16} < 45) \qquad [1.1]$$

$$PP(°C) = 0.571 \cdot X_{MeC16} - 12.240 \qquad (0 < X_{MeC16} < 45) \qquad [1.2]$$

They also proposed correlations between the CP and PP, equations [1.3] and [1.4], with total unsaturated FAME (X_{UFAMEs}) in %(m/m).[65]

$$CP(°C) = -0.576 \cdot X_{UFAMEs} + 48.255 \quad (0 < \%_{UFAMEs} < 84) \qquad [1.3]$$

$$PP(°C) = -0.626 \cdot X_{UFAMEs} + 45.594 \quad (0 < X_{UFAMEs} < 84) \qquad [1.4]$$

The CFPP was correlated with these two parameters, X_{MeC16} and the unsaturated FAME (X_{UFAMEs}), obtaining the relationship given by the equations [1.5] and [1.6].[66]

$$CFPP(°C) = 0.511 \cdot X_{MeC16} - 7.823 \quad (0 < X_{MeC16} < 45) \qquad [1.5]$$

$$CFPP(°C) = -0.561 \cdot X_{UFAMEs} + 43.967 \quad (0 < X_{UFAMEs} < 84) \qquad [1.6]$$

Other correlations were proposed by Park *et al.* using biodiesel from PO, rapeseed oil (RO) and SO. The correlation obtain the CFPP using the content of the unsaturated FAME (X_{UFAMEs}) in %(m/m) given by the equations [1.7] and[1.8].[67]

$$CFPP(°C) = -0.4880 \cdot X_{UFAMEs} + 36.0548 \quad (0 < X_{UFAMEs} < 88) \qquad [1.7]$$

$$CFPP(°C) = -2.7043 \cdot X_{UFAMEs} + 232.0036 \quad (88 < X_{UFAMEs} < 100) \qquad [1.8]$$

Alternatives for biodiesel modification improving the cold flow properties are being explored as for example the conversion of biodiesel to triesters, and the study of π-bonds of unsaturated fatty acids by electrophilic addition to produce branched or bulky esters.[68,69]

The blends of biodiesel was studied by Moser for the CP, PP and CFPP of different biodiesels blends of alternative feedstocks.[70] The blending of different biodiesel could improve these properties as it is possible to see in equations [1.1] to [1.8], it is possible to improve the cold flow properties using blends of biodiesel with lower concentrations of saturated esters.

For the blends of mineral diesel and biodiesel the complexity of the mixture increase. The mineral diesel is composed between 15 to 30 % of *n*-paraffins with a chain length in the region of C8 to C28/C32. The heavier *n*-alkanes when cooled start to precipitate from the fuel. The precipitate is in the form of wax crystals and with the cooling progress the wax crystals grow

with the n-alkanes as low as C18. These *n*-alkanes crystallise with part of the FAME present in the blends that also crystallise when cooled.[71]

The blends with mineral diesel were studied by Dunn and Bagby concluding that this method is only effective to improve the cold flow properties for blends up to 30 %(v/v) of biodiesel. [72] Joshi and Pegg also study studied the low temperature properties of blends and in this study, they developed some correlations between the CP and PP with the volume fraction of biodiesel using blends of methyl esters of fish oil. The correlation obtained are shown below, equation [1.9] and [1.10], where V_B is the volume fraction of biodiesel in %. In these equations is possible to see that these properties get worse when the volume of biodiesel is bigger. [73]

$$CP(^{o}C) = -16.75 + 0.1991 \cdot V_B + 0.000223 \cdot V_B^2 \qquad [1.9]$$

$$PP(^{o}C) = -19.25 + 0.1865 \cdot V_B + 0.000335 \cdot V_B^2 \qquad [1.10]$$

1.4.1.3. Other Components

The process of production of biodiesel can leave some very small concentrations of compounds presents in the crude feedstock, and others resulting from the incomplete conversion and processing of the biodiesel, such as residual oil, glycerides or fatty acids. They have low solubility and high melting points that can lead to the formation of solid residues when stored at low temperatures.

Compounds as sterol glucosides can be present in feedstock oil. The processing after and before the conversion to biodiesel can reduce this molecule content. The presence of these molecules, even in small concentrations, can produce precipitates that settle in the bottom of storage tanks. The high melting point of these molecules and their low solubility in biodiesel or diesel fuel makes them dispersed fine solid particles in biodiesel. This phenomenon can be accelerated by cold weather and sterol glycosides can act as possible seed crystals for developing of larger agglomerates.[74]

Some tests were made for the combinations of soap, water, monoglycerides and sterol glucosides added to distilled biodiesel from soybean oil (SO) measuring the CP and the filtration times. In that study it was concluded that the monoglycerides at concentrations above 6000 ppm had a most significant impact on CP. [75] Combinations of monoglycerides with soap or water had a negative impact on CP and the CP increase a maximum of 3.6 ºC for a concentration of 10000 ppm of monoglycerides, 0 ppm of sterol glucosides, 40 ppm of soap

and 500 ppm of water. The sterol glucosides did not have a negative effect on CP. The filter test was more sensitive to sterol glucosides and soap.[75]

On blends of biodiesel and mineral diesel these impurities could also influence the cold flow properties as was investigated, comparing the properties of biodiesel, diesel blends and their tendency to form solid residues while stored at 4 ºC for 24 h.[76,77] The biodiesel used was biodiesel from SO, PO and yellow grease (YG). This study concludes that the biodiesel from PO has a much greater insoluble mass when compared with YG biodiesel and biodiesel from SO. This precipitate is a consequence of the presence of monoglyceride in the biodiesel from PO and of sterol glucosides for the biodiesel from SO.[65] The CP, PP and CFPP of the biodiesel from PO, YG and SO are a function of the biodiesel concentration and increase with its concentration, depending also on the saturation of the biodiesel. As discussed before it was again confirmed that the CP and PP increase with the saturation of the FAME. It was also observed that the CFPP is almost the same as the CP for the biodiesel from PO B20 and B50, while the CFPP is close to the PP for the biodiesel of YG and SO samples.[65]

On another study using biodiesel from SO, cottonseed oil (CSO) and poultry fat (PF), the biodiesel from SO shows a greater mass of precipitates. The precipitates formation are related with the feedstock and blend concentration, being the solvency effects of biodiesel blends more pronounced at low temperature than at the room temperature. The main cause of the formation of precipitates is the presence of steryl glucosides in the biodiesel from SO, while in the PF biodiesel the precipitates are caused mainly by the presence of monoglycerides and in the biodiesel from CSO are due to the presence of both components. [63][78] Again the CP, PP and CFPP shows a dependence of the biodiesel concentration increasing with the biodiesel concentration. It was also verified that the CFPP is close to CP at low concentrations of biodiesel and with the increase of the concentration the CFPP approaches the PP. [63]

1.4.1.4. Additives

The use of additives is also a common method used to improve the cold flow properties. The most common additives used to improve the cold flow properties of biodiesels are the same used to improve the cold flow properties of petroleum distillates. These additives are divided into two categories PP depressants and wax crystallization modifiers.

The **PP depressants** were used to improve the flowability of oils. These additives inhibit crystalline growth and eliminate agglomeration. PP depressants are normally composed by low

molecular weight copolymers similar to n-alkane paraffin molecules. These additives have a negligible effect on CP and only affect CFPP at high concentrations.[27,79]

Numerous studies were made with additives with and without blends with diesel. In the study of Chiu *et al.* two of the four additives significantly decreased the PP of the blends of biodiesel from SO, but any of the additives had effects on CP, this was also observed in other studies like the study made by Dunn *et al.* where they concluded that the copolymer used as PP depressant for conventional diesel was also effective in biodiesel or blends concluding that the mechanism associated with the crystalline growth habit is similar for biodiesel.[57,80] A mixture of 0.2 % of additive, 79.8 % biodiesel, and 20 % kerosene reduced the PP by 27 ºC. [80]

The PP depressants are studied with biodiesel from Mahua oil with the objective of injecting this biodiesel in CI engines in cold climates. A significant reduction in PP was verified using ethanol, kerosene and a commercial additive. They conclude that the use of ethanol reduces the emissions and its blend with this biodiesel is a totally renewable, viable alternative fuel for improved cold flow behaviour and better emission characteristics without affect the engine performance. [81]

The **wax crystallization** modifiers attack one or more phases of the crystallization process, like nucleation, growth or agglomeration. Their combined effect is promoted the formation of a greater number of smaller, more compact wax crystals. They were categorized as CFPP improvers, CP depressants and wax antisettling flow improvers.[27]

Knothe *et al.* synthetized fatty diesters with bulky moieties and investigated the potential of this as additives for improving the cold flow properties of biodiesel. The compounds studied shown that the bulky moieties in the short chain alkyl group reduced PP. In contrast to the treatment with copolymer PP depressants these esters reduced CP values. So, this result shown that the bulky moieties also interfere with formation of clusters of molecules that precede nucleation. The additives studied were evaluated at loadings of 2000 ppm having only minor effects on CP or PP.[79]

1.4.2. Limits and Methods

The European normative for the biodiesel in the EN 14214:2013 established that each country should detail requirements for a summer and a winter grade.

For the biodiesel B100 in Portugal the limits and grads are only imposed for a maximum value of CFPP and are specified in Table 1.10 for temperate and arctic climates. All the

measures should be made according to the method EN 116 and the units are in ºC. Another test methodology could be found in ASTM D6371.

Table 1.10 – Requirements grades of CFPP temperature for B100 fuel in function of Climate. /ºC

Temperate Climates	**Grade A**	**Grade B**	**Grade C**	**Grade D**	**Grade E**	**Grade F**
	+5	0	-5	-10	-15	-20
Arctic Climates	Class 0	Class 1	Class 2	Class 3	Class 4	
	-20	-26	-32	-38	-44	

In Portugal the B100 for diesel engines should respect the classes in Table 1.11.

Table 1.11 - Adopted classes in Portugal for B100.

Season	**Class**
1 of April to 14 of October	B
1 of March to 31 of March and 15 of October to 30 of November	C
1 of December to 28/29 of February	D

The principle for the measurement of the CFPP is the test of a sample portion of the biodiesel cooled under the specified conditions and drawn into a pipette under a controlled vacuum through a standardized wire mesh filter. The procedure is repeated as the fuel continues to cool, for each 1 ºC below the first test temperature. The test is continued until the amount of wax crystals which was separated out of solution is enough to stop or slow down the flow so that the time taken to fill the pipette exceeds 60 s or the fuel fails to return completely to the test jar before the fuel has cooled by a further 1 ºC.

For the preparation of the sample should be filter approximately 50 mL of the sample at a laboratory ambient temperature, but in any case, not below 15 ºC, though a dry filter paper.

The test could be made in an automated equipment or by a manual equipment. The procedure to mount the experiment is described in EN 116. The results should report the temperature read or indicated at the beginning of the last filtration to the nearest 1 ºC as the CFPP. The final scheme for the test apparatus should be similar to the represented in Figure 1.12.

For the biodiesel used in blends, the biodiesel should fulfil the requirements before the application of any additives. For the blends of biodiesel with mineral diesel a specific combination of CP and CFPP maximum temperature should be chosen from Table 1.12 and a maximum monoglyceride content from Table 1.13. The CP should be measured by the test

method EN 23015 and the CFPP by the test method EN 116. The monoglyceride content should be measured by EN 14105 and the values are present in %(m/m).

Table 1.12 - Standards for the cold flow properties for biodiesel and mineral diesel blends.

Property	Grade a	Grade b	Grade c	Grade d	Grade e	Grade f
CP / ºC	16	13	9	5	0	-3
CFPP / ºC	13	10	5	0	-5	-10

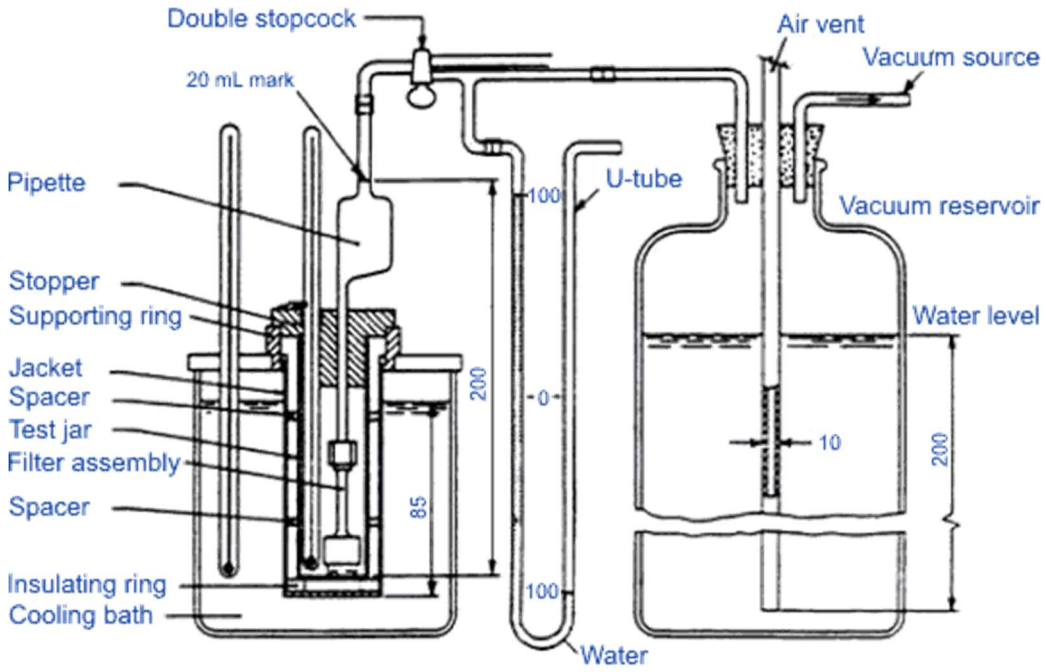

Figure 1.12 - General arrangement of apparatus to measure the CFPP.

Table 1.13 - Monoglyceride content standards for biodiesel and mineral blends.

Property	Grade 1	Grade 2	Grade 3	Grade 4	Grade 5	Grade 6
Monoglyceride content / %(m/m)	0.15	0.30	0.40	0.50	0.60	0.70

For blends up to 7 %(v/v) the classes adopted in Portugal are given in Table 1.14. The classes are represented by a letter that defines a maximum for CP and CFPP and a number that defines the maximum limit for the monoglyceride content.

Table 1.14 - Adopted classes in Portugal for blends up to B7.

Season	Class
1 of April to 14 of October	a1;b1;b2;c1;c2;c3;d1;d2;d3;d4;d5;e1;e2;e3;e4;e5;e6; f1;f2;f3;f4;f5;f6
1 of March to 31 of March and 15 of October to 30 of November	a1;b1;b2;c1;c2;d1;d2;d3;d4;e1;e2;e3;e4;e5;e6; f1;f2;f3;f4;f5;f6
1 of December to 28/29 of February	a1;b1;c1;c2;d1;d2;d3;e1;e2;e3;e4;e5; f1;f2;f3;f4;f5;f6

To measure the CP the method should follow the procedure in EN 23015 (ISO 3015), or ASTM D2500 depending on the country that will be applied, the EN 23015 specifies the method as a measurement of the temperature that in layers of 40 mm, in thickness, the product is transparent. In this test the sample is cooled at a specified rate and examined periodically. The temperature at which a cloud is first observed at the bottom of the test jar is recorded as the CP.

To measure the CP the sample should be initially at a temperature at least 14 ºC above the approximate CP but not above 49 ºC. The sample should be initially filtered or should be used another method to remove any moisture present. After this, the sample should be analysed in the apparatus for CP test (Figure 1.13). The sample should be taken quickly but careful at each temperature to analyse the presence of crystal and put again in the apparatus. The bath to cool down the sample should be maintained in a constant temperature in function of the sample temperature range (Table 1.15). [56]

Table 1.15 - Bath temperature in functon of the sample temperature for measure CP. [56]

Bath temperature range / ºC	**Sample temperature range** / ºC
-1 to +2	Start to +10
-18 to -15	+9 to -7
-25 to -32	-8 to -24
-52 to -49	-25 to -41
-69 to -66	-42 to -58

The CP temperature value is reported as the nearest 1 ºC, at which any cloud is observed at the bottom of the test jar.

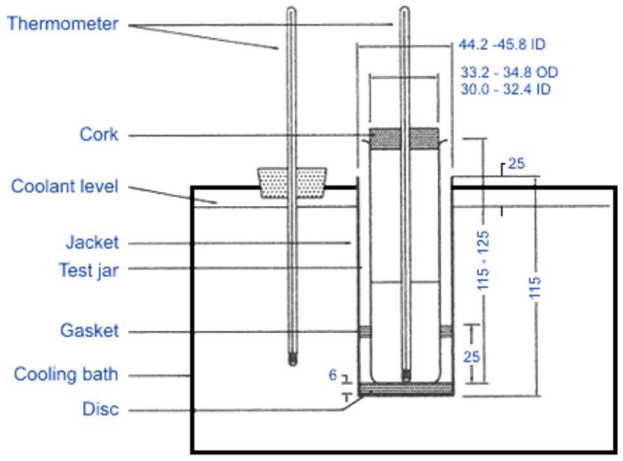

Figure 1.13 - Apparatus for CP test. [56]

The pour point is not a necessary measure for fuels in the European Union but is used in another countries. The ASTM D97 is an American standard for measure the pour point. A summary of this test method described a preliminary heating of the sample, that is after this cooled at a specified rate and examined at intervals of 3 ºC for flow characteristics. The lowest temperature at which movement of the specimen is observed is recorded as the pour point. The apparatus for this experiment is similar to the cloud point show in Figure 1.13.[82]

1.5. Stability of Biodiesel

According to Westbrook, [18] the "stability of the biodiesel is its ability to resist the physical and chemical changes caused by interacting with the environment". In the oxidation tests the period of time which passes between the moment when the oxidation starts and the moment when the formation of oxidation products rapidly begins to increase is called induction period (IP), this point is an important value to measure and define the stability of a fuel showing the physical and chemical capacity that the fuel has to resist to the environment imposed by the test conditions.

The stability of the biodiesel is one of the most important properties of FAMEs, because at this moment is another of the main problems of the use of biodiesel as a substitute of the mineral diesel. The stability of biodiesel is lower than common mineral diesel fuel increasing the risk of problems that can result in a fuel without quality, by the increase of viscosity, formation of gums sediments and other deposits originated by the oxidation process.

The oxidative stability (OS) is a very complex process which involves a number of mechanisms that produces different chemical components such as aldehydes, acids, ketones, and oligomeric compounds. The OS is dependent of the composition of the fuel, the storage conditions or other factors that can change, increasing or decreasing the rate of the oxidation process. [7,12,27,83,84] Another important factor that can affect the process of oxidation is the fact that the modern diesel fuel systems operate at higher pressures and temperatures, which will intensify the oxidation and decomposition of the chemically unstable components of diesel fuels, being this, more critical in fuels with biodiesel. [85]

The OS is normally tested by two methods, the Rancimat method and PetroOxy test, these will be explained in more detail in the subchapter 1.5.5.

1.5.1. Consequences

As for the cold properties of biodiesel, the fuel composition also shows a big impact in the OS. During oxidation the biodiesel breaks into unwanted smaller chain compounds such as aldehydes, small chain esters, high molecular weight materials and other, explained further in this work, becoming chemically unstable [7,27] The compounds formed during the oxidation process deteriorates the fuel quality, some of these compounds can form products like insoluble gums and acids that can cause problems (Table 1.16) such as corrosion of metal, injector coking, fuel filter clogging and formation of deposits in various components of the fuel system including the combustion chamber. [7,27]

Table 1.16 - Problems caused by oxidation products of biodiesel. [7,54]

Oxidation Impact	Impact on fuel injection	Influence on engine
Insoluble Polymers	Deposit formation Injector coking Seizure of moving parts Filter clogging	No start Increased smoke Filter clogging Poor performance
Soluble Polymers	Resins Formation Formation of insoluble	Poor performance No start
Total acid	Corrosion of metal parts Foam from soap formation	Poor performance Increased smoke No start Corrosion of metal

In blends of oxidize biodiesel with mineral diesel can appear other problems, such as reported by Bondioli *et al*., some polymers formed during storage under controlled conditions are soluble in oxidised biodiesel, due to its high polarity but become insoluble only when mixed with mineral diesel fuel.[86]

In Figure 1.14 is shown an example of the deposits formed due to the oxidation process.

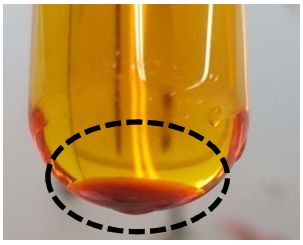

Figure 1.14 - Oxidation product formed during an OS test.

The stability of biodiesel can be classified into three types, thermal stability, storage stability and OS that will be explored in more detail in the next subchapters.

1.5.2. Thermal stability

The thermal stability is the stability of the molecule at high temperatures.[87] This high temperature (cooking temperature) can create some oxidation problems. The methylene interrupted polyunsaturated olefin structure begins to isomerize to a more stable conjugated structure, after this a conjugated diene group from one fatty acid chain can react with a single olefin group from another fatty acid chain to form a cyclohexene ring.[7,58] This reaction has a big importance at temperatures between 250 to 300 ºC. It is a Diels-Alder reaction involving a conjugated di-olefin and a mono-olefin group and originate products called dimers.[7,83,88]

1.5.3. Storage stability

The storage stability is the ability of the liquid fuel to resist to changes in its physical and chemical characteristics by its interaction with its environment. This problem increases with storage conditions like the presence of air, light, high temperature or the presence of metals in the container, as well as the nature of storage container.[7,27,88] During the storage, the visible effects of oxidation can be either deposit formation or the change in colour of the biodiesel.[18]

Some properties are typically analysed when the storage stability is studied as viscosity, acid value, peroxide value and insoluble impurities. These properties were studied for biodiesel from Brassica Carinata oil stored by 12 months and it show be very stable with no increment in viscosity, acid value and peroxide value, if the biodiesel is not allowed to come in contact of moisture and oxygen.[89] Other authors studied long term storage stabilities of different biodiesels and suggested that the viscosity, density, peroxide value, and acid value of biodiesel increases, and the heat of combustion decrease along the time.[27,90,91] Other studies presents the relationship between acid number, kinematic viscosity, peroxide value and insoluble impurities.[18,91–94]

Bondioli *et al*, studied the stability of biodiesel under commercial storage conditions with distilled or undistilled biodiesel and with or without additives, over one year, showing that the IP change dramatically along the storage and depend of the storage conditions. The IP decreases for each sample over time except for samples with a low initial value. In these samples the additization increases the IP but after this, the value also tends to decrease over time. In this

work was also observed that the rate decreases in function of the quality of the product and the contact with air and agitation have a strong impact in the biodiesel stability. [92]

The pure biodiesel regardless of the initial induction time, starts to oxidize immediately during storage and when is blended with mineral diesel the biodiesel stability shows be the main factor that affects the stability of B5 and B20 blends, independent of diesel fuel aromatic content, sulphur level, or stability. The degradation rate in blends with mineral diesel is higher when compared with blends of biodiesels.[18,95,96]

Tennison and Anand studied the effects of biodiesel composition in 10 months of storage of two different biodiesels, coconut (high percentage of saturated methyl esters) and Karanja (higher amounts of unsaturated methyl esters). They made 6 samples 2 neat biodiesel fuels and 4 blends of karanja or coconut with mineral diesel in direct contact with air and sunlight, only direct contact with air, only direct contact with sunlight, and non-contact with air or sunlight. These samples shown a higher degradation for the karanja biodiesel as expected, the blend of the biodiesels reduce the rate of degradation on the long term storage and the blend with the mineral diesel results in a higher rate of degradation when compared to the bio-mix. [96]

The metal presence is also a strong influence in the storage stability. Independently of the metal there isn't variations in the decrease rate of the OS during the storage. The difference in the IP is just due to the initial IP and is just in this parameter that the type of metal has influence in the OS even in presence of antioxidants (AO).[97] The influence of metal and water will be explained in more detail in 1.5.4.2.

1.5.4. Oxidative stability

The oxidation of biodiesel is related with the composition, particularly with the unsaturation in fatty acid chain and affects biodiesel during the extended storage.[87] Biodiesel is poorly resistant to oxidation when exposed to air, light and moisture. The chemistry of oxidation is difficult to define because fatty acids usually occur in complex mixtures, with minor components in this mixture catalysing or inhibiting oxidation. [98]

The auto-oxidation is promoted by different factors as:

- Polyunsaturation;
- The position of the C-C double bond;
- Number of bis-allylic sites.[18]

For example, in methyl linoleate and methyl linolenate the double bonds are prone to oxidation. Counting from the carboxylic acid end, the carbon chain of methyl linoleate has

carbon–carbon double bonds at the 9th and 12th position respectively. Due to his arrangement, one bis-allylic site is created at the 11th Carbon. A hydrogen radical can be easily extracted from these bis-allylic sites during the initial stage of oxidation which is called 'Initiation'. Therefore the bis- allylic positions are more likely to undergo autoxidation than the corresponding allylic sites. [18]

During the oxidation process the peroxides and hydroperoxides are formed which further form shorter-chain compounds such as ketones, aldehydes, alcohols and low molecular weight acids.[99,100]. There could also be formed higher molecular weight products due to the tendency to polymerize of the double bonds. This leads to the formation of insoluble compounds and to the increasing of viscosity of biodiesel which can cause serious problems in the use of this type of fuel as described in subchapter 1.5.1. [86]

The oxidation process is separated in primary oxidation and secondary oxidation

The **primary oxidation** occurs in 4 reactional steps categorized as initiation, propagation and termination.

$$\text{Initiation: } RH + I^{\bullet} \longrightarrow R^{\bullet} + IH \quad [1.11]$$

$$\text{Propagation: } R^{\bullet} + O_2 \longrightarrow ROO^{\bullet} \quad [1.12]$$

$$ROO^{\bullet} + RH \longrightarrow ROOH + R^{\bullet} \quad [1.13]$$

$$\text{Termination: } R^{\bullet} + R^{\bullet} \longrightarrow R - R \quad [1.14]$$

$$ROO^{\bullet} + ROO^{\bullet} \longrightarrow \text{Stable products} \quad [1.15]$$

In the first step, initiation, occurs the removal of a hydrogen from a carbon atom producing a carbon free radical. The initiator is a free radical normally produced by thermal dissociation of hydroperoxides or catalysed by metal decomposing of the hydroperoxides already present or produced by photooxidation. This last is much faster than the first.[98] The time that this process take place is similar to the IP, in this period the concentration of free radicals increases until the autocatalytic propagation steps become dominant and the hydroperoxide have only a small increase.[7,18,58,87,101]

The second step, propagation, is divided into two other steps. In the first step of propagation the presence of molecular oxygen makes an extremely fast reaction, not allowing substantial alternatives for the carbon-based free radical. The reaction of oxygen with the carbon free radical produces a peroxy radical. The second reaction of propagation is the removal of hydrogen from a carbon by the peroxy radical. This reaction is slow, producing a hydroperoxide and a new carbon radical that continues the chain reaction. The hydroperoxide is relatively stable at room temperature and in the absence of metal contaminants, however in

high temperatures or high concentrations, leads to their decomposition to alkoxy radicals. This step is the rate-determining step and is selective for the most readily abstracted hydrogen, normally when the biodiesel is composed by methyl linoleate, the hydrogen is abstracted from the bisallylic methylene group of the fatty acid ester. [7,18,58,87,101]

The third and last step is the termination, this step is based on reactions that remove radicals that would otherwise produce more carbon radicals, like the reaction of two hydroperoxide radicals or the reaction of a free radical with an AO.[7,58,87,101]

When the methyl linoleate is present, the abstracted hydrogen, forms a radical that undergoes resonance to form another free radical containing a conjugated diene. The radicals react with oxygen and the resulting peroxides with the conjugated diene group form the major portion of the product. At high temperature, conjugated dienes formed can react with a single olefinic group of another fatty acid ester by Diels-Alder reaction. Forming a cyclohexene ring. This could react with another diene to form oligomers. So, the biodiesel with high content of mono and polyunsaturation is more prone to form polymers at high temperatures. [101]

The hydroperoxide levels can either peak and then decrease or increase and plateau at a steady state as oxidation progresses. The explanations for these two different activities remains unclear.[7,49,58,87]

The **secondary oxidation** is related to the hydroperoxides double bonds change or undergo *cis*/*trans* isomerization. They are unstable and can easily form secondary oxidation products.[98] The secondary oxidation products include chain carboxylic acids, alcohols, high molecular weight oligomers, and aldehydes. This happens by the continuation of hydroperoxide decomposition and interaction. This oxidation originates products like hexanals, heptanals, propanal, pentane and 2,4-heptadienal. The formation of shorter chain fatty acids by oxidation of fatty oils and biodiesel produces an increase of acidity. This oxidation reaction continues until the reactive sites or available oxygen is completely depleted. [7,87]

Some studies analyse the products of the oxidation, showing that its products also depends of the composition of the biodiesel. Oxidation of biodiesel from RO forms C19 epoxy as the main oxidation product, short-chain oxidation products (alkane, alkene, aldehydes, ketones, alcohols and acids). The higher molecular weight products are formed at an advanced level of oxidation. [102,103] Other study measure the emission of SO biodiesel oxidation by Rancimat method found nine carboxylic acids (formic, acetic, propionic, butyric, succinic, oxalic, lactic, pyruvic and citric), six inorganic ions (sodium, potassium, ammonium, chloride, nitrate and phosphate) and small quantities of acids (lactate and formate).[104]

The process of oxidation is complex and have many factors that affect the OS of biodiesel. These factors could be divided in two groups: The **internal factors** like the fatty acid composition and the molecule unsaturation in the fatty acid chain or **external factors** like temperature. the presence of metals, air, light, enzymes, impurities or moisture that can catalyse the oxidation of biodiesel.[87]

1.5.4.1. Internal Factors

The internal factors are characterized by the composition of biodiesel. The presence of double bonds in the alkyl chains is the main reason for autoxidation, they have a high level of reactivity with oxygen, especially in contact with air/water. The rate of autoxidation also depends on the number and position of the double bonds. The most susceptible position for oxidation is the CH_2 position allylic to the double bonds. [7,46,105,106] For example in the case of oleates, linoleates and linolenates the relative rates of oxidation are 1, 41 and 98 respectively.[106] Carvalho *et al*, study the reaction of oxidation and conclude that in Rancimat test, the polyunsaturated FAME (methyl linoleate and methyl linolenate) accounted for 92 % of the biodiesel that reacted during the test.[104] A small concentration of the more highly unsaturated fatty compounds has a disproportionately strong effect on oxidative stability even greater than the caused by external factors. [27,46,99,106–108] The conformational *cis* and *trans* isomerization have also influence in the OS. While the *trans* is more stable than a *cis* unsaturation, conjugated *trans* unsaturations are more sensitive to oxidation.[108,109]

For blends with mineral diesel the composition of the biodiesel is not the most important factor affecting the OS. The results obtained by Karavalakis *et al*. show that although it is believed that the type of feedstock and the chemical composition may affect the OS, these factors were not significant on the stability of the final blends. The OS of blends seems to be mostly affected by the stage of oxidation of the methyl ester (fresh or aged), the quality of the base diesel fuel and the presence of additives.[70,109]

When it was compared the IP of biodiesel with blends with diesel with low sulphur and ultra-low sulphur it was shown that the absence of sulphur and aromatic compounds in the fuels reduce the IP. The sulphur compounds may act as natural oxidation inhibitors in the fuel oil and their presence usually slows down the aging of the fuel and prevents the formation of acids and sludge.[109] The absence of cracked stocks in the base diesels can improve the OS of the blends.[109]

Park *et al.* studied a predictive equation for the OS (in hours) of biodiesel that depends only on the concentrations of linoleic and linolenic acids.[67] The correlation obtained is given in equation [1.16], where X is the content in %(m/m) of the linoleic and linolenic acids $X_{MeC18:2\ \&\ MeC18:3}$

$$OS = \frac{117.9295}{X_{MeC18:2\ \&\ MeC18:3}} + 2.5905 \qquad (0 < X_{MeC18:2\ \&\ MeC18:3} < 100) \qquad [1.16]$$

Other correlations where made with blends of biodiesel from PO, JO and PoO. The correlation of the OS (in hours) with the palmitic acid methyl ester (X_{MeC16}) in %(m/m) is given in equation [1.17].[110]

$$OS = 0.214 \cdot X_{MeC16} + 0.671 \qquad (0 < X_{MeC16} < 45) \qquad [1.17]$$

There was also studied a correlation between the OS (in hours) and the total unsaturated FAME (X_{UFAMEs}), in %(m/m), given by the equation [1.18].[110]

$$OS(h) = -0.234 \cdot X_{UFAMEs} + 22.318 \qquad (0 < X_{UFAMEs} < 84) \qquad [1.18]$$

1.5.4.2. External factors

The OS is not only affect for the composition but it is also influenced by temperature (heat), catalyst, air, light and the presence of metals that can catalyse the oxidation of biodiesel.[7,98,106,111,112]

The presence of metals influences the OS but the influence of the compounds structures has a greater influence.[99] Bondioli *et al* studied in different conditions the storage stability of biodiesel from RO concluding that the storage container (iron or glass) influence strongly the biodiesel oxidation. [113]

Knothe *et al.* studied the influence of metals in the OS of biodiesel in presence of iron, nickel and copper. [99] Was observed that this last metal, copper, has the strongest catalytic effect, and the effect of the presence of Cu change with the type of biodiesel and change with blends of biodiesel showing a stronger effect on blends. The effect of metals is catalytic, as small amounts of metal have nearly the same influence in the OS as larger amounts, however it depends on the particle size.[97–99,111] Knothe and Steidley recently show also that the Cu is

the metal that most strongly promote the oxidation and Mo and Re, shown an inhibitory effect on biodiesel oxidation. [112]

This effect is also studied by Jain and Sharma in the biodiesel from JO, and the results are shown in Figure 1.15.[114]

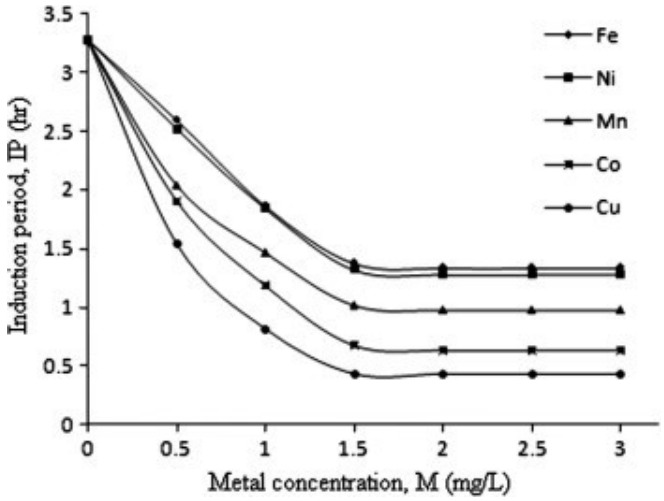

Figure 1.15 - Influence of metal contamination in the IP of biodiesel from JO.

Sarin *et al*. published a work about the effect of metal contaminants and AOs on the OS of the biodiesel from PoO, JO and PO.[115–117] The metals as iron, manganese, cobalt and copper were blended with these methyl esters. The results confirmed one more time that copper has a greater influence, inducing the strongest catalytic effect in all the cases. For all the metals and methyl esters it is possible to observe that the IP value became almost constant as the metal concentration increase, confirming the catalytic influence of the metals.

Another contaminant that could be present in the storage container of the commercial biodiesel or blends is the water. Yang *et al*, study the storage at 15 ˚C and 40 ˚C of two commercial available biodiesel and their blends with diesel and conclude that the presence of water did not contribute significantly to the degradation of all tested samples over time, being the higher temperature the most critical factor for the degradation of unsaturated FAMEs. [118]

The oxidation of biodiesel cannot be entirely prevented. It is only possible improve the OS or decelerate the oxidation rate, this can be made mainly by preventing the contact with air, with pro-oxidants, avoiding elevated temperatures or the presence of light, for this should be used three different ways: use of antioxidants, metal deactivators or blending.[119]

1.5.4.3. Antioxidants

The Antioxidants (AO) are compounds that are used to delay, controls or inhibits autoxidation process of substrates and decrease the yields of unwanted secondary products, normally is when the AO is exhausted that the oxidation initiates. As said before the fuels more unsaturated are more suitable for oxidation but even highly saturated biodiesel loses its stability rapidly if it contains a low level of natural AO. The biodiesel produced from land animal fats contain more saturated esters, but they present poor stability because they contain a lesser amount of natural AO. The vegetable oils contain some natural AOs, such as tocopherols, sterols and tocotrienols so the unrefined vegetable oils usually have higher OS than the refined oils. For example, the Amazonian buriti oil (highly unsaturated) has more OS irrespective of its high oleic acid content because of the presence of large amounts of tocopherols and carotenoids. These natural AOs are destroyed after transesterification, during distillation and purification process. Because of that it is necessary to add natural or synthetic AOs to biodiesel to optimize their oxidation behaviour. The addition of appropriate AOs improves OS and also reduces the NO_x formation during the combustion. [40,119–122]

The AOs should have some basic characteristic to be applied in biodiesel fuels as no toxic, low volatility, effective in low concentrations, available, long shelf life, high solubility in biodiesel, long shelf life, inexpensive, high thermal and light stability. [119] The addition of these AOs should be made immediately after the production of biodiesel. If the addition of AO was made during the oxidative process, when the biodiesel has started to get rancid, the addition of AOs will not be useful. [119]

The AO can be defined in different ways, phenolic-type or aminic-type, classified in natural or synthetic AOs and chain breaking (primary antioxidants) and hydroperoxide decomposers (secondary antioxidants).[119] The **primary antioxidants** are free radical quenchers, they remove the free radicals formed during the initiation and propagation steps by donating hydrogen atoms delaying or interrupting the reaction. The phenolic compounds, secondary aromatic amines, and thiophenols are the common primary AO. The amines and phenols have a hydrogen atom that can be donated to the peroxy radical to interrupt the chain reaction, they are called chain-breakers. [7,98] Some natural AO as tocopherols and flavonoids are also in this class. [119] The **secondary antioxidants** are the hydroperoxide decomposers, which break hydroperoxides into non-reactive stable products before they get converted into radicals or replenish hydrogen to chain breaking AO or scavenge singlet oxygen, metal ions and pro-oxidative enzymes. Normally are organic phosphite esters and sulphides. [101,119]

The hybrid or bifunctional AO such as amino phenols, hydroxy hydro quinolines, and hydroxyl benzimidazoles have increase the use because their effectiveness in scavenging free radicals.[119]

The AOs could be produced or found as natural AOs. Nowadays most of the AOs used for biodiesel are from food AOs such as the vegetable oils AOs. The natural AOs are for example the ascorbates, carotenoids, caffeic acid, citric acid, chlorophylls, ferulic acid, gossypol, acid gallic, lignin, polyphenols, rosemary, sesamol, soluble polyphenols, tocopherols (α-, δ-, γ-) and tocotrienols. The other alternative as AOs is the synthetic AOs as butylated hydroxytoluene (BHT), butylated hydroxyanisole (BHA), *tert*-butylhydroquinone (TBHQ), di-*tert*-butylhydroquinone (DTBHQ), ionol BF200 (IB), 2,2'-methylenebis (4-methyl-6-*tert*-butyphenol) (MBEBP), *tert*-butylated phenol (TBP), octylated butylated diphenyl amine (OBPA), Ethoxyquin (EQ), diphenyl-p-phenylenediamine (DPD), octyl gallate (OG), pyrogallol (PY) and propyl gallate (PG). [40,119–122]

Some studies analyse blends of biodiesel and mineral diesel. Karavalakis *et al.* studied the OS of nine biodiesels with or without AOs additives and blends with another mineral diesel. Was analysed the OS of the pure biodiesels with 3 weeks of space between measurements. Four of the samples analysed were well below the minimum IP of 8 h. These samples were comprised mainly of unsaturated methyl esters and free of AOs. In this test the influence of compound structure of the fatty esters and the level of unsaturation show a high importance on the deterioration of these fuels.[109] For the blends it was used a mineral diesel with low sulphur content. The results shown that the biodiesel made by transesterification of used frying oils is the only that failed the minimum of 20 h for the IP for blends of 5, 7 and 10 %v/v. All the other blends shown values above the IP minimum despite some of them failing to achieve the IP minimum in B100. There is a weak correlation between the biodiesels with AO additives and those without.[109]

Other phenomena were also study, the Synergism of AOs is the combined use of two or more AO to produce and effect greater than the sum of any individual AO. The synergism not only improves stability but also reduces the amount of AOs need and the cost of additives. [119] Christensen *et al*, study the re-additization of commercial biodiesel blends (B20) during long-term storage and show that the addition of AO during the storage with the monitoring of IP and acid number can increase significantly the storage life of biodiesel blends. [123]

There is a lot of published papers regarding the effect of natural, synthetic and synergism between AOs in different conditions, presence of metal, blends and pure biodiesel.

Studies related only with natural AOs shows that the natural AOs have a limited AO activity in biodiesel when compared to synthetic AO and most of the studies regarding only natural AOs are centred in tocopherols (vitamin E). [119] Natural AOs such as tocopherols, carotenoids, lycopene, zeaxanthin, canthaxanthin, astaxanthin, gallic acid, caffeic acid, vanillic acid, vanillin, ferulic acid, protocatechuic acid, p-coumaric acid, eugenol, sesamol, cinnamic acid, sinapic acid, resveratrol are produced commercially on a large scale and some herbal extracts of sage, rosemary, clove, allspice, thyme, cinnamon, oregano, marjoram, eucalyptus, artichoke, and turmeric have been identified as effective AOs. However, except for tocopherols, only very few studies have made on biodiesel fuels. [119]

Regarding the tocopherols, there are four forms of tocopherols in nature, α, β, γ, δ. The α- and γ- tocopherols are present in vegetable oils and the α-tocopherol is common in animal fats. [119] Tocopherols are effective only if their concentration is approximately equal to their concentration in vegetable oils and at a higher level, they could act as a prooxidant.

Some results shown that the stabilizing effect of tocopherols follow the δ- > γ- > α-tocopherol in studies of α-, γ- and δ-tocopherols from 250 to 2000 $mg \cdot kg^{-1}$ in sunflower, recycled vegetable oil, rapeseed and tallow methyl esters. The tocopherols stabilise methyl esters reducing the rate of peroxide formation. [124]

Other potent natural AO is β-carotene, but its effectiveness mainly depends on the partial pressure of oxygen in contact. At higher oxygen concentration β-carotene acts as a prooxidant and favour oxidation. [119]

In the studies regarding synthetic AOs phenolic AOs are the most common used in biodiesel because their cost, availability and performance. The major phenolic AO used is BHT, BHA, TBHQ, PG, OG, PY and EQ. [119] In most of the cases the PY and PG is consistent in the most efficient AOs regarding the pure biodiesel from vegetable oil and TBHQ for biodiesel from animal fat. [119,122,125–130]. In some situations, other AOs also have good results depending on the fuel tested.

In 2003 Mittelbach and Schober studied the OS of biodiesel produced from RO, sunflower oil, used frying oil, and beef tallow, both undistilled and distilled. The study used four synthetic AOs PY, PG, TBHQ, and BHA. In Figure 1.16 and Figure 1.17 are plotted the results of this study.[122]

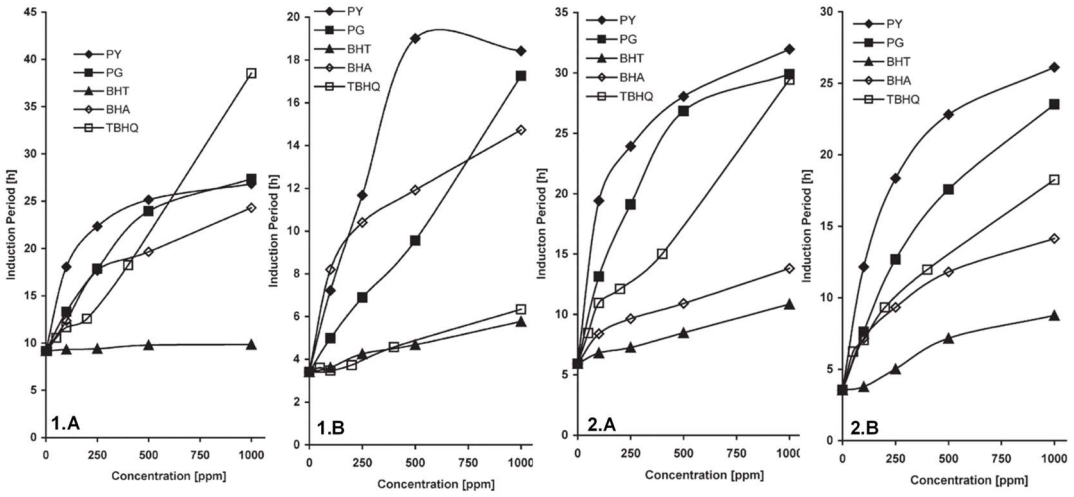

Figure 1.16 - Influence of AOs concentration on the OS using biodiesel from RO (1) and used frying oil methyl esters (2): Undistilled (A) and distilled (B). [122]

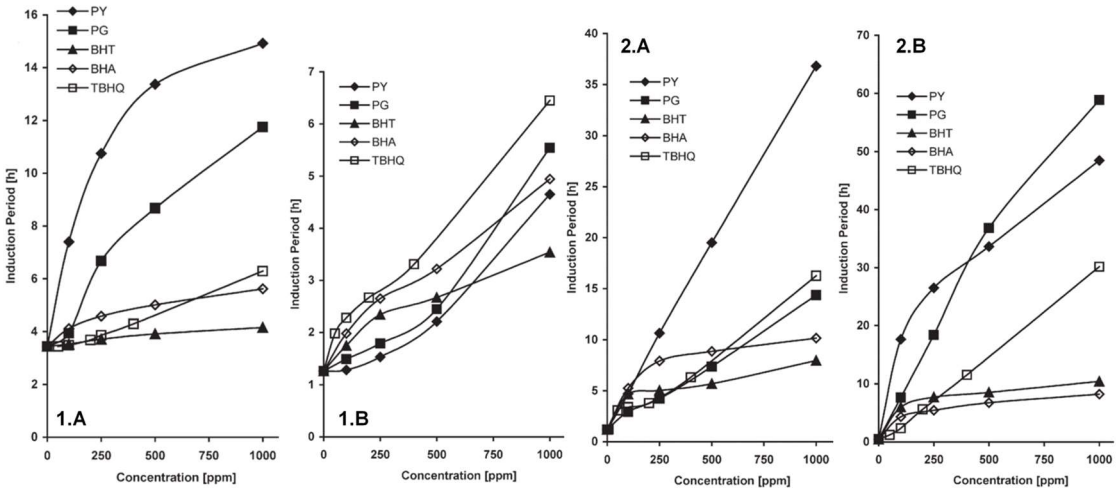

Figure 1.17 - Influence of AOs concentration on the OS using sunflowerseed oil methyl esters (1) and used tallow methyl esters (2): Undistilled (A) and distilled (B).[122]

Sendzikiene *et al.* compared the FAME from vegetable oil and from animal fat concluding that the biodiesel from vegetable oils are more stable. The study of the AOs addition shows that the addition of 400 ppm of BHA or BHT is the correct quantity for stabilization of the fuels. The optimal stability is obtained when for mixtures of 80-90 % of FAME of animal fat and 10-20 % of FAME of vegetable oil with synthetic AOs added.[131] The mixtures with AOs with a higher concentration of FAME from animal fat present a higher IP when compared with FAME from vegetable oil. This is not verified when the FAME from animal fat don't have AOs.[122,131]

Some studies regarding the stability with BHA, BHT, PG, TBHQ, and PY was made with different biodiesels. In biodiesel from Camelina the TBHQ show to be the most efficient and 3000 ppm can maintain satisfactory OS for one year, the other AO follow the other PG>BHT>BHA.[132] In pure biodiesel and blends from RO (50 %), sunflower oil (20 %) and used frying oil (30 %) show that the PG and PY are the most strong AO in pure biodiesel and blends. [128] The PY shows be the most efficient AO also for blends of biodiesel from karanja oil or Jatropha. [129,130] There are studies that also consider another AO as OBPA, DPD, DTBHQ as the study from Rizwanul Fattah *et al*, where is studied the effect of AO in biodiesel from vegetable and animal feedstocks. Despite the addition of this AO the PY was also the most effective AO in almost all the biodiesels studied, due to its higher number of labile hydrogens. The other AO was ranked by the following order OBPA=DPD<BHT<DTBHQ=TBHQ<PG for vegetable oils and for animal oil the rank was BHA=BHT<PG<TBHQ. [126] Study of biodiesel from SO, CSO, PF and YG with additives as DTBHQ, and IB enhance the OS for the different biodiesels0. The biodiesel from SO, YG, CSO and distilled SO could be improved significantly with PY, PG and TBHQ while PY, BHA and BHT show the best results for biodiesel from PF. Regarding this studies the effect of AO on biodiesel differs with the fuel composition. [127]

The effectiveness of this AO could vary with the test methods used, Zhou *et al*, show that the PY and PG was the more efficient in inhibiting biodiesel oxidative degradation compared with BHA and BHT. The TBHQ displays the weak test to the AO activity in the PetroOXY test, inconsistent with the best stabilizing effects in the Rancimat method. [125]

The studies regarding natural and synthetic AO are also extensively studies for pure biodiesels. The presence of these compounds shown a positive impact in the OS. The phenols polysubstituted with the substituents in *ortho* and *para* positions tend to show the largest improvement in stability.[133]

The study in 2012 regarding the gossypol, BHT and γ-tocopherol as AOs in various biodiesels (YG, SO and methyl oleate) with concentrations of 250 and 500 ppm conclude that the γ-tocopherol is more suitable for biodiesel with low concentrations of endogenous tocopherols (YG and MO). [134] The results are shown in Table 1.17.

Other study in 2012 investigated the impact of various synthetic phenolic AOs on the OS and storage stability of biodiesel from PoO. The PY was reported to be the best AO showing the best improvement in the oxidative stability of biodiesel from PoO, the IP was enhanced to 34.35 h at a PY concentration of 3000 ppm at 110 ºC Other AOs were also studied, their results being in Table 1.18.[90]

Table 1.17 - Influence of AOs in different biodiesels.[134]

Biodiesel source	**SO**		**YG**		**MO**	
Time /day	**0**	**90**	**0**	**90**	**0**	**90**
IP 110ºC /h	5.5	4.9	4.2	3.2	10.3	10.2
IP with BHT 250 ppm /h	6.7	5.3	5.8	5.0	12.8	12.2
IP with BHT 500 ppm /h	7.7	6.1	6.9	6.2	14.6	14.5
IP with γ-tocopherol 250 ppm /h	5.9	4.8	7.0	6.0	19.9	17.1
IP with γ-tocopherol 500 ppm /h	5.9	4.9	8.3	6.8	22.7	19.2
IP with Gossypol 250 ppm /h	7.2	6.6	5.4	4.3	11.7	11.4
IP with Gossypol 500 ppm /h	8.5	7.7	5.7	4.8	17.4	12.9

Table 1.18 - Values of IP for biodiesel from PoO with different concentrations of AOs. [90]

AOs	**0 ppm**	**500 ppm**	**1000 ppm**	**2000 ppm**	**3000 ppm**
BHT /h	0.33	0.80	1.76	3.14	4.88
BHA /h	0.33	0.76	1.70	2.96	5.02
TBHQ /h	0.33	0.86	1.54	2.91	6.19
Gallic Acid /h	0.33	0.67	0.76	0.82	0.88
PY /h	0.33	2.86	4.99	25.02	34.35

The efficiency of natural and synthetic AOs was compared for distilled biodiesel from PoO and JO and in both situations the synthetic AOs reveal a higher efficiency. [121,135] For example the α-Tocopherol required 1000 ppm to improve the IP for 6.17 h and the synthetic AOs BHT and TBHQ only needed 50 ppm to obtain 6.42 and 8.85 h, respectively. [121,136] The order of efficiency for biodiesel from JO is TBHQ>BHT>TBP>OBPA>α-Tocopherol. [135] For biodiesel from SO with AO the order effectiveness is Caffeic acid>ferulic acid> *tert*-butylhydroquinone. [137]

Tang *et al*. studied the effectiveness of natural and synthetic AOs like the α-tocopherol, BHA, BHT, TBHQ, di-TBHQ, IB, PG and PY to improve the OS of biodiesel from SO, CSO, PF, and YG in a range of concentrations between 250 to 1000 ppm. The natural AOs play a significant role in the OS. The IP of the biodiesel from SO, CSO, YG and distilled SO could be improved significantly with PY, PG and TBHQ, while PY, BHA, and BHT show the best results for PF biodiesel. Moreover, it was shown that the effect of AOs on B20 and B100 was similar and the OS of untreated SO biodiesel decreased with the increasing indoor and outdoor storage time, while the IP values, by adding TBHQ to SO biodiesel, remained constant for up to 9 months.[138]

Other important studies in the AOs is the synergetic effect in the mixture of some AOs. In some case there is no advantage in the addition of different AO, for example in SO biodiesel the mixture of BHT with TBHQ or BHA didn't show any improvement in the AO compared

with the BHT pure.[139] The use of natural AO such as rosemary, oregano and basil in SO biodiesel show that the best synergetic effect is obtained with the mixture 50.00 %, 12.50 % and 37.50 %, respectively. [140] The TBHQ is the one of the most effective synthetic AO in many types of biodiesel and exhibits good synergism with BHT or BHA and not with PG. Chelating agents such as citric acid and monoglyceride citrate can be use with TBHQ to enhance the effectiveness of vegetable oil. [119]

The BHT is an AO more effective in animal fat than in vegetable oil. It can be used combined with BHA and TBHQ or PG to improve the effectiveness of the BHT activity.[119] The use of BHA, could prevent the microbial contamination in oils. Can be used in combination with BHT, TBHQ or gallates. In general is less effective in animal fats but in combination with citric acid, it performs better and the IP is almost doubled. [119]

Souza *et al*, study the combination of different AO (TBHQ, BHT, citric acid and rosemary extract) in biodiesel from CSO and conclude that the 1500 mg of TBHQ with 1500 mg of rosemary extract are the best options. [141]

1.5.4.4. Metal deactivators

The presence of metals affects the OS and thus to reduce the influence of the metals in the OS is necessary the use of AOs or metal deactivators. The metal deactivator forms a protective layer between metal ions and fuel, preventing metal-fuel contact. [119] For this is pretend to reduce the metal contamination to a minimum and inactivate the trace quantities of metals that would be of considerable importance in OS. Numerous studies were made to evaluate the effect of AOs and metal deactivators as deactivators for different metals.

Morris *et al*. studied the efficacy of some metal deactivators for copper, iron, nickel, and tin in lard and concluded that the ascorbyl palmitate, potassium ascorbyl palmitate, ascorbic, tartaric, citric, phosphoric acids and N,N′-dialicylidene-1,2- diaminopropane were the most effective. This deactivation could be in part explained by the synergetic effect of these compounds with phenolic AOs.[126,142] There were made studies of blended diesel stabilization with combinations of AOs and metal deactivators that show improvements in stabilization of blended diesel fuels.[143,144]

In Table 1.19 are represented the IP values for some studies with the presence of metals or not with some AOs and different types of biodiesel.

Table 1.19 - Influence of metals and AOs in biodiesel from PoO, JO and PO.

	Without metal		With metal 2 ppm of Cu		Ref
	Without AO	**AO necessity to achieve 6 h of IP**	**Without AO**	**AO necessity to achieve 6 h of IP**	
Pongamia	2.54 h	250 ppm BHT	≈0.27 h	1050 ppm of BHT	[115]
Jatropha	9.24 h	0	≈2.9 h	150 ppm of TBHQ	[117]
Palm	3.95 h	200 ppm of BHT	≈0.4 h	1000 ppm of BHT	[116]

The PY in metal contaminated biodiesels is the most effective. For biodiesel contaminated with copper or lead the PY show the best AO performance below 3000 ppm and TBHQ the best above 3000 ppm followed by PG, BHA, BHT and α-tocopherol.[145] In blends PY also revealed be the most effective AO for this situation with Jatropha biodiesel. [146] Jain and Sharma developed correlations between the IP, with metal and the PY the correlations found in this study are presented in Table 1.20.[114]. In these correlations X_{AO} is the concentration of AO in ppm and X_M is the relative metal concentration in $mg \cdot L^{-1}$.

Table 1.20 - Correlation between induction period (hours) with metal and AO concentration. [114]

Metal	Correlation	Nº eq.	Regression coefficient
Fe	$IP = 0.1255(X_{AO})^{0.7334}(X_M)^{-0.472}$	[1.19]	0.93
Ni	$IP = 0.11735(X_{AO})^{0.7279}(X_M)^{-0.4663}$	[1.20]	0.92
Mn	$IP = 0.0932(X_{AO})^{0.7578}(X_M)^{-0.477}$	[1.21]	0.95
Co	$IP = 0.0841(X_{AO})^{0.7648}(X_M)^{-0.5871}$	[1.22]	0.95
Cu	$IP = 0.063(X_{AO})^{0.7986}(X_M)^{-0.7599}$	[1.23]	0.94

Sarin *et al*. studied the synergistic effect of metal deactivator and AOs on the OS of jatropha biodiesel, with metal contamination (2 ppm). In this study it was found that the quantity of AO can be reduced by 30-50 % even if a very small amount of metal deactivator was used meeting the 6 h of IP.[147]

1.5.4.5. Blending

The OS can also be improved by blending different biodiesels or blending of biodiesel with mineral diesel that have a much greater OS. The study of blends of biodiesel from PoO,

jatropha and PO, with the results represented in Figure 1.18, Figure 1.19 and Figure 1.20, show a linear increase of the IP of the blend with the increase of the most stable biodiesel.[110]

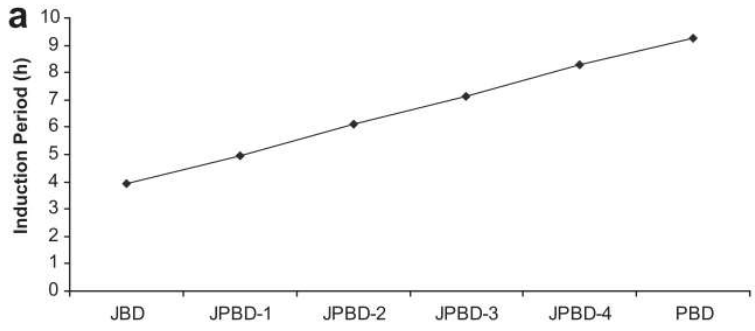

Figure 1.18 - IP of blends of biodiesel from JO and PO. [110]

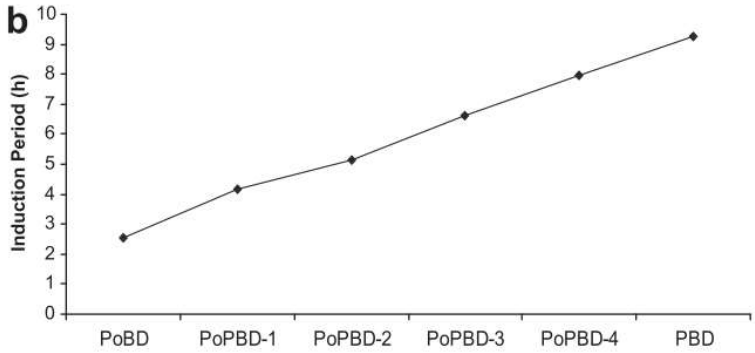

Figure 1.19 - IP of blends of biodiesel form PoO and PO. [110]

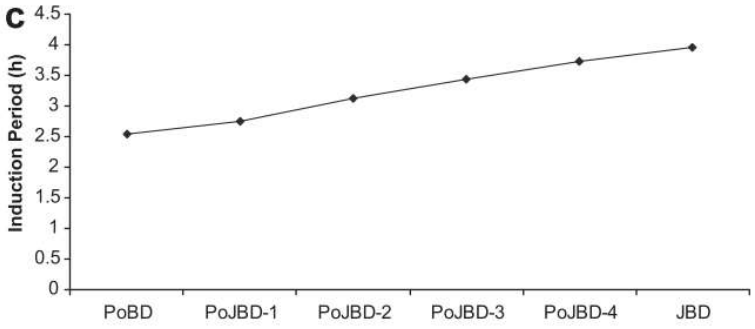

Figure 1.20 - IP of blends of biodiesel from PoO and JO. [110]

In this work it was also studied a ternary mixture of these biodiesels. The results of this mixture allowed the development of a correlation of the dependence of the OS on methyl esters of the fatty acid compositions, this correlation was shown in the equations [1.17] and [1.18].

Cremonez *et al*, study the addition of biodiesel from vegetable sources or swine fat, to the SO biodiesel and concluded that the addition of vegetable esters improve the IP, whereas swine fat esters decline the IP when blended with SO biodiesel.[148]

José T. and Anand K. study the effects of blending in long term storage and verified that mix karanja (highly unsaturated) with coconut (highly saturated) biodiesel reduce the rate of degradation and blending with diesel present a higher rate of degradation when compared with blends of biodiesel. [96]

Karavalakis *et al.* studied the effect of blend in different biodiesels with low-sulphur diesel and reported the effect of different concentrations of biodiesel. The results of these different blends are shown in Figure 1.21. The values for the B-1, B-2, B-3, B-4, B-5, B-6, B-7, B-8 and B-9 of IP are 3.51, 5.72, 6.59, 17.38, 7.99, 9.74, 3.81, 18.57, 8.75, respectively. [109]

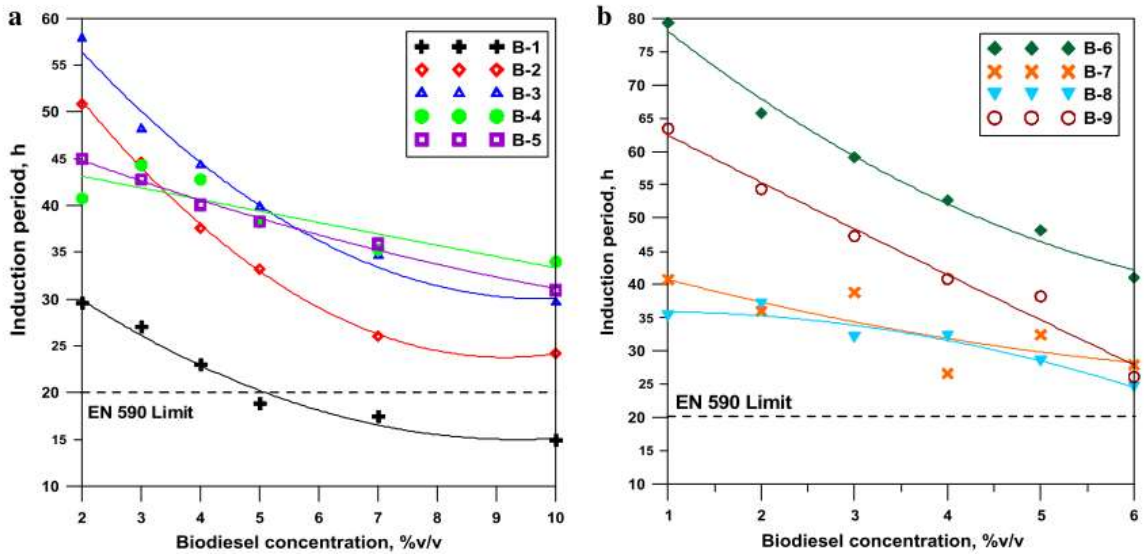

Figure 1.21 - IP of blends of biodiesel with diesel with different concentrations. [109]

1.5.5. Measurement, limits and methods

During the IP the concentration of ROOH remains very low and when it end there is a sudden rise in the hydroperoxides levels. [18] This sudden rise of the hydroperoxides levels could be measured to determine the time of the OS. It is measured usually in a Rancimat test or by OS Index. The Rancimat test is defined in the European normative EN 14112 and for the biodiesel the EN 14214:2013 requires an OS at 110 ºC with a minimum IP of 8.0 h.

In this normative the OS is defined as the "IP determined according to the procedure specified in this European Standard and is expressed in hours. The system for measure the OS should be like the represented in the Figure 1.22 or as said before can be obtained commercially under the trade name Rancimat, model 743, from © Metrohm AG.

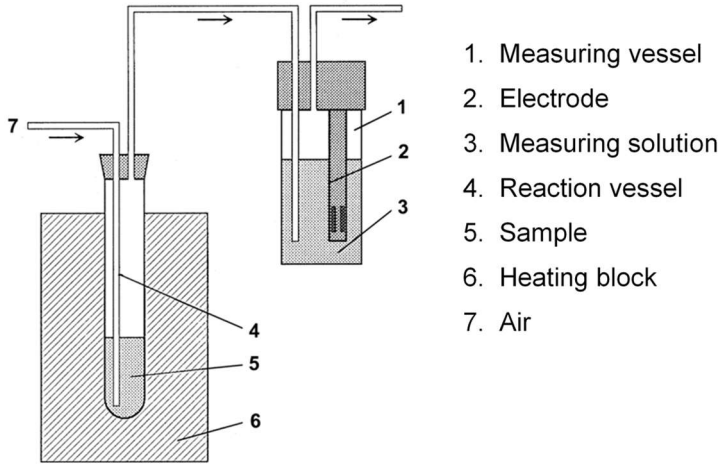

Figure 1.22 - Schematic representation of EN 14112 apparatus.

In this equipment the oxidation is induced by passing through the biodiesel sample of 3 g at a constant temperature of 110 ºC, a flow of air at a rate of 10 $L \cdot h^{-1}$. The oxidation produces vapours that are released together with air and bubbled into 50 ml of demineralized water. The conductivity of this water is measured with an electrode. and recorded in a device which will show the end of the IP by the increase of carboxylic acids produced during the oxidation process and absorbed in water. The result of this test should be similar to that reported in Figure 1.23. Some studies show that the method with the second derivative return slightly higher estimates for the IP. [149]

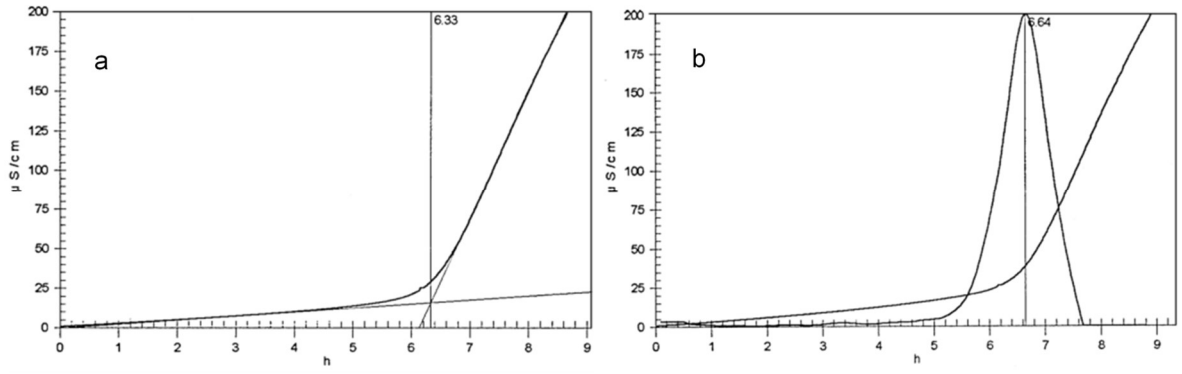

Figure 1.23 - Example of conductivity curve obtained in Rancimat method. a) IP obtained manually; b) IP obtained automatically.[150]

To measure the OS of blends of Biodiesel with diesel was produce a normative EN 15751:2014 where the apparatus is similar with changes only in the volume of demineralized water that is 60 ml and the mass of sample that is 7.5 g. This normative could also be applied for pure biodiesel. For blends of biodiesel and mineral diesel up to 7 %v/v the IP has a minimum value of 20 h.

The oxidative stability could be related also with the iodine value. The OS and the iodine value both depend on saturation. The iodine value measures the amount of iodine in grams *per* 100 g of sample that can be added to the double bonds of a fatty acid. [27]

The other method to measure the OS is known as PetroOXY method. This method is described in ASTM D 525. This method includes all volatile and non-volatile oxidation products unlike the Rancimat method.

In a small and hermetically sealed test chamber is analysed 5 mL of sample is combined with oxygen at a pressure of 700 kPa and heated to a temperature of 140 ºC. This test measures the pressure drop that is directly related to the OS of the fuel. In this test the IP is characterized by the time elapsed between starting the test and the breaking point, which is defined as a pressure drop of 10 % below the maximum pressure.

The ASTM (ASTM D4625) have also a test method for distillate fuel storage stability. In this test the sample is stored at 43 ºC for 24 weeks in a sealed vessel with a defined air space. The accelerated storage at 43 ºC corresponds to about 4 times the storage time at 21 ºC. [151]

2. Aim work strategy

The initial aim of this PhD was the understanding and minimization of the impact of the use of biodiesel, focusing on its oxidative properties and low temperature behaviour.

Concerning these two properties the Figure 2.1 shows a scheme highlighting what affects them and how, ways to improve the characteristics of the blends and the main strategies adopted in this work to better understand their dependence on the composition and storage conditions of biodiesel fuels.

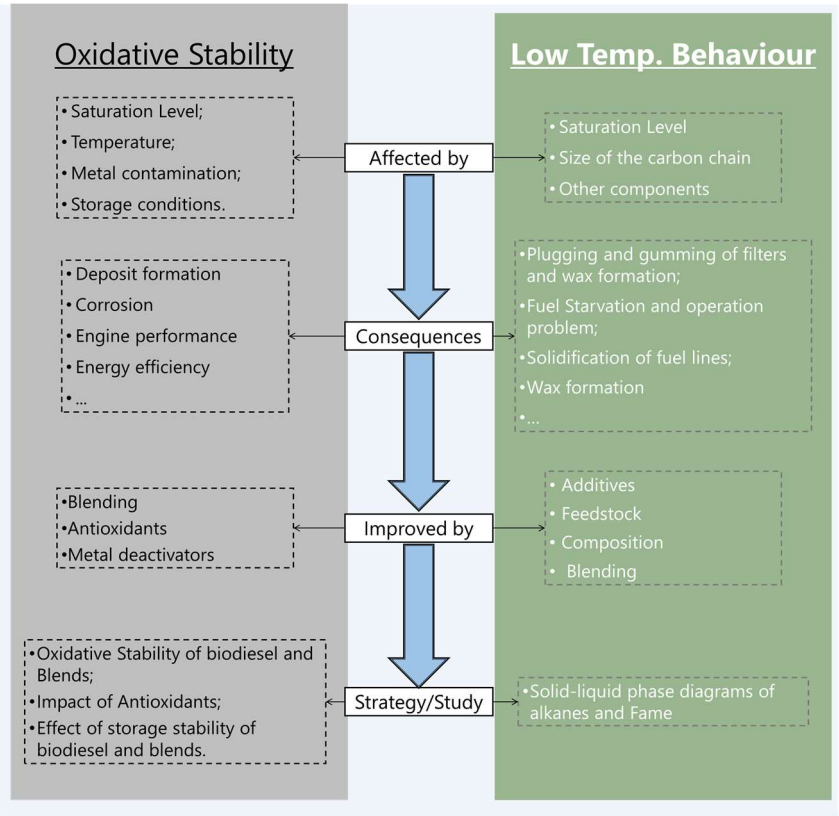

Figure 2.1 - Schematic representation of the work plan for understanding the biodiesel influence in the OS and low temperature properties.

As schematically represented in Figure 2.1 this work was subdivided in two parts:

PART A. (Chapter 3). The study of low temperature behaviour of biodiesel and mineral diesel blends.

PART B (Chapter 5). Study of the oxidative stability of biodiesel and its blends with mineral diesel.

A succinct description of the strategy and of each part is given in the next subchapters.

2.1. Part A. The study of low temperature behaviour of biodiesel and mineral diesel blends

This part of the work concerns the study of the solid-liquid phase diagrams of binary mixtures of alkanes and fatty acid methyl esters by differential scanning calorimetry (DSC), optical microscopy and X-ray powder diffraction (XRD). In the DSC is possible to measure the phase transition temperatures and enthalpies in the mixtures studied, and with this the corresponding phase diagrams can be obtained. An example of a typical result of a thermal behaviour of a binary mixture obtained in the DSC of different compositions is show in Figure 2.2.

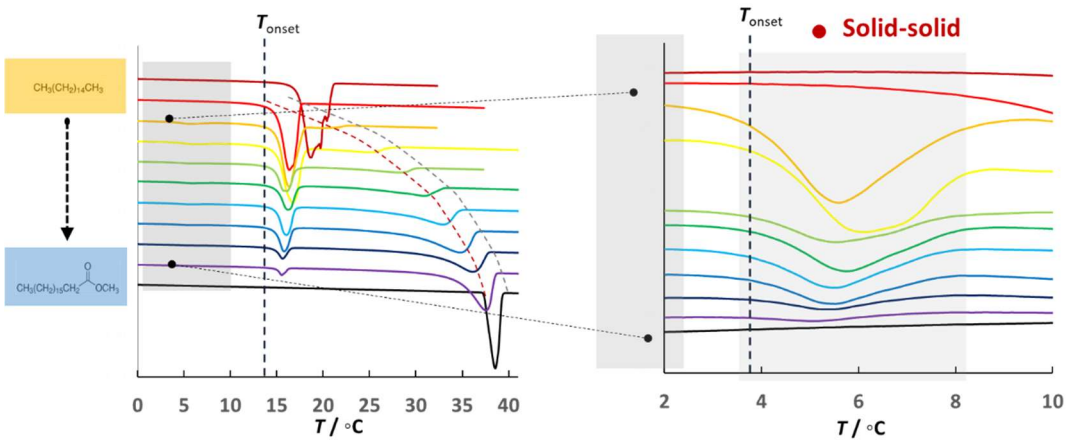

Figure 2.2 - Illustration of the thermal behavior of the different binary mixtures for the system methyl stearate with hexadecane as evaluated by DSC.

With this work was possible to evaluate the crystallization behaviour, effect of the molecular structure and its molecular interactions (Figure 2.3).

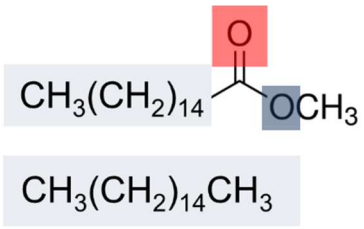

Figure 2.3 - Illustration of the similar molecular size and its possible molecular interactions.

The experimental strategy followed to obtain these results is schematically represented in Figure 2.4 where is shown the steps followed and the objective of the apparatus used.

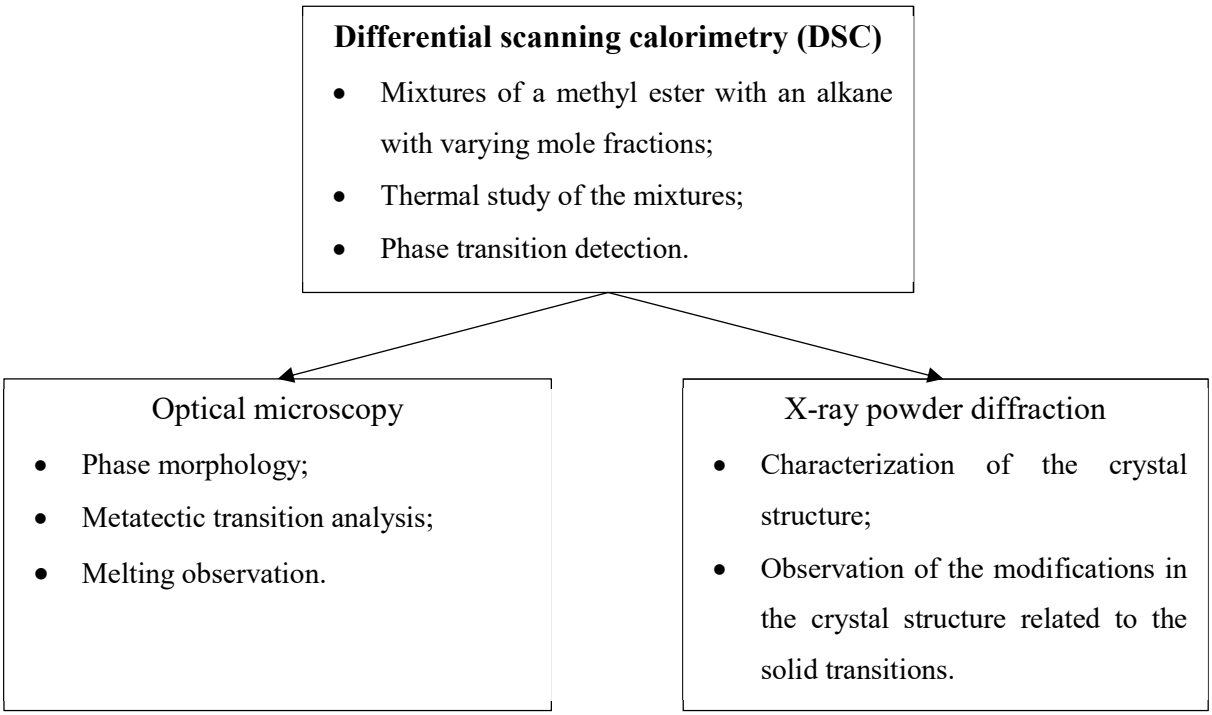

Figure 2.4 - Schematic representation of the strategy for the low temperature studies.

2.2. Part B. Study of the oxidative stability of biodiesel and its blends with mineral diesel.

This part of the work was explored measuring the induction period of the biodiesel or the biodiesel blends according the standard EN 14112, using commercial biodiesels from different sources in Portugal.

The long period of analysis by this method and the big uncertainty associated to the commercial apparatus (Rancimat) demanded the development of a new apparatus where is possible to control the temperature and the air flow with high precision, thus reducing the uncertainty of the results. With the development of this apparatus the number of analyses measured simultaneously increase, making possible obtain more precise results avoiding the aging of the fuel when storage. The development and test of this new apparatus is explained in chapter 4.

To understand the oxidative stability was made an experimental strategy that explored the effects of biodiesel concentration, the concentration of AOs and of storage conditions on the stability of pure biodiesel and biodiesel blends. All the samples of biodiesel were studied by gas chromatography to analyse the composition of the fuel and understand the influence of the

fuel's composition on OS. The strategy followed to understand this property was enumerated in the next points:

- For the concentration study were made blends with concentrations near the actual industrial values and concentrations that can be adopted in the future. In this study were used different types of biodiesel and mineral diesel to explore the influence of the production process and the influence of the unsaturation level.
- For the study of the AOs was used a synthetic and a natural AO in different concentrations in two types of biodiesel. This effect was also studied in blends to explore the existence of a synergistic effect of the mineral diesel and the AO.
- The study of the storage stability was explored by storing blends and pure biodiesel in a dark place (Figure 2.5) with constant temperature to avoid changes in the oxidation kinetics and making periodical analysis of the samples. For this was planned to explore blends of B7 and B14 in the following conditions:
    - Blends under nitrogen atmosphere;
    - Blends under dry air atmosphere;
    - Blends with a metal (nitrogen and dry air atmosphere);
    - Blends with water (nitrogen and air atmosphere);
    - Blends with water and a metal (nitrogen and air atmosphere).

Figure 2.5 - Stored samples of biodiesel blends.

3. Phase diagrams of mixtures of methyl esters and alkanes

The solid-liquid equilibrium of fatty acid methyl and ethyl esters has been extensively studied [152–155], nevertheless the phase behaviour of binary mixtures of fatty acid esters and paraffin's have been poorly investigated. There are only a few studies of ethyl esters or methyl esters with aromatic hydrocarbons [156] and linear alkanes [157–160]. Typically, the phase diagrams of these mixtures exhibit invariant points, such as eutectics and peritectics. The interpretation of their phase diagrams is fundamental for the understanding the low temperature phase behaviour of blends of biodiesel and diesel fuels [153,156–159].

The binary mixtures of FAMEs composed by methyl myristate, methyl palmitate and methyl stearate were studied by Costa *et al*, [155] that shown that these mixtures present very complex phase behaviour with multiple phase regions and peritectic and metatectic reactions.

Maximo *et al*. [153] studied the blends of FAME with FAEE with mixtures as ethyl palmitate, ethyl stearate or ethyl oleate with methyl palmitate. These systems shown also a very complex behaviour with the formation of solid-solutions, peritectic reactions and metatectic transitions. The authors proposed that the mixtures of FAME with FAEE could be used to improve their cold flow properties when compared with mixtures of FAMEs.

The systems of FAMEs with aromatics were studied by Benziane *et al*, [156] that concluded that all the mixtures studied presented a simple eutectic behaviour. In another work Benziane *et al*, [157] studied the FAMEs (methyl palmitate and methyl stearate) in mixtures with heavy alkanes (*n*-eicosane, *n*-tetracosane and *n*-octacosane) again reporting that these mixtures had a simple eutectic behaviour. A similar conclusion was made by Lobbia *et al*, with the study of the crystallization curve of the methyl stearate, methyl nonadecanoate, ethyl stearate and methyl palmitate with hexadecane.[160]

Mixtures between FAEE and alkanes were studied by Robustillo *et al*, [158] reporting systems of ethyl laurate, ethyl palmitate and *n*-decane and by Chabane *et al*, [159] which studied mixtures of ethyl myristate with n-tetradecane and n-hexadecane and ethyl palmitate with n-octadecane. All the systems were reported to present a simple eutectic behaviour except for the system ethyl laurate and *n*-decane were a peritectic point was identified. Some of these systems show the presence of solid-solid transitions.

Since pure biodiesel is seldom used, blends with mineral diesel it would be very important to study the phase behaviour of the mixtures of saturated fatty acid methyl esters more abundant in biodiesel with n-alkanes. The mixtures of dissimilar size are well established to produce simple eutectic systems with a near ideal behaviour. [157–159]

This chapter presents a systematic study of the phase behaviour of binary mixtures composed by combination of the most abundant saturated FAMEs with the n-alkanes with similar size as depicted schematically in Figure 3.1. The phase diagrams of these two FAMEs, methyl palmitate (MeC16) and methyl stearate (MeC18) with hexadecane (C16), octadecane (C18) and eicosane (C20) were studied in detail using differential scanning calorimetry (DSC), temperature controlled polarized optical microscopy and x-ray powder diffraction, XRD. The results and its relevance to the behaviour of blends of diesel with biodiesel will be discussed below.

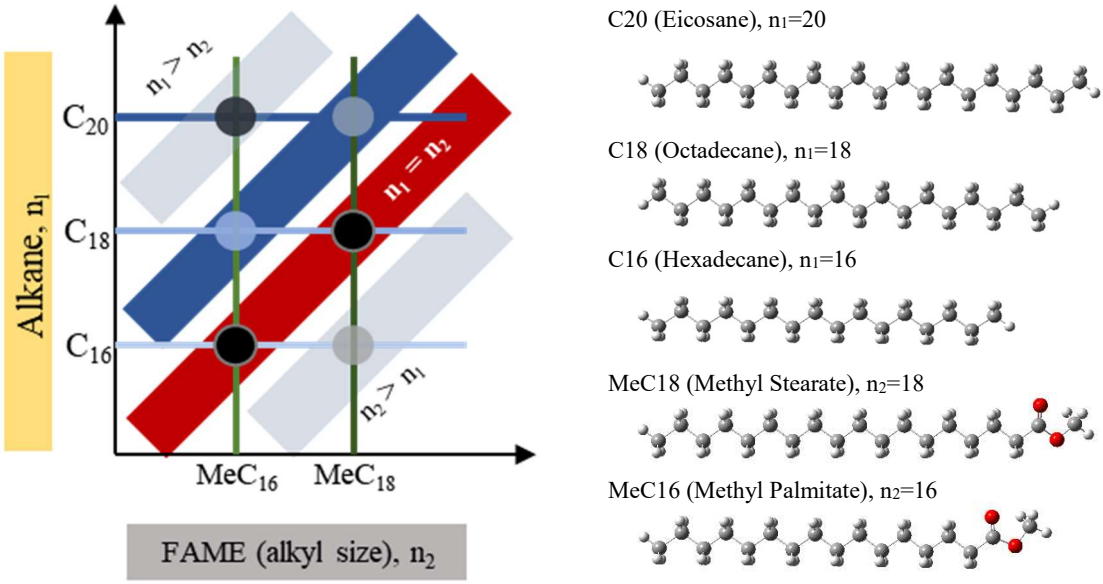

Figure 3.1 - Schematic representation of the binary mixtures between methyl esters and alkanes studied in this work. Alkanes: Eicosane, C20H42, (C20); Octadecane, C18H38, (C18); Hexadecane, C16H34, (C16); FAMEs: Methyl stearate, C19H38O2, (MeC18); Methyl palmitate, C17H34O2, (MeC16).

3.1. Materials

All the compounds used in this study were supplied by Sigma-Aldrich. The stated purity presented by the supplier and the purity of the samples evaluated in our laboratory using gas chromatography (GC) (HP 4890 equipped with a cross-linked, 5 % diphenyl and 95 % dimethylpolysiloxane column), is depicted in Table 3.1. The relative atomic masses used were those recommended by IUPAC in 2013.[78] Due to their high quality the samples were handled without any further purification.

Table 3.1 - Compounds description, purities (%(m/m)) and suppliers

Chemicals name	**Chemical formula**	**Molecular Weight / g·mol^{-1}**	**CAS no.**	**Purity /** GC	**Purity /** supplier
Hexadecane	$C_{16}H_{34}$	226.42	544-76-3	99.6	>99
Octadecane	$C_{18}H_{38}$	254.47	593-45-3	99.1	99
Eicosane	$C_{20}H_{42}$	282.52	112-95-8	99.6	99
Methyl Palmitate	$C_{17}H_{34}O_2$	270.43	112-39-0	99.8	>99
Methyl Stearate	$C_{19}H_{38}O_2$	298.48	112-61-8	99.7	99

The binary mixtures of around 200 mg with different compositions (molar fraction between 0.0 to 1.0 in 0.1 mole fraction steps) were prepared gravimetrically (using an analytical balance, Mettler Toledo, model AG245, with a mass resolution of 0.01 mg) and kept in sealed glass bottles to avoid contamination and evaporation of the components (Figure 3.2). Some additional binary mixtures compositions were prepared whenever necessary to increase the definition/resolution of the phase diagrams. The mixtures were heat to a high temperature (315 K) and kept overnight in order to obtain a homogeneous solution. The overall uncertainty of the experimental mole fraction was estimated to be approximately $\pm 1 \times 10^{-3}$.

Figure 3.2 - Example of the samples bottles for the mixtures of methyl stearate and hexadecane.

3.2. Differential scanning calorimetry

The thermal study of each sample was evaluated by DSC, using two different commercial DSC instruments (Perkin-Elmer model Pyris Diamond DSC and NETZSCH 200F3 DSC, (Figure 3.3) using in the both instruments high purity (99.999 %) gaseous nitrogen as protective gas (50 ml·min^{-1}). The temperature and heat flux scales of the power compensation DSC (Perkin-Elmer model Pyris Diamond) were calibrated by measuring the temperature and the enthalpy of fusion of reference materials [161–163] namely, benzoic acid, 4-methoxybenzoic acid, triphenylene, naphthalene, anthracene, 1,3,5-triphenylbenzene, phenylacetic acid, perylene, *ortho*-terphenyl, and 9,10-diphenylanthracene, indium and water at different scanning rates (2, 5, and 10 K·min^{-1}). The temperature and heat flux scales of the NETZSCH 200F3 DSC were calibrated based in the temperature and the enthalpy of fusion of the following reference materials: benzoic acid, *o*-terphenyl, cyclohexane, adamantane, undecane and water were used. [161–163]

Figure 3.3 - Picture of the Perkin-Elmer model Pyris Diamond DSC (left) and NETZSCH 200F3 DSC (right).

For the thermal study small quantities of each sample were sealed in an aluminium crucible (30/50 μg) and heated at a rate of 5 K·min^{-1} to 323.15 K under nitrogen atmosphere. The sample was maintained at this temperature for 5 min and was then cooled at a rate of 5 K·min^{-1} to a temperature of 223.15 K and maintained at this temperature for 10 min. After this isothermal step, the sample was then heated at a rate of 2 K·min^{-1} until the complete melting and an isothermal step of 5 min (Figure 3.4).

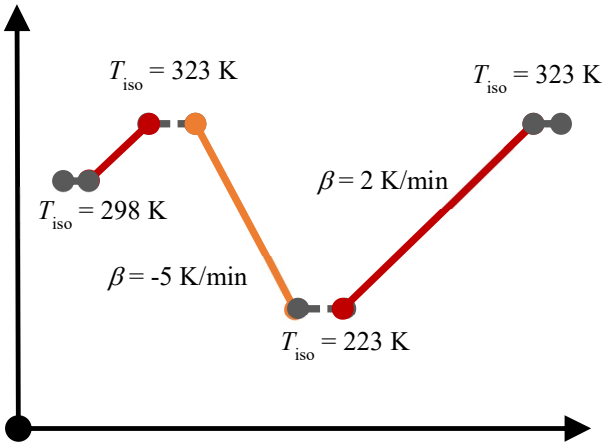

Figure 3.4 - Schematic representation of the thermal profile used in the DSC.

Due to peaks overlapping, which prevents the direct evaluation of the onset temperature, the solid-solid and solid-liquid transitions were determined based on the peak temperatures [152,153,155,164] and corrected to the temperature delay previously derived for each scanning rate. The uncertainty of the experimental results was taken as the overall standard deviation for the enthalpies of melting, σ, and was estimated ± 0.5 K for the temperature and 2 % for the heat involved in the melting process (typical ± 4 $J \cdot g^{-1}$ considering the size and the average molar mass of the samples) using the described methodology (scanning rate, sample mass, crucibles).

3.3. Phase transition morphology analyses

The morphology analyses of the solid phases of the mixtures and solid-solid and solid-liquid events previously observed in the DSC was explored by optical microscopy using an Olympus optical system, model BX51, equipped with a Linkam T95-PE temperature controller with LTS120, a camera Olympus DP71 with U-CMAD3/U-TV1x-2 and a camera Olympus C-5060 Wide zoom.

The quantitative and qualitative characterization of the crystal structures of the solid phases was evaluated by x-ray powder diffraction in a Panalytical XRD apparatus model Empyrean, operating with an anode of Cu ($K_{\alpha1}$= 1.5406 Å; $K_{\alpha2}$= 1.5444 Å). The low temperature chamber was an Anton Paar model TTK450, the temperature controller an Anton Paar TCU100 and the chamber was cooled using liquid nitrogen. Diffraction data were collected in the 2θ range from 3◦ to 50◦ in steps of 0.02 and a time per step of 50 s using a linear detector PIXEL 1D with an active length 3.347º, with incident slit of 1/4º and diffracted beams anti-

scatter slits of 7.5 mm. The diffractograms acquired for these mixtures did not have enough resolution to allow the crystal structures to be derived from them. They were only used to identify differences between the solid regions. The sample were heated or cooled until the desired temperature at which the diffraction data were collected. The heating or cooling process of the sample was conduct by the temperature controller with no programmed temperature rate.

3.4. Results and discussion

Given the limited information available about the phase behaviour of systems composed of fatty acid methyl esters and alkanes, main components of waxes forming in biodiesel and mineral diesel, the phase diagrams of several of these mixtures are here derived and analysed.

The phase diagrams reported below are the result of the interpretation of the DSC thermograms, from which, whenever possible Tammann plots are presented to help identification and interpretation of eutectic points and the solid solution domains. These results were complemented with information derived from optical microscopy where it is possible to observe some visual changes in solid structure or the initial/final melting temperatures. The results are further supported by XRD where is possible to study the crystal structures modification at different temperatures or concentrations. The melting properties of the pure compounds are reported in Table 3.2.

Table 3.2 - Melting data concerning the studied pure compounds.

Component name	**T_{fus} / K this work**	**T_{fus} / K literature**	**ΔH_{fus} / J·g^{-1} this work**	**ΔH_{fus} / J·g^{-1} literature**
Hexadecane	290.9 ± 0.5	291.1 [a]	235 ± 4	228.79 ± 0.4 [a]
Octadecane	300.3 ± 0.5	301.3 [a]	235 ± 4	241.29 ± 0.4 [a]
Eicosane	309.2 ± 0.5	309.7 [a]	260 ± 5	238.21 ± 0.4 [a]
Methyl Palmitate	301.7 ± 0.5	300.53 ± 0.02 [b] 305.15 [c] 302.2 [d]	202 ± 4	209.0 ± 4.6 [b] 207.05± 7.8 [c] 215 [d]
Methyl Stearate	310.5 ± 0.5	310.16 ± 0.05 [b] 310.9 [c] 311.0 [d]	218 ± 4	222.0 ± 1.8 [b] 206.7± 5.7 [c] 240 [d]

"a" - reference [165]; "b" - reference [166]; "c" – reference [167]; "d" – reference [168]; Temperature and specific enthalpy uncertainty: taken as the overall standard deviation, σ, including the calibration uncertainty. Estimated as σ (temperature) = ± 0.5 K and σ (specific enthalpy of fusion) = ± 4 J·g^{-1}).

The phase behaviour results were compared with the prediction of an ideal eutectic behaviour described by the Schröder-van Laar model [169] as presented in equation [3.1] for the dependence of the liquidus line temperature with the mole fraction, $T(\chi_i)$, where the liquid mixture is assumed as an ideal liquid solution and neglecting the correction effect of the difference in the heat capacities of the solid and liquid phase.

$$\ln(x_i) = \frac{\Delta H_{fus}}{R}\left(\frac{1}{T_{fus_i}} - \frac{1}{T(xi)}\right) \qquad [3.1]$$

where, χ_i is mole fraction of the component, $T_{fus\ i}$ and ΔH_{fus} are the melting and heat of fusion of the pure component and R is the universal gas constant. The Schröder-van Laar model was only used for comparative proposals between the different binary systems and should not be considered as a modellation attempt of the observed thermal behaviour.

3.4.1. Phase behaviour of the binary mixture methyl stearate + hexadecane (MeC18 + C16)

Figure 3.5 depicts the derived solid-liquid phase diagram measured at atmospheric pressure (p=0.10 ± 0.01 MPa) for the binary mixture system composed by methyl stearate and hexadecane (MeC18 + C16). It was found that the (MeC18 + C16) system presents a simple eutectic type behaviour with an eutectic composition close to χ_A=0.15 and an eutectic temperature of 289 K in good agreement with the results published by Lobbia *et al* [160]. An invariant solid-solid transition at 278 K was found in this binary mixture in the intermediate binary mixtures' compositions.

The solid-solid transition founded by DSC is not detectable by optical microscopy, and shows a small endothermic and reversible heat of transition which was correlated with the hexadecane (C16) content as shown in the Tammann plot presented in Figure 3.6. This suggests that the solid phase that undergoes the solid-solid transition is formed by hexadecane crystallizing on a solution of MeC18 on a structure not present when hexadecane is crystallized from the melt.

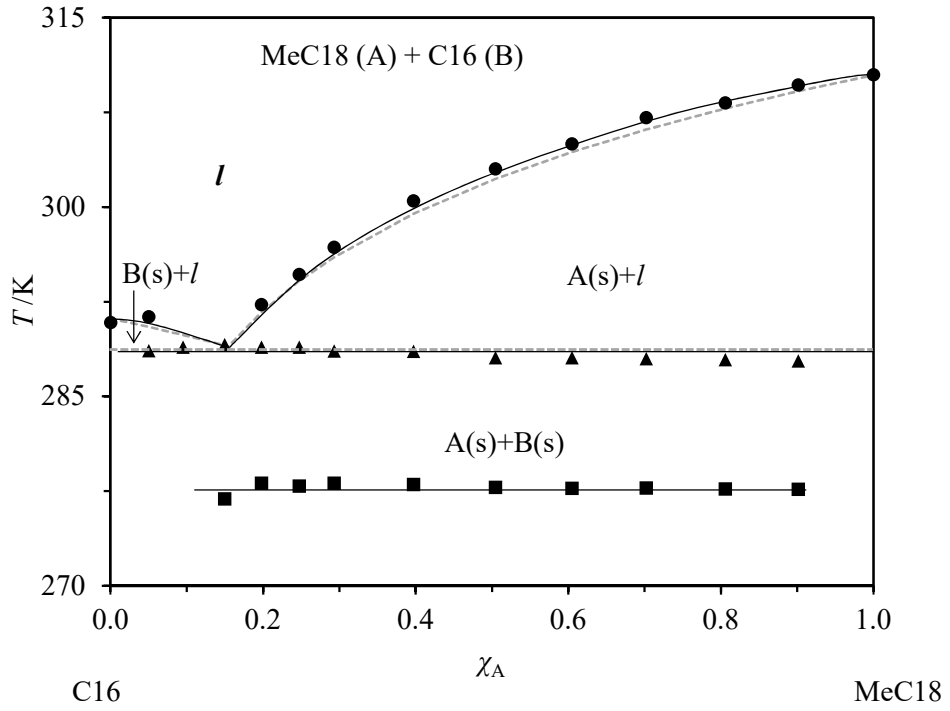

Figure 3.5 - Solid-liquid phase diagram (p=0.10 ± 0.01 MPa) for the binary system methyl stearate (A) and hexadecane (B). ● – liquidus line; ■ – solid-solid transition; ▲ – eutectic transition. Dot grey lines (▪▪▪▪) indicates the ideal eutectic liquidus line.

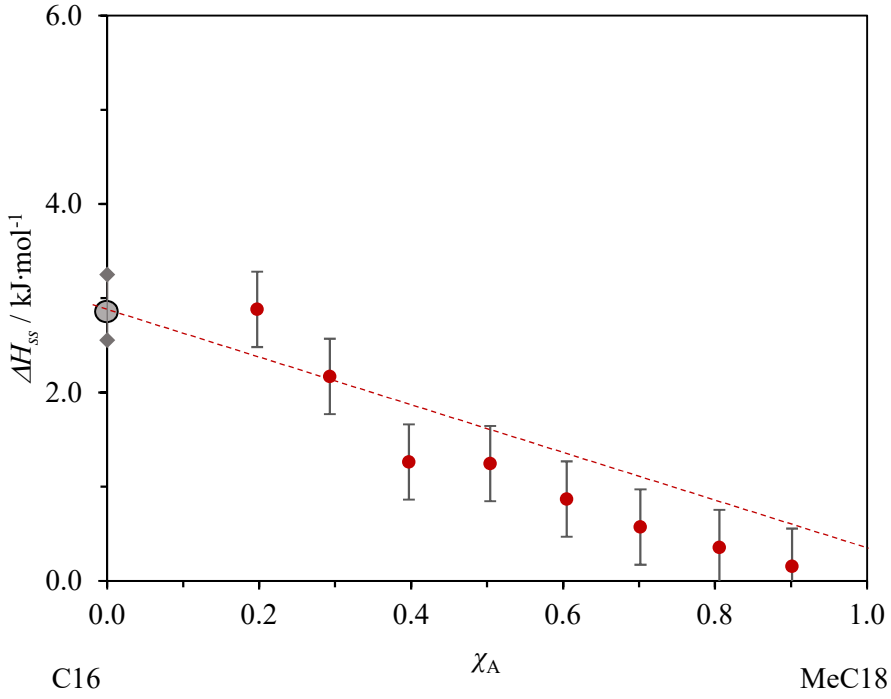

Figure 3.6 - Tammann diagram for the solid-solid transition for the binary system methyl stearate (A) + hexadecane (B). Solid-solid transition observed at T = 278 ± 1 K. Linear dependence with hexadecane mole fraction, converging to χ_A = 1.0, ΔHss = 2.5 ± 0.5 kJ·mol^{-1} (hexadecane).

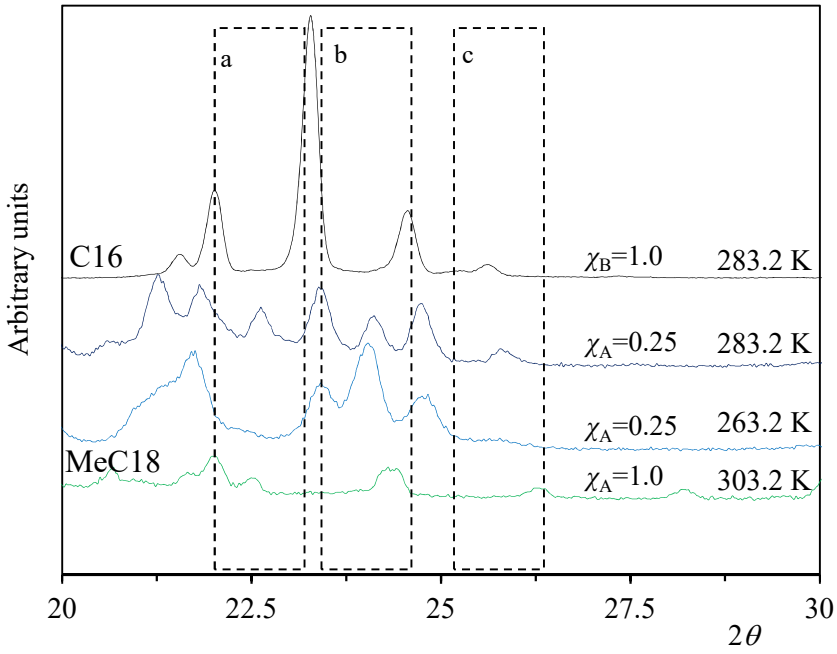

Figure 3.7 - XRD spectra for the solid-solid transition observed in binary mixtures system composed by methyl stearate (A) and hexadecane (B) at different compositions.

The structural change involved in this solid-solid transition was explored by XRD. The change in the XRD spectra with the temperature is depicted in Figure 3.7 for the mixture composition of χ=0.25 of methyl stearate. The XRD data of the mixtures was compared with XRD of the pure compounds. In the spectra regions highlighted by the regions "a" and "c" two new diffractions peaks at 2θ= 23º and 2θ= 26º, are depicted, as well as a decrease of the peak intensity at 2θ= 24º, region "b", supporting the existence of a structural change in the crystal which is not observed in the pure alkane C16. In Figure 3.8 is represent the results of the optical microscopy where is possible to see the partial melting at 293 K and the increasing of the presence of liquid when the temperature increase to 294.5 K.

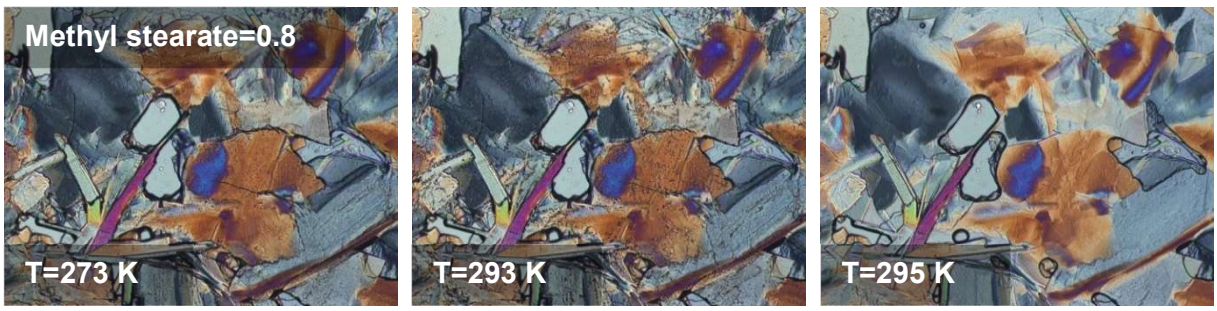

Figure 3.8 - Microscopy pictures of the crystals of the binary system methyl stearate and hexadecane at different temperatures, x100 magnification.

3.4.2. Phase behaviour of the binary mixture methyl stearate + octadecane (MeC18 + C18)

The solid-liquid phase diagram for the binary mixture of methyl stearate + octadecane (MeC18 + C18) is presented in Figure 3.9. This binary mixture presents novel features when compared with the previous phase diagram (MeC18 + C16). We found evidences to the formation of an intermediate compound, with a composition of χ_A= 0.66, which suggests the 2:1 stoichiometric of FAME to alkane. The eutectic point was found at T= 298 K and a molar fraction χ_A= 0.2. The intermediate compound (2:1), decomposes at T= 300 K with the formation of a peritectic point at a composition close to χ_A= 0.5. The composition ratio of the intermediate compound (2:1) was further supported by the Tammann plot of the solid-solid transition observed at 275 ± 1 K which converges to χ_A= 0.66 as depicted in Figure 3.10. Figure 3.11 presents the XRD spectra of the two pure compounds and the intermediate compound (2:1). The comparative analysis the XRD data supports the formation of the intermediate compound.

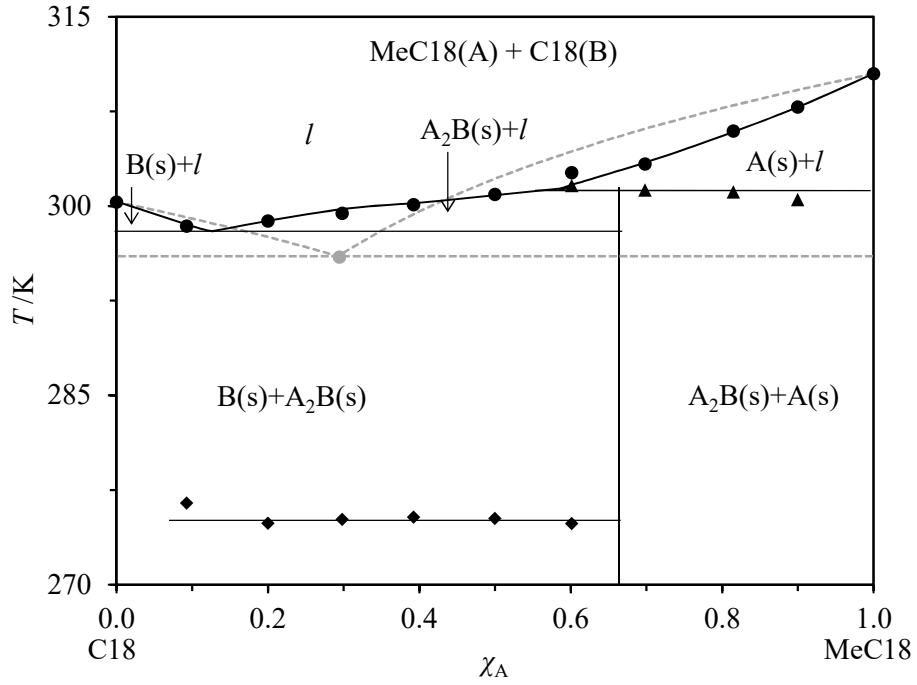

Figure 3.9 - Solid-liquid phase diagram (p=0.10 ± 0.01 MPa) for the binary system methyl stearate (A) and octadecane (B). ● – liquidus line; ♦ – solid-solid transition; ▲ – peritectic transition. Dot grey lines (▪▪▪▪) indicates the ideal eutectic liquidus line.

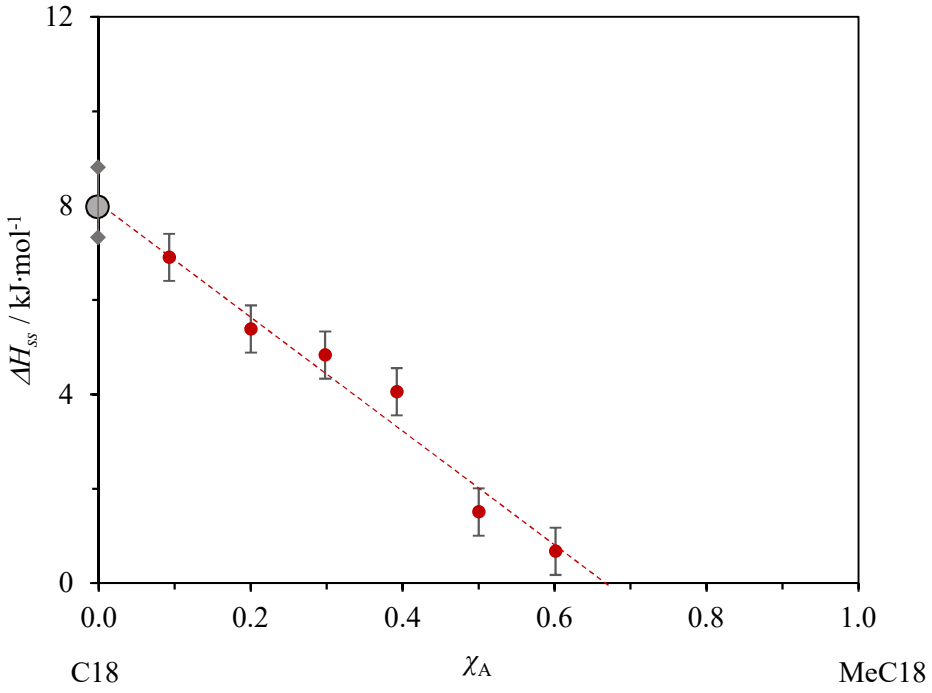

Figure 3.10 - Tammann diagram for the solid-solid transition for the binary system methyl stearate (A) and octadecane (B). Solid-solid transition observed at $T = 275 \pm 1$ K. Linear dependence with octadecane mole fraction, converging to $\chi_A = 0.66$, $\Delta Hss = 8.0 \pm 0.5$ kJ·mol^{-1} (octadecane).

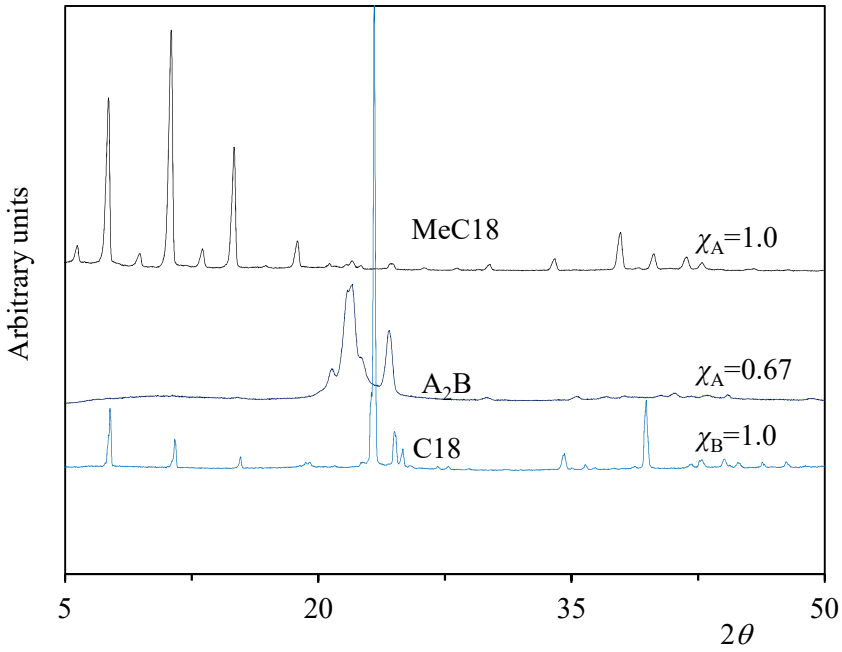

Figure 3.11 - XRD spectra for the pure compounds methyl stearate (A) and octadecane (B) at 298.2 K and the A_2B co-crystal formed at the 2:1 composition.

Moreover, as mentioned above, this system shows a solid-solid transition at about 275 K which is observable by DSC and XRD. The change in the crystal structure are supported by the XRD data as reported in Figure 3.12 ($2\theta = 30^{o}$ peak disappearance) highlighted in the dash line box. We found a strong indication that this solid-solid transition is associated to the octadecane as supported by the Tammann plot presented in Figure 3.10. It is also quite interesting to observe that the octadecane solid-solid seems to be induced by the binary mixtures solution as it was not observed in pure octadecane.

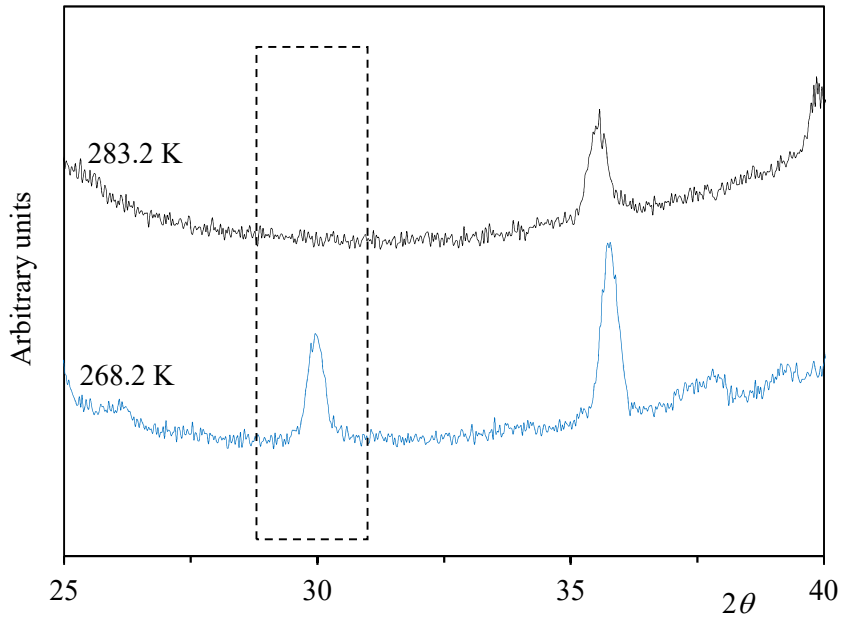

Figure 3.12 - XRD spectra for the binary system composed by 40 % (mol/mol) methyl stearate and octadecane.

The optical microscopy (Figure 3.13), didn't show a visible solid-solid transition using a polarize light. In these results it is only possible to see the fusion at temperatures between the eutectic and peritectic line and the liquidus line.

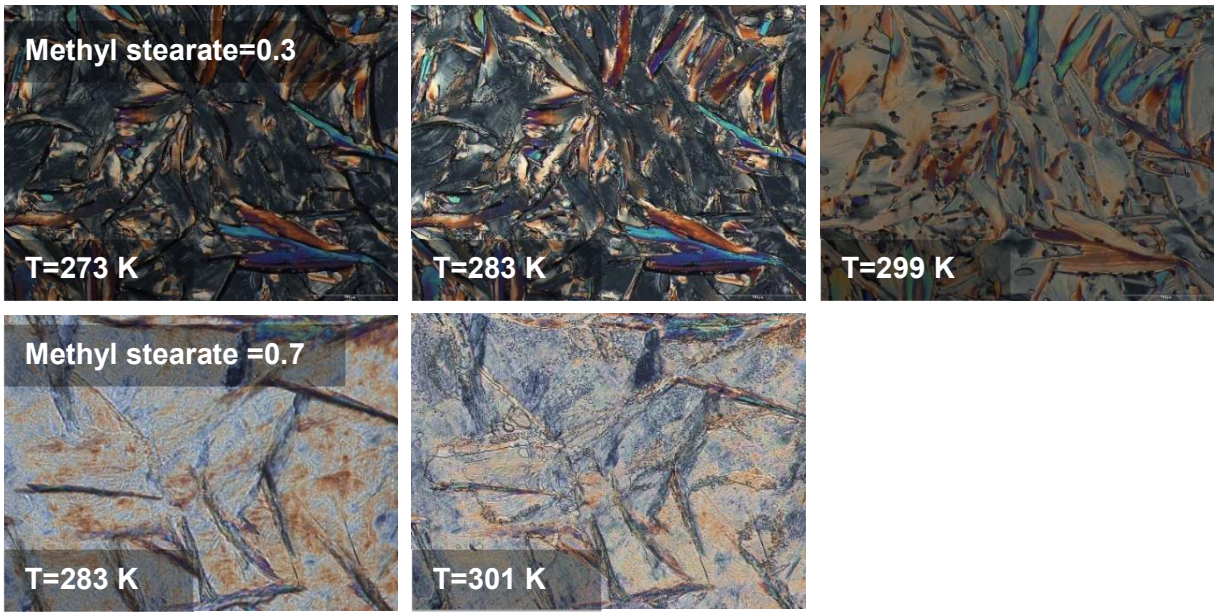

Figure 3.13 - Microscopy pictures of the crystals of the binary system methyl stearate and octadecane at different temperatures, x100 magnification.

3.4.3. Phase behaviour of the binary mixture methyl stearate + eicosane (MeC18+C20)

The phase diagram for the binary system methyl stearate + eicosane (MeC18 + C20) is significantly more complex than the phase diagrams discussed previously. A significant number of phase transitions were observed by DSC at lower temperatures which indicates a much more complex behaviour. Figure 3.14 presents our interpretation of the solid-liquid phase diagram for this binary mixture based in rationalization of the DSC thermograms. In the region on the left-hand side, close to the pure eicosane, we found an indication to the formation of a solid-solution. In this region of the phase diagram, there is the indication to the formation of a peritectoid at composition χ_A= 0.2 and *T*=308 K induced by the solid-solution SS''. The initial melting of the mixture of molar fraction χ_A= 0.10 at 308 K was detected by optical microscopy and is present in Figure 3.15.

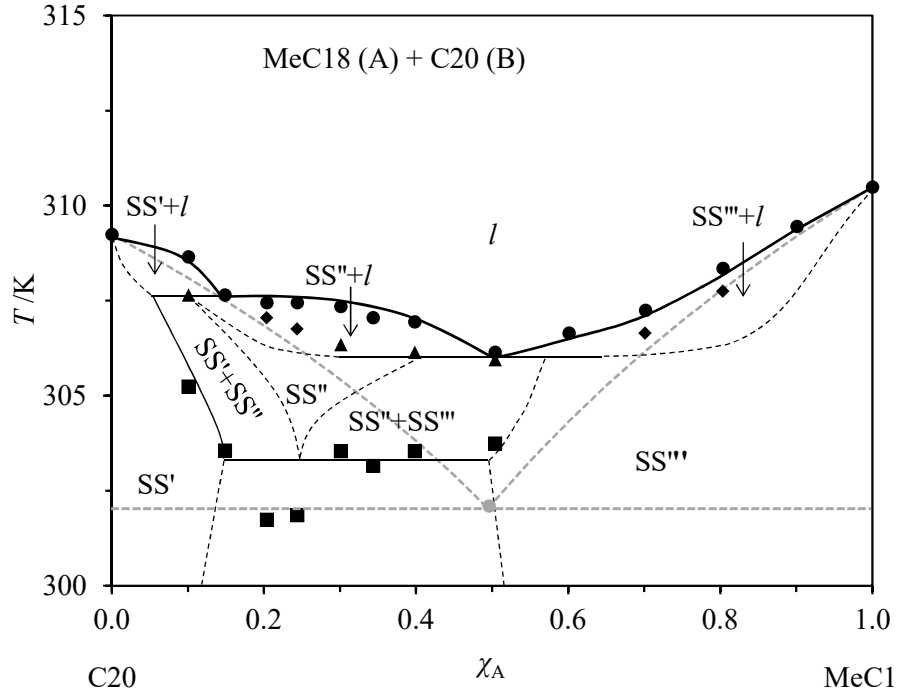

Figure 3.14 - Solid-liquid phase diagram (p=0.10 ± 0.01 MPa) for the binary system methyl stearate (A) and eicosane (B). ● – liquidus line; ■ – solid-solid transition; ▲ – solidus line ♦ - possible metatectic transition. Dashed lines represent hypothetical transitions for which no evidence from DSC was available. Dot grey lines (▪▪▪▪) indicate the ideal eutectic liquidus line.

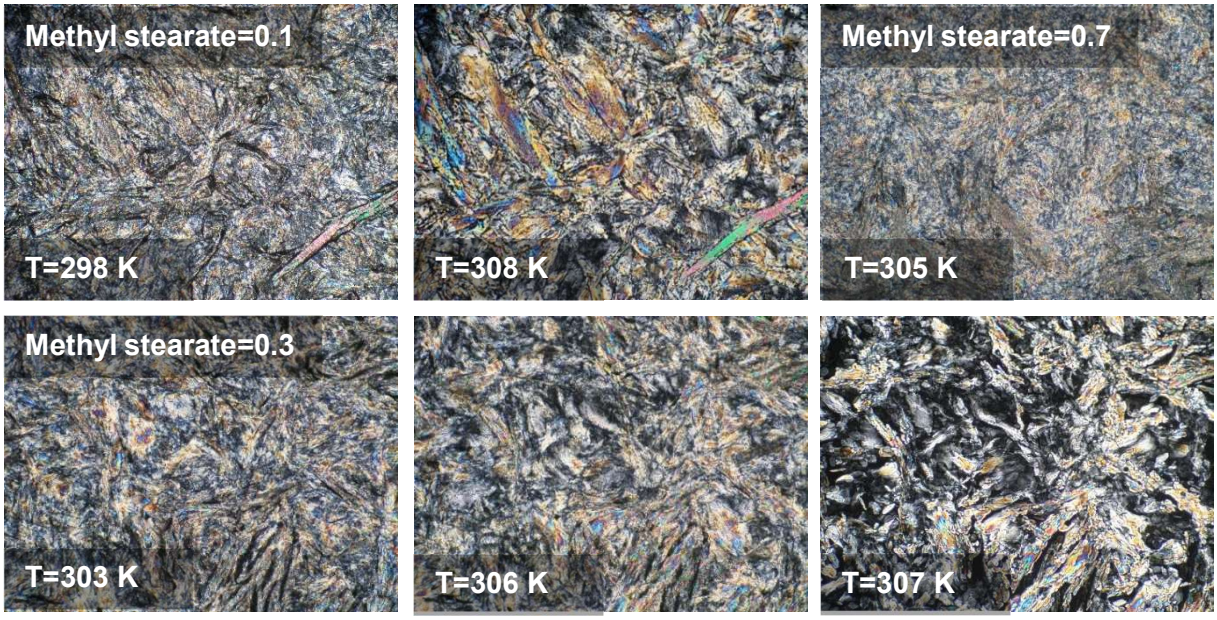

Figure 3.15 - Microscopy pictures of the crystals of the binary system methyl stearate and eicosane at different temperatures, x100 magnification.

An eutectoid point was also observed at the composition χ_A= 0.5 and T= 306 K. The melting of the intermediate solid solution SS'' was observed by optical microscopy at χ_A= 0.3 and T=307 K which is presented in Figure 3.15. At the composition between χ_A= 0.1 and χ_A=

0.5, an invariant transition at T=303 K was found. At the same composition region, but at higher temperature we found the indication for the formation of two-solid solution regions, SS'+SS'' and SS''+SS'''.

Based on the analysis of the XRD spectra for the different binary compositions depicted in Figure 3.16 and Figure 3.15 we found the indication of a distinguished crystal structure pattern for the different compositions supporting the existence of the solid solution. The binary system MeC18 + C20 is characterized by the significant solid phase stabilization as indicated by the rise of the liquidus line temperature when compared with the hypothetical ideal behaviour.

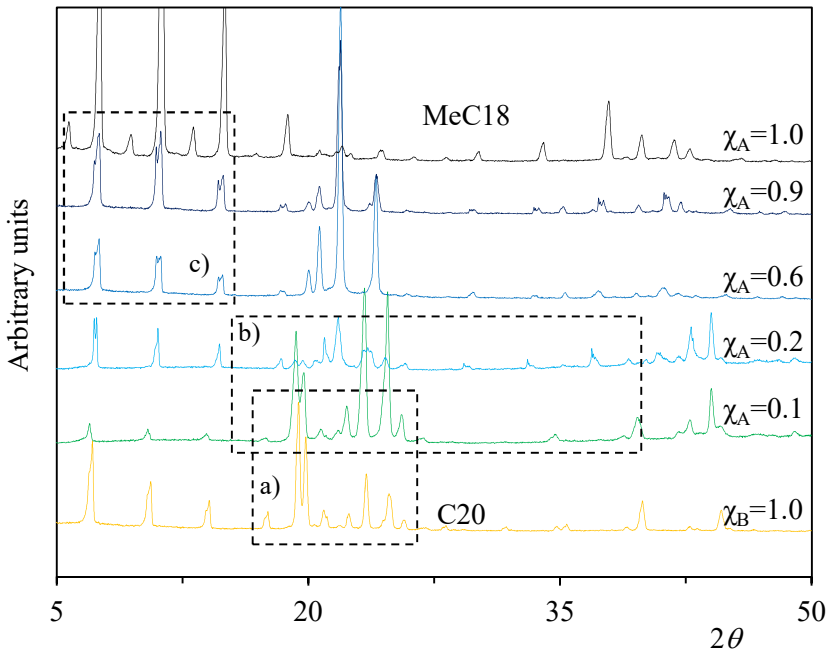

Figure 3.16 - XRD spectra for the binary system formed composed by methyl stearate (A) and eicosane (B) at different compositions and 300 K.

3.4.4. Phase behaviour of the binary mixture methyl palmitate + eicosane (MeC16+C20)

The binary system methyl palmitate + eicosane (MeC16 + C20), represented in Figure 3.17, presents a solid-liquid phase diagram, similar to the MeC18 + C16 system, with the formation of an eutectic point around 295 K and a composition of χ_A= 0.8 as well as solid-solid

transition. The lower temperature transition is an invariant solid-solid transition around 280 K which was detected in the composition region between χ_A= 0.1 and χ_A= 0.7.

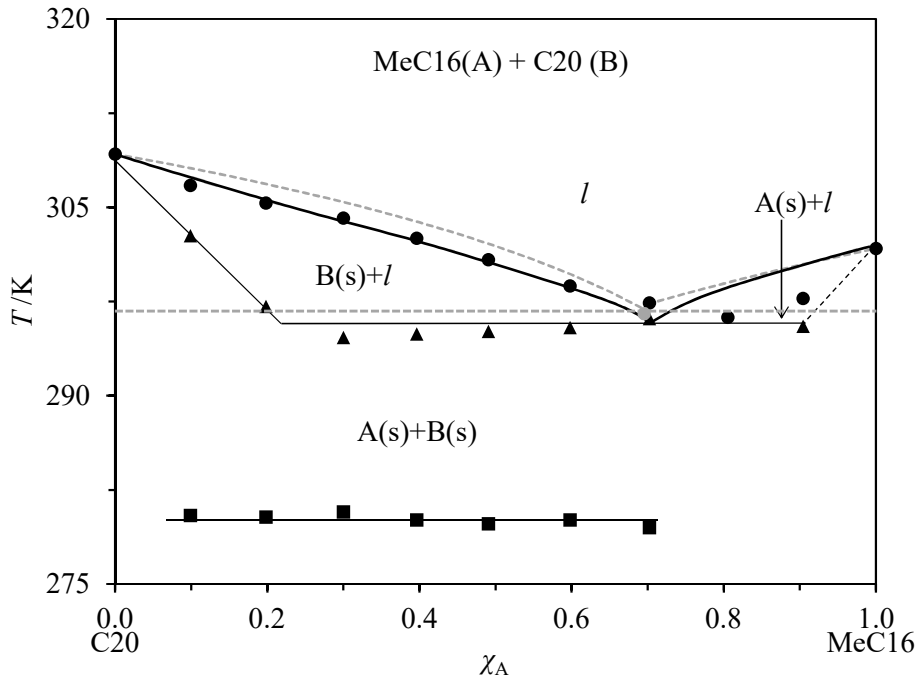

Figure 3.17 - Solid-liquid phase diagram (p=0.10 ± 0.01 MPa) for the binary system methyl palmitate (A) + eicosane (B). ● – liquidus line temperature; ■ – solid-solid transition; ▲ – solidus line. Dot grey lines (▪▪▪▪) indicate the ideal eutectic liquidus line.

3.4.5. Phase behaviour of the binary mixture methyl palmitate + hexadecane (MeC16+C16)

The solid-liquid phase diagram for the binary mixture methyl palmitate + hexadecane, (MeC16 + C16) is depicted in Figure 3.18 and presents solid-liquid phase diagram similar than the MeC18 + C18 system.

The liquidus line is in good agreement with the data published by Lobbia *et al* [160]. However, our solid-liquid phase diagram results highlights some novel details not reported previously. For molar fractions above χ_A= 0.5, DSC data suggest the existence of a metatectic transition which was further confirmed by optical microscopy. Moreover, the formation of a co-crystal at a 1:1 stoichiometric proportion (AB) was confirmed by the the Tammann plot representation of the solid-solid transition at T=259 K (Figure 3.19) indicating the existence of a peritectic point at compositions close to 0.4. This transition is also supported by the XDR data depicted in Figure 3.20 (disappearance of the peak at 2θ = 30º at higher temperatures).

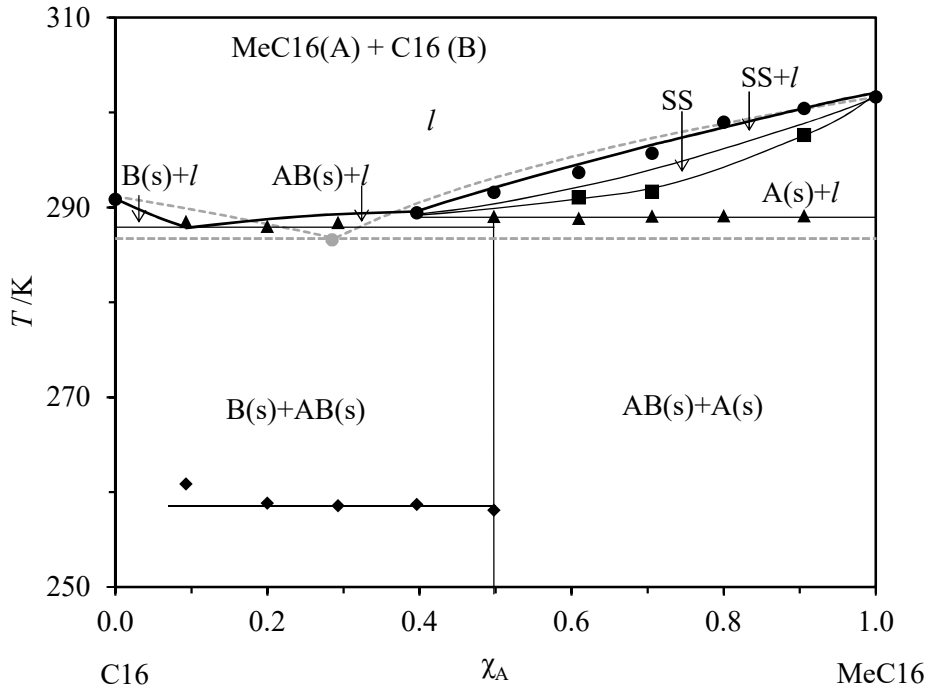

Figure 3.18 - Solid-liquid phase diagram (p=0.10 ± 0.01 MPa) for the binary system formed by methyl palmitate (A) and hexadecane (B). ● – liquidus line; ■ – metatectic transition; ▲ – solidus line; ♦ – solid-solid transition. Dot grey lines (▪▪▪▪) indicate the ideal eutectic liquidus line.

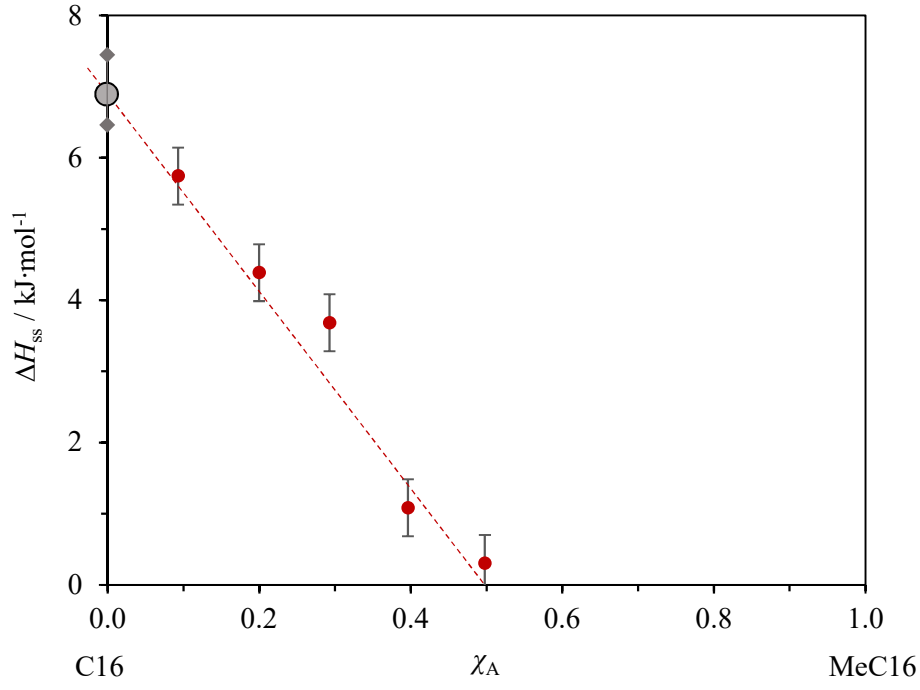

Figure 3.19 - Tammann diagram for the solid-solid transition for the binary system methyl palmitate (A) and hexadecane (B). Solid-solid transition observed at T = 258 ± 1 K. Linear dependence of hexadecane mole fraction, ΔHss = 7.0 ± 0.5 kJ·mol^{-1} (hexadecane).

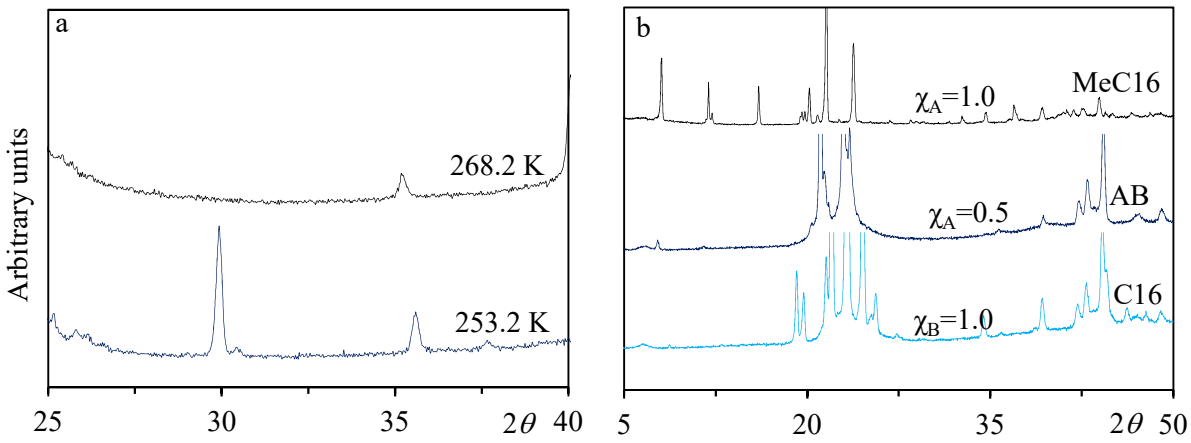

Figure 3.20 - XRD spectra of the binary system composed by methyl palmitate (A) and hexadecane (B). a) 30 % (mol/mol) methyl palmitate; b) At 283 K and the AB co-crystal formed by the 1:1 mixture.

We tried to find a metatectic transition by optical microscopy (Figure 3.21) but it isn't clear the existence of this phase and in the microscopy results just show the melting process.

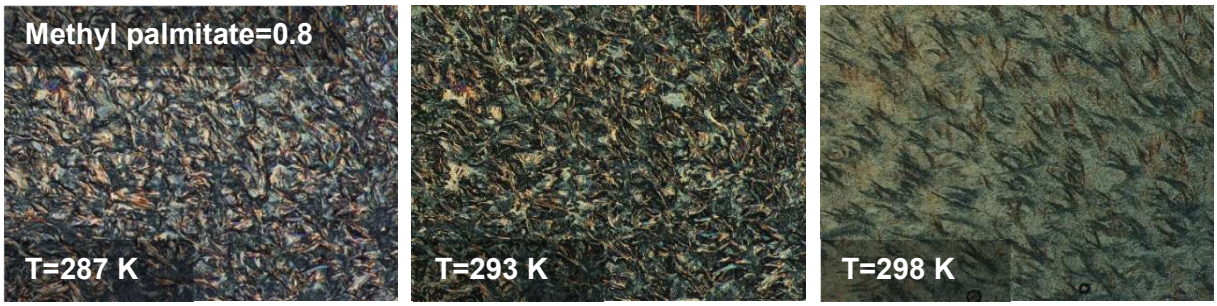

Figure 3.21 - Microscopy pictures of the crystals of the binary system methyl palmitate and hexadecane at different temperatures, x100 magnification.

3.4.6. Phase behaviour of the binary mixture methyl palmitate + octadecane (MeC16+C18)

The solid-liquid phase diagram of the system methyl palmitate + octadecane (MeC16 + C18) is presented in Figure 3.22. This binary mixture presents a behaviour very identical than the methyl stearate + eicosane (MeC18+C20) system, with the indication to the formation of a solid-solution.

In this binary mixture we found the indication to the formation of a peritectoid point in the alkane rich region (molar fraction of around χ_A= 0.2 and 299 K). The eutectoid appear at 293 K between χ_A= 0.3 - 0.4. This transition is supported by the XRD data presented in Figure

3.23. At the molar fraction of χ_A= 0.2 some new diffraction peak were found which supports the structural modification.

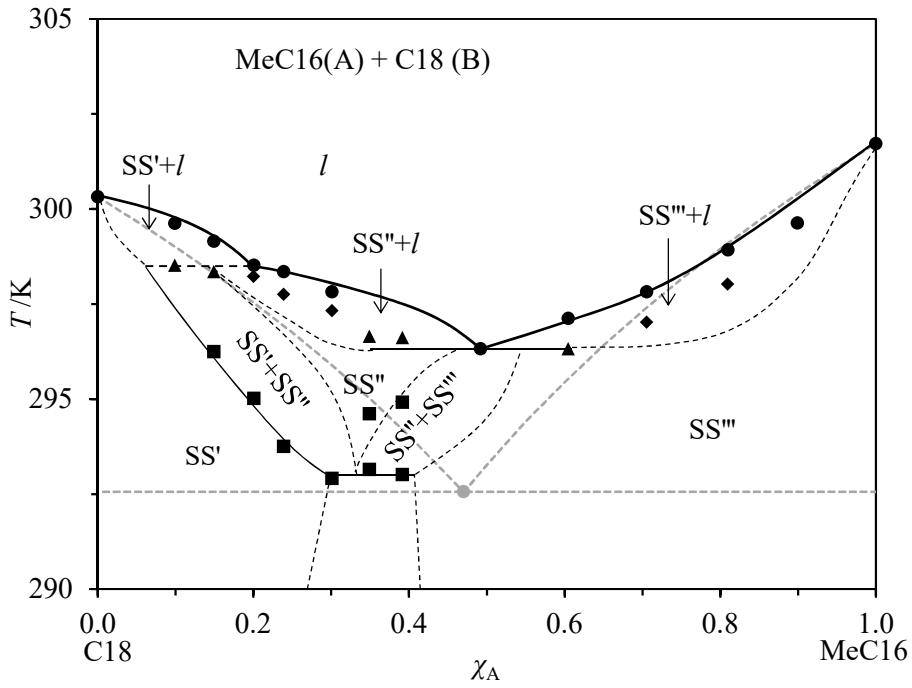

Figure 3.22 - Solid-liquid phase diagram (p=0.10 ± 0.01 MPa) for the binary system methyl palmitate (A) + octadecane (B). ● – liquidus line; ■ – solid-solid transition; ▲ – solidus line, ♦ - possible metatectic transition. Dot grey lines (▪▪▪▪) indicate the ideal liquidus line.

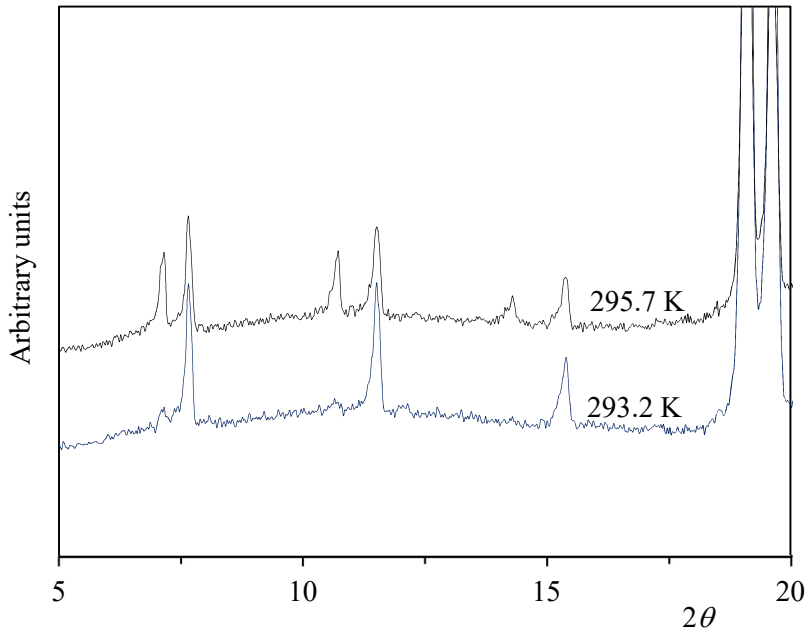

Figure 3.23 - XRD spectra for the binary system composed by 20 % (mol/mol) methyl palmitate and octadecane.

The eutectic point was found at the molar fraction of χ_A= 0.5 and *T*=296 K. At the methyl palmitate rich region an extensive region solid solution is observed. As for the system methyl stearate + eicosane the existence of the solid solution region is supported XRD data and optical microscopy as shown in Figure 3.24 and Figure 3.25, respectively.

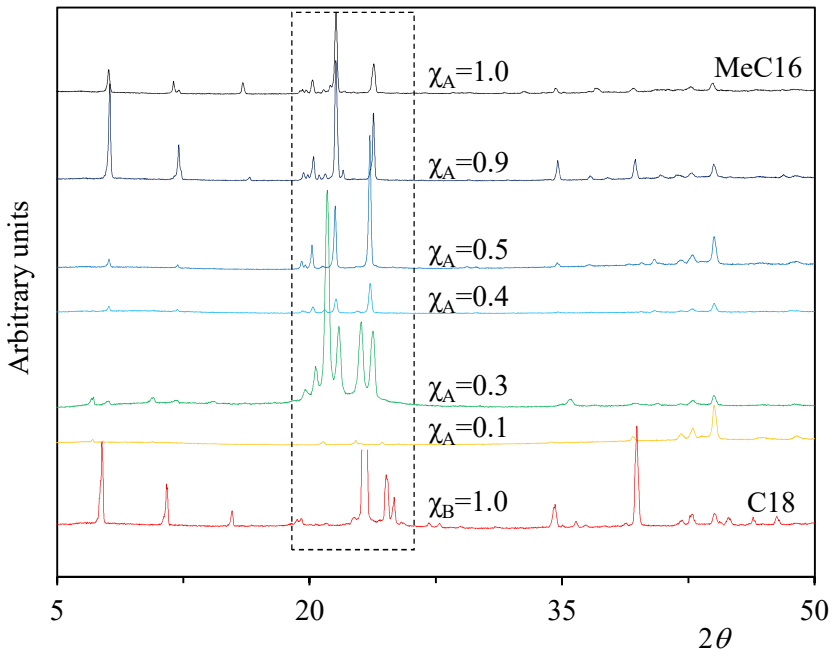

Figure 3.24 - XRD spectra for the binary system composed by methyl palmitate (A) and octadecane (B) at different compositions and 295 K.

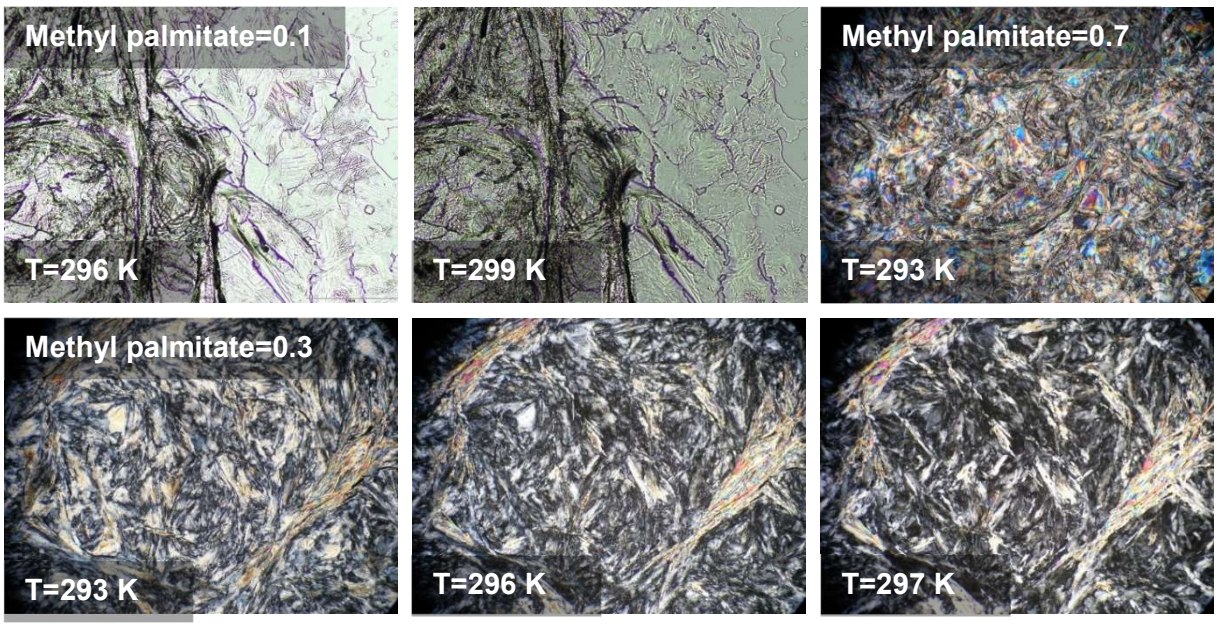

Figure 3.25 - Microscopy pictures of the crystals of the binary system methyl palmitate and octadecane at different temperatures, x100 magnification.

3.5. Conclusions

The solid-liquid phase diagram of the series of the saturated methyl esters and alkanes binary mixtures show a more complex behaviour than the data previously reported. The phase diagram behaviour follows a pattern that seems to be related with the balance between the size of the methyl ester and the alkane. We found the formation of co-crystals, peritectic and metatectic reactions in mixtures with equal alkyl chain size, and the formation of solid solutions in mixtures with an alkane alkyl size two carbon bigger than the methyl esters. The molecular understanding/interpretation of the phase behaviour schematically represented in Figure 3.26.

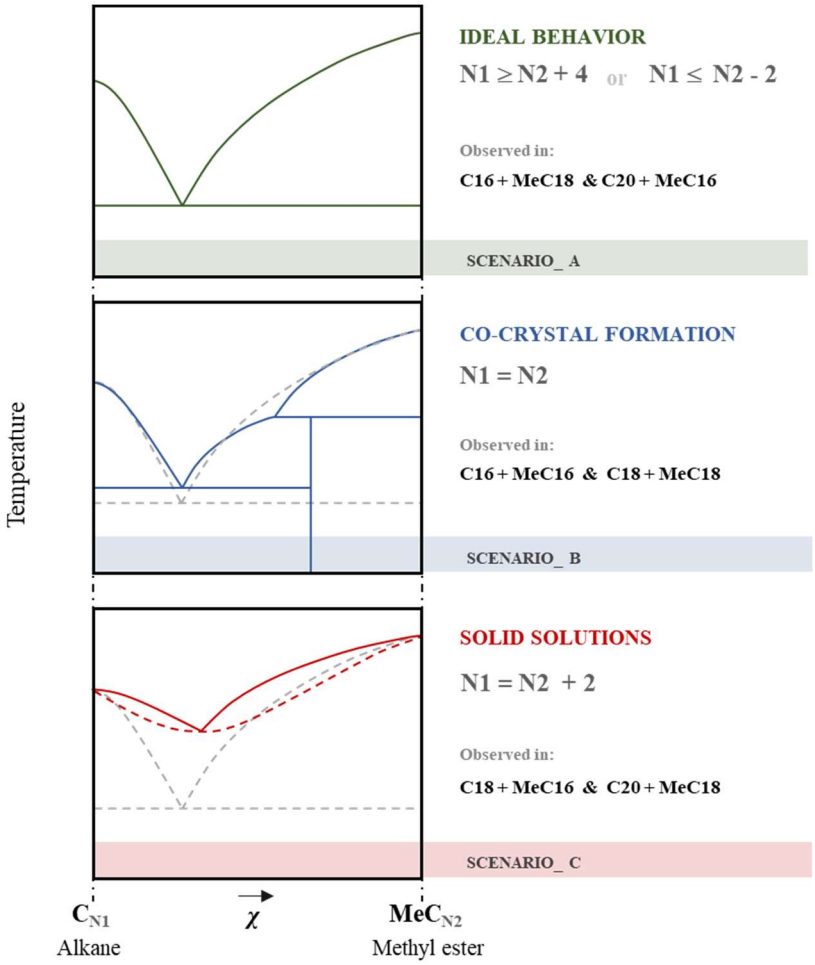

Figure 3.26 - Schematic diagram of the phase behaviour of binary mixtures of saturated methyl esters and alkanes and their dependence with the alkyl size balance. Dashed line depicts the ideal behaviour described by the Schröder-van Laar model.

The observed behaviour could be divided in tree typical scenarios organized according the differences in size between the alkyl chains of the mixture components which seem to rule

the phase stability. The comparation with the ideal eutectic model show a good agreement with the results near the pure compounds and the conclusion are in good agreement with the results published of Lobbia *et al*, where a deviation to the ideal eutectic point in the system C16+MeC16 and an ideal eutectic behaviour as observed for C16+MeC18 and C16+MeC19. This last system confirms the conclusion that the ideal eutectic for the interval represented in Figure 3.26, scenario A.

This understanding could be extended to the diesel /biodiesel blends phase behaviour interpretation and can be a good model to the interpretation of the increase of the cloud and pour points in biodiesel blends with a rich fraction of methyl palmitate or methyl stearate when combined with mineral diesel with a rich fraction in octadecane or eicosane respectively. The formation of the solid solution in a wide range of concentrations, could have important impact on the wax formation as well as in the performance of additives used to improve the low temperatures behaviour of diesel blends. We found that the solid-solid transitions found in the alkane rich region is related with the alkane crystals and seems to be promoted by the presence of the methyl esters.

4. RANCITECH: Design, construction and test of a new high precision oxidative stability apparatus

The RANCITECH apparatus was developed in order to increase the number of available oxidative stability essays, which could be done simultaneously, as well as to improve their accuracy and precision. The design of the apparatus was based in two similar sides (A and B), with 8 samples essays in each thermostable block. Figure 4.1 depicts the general overview picture of the RANCITECH apparatus. In Figure 4.2 is presented a schematic diagram of the electrical circuit, data acquisition, air flow control and temperature control systems.

The thermostable blocks, the temperature control electrical circuits, the temperature controllers, the air flow regulators and other auxiliary devices are supported by a standard aluminium profile from ©MayTec. The two thermostable blocks were thermal isolated using corkboard (ICB) from Isocor. The cavities of the thermostable block are located at the surface and the top surface of the thermostable block is isolated by 20 mm thickness Teflon.

Figure 4.1 - General overview of the high precision oxidative stability apparatus (RANCITECH v16.2).

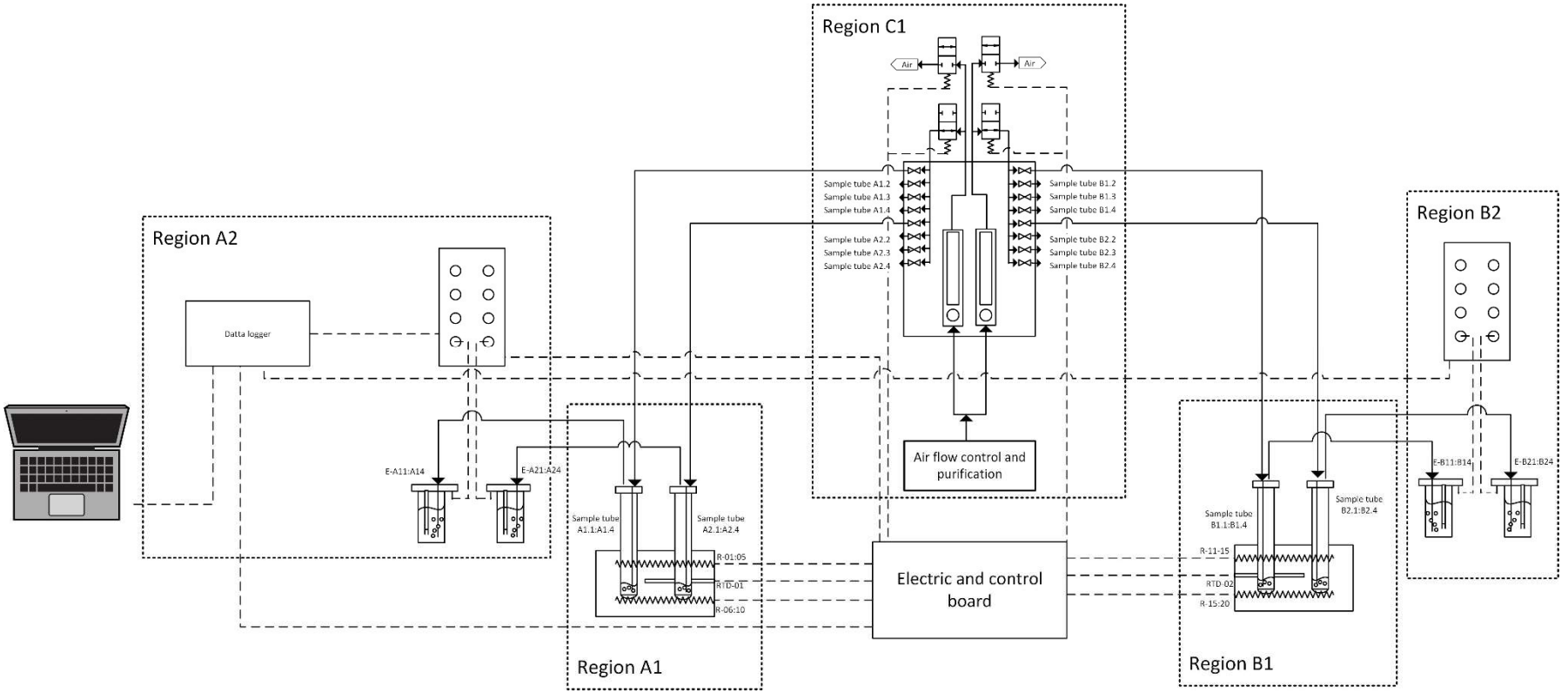

Figure 4.2 - Schematic diagram of the oxidative stability apparatus “RANCITECH”, electrical circuit, data acquisiton, air flow control and temperature control system. – – Electrical signal;.— Mass flow; ---- Region box

4.1. Thermostable blocks

The thermostable blocks, (two independent blocks, regions A1 and B1), are used to keep the samples at desired temperature (110 ºC). The blocks were constructed of aluminium in order to achieve a good temperature homogeneity. Each block allocates 8 sample cavities located symmetrically as depicted in Figure 4.3, Figure 4.4 and Figure 4.5. A good heat power distribution was guaranteed by the use of 10 heaters of 50 W which are located symmetrically in each aluminium block. The temperature control with a resolution of ± 0.1 ºC was achieved using a high resolution PID controller connected to a Pt-100 temperature sensor.

Some details of the blocks along the construction and system assembly are presented in a 3D schematically representation (Figure 4.3) and a series of pictures are depicted in Figure 4.4 and Figure 4.5.

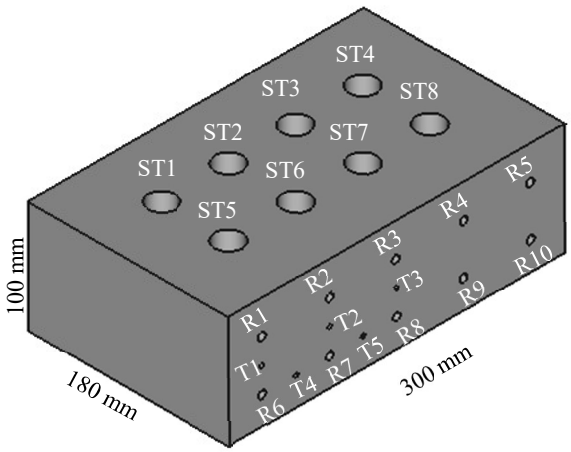

Figure 4.3 - 3D representation of one thermostable block. STx – Sample tube cavities; Rx – Heaters cavities; Tx – Pt-100 cavities.

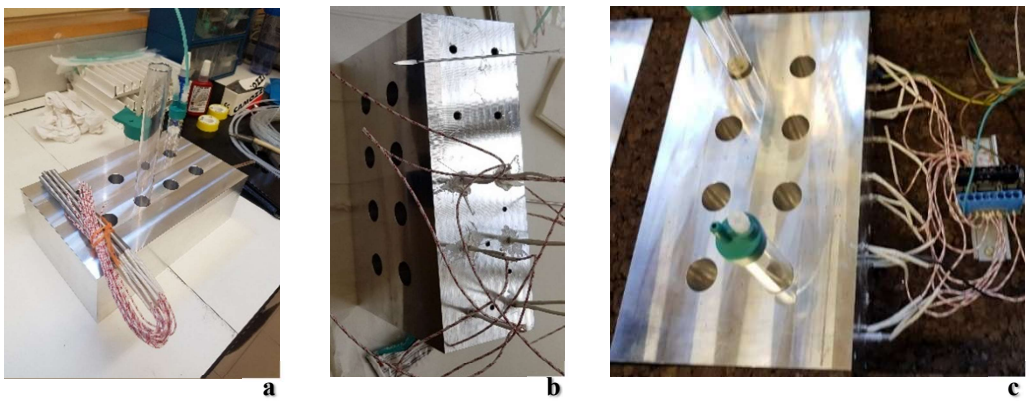

Figure 4.4 - Constructions details of the thermostable blocks. “a” - Thermostable block without heaters cavities; “b” - Details of the heaters cavities; “c” - Block with heaters connected.

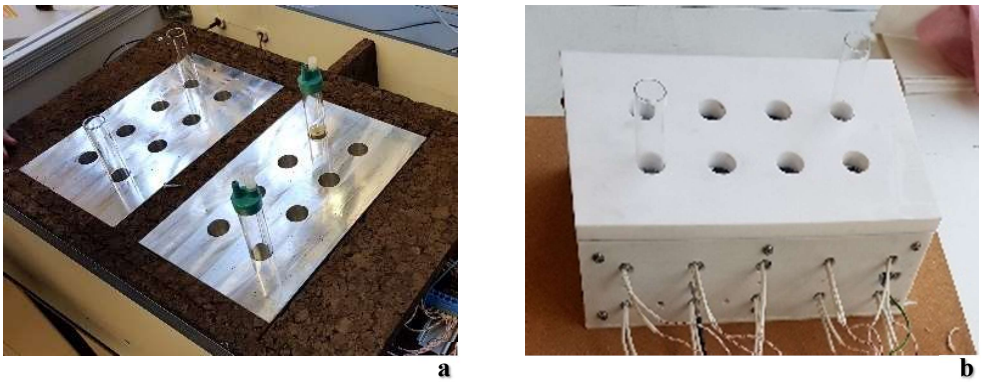

Figure 4.5 - Constructions details of the thermostable blocks. “a” - Blocks with isolation cork; “b” - Side/top view of the block with teflon cover.

The thermostable blocks and cavities were designed to have a good contact between the sample tube and the block according to the EN 14112 standard procedure for the evaluation of the oxidative stability. For this reason, the bottom of the cylinder cavity was designed with the same format than the reaction vessel and is deep enough to guarantee a good temperature homogeneity of the sample as show in Figure 4.6.

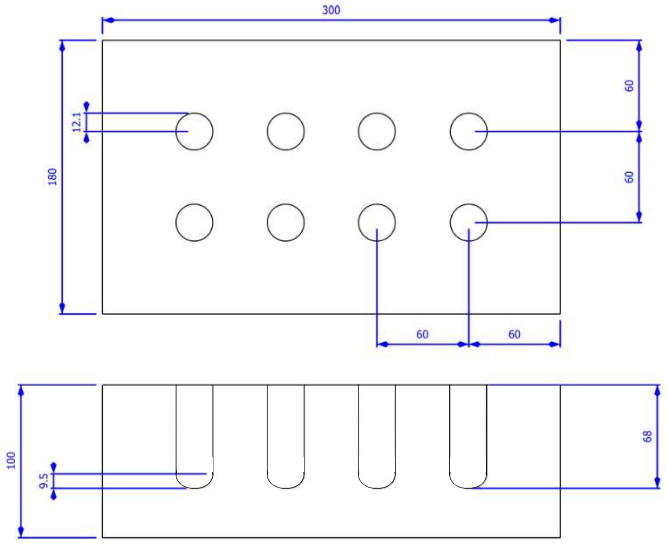

Figure 4.6 - Upper and cutted side view of the thermostable block. Sizes and dimensions in milimeters.

The thermal contact between of the heaters and the Pt-100 sensor with the aluminium block was guarantee using a thermal contact component (Dow Corning 340). The Figure 4.7 depicts the drawing of the side view of thermostable block.

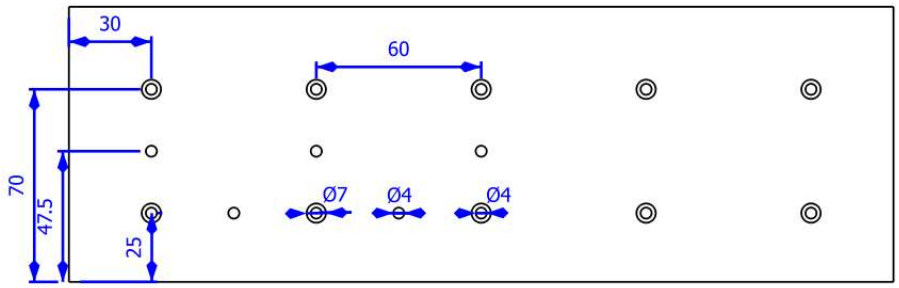

Figure 4.7 - Draw of the side view of the thermostable block including the location of the heaters and the Pt-100 cavities. Sizes and dimensions in milimeters.

In order to optimise the better conditions for the temperature control several locations of the Pt-100 temperature sensor and the heater power distribution were tested. A list of the specifications of the components used are listed in Table 4.1.

Table 4.1 - List of components used in the thermostable blocks and temperature control and its specifications.

	Brand/model	**Specification**
Resistance	Resisterma	50 W 230 VAC Ø6.5 x 175 mm
RTD	Pt-100	Class A 4 wires Ø4 x 150 mm
PID Temperature controller	Omron/E5DC	230 VAC 50 Hz
Solid-state relay	Omron/G3PE-215B	Input 24 VDC Load voltage 230 VAC

The thermal power input distribution was achieved using 10 heaters (50 W each) wired in parallel, and the location T2 of the Pt-100 (Figure 4.3) was found to be the best combination for a good temperature control. The temperature control of each thermostable block was made using a PID temperature controller (model Omron E5DC) and a solid-state relay (SSR) as a power actuator. Figure 4.8 depicts a schematic diagram of the temperature control system.

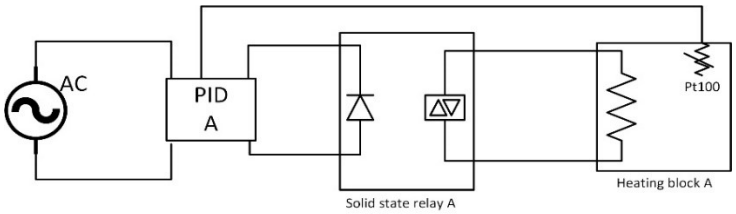

Figure 4.8 - Schematical electric diagram of the temperature control system of each thermostable block.

The temperature homogeneity evaluation and temperature calibration of each block was made by comparation of the PID controlled temperature with the temperature measured inside the sample tube using a calibrated thermometer (Fluke model 51 &52 Series II: certified K type thermocouple SN-25690313WS), in all the samples holes, with the air flowing as in the working operation. The deviation from the set point temperature was found to be less than ± 0.2 K in all the cavities. The average deviation was corrected in the PID temperature controller, taken as an offset value. The temperature of the samples in the conditions described before was checked periodically.

4.2. Air flow and control

The stability and accuracy of the air flow is essential to achieve a high precision measurement of the OS. The air flow regulation and control system (represented by the region C1, Figure 4.2) are depicted in Figure 4.9.

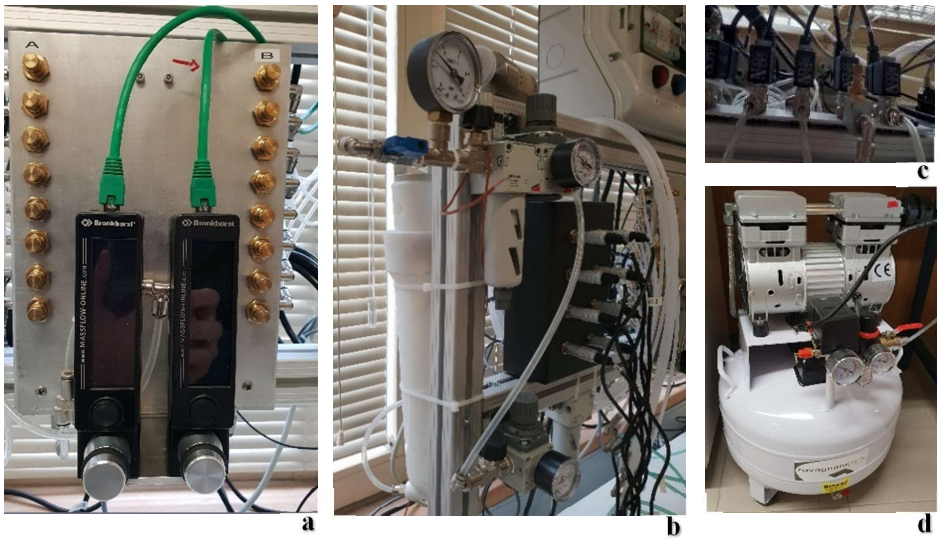

Figure 4.9 - Pictures of the air flow control system. “a” - Air flow control valves and mass flow regulator (Bronkhorst MV302); “b” - Air pressure regulation and micro filtration; “c” - Valves for air control (on/off) side A and B; “d” - Dry and oil free air compressor (Ravagnani SD70/8).

The air flow needs to be controlled and cannot have oscillations due to the pressure oscillations of the air compressor tank. To minimize the inlet pressure oscillations, two pressure regulators in series were installed as well as, an additional 1 litters tank installed at the low-pressure stage gas circuit. Both sides (A and B) should be able to work independently, and the working stage of each side should not lead to a significant perturbation in the inlet pressure. A scheme of the air flow control is presented schematically in Figure 4.10 and the list of components/parts in presented in Table 4.2.

Table 4.2 - list of components/parts used to assemble the air flow control system.

	Brand	**Model**
Air Compressor	Ravagnani	SD70/8
Filters	Camozzi	MC104-F00 MC104-F10
Control valve	Camozzi	RFU 482-1/8
Pressure regulator	Camozzi	MC104-R00 MC104-R10
Solenoid valves	Camozzi	G7J A322-1C2-NO A321-1C2-NC
Mass flow regulator	Bronkhorst	MV302

The pressure of the oil free air source of the compressor tank is based in an ON/OFF control type with a large pressure hysteresis (8 - 12 bar). To minimize this oscillation a reduction/regulation of the pressure was designed in three regulation stages. The pressure regulator in the compressor was set to 4 bars (stage 1). The inlet pressure of the air is after regulated in series by the use of two additional pressure regulators to 3 bar (stage 2) and 2 bar (stage 3). These reductions prove to be enough to stabilize the initial pressure oscillations of the compressor tank. A silica gel filter/tank was used to reduce the content of water and to increase the volume of line at the low-pressure stage (stage 3) in order to minimize the pressure oscillation which may affect the stability of the air flow regulation system. At the low-pressure level, the air stream is divided in two similar paths which are feeding the sides, A and B of the apparatus. The inlet air flow paths of side A and side B are close/open using a solenoid valve which is controlled by the software or by the operator in the switchboard. To avoid pressure oscillations, when any air path is closed, the air flow of the closed path is purged to an escape outlet with a similar flow regulation (typically 80 $L \cdot h^{-1}$). In each side (8 channels) the total air flow (typically 80 $L \cdot h^{-1}$) is regulated and measured by means of a mass flow controller, (Bronkhorst model MV302). The individual air flow of each channel is regulated by a needle

control valve (Camozzi, model RFU 482-1/8). The air flow adjustment of each channel was done using a calibrated digital flowmeter (Varian Intelligent Digital Flowmeter, model 1000 Series with the SN-US08C35194).

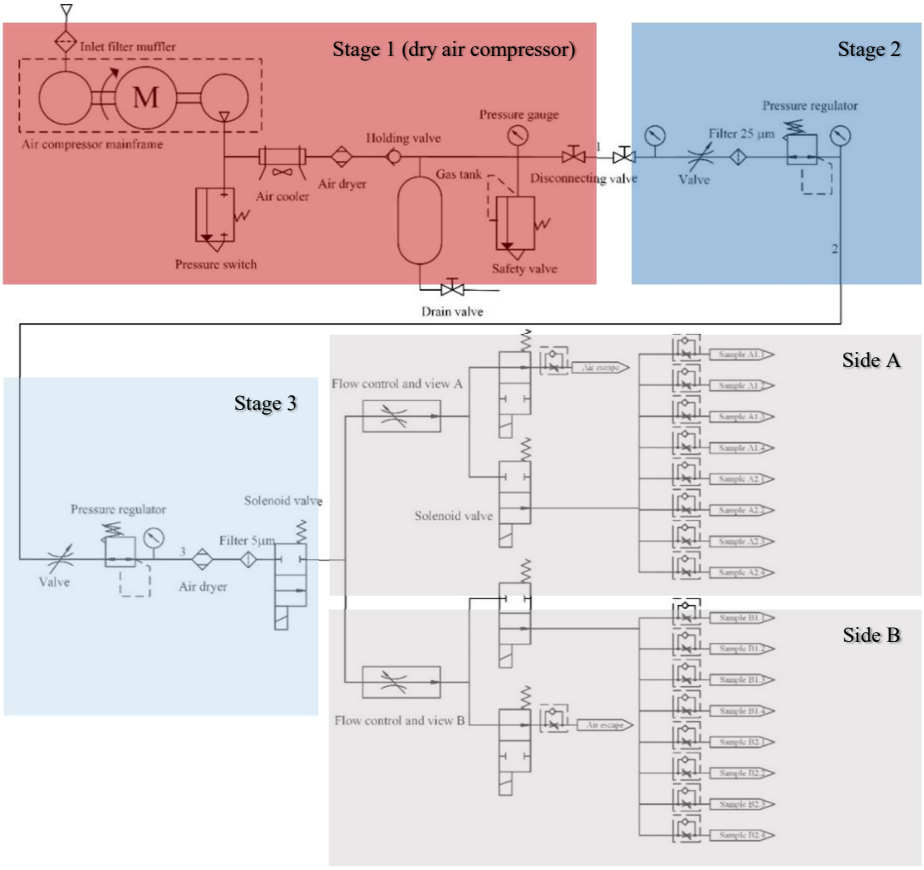

Figure 4.10 - Schematic representation for the air flow control system. Stage 1 – Dry air compressor; Stage 2 – Pressure reduction to 3 bar; Stage 3 – Pressure reduction to 2 bar; Side A and side B - fine flow regulation.

4.3. Data acquisition and control system

The data acquisition and control system are presented schematically in Figure 4.2 (region A2 and B2) and is responsible to measure the electrical conductivity of the detector cell. In Figure 4.11 it is represented a schematic diagram of the electric circuit used to measure the electrical conductivity of each cell (side A or B).

The electric alternated potential source was set with an electrical transformer, 240 VAC / 50 Hz to 8 VAC / 50 Hz. In order to increase the stabilization, the output sign and to avoid the risk of short circuit in the measuring cell a resistor of 120 ohms was installed in

series with each conductivity cells as represented in Figure 4.11. The electrical circuit includes also a circuit which is used to measure the electric alternated potential source (channel 101).

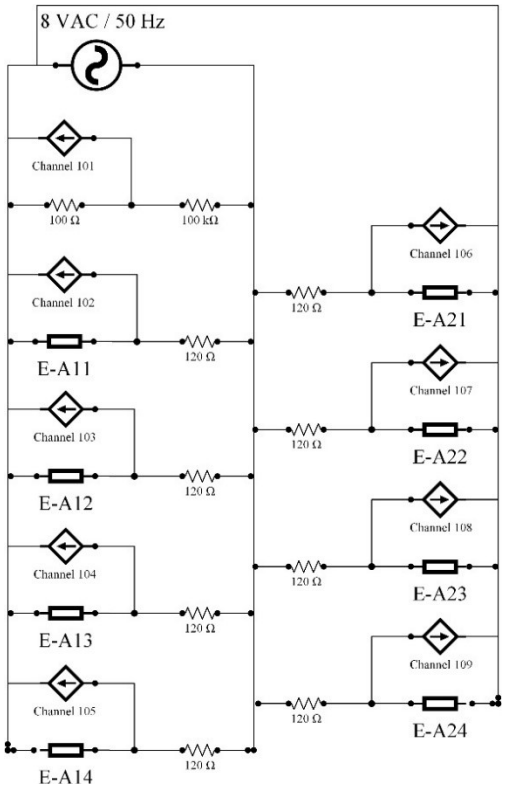

Figure 4.11 - Schematica diagrama of the electric circuit for the data acquisition (side A or B).

The data acquisition and control system were developed using a 6½ digits Data Acquisition/Data Logger Switch Unit (Agilent model 34972, using a 22 channels multiplexer (34901A) and 20 channels Actuator/GP Switch (34903A) boards). An overview of the data acquisition and control system is depicted in Figure 4.12.

a b

Figure 4.12 - Pictures of the data acquisition and control system and conductivity cell. “a”- Data Acquisition/Data Logger Switch Unit; “b” – Electrical onductivity cells.

4.4. RANCI_Data: Software for data acquisition and data analysis

A customized software application developed in VEE-Pro 9.33 (From Keysight) "RANCI_Data" was developed to perform the data acquisition and control of the RANCITECH apparatus. A simplified diagram of the software "RANCI_Data" is presented schematically in Figure 4.13.

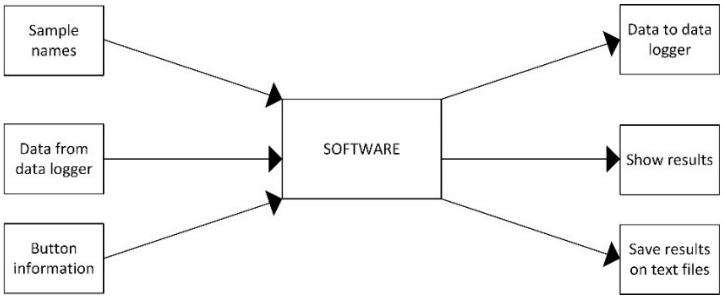

Figure 4.13 - Simplified schematic diagram of the software "RANCI_Data".

The software application is divided in two main functionalities:

- Experiments control and design: For this purpose, the software is switching the air flow and programming data logger system for the reading of a specific channel according the optimized procedure.
- Data Logging: The raw data is acquired in VAC and converted by software to conductivity units using the equation [4.1]. The results are saved in text format and shown in real time as a plot of conductivity versus time for each measuring channel.

$$k = \left(R_c \left(\frac{V_{source}}{V_{channel}} - 1 \right) \right)^{-1} K_{cel} \qquad [4.1]$$

In addition, the software also creates a LOG file in where all the actions taken by the user or by software are written and saved. To obtain this final result the data follows a path as schematically represented in the simplified flow diagram. Figure 4.14 depicts a scheme of information flow implemented in software.

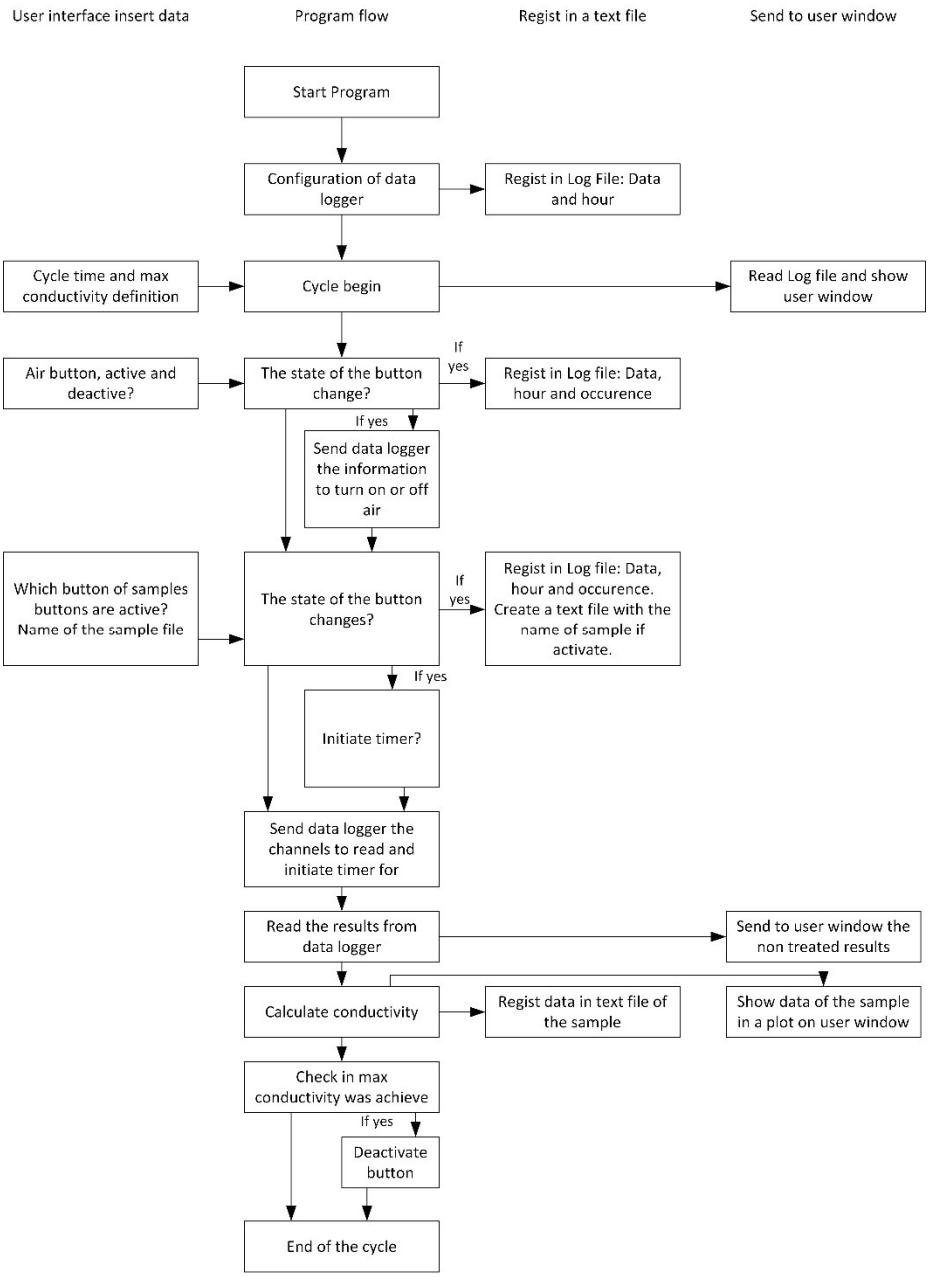

Figure 4.14 - Flow of information implemented in the software RANCI_Data.

A typical screen shot of the software RANCI_Data is depicted in Figure 4.15 (end of all (16) measuring cells experiments). In this figure (example of typical software output screen) all the samples achieved the threshold value of the programmed maximum conductivity.

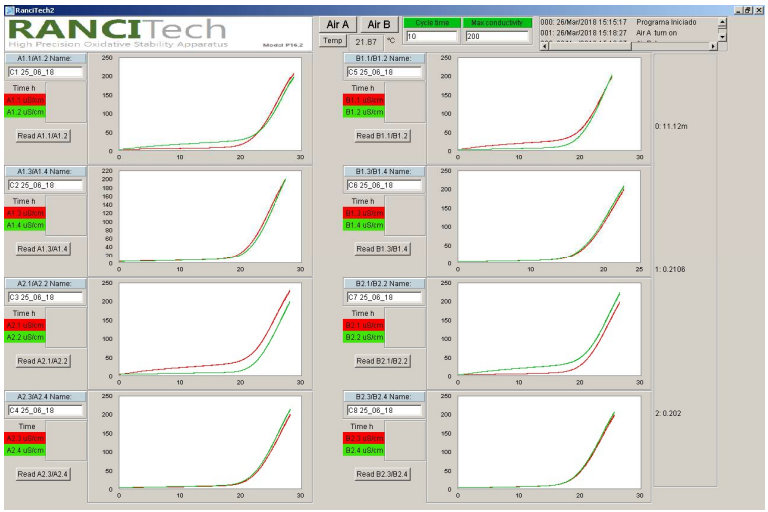

Figure 4.15 - Typical screen shot view of the software RANCI_Data .

4.5. RANCI_Cal: Software for OS data analysis

In order to increase the accuracy and repeatability of the calculation of the oxidative stability time (induction period) a customized software application "RANCI_Cal" was developed in Visual Basic using EXCEL platform as well as in VEE Pro. Both applications are fully compatible with data format used by the RANCI_Data software which avoids the data manipulation and conversion errors. The OS time (induction period, IP) was derived from the interception of the two time/conductivity linear regions as described in the chapter 1.5.5. An example of the software developed in the EXCEL platform is shown in Figure 4.16.

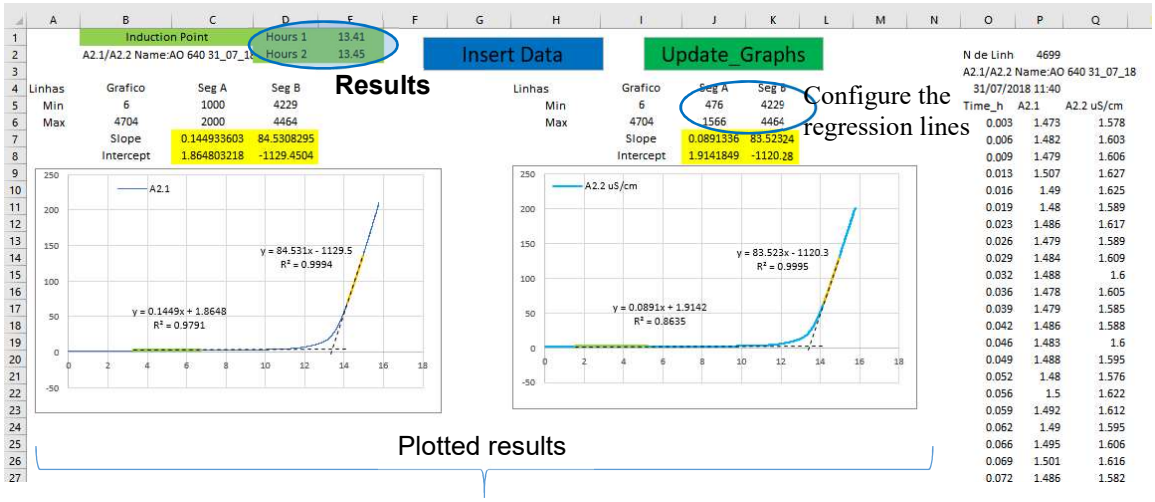

Figure 4.16 - Screen shot of the program developed in a Excel platform for the calculation and visualization of the experimental results.

The RANCI_Cal analysis software (version developed in VEE Pro) is depicted in Figure 4.17.

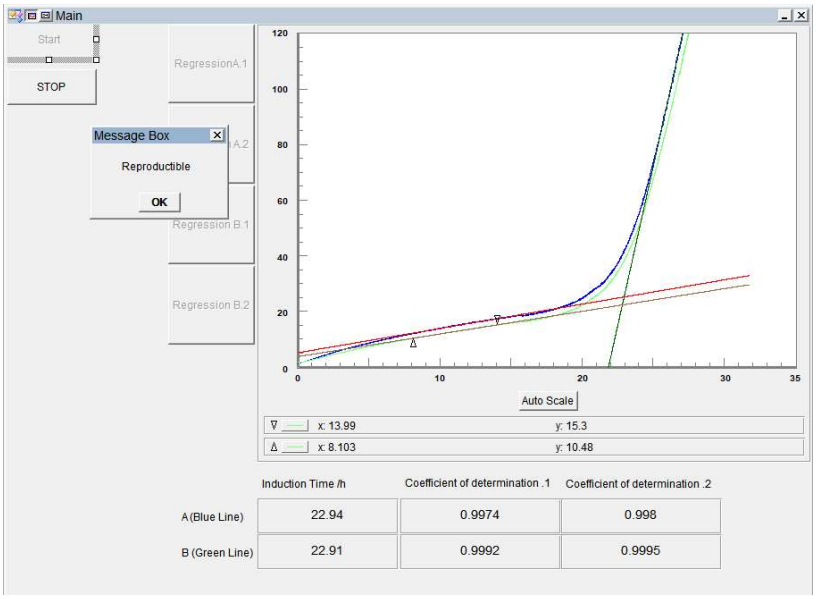

Figure 4.17 - Example of the program RANCI_Cal developed in VEE pro software for the calculation and visualization of the experimental results.

4.6. Test and Optimization of the RANCITECH apparatus

The evaluation of the repeatability of the results obtained in the RANCITECH apparatus a series of measurements have been done using the same batch of biodiesel in all the sample cavities/channels. The essays were done in four consecutive days according the EN14112 procedure. The biodiesel sample was kept under nitrogen atmosphere to avoid the oxidation.

The results obtained in the 16 sample cavities/channels (4 consecutive days) are presented in Figure 4.18. The test results obtained in the RANCITECH apparatus feet the repeatability criteria defined in the European normative 14112, described in equation [4.2]

$$r = 0.09 \cdot \overline{IP} + 0.16 \qquad [4.2]$$

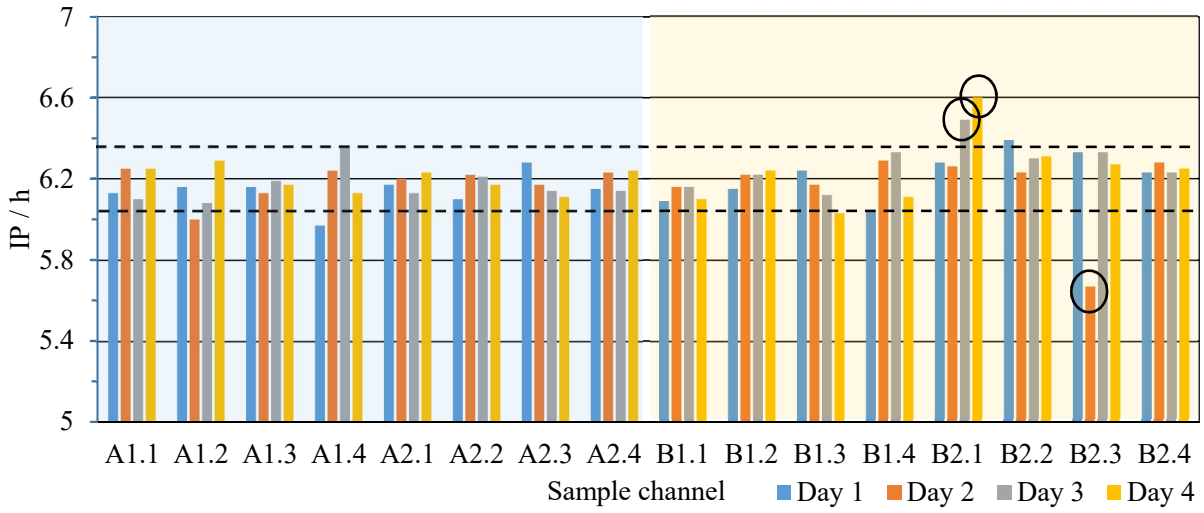

Figure 4.18 – Induction period, IP for the test series results. "---" lines indicate the uncertainty interval (for 95 % degree of confidence).

The overall mean value of 6.20 h with a standard deviation of 0.124 h was derived. Some (3 data points) test results were after considered as outliers results using the criteria of excessive deviation from the normal distribution (which could occur by erroneous sampling or irregular air flow condition in the essay). The outlier results are highlithed by "circule marks" in Figure 4.18. The obtained overall average (after removal of the average outliers' results) is 6.20 h and a standard deviation of 0.073 h is very similar than the initial average but presents a significant lower standard deviation.

Based on results obtained in this study, and in the uncertainty propagation of the partial uncertainties of air flow, time interval, temperature oscillation, and sampling, the following uncertainty equation (equation [4.3]) was derived for the estimation of the measuring uncertainty (95 % of confident interval).

$$IP = \overline{IP} \pm (0.02 \cdot \overline{IP} + 0.1) \qquad [4.3]$$

The uncertainty results obtained by the derived uncertainty equation (which was derived adopting very conservative uncertainty criterions) are in agreement with the uncertainty results obtained in the test set results and could be compared with the equation [4.2] for repeatability interval needed to by satisfy the EN 14112 for the measurement of the induction period (IP).

The results obtained in the RANCITECH apparatus were also compared with the of results obtained in a commercial apparatus, (Metrohm, Rancimat model 743) using the same

sample batch. The obtained results are presented in Figure 4.19 and are in excellent agreement and fulfil the repeatability interval needed to satisfy the EN 14112.

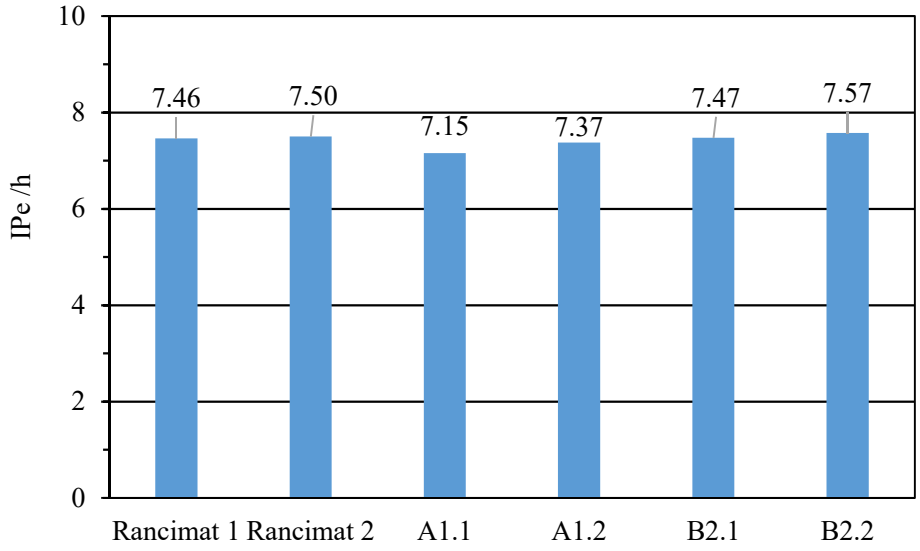

Figure 4.19 - Comparation of results of the RANCITECH with a commercial apparatus (Metrohm, Rancimat model 743).

Comparing the results obtained in both studies it was possible to conclude that the RANCITECH can produce reliable values for the OS with a higher reproducibility and lower uncertainty. These results could also be compared with the equation for the reproducibility where is verified that the values are inside the error given by the equation [4.4].

$$r = 0.26 \cdot \overline{IP} + 0.23 \qquad [4.4]$$

The obtained higher reproducibility and repeatability of the RANCITECH apparatus is due to the improved air flow control and the better temperature control and homogeneity of the thermostable block.

5. Oxidative stability study

The understanding of the oxidative stability (OS) of the biodiesel and its blends with mineral diesel is crucial to the development of new technological approach in order to improve the quality and applicability of this fuels. Subchapter 1.5 presents several works describing the study the behaviour of biodiesel and mineral diesel blends. The studies presented in the literature are dispersed, and it was not possible to draw conclusions about the critical conditions for the OS of the biodiesel and mineral diesel blends used in Portugal.

5.1. Experimental

Herein, the OS was extensively studied in different conditions in order to understand major factors which could be affecting the oxidative stability of biodiesel and biodiesel blends with mineral diesel. The following effects/condition were explored:

- Concentration effect in different biodiesel blends (5.2.1);
- Different concentrations of antioxidants in pure biodiesel (5.2.2);
- Concentration effect of biodiesel and antioxidants in the oxidative stability (5.2.3);
- Different antioxidants in a biodiesel blend (5.2.4);
- Different mineral diesels with biodiesel blends with antioxidants (5.2.5);
- Storage stability of pure biodiesel (5.2.6);
- Storage stability on biodiesel blends B7 and B14 (5.2.7);
- Effects of metal in storage stability of biodiesel blends B7 and B14 (5.2.8);
- Effect of water in storage stability of biodiesel blends B7 and B14 (5.2.9);
- Synergistic effect of metal and water in storage stability of biodiesel blends B7 and B14 (5.2.10).

5.1.1. Oxidative stability measurements

To measure the OS of the different sample two oxidative stability apparatus were used: a commercial apparatus from Metrohm (model Rancimat 743) and the RANCITECH apparatus, described in the chapter 4. The OS was measured following the procedure described in EN 14112. The value of the IP was obtained "manually" as described in the chapter 1.5.5. In Figure 5.1 is represented a schematic description of the IP meaning, as the end of the Initiation step (Region A), obtained by the interception of the two linear regimes (Region A and Region B).

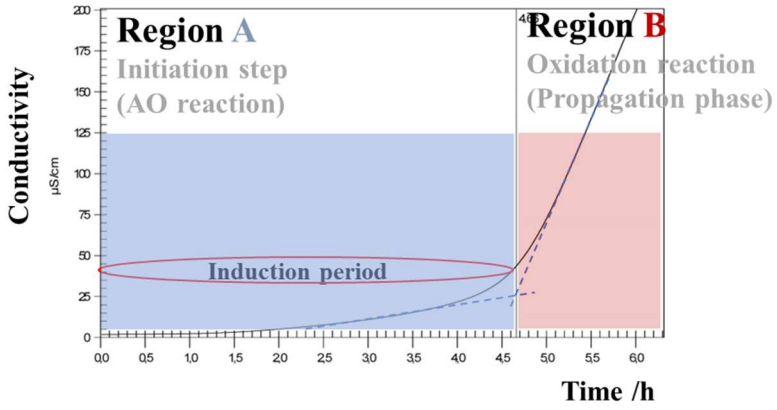

Figure 5.1 – Schematical representation of a typical OS result.

The biodiesel samples were analysed whenever possible upon reception. These samples were stored in a dark place without air contact (deposit full) and under nitrogen atmosphere.

5.1.2. Materials

For this study different sources, of mineral diesel and biodiesel batches were used, produced as recently as possible before the experiment or the preparation of the sample for storage to avoid uncontrolled oxidation during storage and for this reason it was necessary a new fuel for each experiment starting at different times. The biodiesel received was used in different studies and to facilitate the understanding of the results in Table 5.1 is given a name for each fuel, described the company that supplied the fuel and the subchapters of the thesis where these fuels are mentioned.

Table 5.1 - Fuels used, name, feedstock, source company and subchapters where the fuels are mentioned.(UCO – Used cooking oil)

Fuel Type	Batch Name	Feedstock composition	Source Company	Studies (subchapter)
Biodiesel	A	80 % UCO + 20 % Colza oil	Prio Energy	5.2.6; 5.2.7; 5.2.8; 5.2.9; 5.2.10 .
Biodiesel	B	80 % UCO + 20 % Colza oil	Prio Energy	5.2.6; 5.2.7; 5.2.8; 5.2.9; 5.2.10 .
Distilled biodiesel	C	85 % UCO + 15 % Animal fat	Enerfuel S. A.	5.2.1; 5.2.2; 5.2.3; 5.2.4; 5.2.5 .
Biodiesel	D	60 % UCO + 30 % Soy oil + 10 % Colza oil	Torrejana, S.A.	5.2.1; 5.2.2; 5.2.3 .
Biodiesel	E	80 % UCO + 20 % Colza oil	Prio Energy	5.2.1 .
Mineral diesel	X		Galp (Matosinhos)	5.2.6; 5.2.7; 5.2.8; 5.2.9; 5.2.10
Mineral diesel	W		Galp (Matosinhos)	5.2.1; 5.2.3; 5.2.5 .
Mineral diesel	Z		Galp (Sines)	5.2.1; 5.2.4; 5.2.5 .

The composition of the biodiesel samples used were analysed by gas chromatography (Agilent 6890N equipped with a DB-Wax) following the method described in EN 14103 showing the composition reported in Table 5.2 and Figure 5.2. The mineral diesels were analysed by gas chromatography (HP 5890 Series II with a HP-PONA) with an injector at 280 ºC and a detector at 270 ºC (temperature: 35 ºC hold for 20 min, programmed at 5 ºC.min^{-1} up to 250 ºC, hold for 30 min, programmed at 10 ºC.min^{-1} up to 310 ºC and hold for 21 min). The aromatic content was analysed externally, following the EN 12916:2016 at Sines refinery. The composition of paraffines that were possible to determine, and the aromatic content in the mineral diesel used is present in Table 5.3 and Figure 5.3. This table doesn't have the total composition of the mineral diesels and it was only used for comparative purposes.

Table 5.2 - Composition of the biodiesel batches used. (%(m/m)). Cx:y (x:alkyl chain syze; y: number of double bonds)

Compound	A	B	C	D	E
C6:0	-	0.01	0.00	0.00	0.00
C8:0	0.03	0.06	0.04	0.02	0.05
C10:0	0.02	0.03	0.02	0.01	0.02
C11:0	-	0.00	0.00	0.00	0.00
C12:0	0.10	0.08	0.04	0.02	0.08
C13:0	-	0.06	0.14	0.02	0.02
C14:0	0.409	0.64	0.53	0.23	0.43
C16:0	13.43	12.84	11.50	10.26	15.91
C16:1	0.61	0.90	0.77	0.41	0.44
C18:0	5.01	6.68	5.85	4.12	4.22
C18:1	32.00	37.51	42.64	34.47	38.26
C18:2	35.97	29.17	31.92	38.05	27.45
C18:3	3.14	3.00	0.44	3.94	3.31
C20:0	0.37	0.54	0.33	0.38	0.40
C22:0	0.40	0.04	0.28	0.45	0.34
C22:1	0.10	0.06	0.00	0.06	0.00
C24:0	0.15	0.17	0.07	0.16	0.12
C24:1	0.00	0.00	0.00	0.00	0.00
Saturated	19.92	21.15	18.80	15.67	21.59
Unsaturated	71.82	70.64	75.77	76.93	69.46

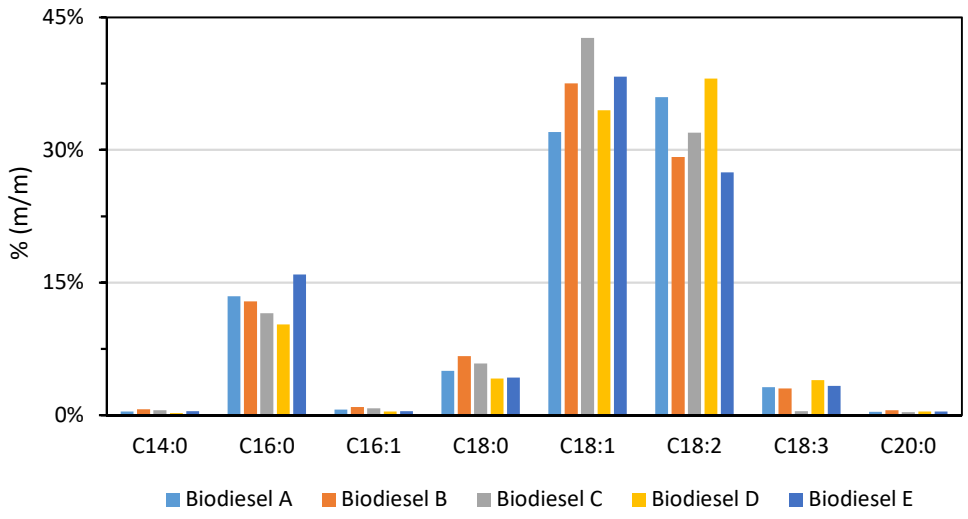

Figure 5.2 – Main composition of the diferent biodiesels batches used in this work.

Table 5.3 - Partial composition of the mineral diesels batches used In %(m/m). Cx (x: alkyl chain size); "()" - normalized fraction (%) (alkane composition).

Compound	X	W	Z
C7	0.02 (0.08)	0.02 (0.12)	0.07 (0.32)
C8	0.07 (0.30)	0.00 (0.01)	0.21 (0.90)
C9	0.14 (0.64)	0.23 (1.11)	0.54 (2.31)
C10	0.31 (1.42)	0.41 (2.00)	1.06 (4.51)
C11	0.54 (2.48)	0.60 (2.94)	1.19 (5.05)
C12	0.96 (4.42)	1.16 (5.72)	1.51 (6.45)
C13	1.88 (8.66)	2.26 (11.2)	2.30 (9.80)
C14	2.40 (11.1)	2.50 (12.3)	2.42 (10.3)
C15	2.54 (11.7)	2.77 (13.7)	2.57 (11.0)
C16	2.10 (9.65)	2.25 (11.1)	2.16 (9.21)
C17	2.19 (10.1)	2.26 (11.1)	2.16 (9.22)
C18	1.88 (8.66)	1.81 (8.91)	1.72 (7.33)
C19	1.91 (8.79)	1.29 (6.38)	1.63 (6.96)
C20	1.50 (6.90)	0.93 (4.57)	1.07 (4.56)
C21	1.11 (5.10)	0.67 (3.28)	0.81 (3.47)
C22	0.77 (3.53)	0.40 (1.96)	0.68 (2.88)
C23	0.57 (2.64)	0.29 (1.42)	0.52 (2.21)
C24	0.40 (1.85)	0.22 (1.08)	0.36 (1.52)
C25	0.23 (1.07)	0.15 (0.76)	0.22 (0.91)
C26	0.15 (0.69)	0.01 (0.02)	0.15 (0.64)
C27	0.07 (0.30)	0.07 (0.33)	0.11 (0.49)
Mono-aromatic	-	19.6	19.1
Di-aromatic	-	2.5	2.2
Tri-aromatic	-	0.2	0.1

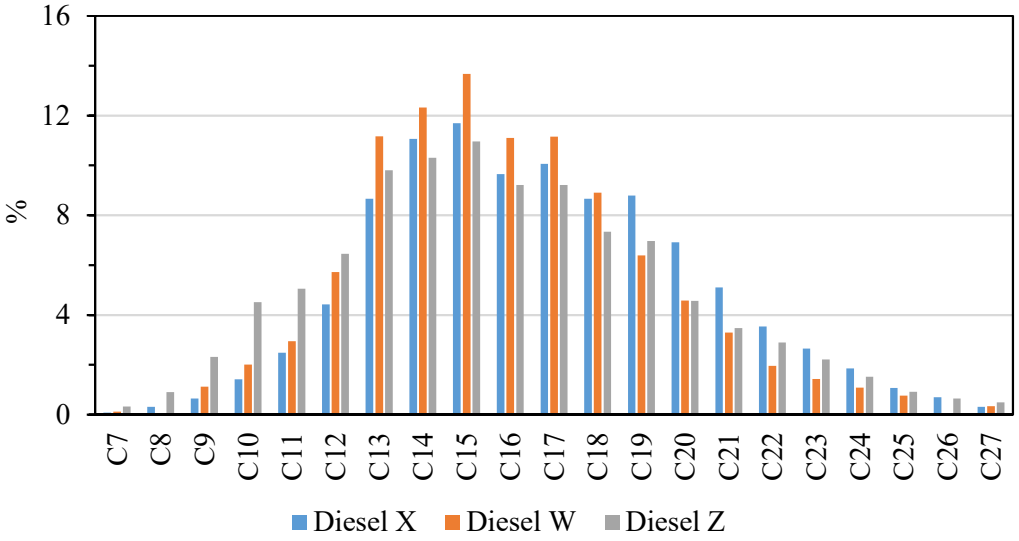

Figure 5.3 – Normalized fraction (alkane composition) of the diferent batches of mineral diesel.

The properties of all these fuels were analysed by the Matosinhos refinery laboratory technicians, and the results for the biodiesel analysis are shown in Table 5.4 (biodiesel) and Table 5.5 (mineral diesel).

Table 5.4 – Overview of the relevant properties of the biodiesel batches.

Property	Unit	A	B	C	D	E
Ester content	(m/m)	95.5	98.4	98.4	96	94.5
Density at 15 ºC	$kg \cdot m^{-3}$	883.8	880.5	880.4	883.9	883
Viscosity at 40 ºC	$mm^2 \cdot s^{-1}$	4.468	4.289	4.256	4.343	4.573
Flash point	ºC	162	170	182	145	152
Sulphur content	$mg \cdot kg^{-1}$	11.8	4.5	1.9	3.8	7.2
Water content	(m/m)	0.018	0.072	0.024	0.042	0.014
Total contamination	$mg \cdot kg^{-1}$	<12	>30	2	<12	13
Acid value	mg $KOH \cdot g^{-1}$	0.45565	0.44035	0.3	0.4039	0.48415
Iodine value	g $iodine \cdot 100g^{-1}$	115.6	113.85	100	115.75	95.9
Linolenic acid methyl ester	(m/m)	3.14	3.00	--	3.96	3.32
CP	ºC	--	9	2	3	5
CFPP	ºC	--	-3	-1	-4	-4

Table 5.5 - Properties of the mineral diesel batches.

Property	Unit	X	W	Z
Density at 15 ºC	$kg \cdot m^{-3}$	841.2	839.7	839.0
Viscosity at 40 ºC	cSt	3.461	--	--
Flash point	ºC	73	69.0	--
Water content	(m/m)	0.003	0.007	--
Sulphur	$mg \cdot kg^{-1}$	11.8	9.0	--
CFPP	ºC	-6	-7	--
CP	ºC	-1	-2	--
Cetane number	--	--	51.5	52.4
Cetane Index	--	--	53.8	53.9
Total contamination	$mg \cdot kg^{-1}$	--	14.0	--
Recovered at 250	%(v/v)	26.0	26.2	25.8
Recovered at 350	%(v/v)	87.5	90.1	91.9

In Table 5.4 is given a higher value for the ester content. This is due to the method follow to measure the ester content at the refinery that considers all the points detected in the GC. It is also saw a good agreement between the iodine value and the total unsaturated value obtained except for the biodiesel C.

The AOs used for this test were composed by vitamin E, given by Enerfuel S.A., and the Baynox® plus (2,2'-Methylenebis(4-methyl-6-tert-butylphenol)) supplied by Torrejana S.A. The structures of these molecules are shown in Figure 5.4.

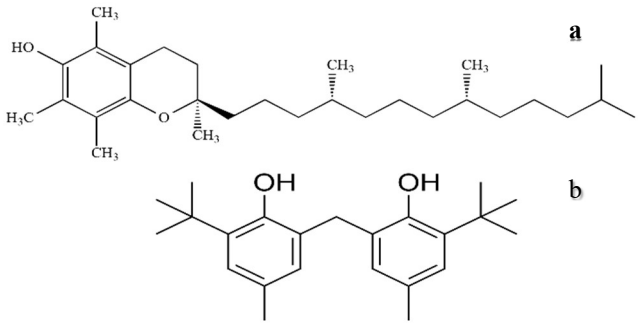

Figure 5.4 - Molecular structures of the AOs used. “a” Vitamin E; “b” - 2,2'-Methylenebis(4-methyl-6-tert-butylphenol).

5.1.3. Sample preparation

For the study of the concentration of biodiesel and AOs, batches of 200 ml of blends in a glass bottle of 250 mL, using a volumetric pipette were prepared. The samples were mixed for 10 min using a magnetic stirrer at 500 rpm. The samples were analysed as soon as possible to avoid oxidation.

The blend used for the storage test stability were prepared in a 10 L glass bottle. The blend (biodiesel + mineral diesel) was stirred 2 hours using a magnetic stirrer at 700 rpm.

This global mixture was then divided by several storage bottles. The storage of the samples under different conditions was made using bottles of 1 L with samples of 500 mL, which make possible the contact of the fuel with the atmosphere. These bottles were closed with a cover prepared for the conditions of storage as exemplified in Figure 5.5. The nitrogen atmosphere was created by passing nitrogen gas above the surface of the fuel and not through the fuel. The dry air atmosphere was made using a silica gel deposit to dry the air that enters the sample and the normal atmosphere samples are equipped with a tube with an empty deposit to avoid contamination.

These samples were stored in a dark place at constant temperature (21 ± 1 ºC) and are not mixed along the time of storage. The samples for the test were sampled from the bulk of the glass bottles using a syringe.

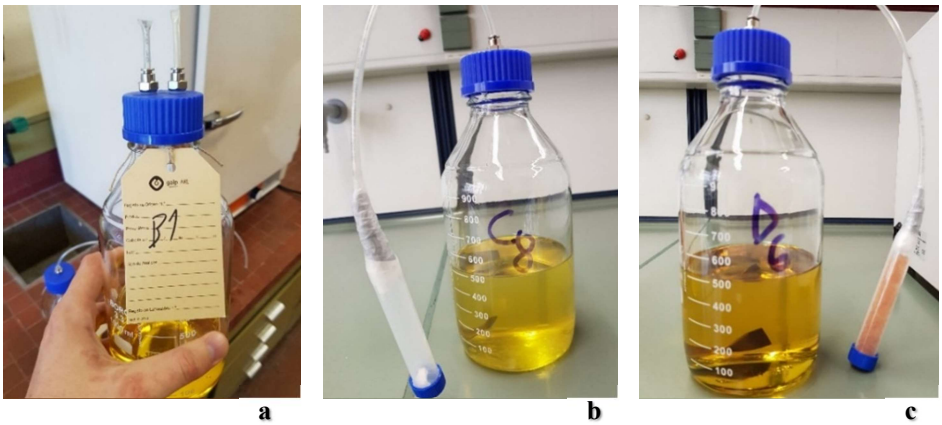

a b c

Figure 5.5 - Example of samples for the study of the storage stability. “a” - Nitrogen atmosphere sample; “b” - Open to normal atmosphere; “c” - Open atmosphere with dry air.

In the storage stability studies that were carried out in presence of a metal, it was used a small metal piece (50x15x1.5 mm) of an alloy (Steel NP-Fe360-2) similar to the material present in the storage tanks at Galp. The steel was analysed by scanning electron microscope (SEM) at CEMUP, to evaluate their composition and morphology (Table 5.6). The silicon present in the steel could be due to sandpaper used to clean the metal surface. The Figure 5.6 depicts an image of the metal piece used and a SEM image of its surface.

Table 5.6 - Average composition of the alloy (Steel NP-Fe360-2).

Element	**Composition** / %(m/m)
C	3.5
O	4.6
Si	0.7
Fe	92.3

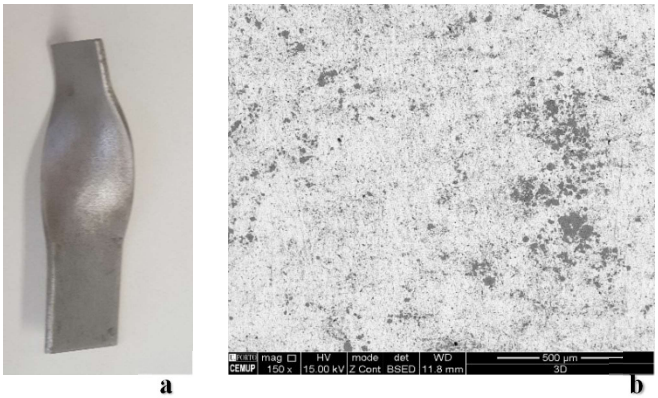

a b

Figure 5.6 - “a” - Picture of the metal piece (50x15x1.5 mm). “b” - SEM image (150 X) of the steel surface used for the study of the metal effect in storage stability tests.

5.2. Results of the oxidative stability studies

For the storage stability study some of the results are scattered and there are some points higher than those previous measured that are meaningless. For that reason, will be present the results for both experiments and the line that represent the decay of the IP as a function of the storage time.

The OS study, based in study of the dependence of the induction period, IP, was analysed in order to establish the relation between the IP and the biodiesel and AO concentration in the blends. The rate of the induction process was related with the inverse of the IP time as expressed in equation [5.1].

$$Rate\ of\ induction\ process = f(\frac{1}{IP}) \qquad [5.1]$$

5.2.1. Concentration effect in different biodiesel blends

The study of the effect of biodiesel concentration on the OS was carried out to understand the influence of the biodiesel and diesel used in the blends. For this purpose, three different biodiesels batches “C”, “D” and “E” with different levels of total unsaturation and/or sample history (e.g. “C” was distilled) were used. These biodiesels are blended with the mineral diesel “W” and “Z”. With these combinations was possible to analyse the effect of the mineral diesel composition, the effect of blends with distilled biodiesel (without natural AOs), and the effect of different biodiesel compositions.

The samples with the same mineral diesel were prepared at the same time and analysed in the RANCITECH apparatus. The results of the different biodiesels with diesel “W” are shown in Figure 5.7 and with mineral diesel “Z” in Figure 5.8. The samples of the blends with mineral diesel “Z” were prepared 75 days after the preparation of the samples with mineral diesel “W”; during this period the biodiesel were stored under nitrogen atmosphere.

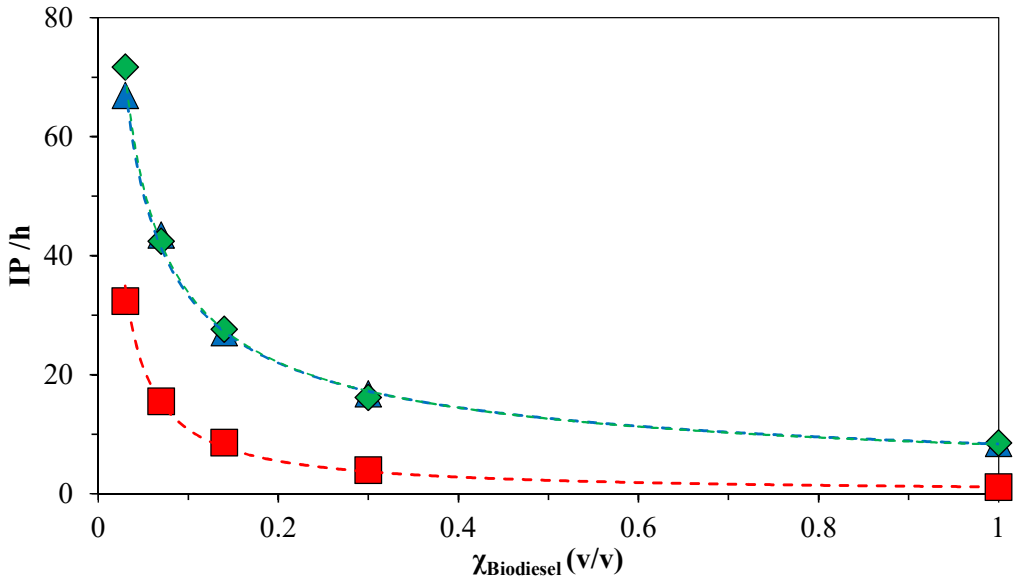

Figure 5.7 - Plot of oxidative stability (IP) as a function of biodiesel blends concentration with mineral diesel "W". ■ - Biodiesel "C"; ▲ - Biodiesel "D"; ♦ - Biodiesel "E".

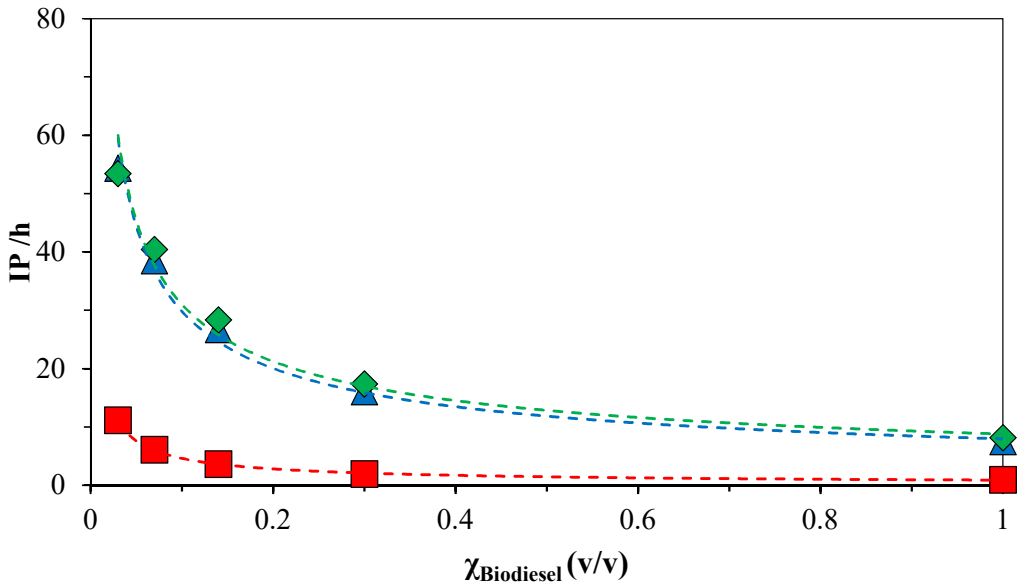

Figure 5.8 - Plot of oxidative stability (IP) as a function of biodiesel blends concentration with mineral diesel "Z". ■ - Biodiesel "C"; ▲ - Biodiesel "D"; ♦ - Biodiesel "E".

Analysing these results, it is observed that the biodiesel concentration has a strong effect in the OS of blends. The dilution of the biodiesel in the mineral diesel have a strong effect in oxidative stability of the blend. The biodiesels "D" and "E" have a similar behaviour along the

concentration profile in both situations. Comparing these two biodiesels the biodiesel "D" has a slightly lower OS. This could be explained by the higher total unsaturation of biodiesel "D".

Comparing the results in Figure 5.7 and Figure 5.8 it is observable a global decrease in the OS due to the lower OS of the intrinsically mineral diesel "Z". The biodiesel "C" has a deviation in the profile, this result could be due to the time difference between samples. This biodiesel doesn't have a natural capacity to resist oxidation, since the distillation process takes out the AOs present naturally in the biodiesel.

Based on these results the dependence of the oxidative stability (given as IP) with the biodiesel concentration was studied and a good linear dependence between the inverse of the IP (related with the rate of the induction process) and the concentration of the biodiesel was found, as depicted in Figure 5.9 and Figure 5.10.

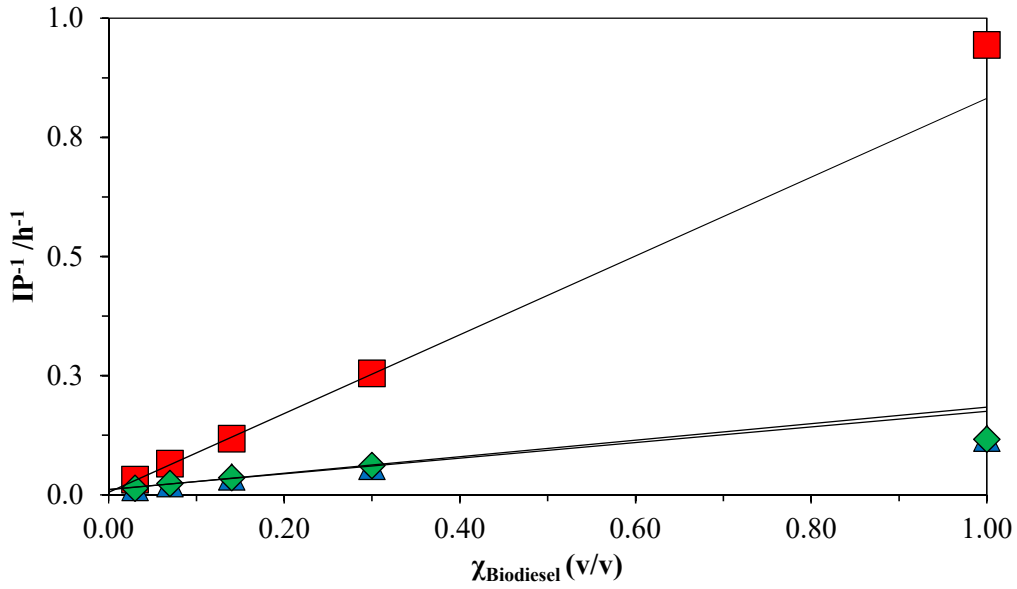

Figure 5.9 - Study of the dependence 1/IP with biodiesel concentration in blends with mineral diesel "W". ■ - Biodiesel "C" (y = (0.8264±0.0146)x + 0.0053±0.0025); ▲- Biodiesel "D" (y = (0.1635±0.0108)x + 0.0116±0.0018); ♦ - Biodiesel "E" (y = (0.1733±0.0088)x + 0.0105±0.0015).

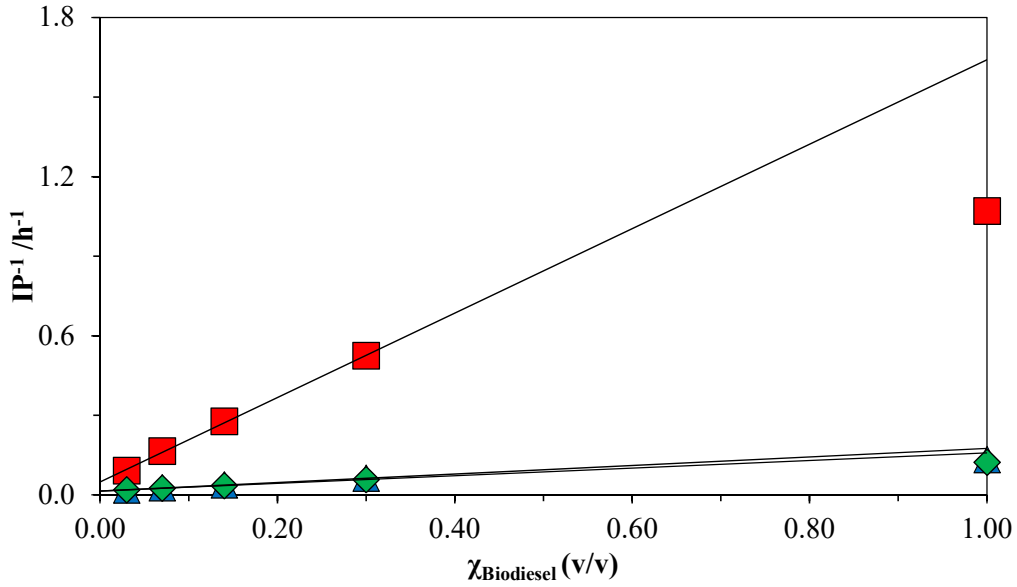

Figure 5.10 - Study of the dependence 1/IP with biodiesel concentration in blends with mineral diesel "Z". ■ - Biodiesel "C" (y = (1.5929±0.0053)x + 0.0482±0.0053); ▲- Biodiesel "D" (y = (0.1610±0.0037)x + 0.0143±0.0006); ♦ - Biodiesel "E" (y = (0.1436±0.0020)x + 0.0147±0.0003).

The fitted dependence coefficients, between the inverse of the induction period (1/IP) and the concentration of biodiesel is very similar between biodiesel "D" and "E" and significantly larger for the biodiesel "C" (distilled).

5.2.2. Different concentrations of antioxidant in pure biodiesel

The AOs are commonly used in industry to achieve the minimum required OS for the pure biodiesel. The selection of the AOs should take in to account the composition or the process of production of the biodiesel. In this work the influence of different concentrations of AOs (vitamin E) in two different biodiesels was studied. Biodiesel "C" and "D" with different concentrations of AO (160 ppm, 320 ppm and 640 ppm) were analysed in RANCITECH (Figure 5.11 and Figure 5.12).

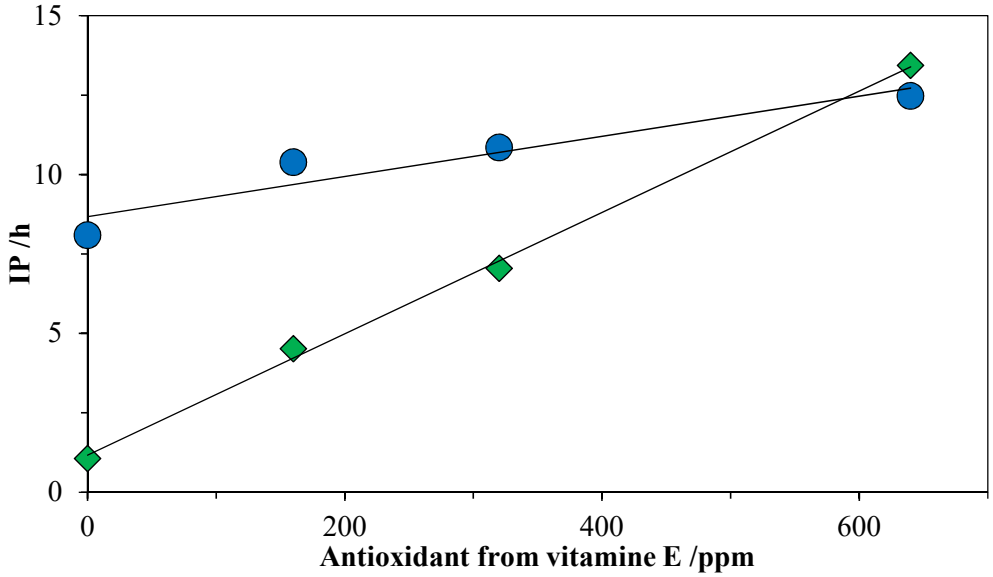

Figure 5.11 - Oxidative stability as a function of the AO concentration from Enerfuel with different biodiesel. ♦ - Biodiesel C; ● – Biodiesel D.

It was found that the induction period, IP show a linear increase with the concentration of AO. The AO has a significant higher effect in the increase of the IP (around 1.9 h /100 ppm) in the biodiesel "C" (distilled biodiesel) than in the biodiesel "D" (0.6 h /100 ppm) which can be related with the impact of the AO naturally present in the biodiesel "D".

5.2.3. Concentration effect of biodiesel and antioxidant in the oxidative stability

In this chapter is presented the study regarding the effect of the presence and concentration of AOs in the OS of biodiesel and mineral diesel blends with different concentrations of biodiesel. For this purpose, blends of biodiesel mineral diesel "W" were prepared using biodiesel "C" and "D" samples with different concentration AOs (vitamin E) as described previously (5.2.2). The effect of biodiesel "C" and "D" concentration (B3, B7, B14, B30) in the blend was study using a fixed AO concentration (320 ppm). The effect AO concentration (640, 320, 160 ppm) was study in biodiesel "C" and "D" blends, B7 and B30. The results are shown in Figure 5.12 (biodiesel "C") and Figure 5.13 (biodiesel "D"), where the concentrations of AO are referred to the concentration of AO in the biodiesel.

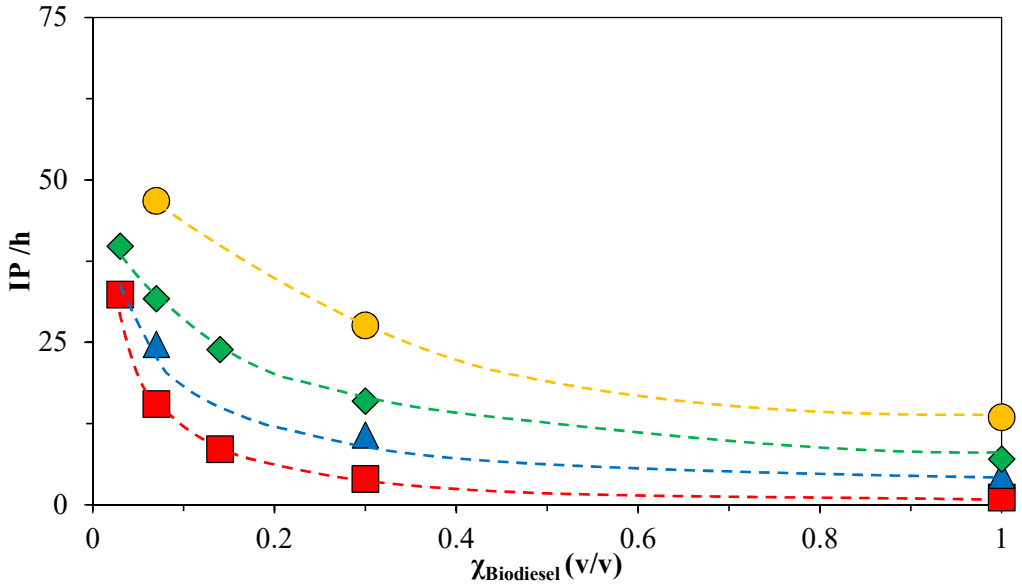

Figure 5.12 - Plot of oxidative stability (IP) as a function of biodiesel "C" concentration with AO and with mineral diesel "W". ■ – 0 ppm; ▲ - 160 ppm; ♦ - 320 ppm; ○ – 640 ppm.

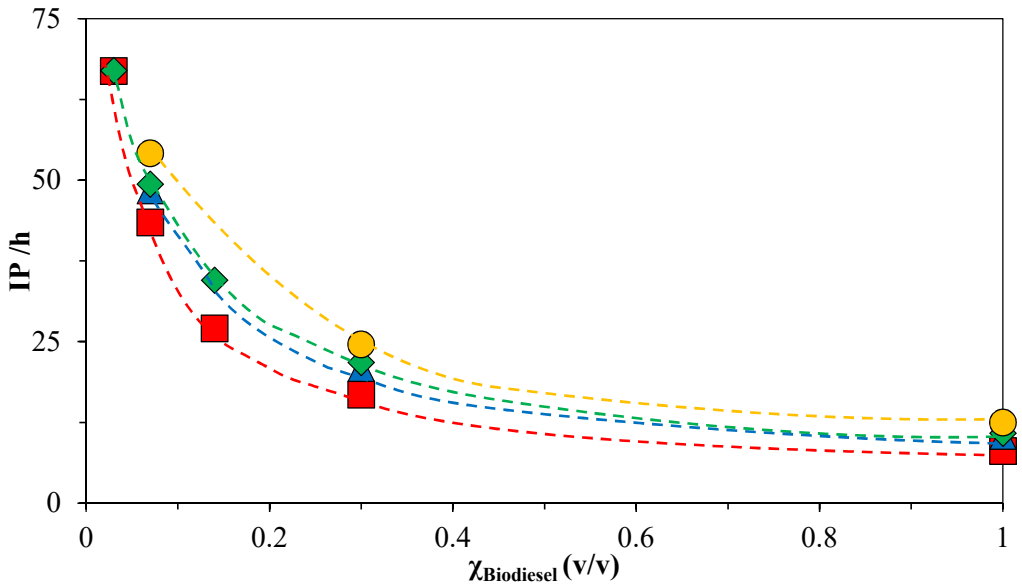

Figure 5.13 - Plot of oxidative stability (IP) as a function of biodiesel "D" concentration with AO and with mineral diesel "W". ■ – 0 ppm; ▲ - 160 ppm; ♦ - 320 ppm; ○ – 640 ppm.

These results were again used to evaluate the correlation between the IP (or 1/IP which is related with the rate of process occurring in the induction period), now in the presence of the AO (Figure 5.14 and Figure 5.15)

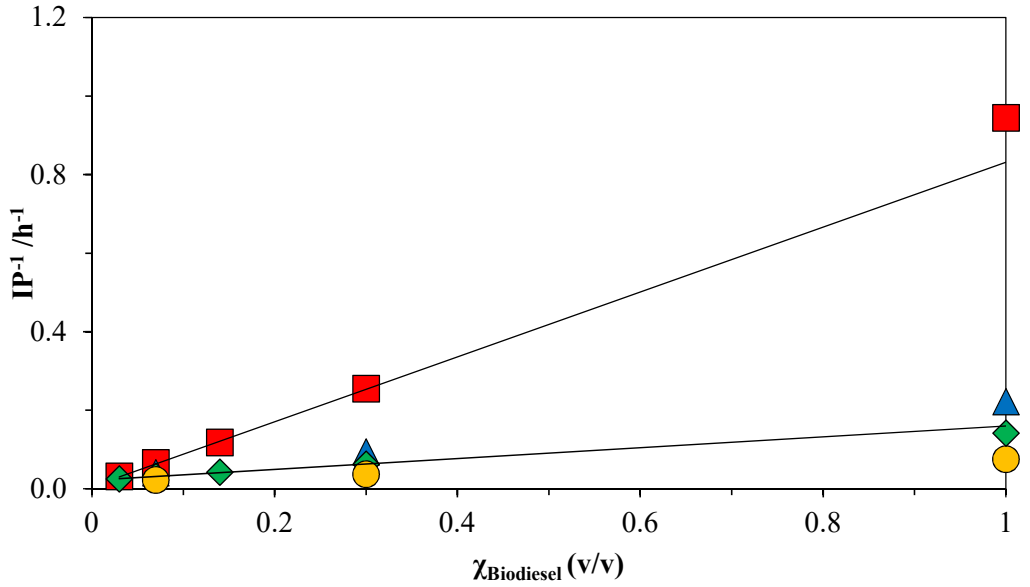

Figure 5.14 - Study of the dependence 1/IP with of biodiesel "C" concentration with AOs (vitamine E) in blend with mineral diesel "W". ■ – 0 ppm (y = 0.8264x + 0.0053); ▲- 160 ppm; ♦ - 320 ppm (y = 0.1383x + 0.0217); ○ – 640 ppm.

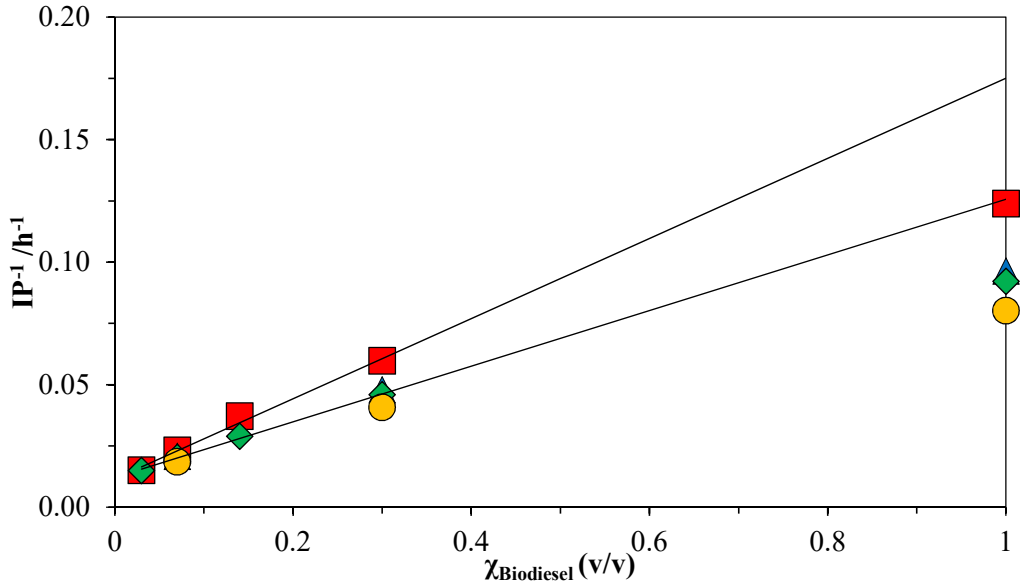

Figure 5.15 - Study of the dependence 1/IP with of biodiesel "D" concentration with AOs (vitamine E) in blend with mineral diesel "W". ■ – 0 ppm (y = 0.1635x + 0.0116); ▲- 160 ppm; ♦ - 320 ppm (y = 0.1136x + 0.0122); ○ – 640 ppm.

Analogous than the observed before a linear dependence was found between the value of (1/IP, inverse of the induction period) and the biodiesel concentration. The blends with biodiesel "C" which have previously distilled (and as a consequence the presence of natural antioxidants is residual) show a marked effect in the OS with the increase of the AO even for lower concentrations of biodiesel.

The AO concentration does not change the linearity dependence of 1/IP with biodiesel concentration but leads to a decrease of the slope with the increase of the AO concentration, reflecting the increase of initial antioxidative stability of the biodiesel by addition of the AO.

The influence of the concentration of AO with the dilution of biodiesel in the blend (B7, B30) and B100 as a function of the concentration of AO is depicted in Figure 5.16 and Figure 5.17.

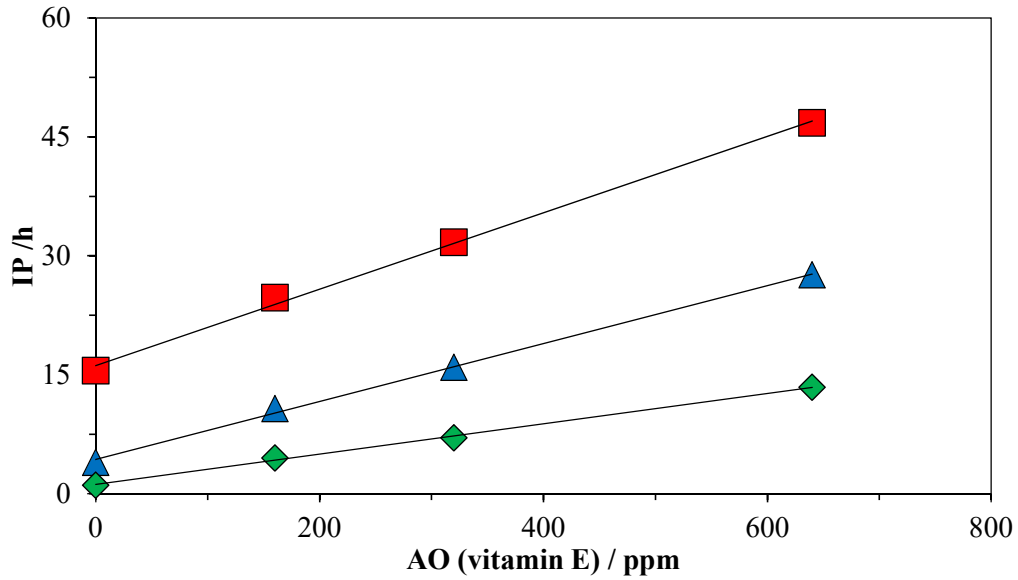

Figure 5.16 - Study of the influence of the AO in blends of biodiesel "C" with mineral diesel "W". ■ – B7 ppm; ▲ - B30; ♦ -B100.

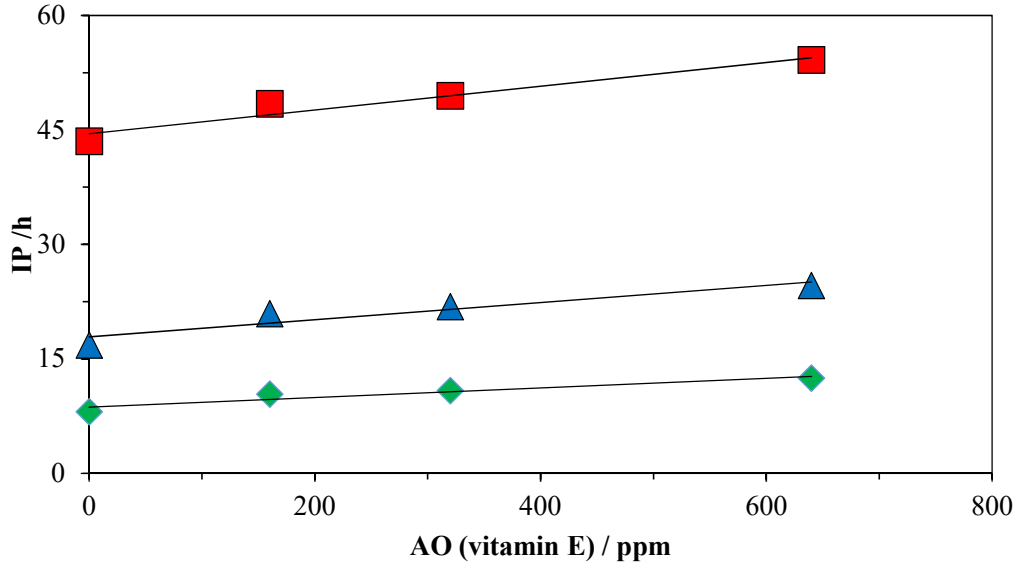

Figure 5.17 - Study of the influence of the AO in blends of biodiesel "D" with mineral diesel "W". ■ – B7 ppm; ▲ - B30; ♦ - B100.

Based on the analysis of the Figure 5.17 is observed that the AO (vitamin E) as a minor effect in the oxidative stability of the blends involving biodiesel "D" (with natural antioxidants). However, in the case of the blends involving biodiesel "C" (without natural antioxidants) the effect of the AO (vitamin E) is quite significant and is progressively stronger with the dilution of the biodiesel in the blend.

5.2.4. Different antioxidants in a biodiesel blend

To understand the AO effect, the effect of the presence of a synthetic AO "BAYNOX plus" [2,2'-Methylenebis(4-methyl-6-tert-butylphenol)] was studied and compared the results with those obtained for the vitamin E. In Figure 5.18 depicts the results of the effect both AOs observed in different blends (B3, B7, B14, B30 and B100) composed by mineral diesel "Z" and biodiesel "C".

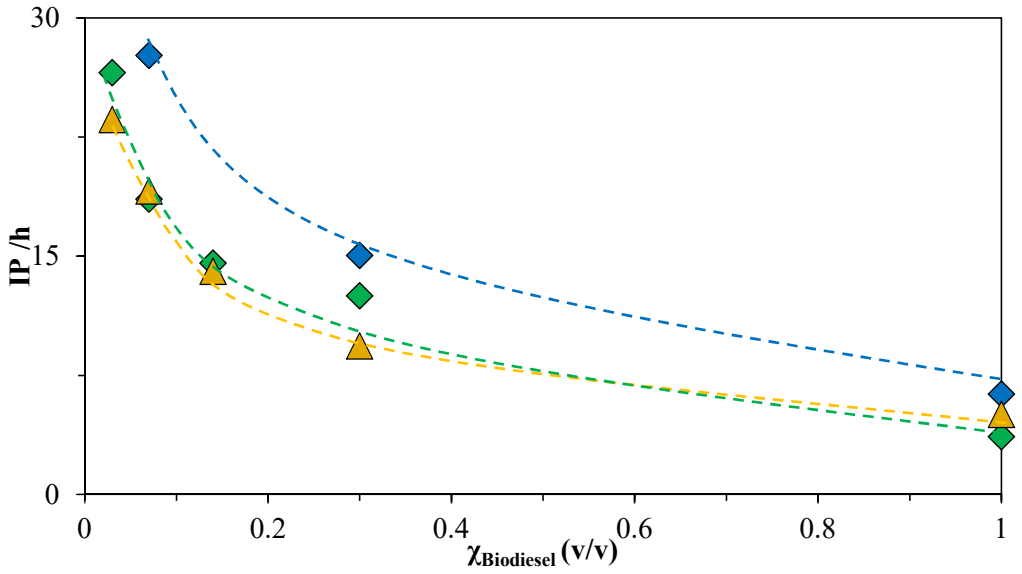

Figure 5.18 - Oxidative stability as a function of biodiesel "C" concentration with mineral diesel "Z", comparing different types of AO. △- 305 ppm "vitamin E"; ♦ - 300 ppm from "BAYNOX plus"; ♦ – 500 ppm "BAYNOX plus".

The results of this study show that the both AOs present the same effectiveness in this biodiesel and blends.

5.2.5. Different mineral diesel with biodiesel blends with antioxidant

To conclude the AO studies, was evaluated if the two different mineral diesels had some influence in the effectiveness of the AO. For this study was prepared blends of mineral diesel "W" with the biodiesel "C" with 320 ppm of AO (vitamin E). The results are shown in Figure 5.19.

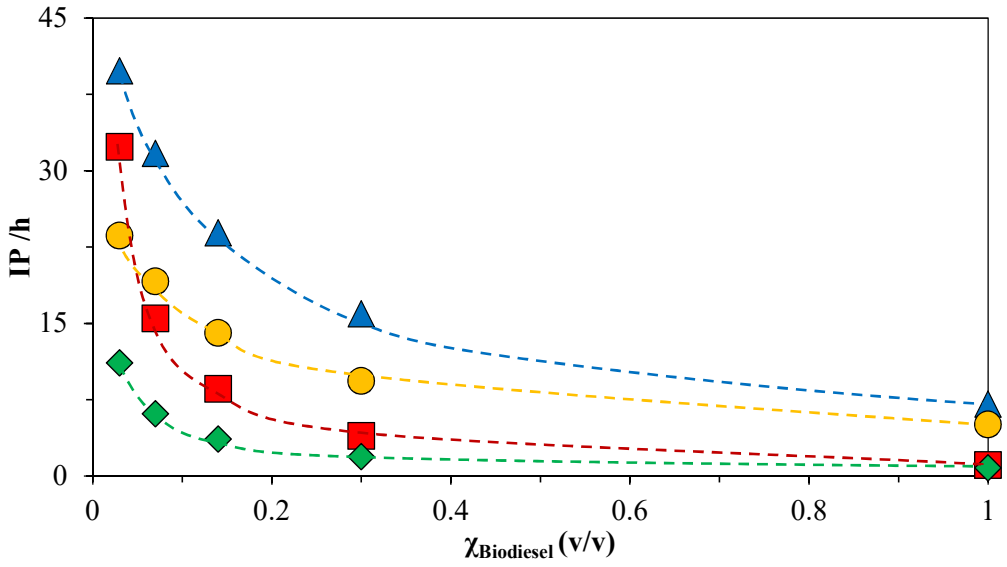

Figure 5.19 - Study of the AO effect regarding the use of two different mineral diesel blended with biodiesel C. ♦ - Blends diesel "Z" with biodiesel "C" 0 ppm; ● - Blends diesel "Z" with biodiesel "C" 320 ppm; ■ – Blends diesel "W" with biodiesel "C" 0 ppm; ▲ - Blends diesel "W" with biodiesel "C" 320 ppm.

These results show the IP increment by the addition of the AO (vitamin E) in both mineral diesels is identical and dependent of the influence of the pure biodiesel and mineral diesel, for the different batches concentrations for the biodiesel "C" (without natural antioxidants).

5.2.6. Storage stability of pure biodiesel

The study of the time evolution of the oxidative stability "storage stability" of pure biodiesels and blends under different conditions was done, analysing the time evolution of the induction period with the storage time.

The study of the storage of biodiesel was carried out to understand the evolution of the induction period (IP) along the storage time. The time evolution of the OS with storage time of pure biodiesel "A" and "B" was study keeping the biodiesel under dry nitrogen and dry air

atmosphere. The samples of biodiesel "A" (Figure 5.20) were stored for a period of 140 days and analyses in the Rancimat apparatus (Figure 5.21).

Figure 5.20 - Pictures of samples of biodiesel "A" under nitrogen (a) and dry air (b).

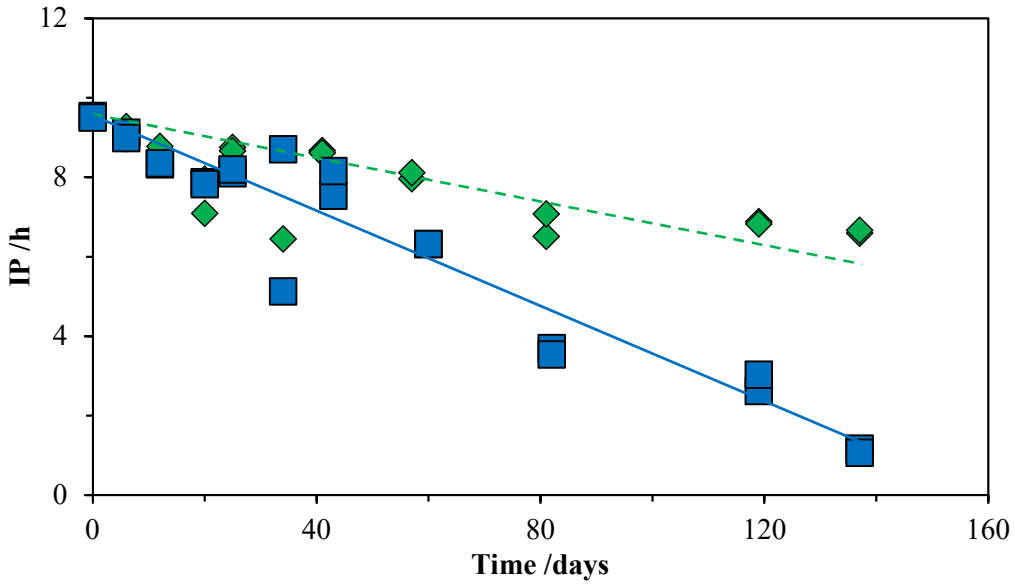

Figure 5.21 - Results for the storage stability over time for biodiesel "A", under nitrogen (---◆) and dry air (—■) atmosphere measured in a Rancimat apparatus.

The samples of biodiesel "B" (Figure 5.22) were analysed in the RANCITECH apparatus during a period of 50 days (Figure 5.23).

Figure 5.22 - Pictures of samples of biodiesel "B" under nitrogen (a) and dry air (b).

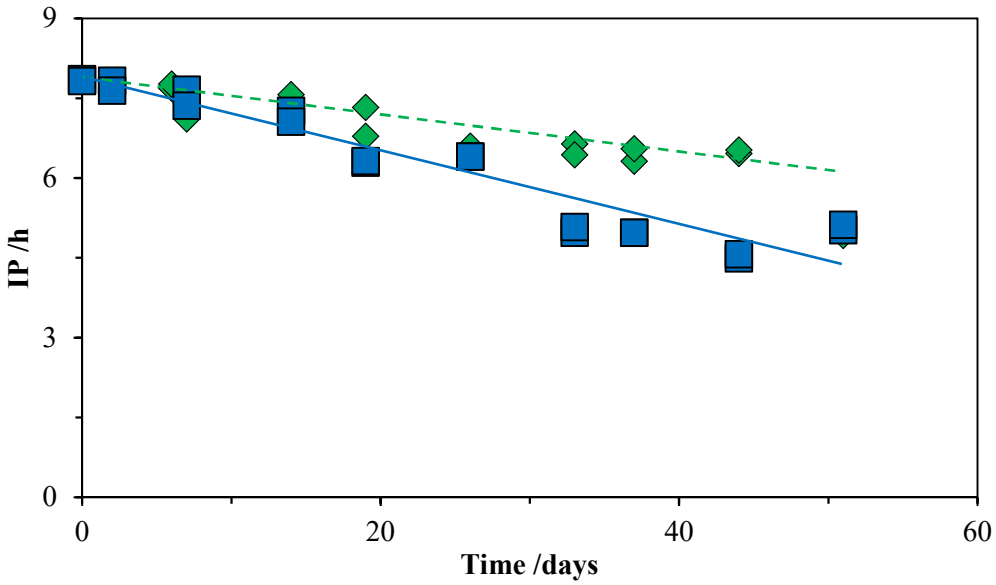

Figure 5.23 - Results for the storage stability over time for biodiesel "B" under nitrogen (---◆) and dry air (—■) atmosphere measured in a RANCITECH apparatus.

The results of these tests show in both cases an approximately linear behaviour on the decay of the OS for the pure biodiesel. The first set of test was study during a longer time period and for this reason the difference between the decay (N_2(g) & Air) is more visible. It was found that in both case the protective nitrogen atmosphere reduces the rate of the IP decay (time evolution of the oxidative stability).

5.2.7. Storage stability on biodiesel blends B7 and B14

This study focus on the storage stability of blends of biodiesel "A" and "B" with the mineral diesel "X" (B7 and B14). To understand the time influence in the OS blends of biodiesel with mineral diesel, were prepared samples in the same conditions as those used for the pure biodiesel (under nitrogen and dry air atmosphere). Similarly to the pure biodiesel samples, the blends with biodiesel "A" (B7) (Figure 5.24) were studied in the Rancimat apparatus during 140 days, and the results are shown in Figure 5.25.

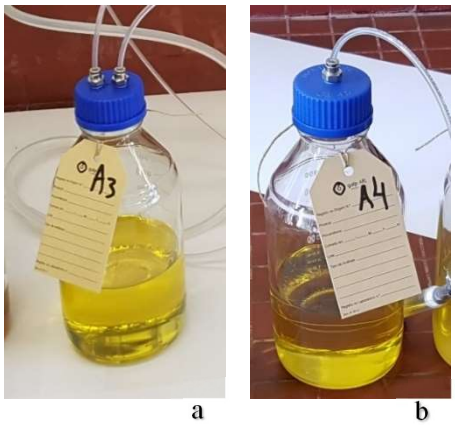

Figure 5.24 - Pictures of samples B7 of biodiesel "A" and diesel "X" under nitrogen (a) and dry air (b).

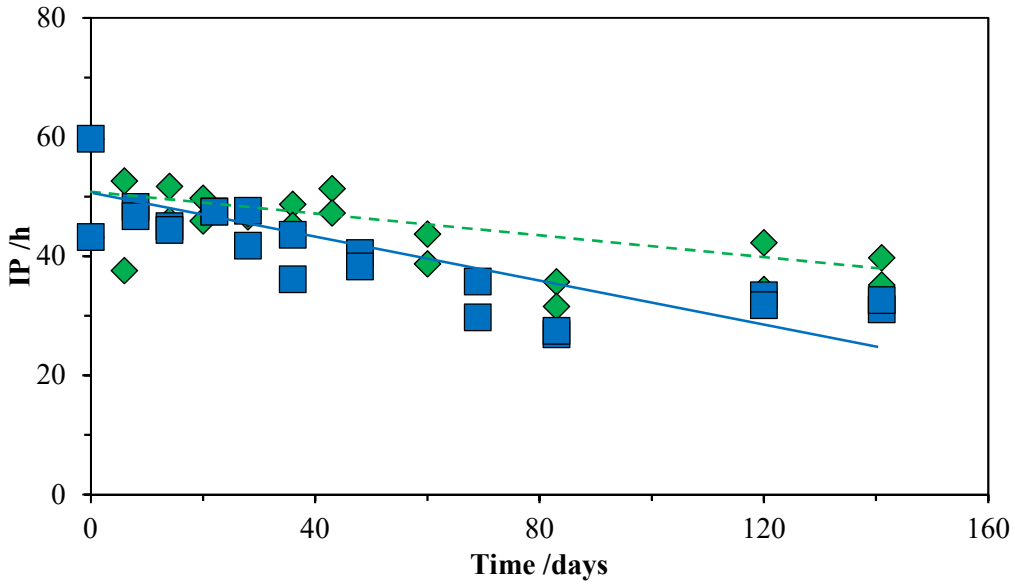

Figure 5.25 - Results for the storage stability of B7 blend with biodiesel "A" with mineral diesel "X" under nitrogen (---◆) and dry air (—■) measured in a Rancimat apparatus.

After finishing the analyses of the B7 samples, samples of biodiesel "A" with 14 %(v/v) (B14) (Figure 5.26) were prepared. This study was made for 130 days in the Rancimat apparatus and the results are shown in Figure 5.27.

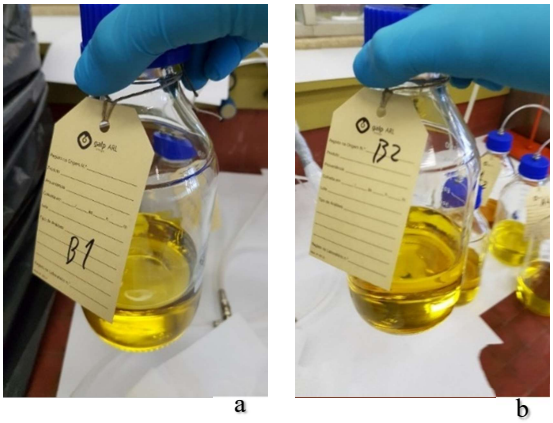

Figure 5.26 - Pictures of samples B14 of biodiesel "A" and mineral diesel "X" under nitrogen (a) and dry air (b).

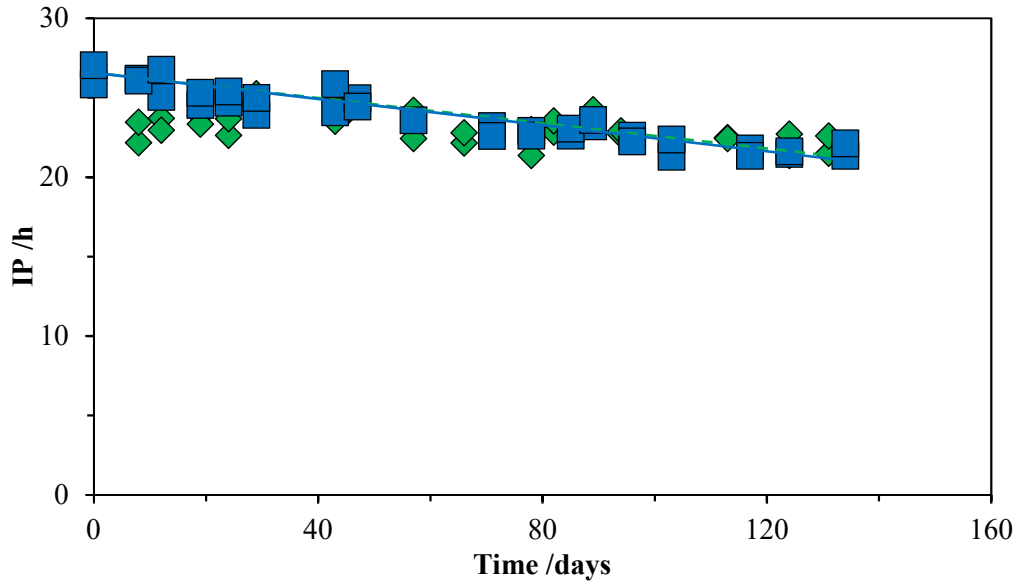

Figure 5.27 - Results for the storage stability of B14 blend with biodiesel "A" with mineral diesel "X" under nitrogen (---◆) and dry air (—■) measured in a Rancimat apparatus.

Regarding these first results for blends it is possible to observe that the mineral diesel has a strong effect in the OS of blends, as mentioned before in 5.2.1. The increase in the biodiesel concentration reduces the OS of the blend to almost half (see Figure 5.25 and Figure 5.27). This

result is also in good agreement with the previous results (5.2.1). The decay in the OS along time didn't show differences between the samples under nitrogen or dry air atmosphere, both set of results show an identical time decay of the IP.

Analogous study, with blends B7 and B14 (Figure 5.28), where made using biodiesel "B" with the same mineral diesel. These samples were analysed along 55 days in RANCITECH apparatus. In this study it should be taken in to consideration that the mineral diesel was stored for 1.5 year. The results for the B7 and B14 are shown in Figure 5.29 and Figure 5.30, respectively.

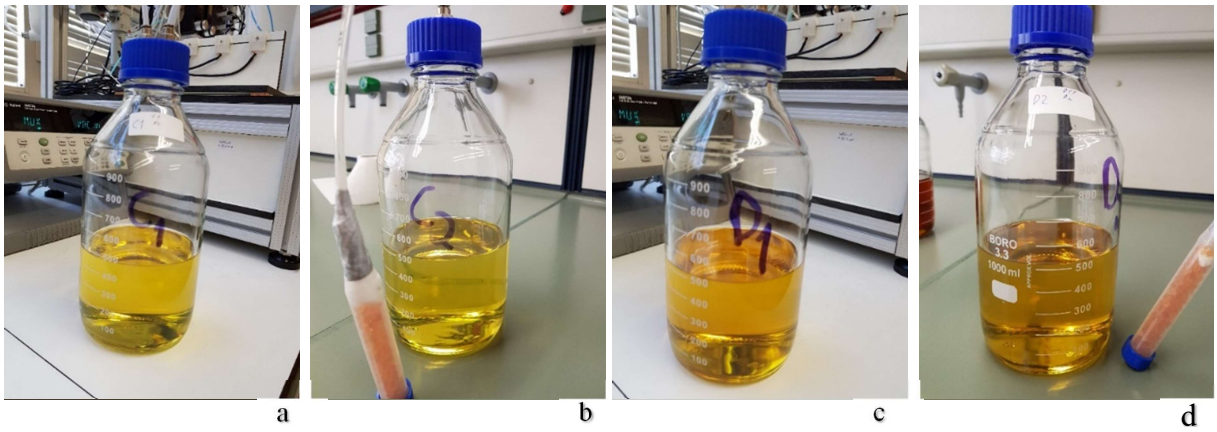

Figure 5.28 - Pictures of samples B7 under nitrogen (a) and dry air (b) and B14 under nitrogen (c) and dry air (d) of biodiesel "B" and diesel "X".

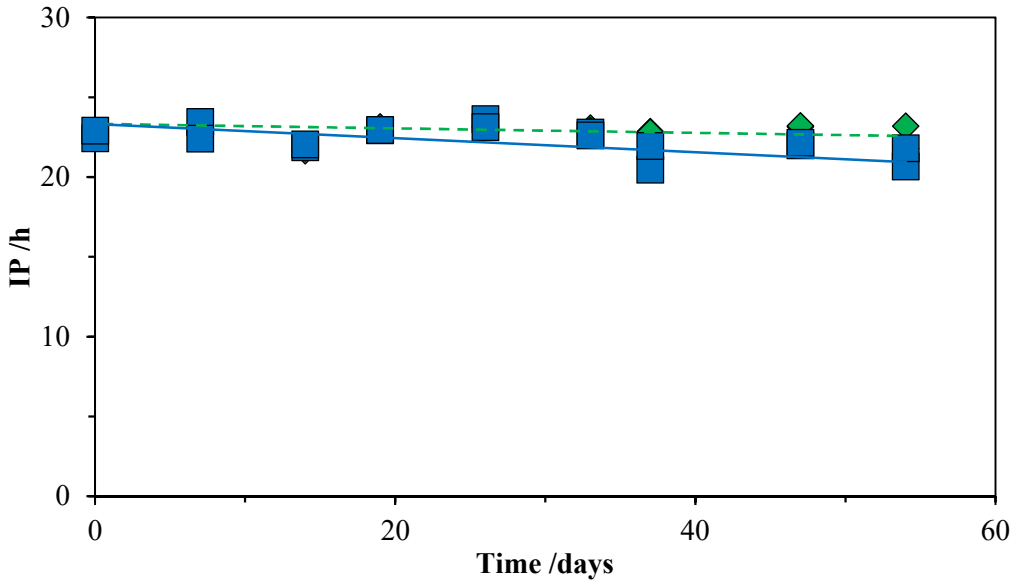

Figure 5.29 - Results for the storage stability of B7 blend with biodiesel "B" with mineral diesel "X" under nitrogen (---◆) and dry air (—■) measured in a RANCITECH apparatus.

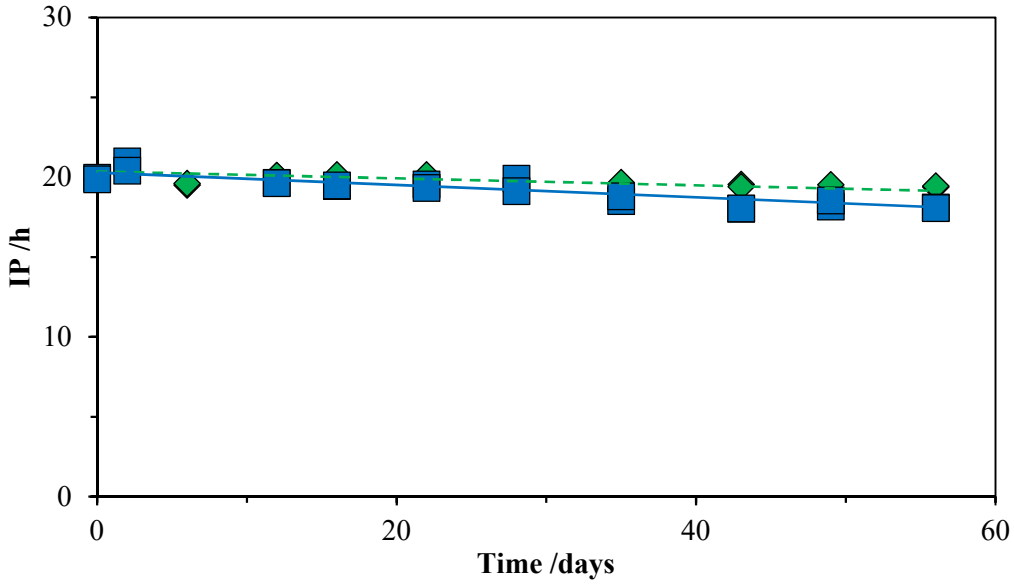

Figure 5.30 - Results for the storage stability of B14 blend with biodiesel "B" with mineral diesel "X" under nitrogen (---◆) and dry air (—■) measured in a RANCITECH apparatus.

From these results it is again verified that storage under dry air or nitrogen atmosphere didn't affect the decay rate in the OS in the Biodiesel/Mineral Diesel in contrast than the observed previously in the pure biodiesel.

5.2.8. Effects of metal in storage stability of biodiesel blends B7 and B14

To better understand the oxidation process in the commercial fuels the influence of metal, similar to the metals used in the industry was also studied.

These samples were prepared and analysed in the same period of time as the blends in 5.2.7. The metal (Steel) used was the one previously reported and characterized in Table 5.6. The blends with biodiesel "A" (Figure 5.31) were studied under dry air atmosphere. The results of this study were compared with the same blend without metal and the results are shown in Figure 5.32 for B7 and Figure 5.33 for B14.

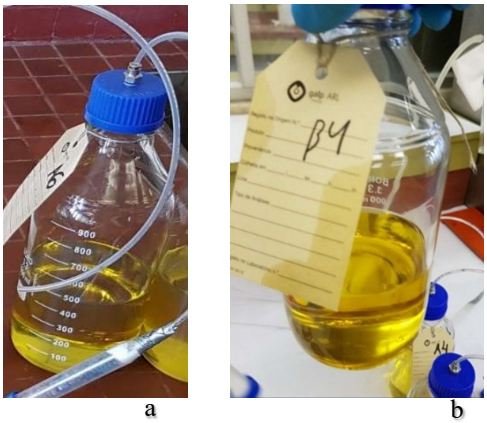

Figure 5.31 - Pictures of samples B7 (a) and B14 (b) of biodiesel “A” and mineral diesel “X” with a metal and dry air.

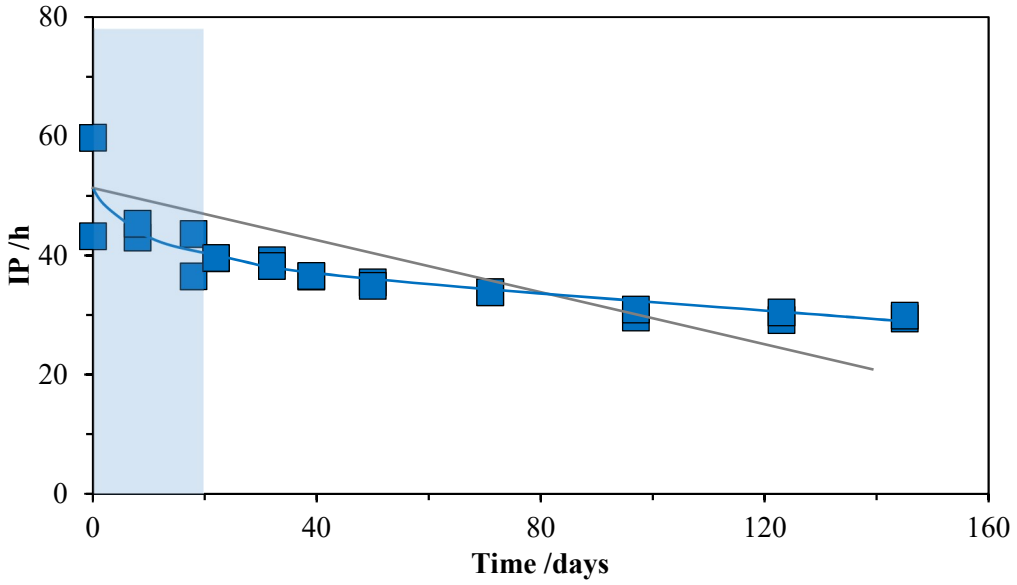

Figure 5.32 - Results for the storage stability of B7 blend study for biodiesel “A” with diesel “X” with metal under dry air (—■) measured in a Rancimat apparatus. (—) results without metal under dry air.

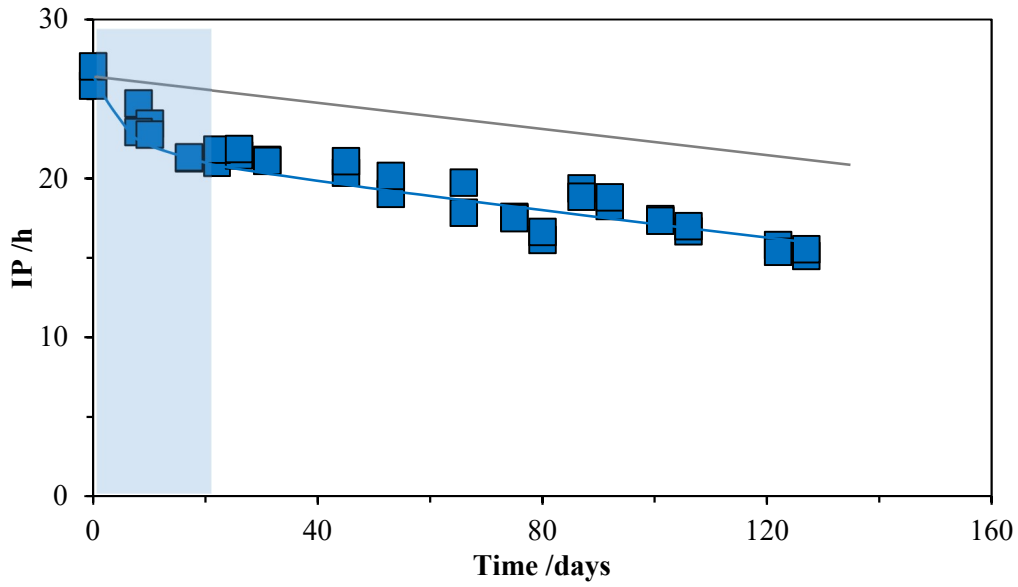

Figure 5.33 - Results for the storage stability of B14 blend study for biodiesel "A" with diesel "X" with metal under dry air (—■) measured in a Rancimat apparatus. (—) results without metal under dry air.

These results highlight the influence of the metal (steel) presence in the time evolution of the IP. The presence of the metal leads to an initial high rate of decay (initial 20 days), and after this period the rate of decay becomes constant and similar as those obtained in blends without presence of the metal. The same study was made using biodiesel "B" (Figure 5.34) in order to evaluate the effect of a protective nitrogen atmosphere using the RANCITECH apparatus.

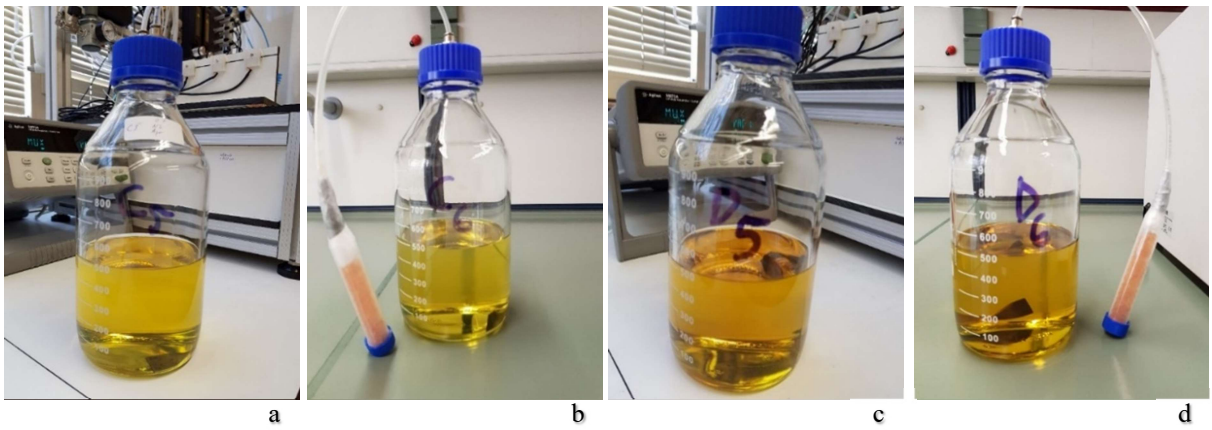

Figure 5.34 - Pictures of samples B7 under nitrogen (a) and dry air (b) and B14 under nitrogen (c) and dry air (d) of biodiesel "B" and diesel "X" with metal.

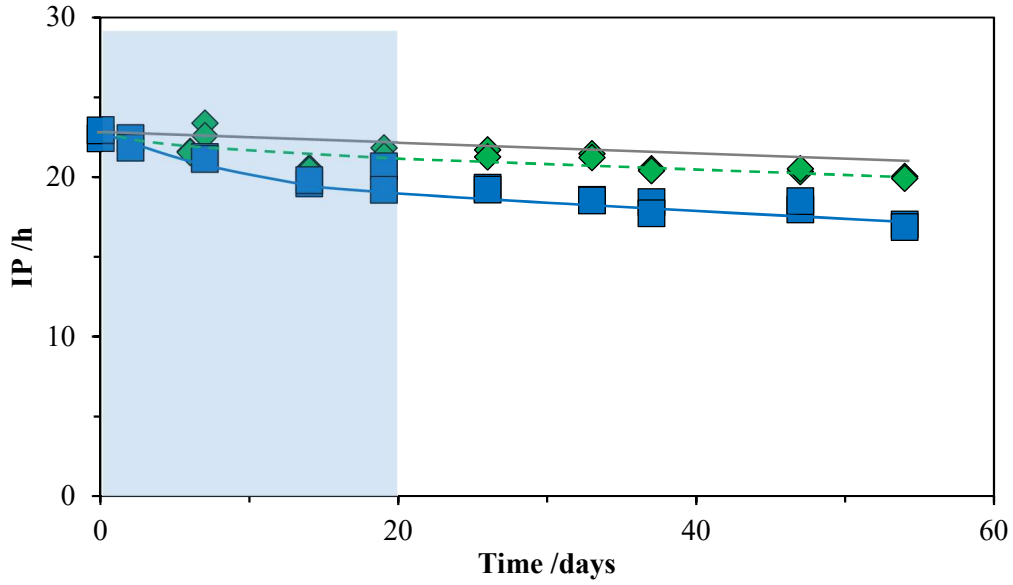

Figure 5.35 - Results for the storage stability of B7 blend study for biodiesel "B" with diesel "X" with metal under nitrogen atmosphere (---◆) and dry air (—■) measured in a RANCITECH apparatus. (—) results without metal under dry air.

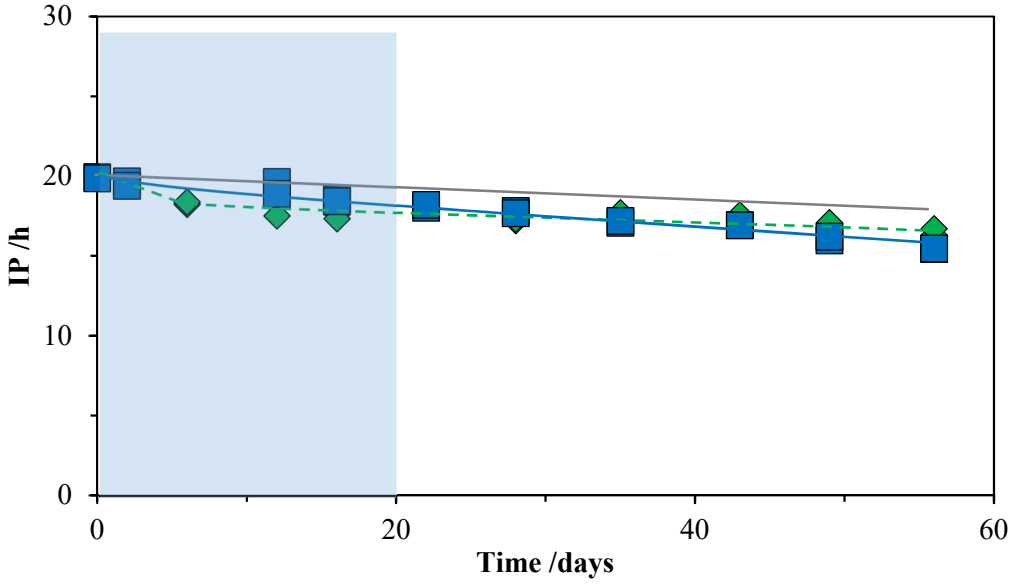

Figure 5.36 - Results for the storage stability of B14 blend study for biodiesel "B" with diesel "X" with metal under nitrogen atmosphere (---◆) and dry air (—■) measured in a RANCITECH apparatus. (—) results without metal under dry air.

It is found again that the nitrogen atmosphere didn't have relevant influence in the storage stability (in a presence of a metal) when compared with dry air. In both cases (N_2 and Air) the presence of metal seems to increase the initial decay rate, however, after this initial period, a constant rate of decay is observed which is similar than the found in the samples without the presence of the metal.

The effect of metal do not seems to have a significant impact in the change of the induction period along time. These results is in agreement with previous study described in a literature. [114]

The initial high rate of IP decay which was observed in the presence of a metal (steel) should be due to the catalyst ability of the metal surface (as discussed in introduction: chapter 1.5). After the fast initial decay, the decay becomes linear and less significant which could be due to the fast passivation of the metal surface in the presence of the blends.

5.2.9. Effect of water in storage stability of biodiesel blends B7 and B14

Study of biodiesel blends "A" and "B" with mineral diesel "X" with the presence of water were made. The samples were prepared in a similar way than the samples for the study of the presence of metal, in this case, the blend was contaminated with 1 ml of deionized water. The results for the blends of biodiesel "A" (B7 and B14) with mineral "X" (Figure 5.37) are shown in Figure 5.38 and Figure 5.39.

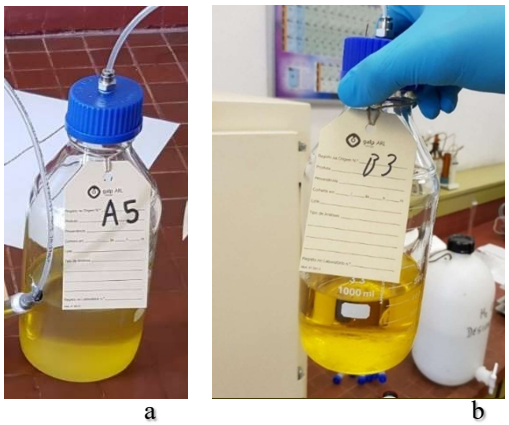

a b

Figure 5.37 - Pictures of samples B7 (a) and B14 (b) of biodiesel "A" and diesel "X" with water (1 mL) open to atmosphere.

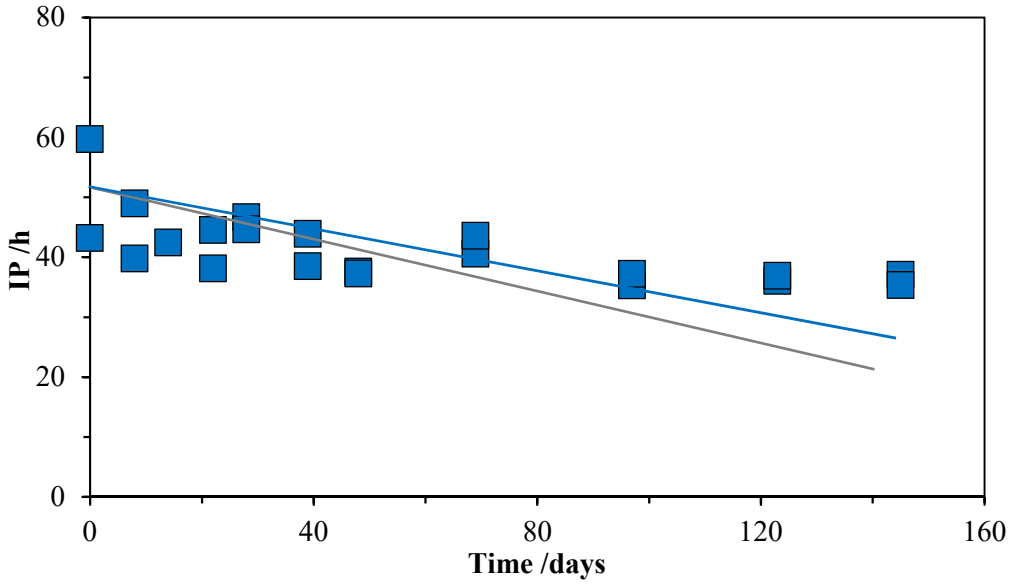

Figure 5.38 - Results for the storage stability of B7 blend study for biodiesel "A" with diesel "X" with water (1 mL) measured in a Rancimat apparatus(—■). (—) results without water under dry air.

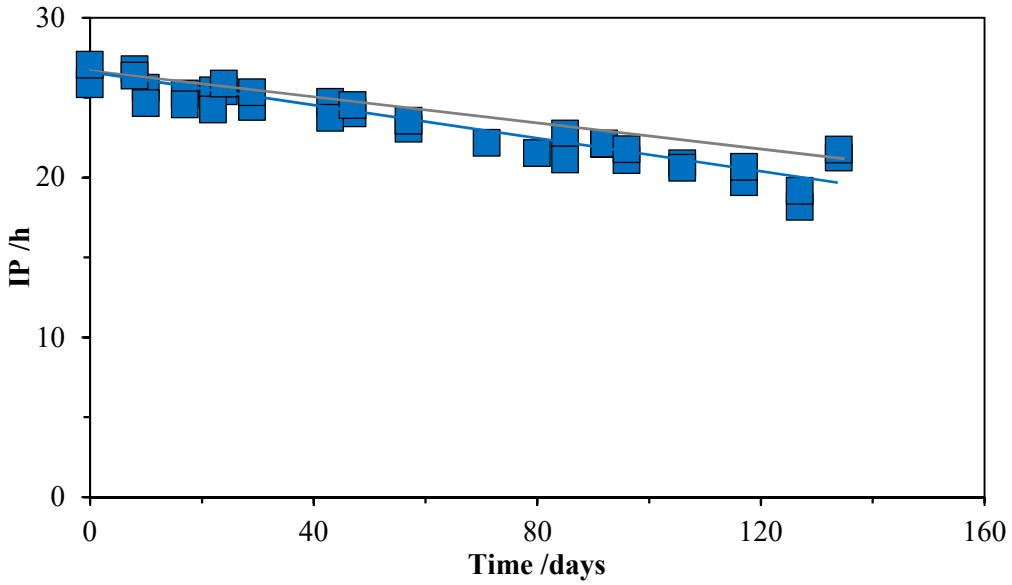

Figure 5.39 - Results for the storage stability of B14 blend study for biodiesel "A" with diesel "X" with water (1 mL) measured in a Rancimat apparatus(—■). (—) results without water under dry air.

In these results was shown that the water doesn't have any significant effect in the storage stability of blends. This study was also made for blends with the biodiesel "B" (Figure 5.40) for B7 (Figure 5.41) and B14 (Figure 5.42) under nitrogen atmosphere or air.

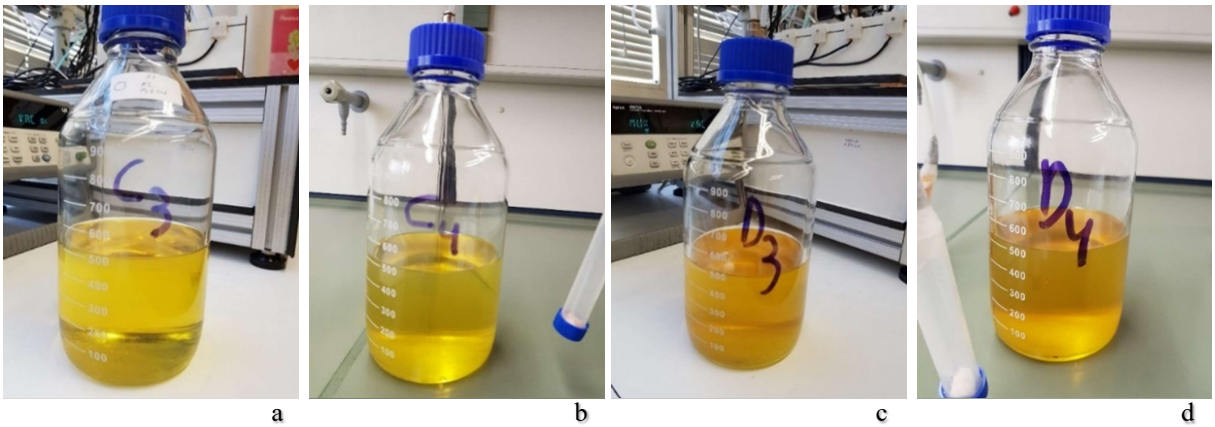

Figure 5.40 - Pictures of samples B7 under nitrogen (a) and dry air (b) and B14 under nitrogen (c) and dry air (d) of biodiesel “B” and mineral diesel “X” with water (1 mL).

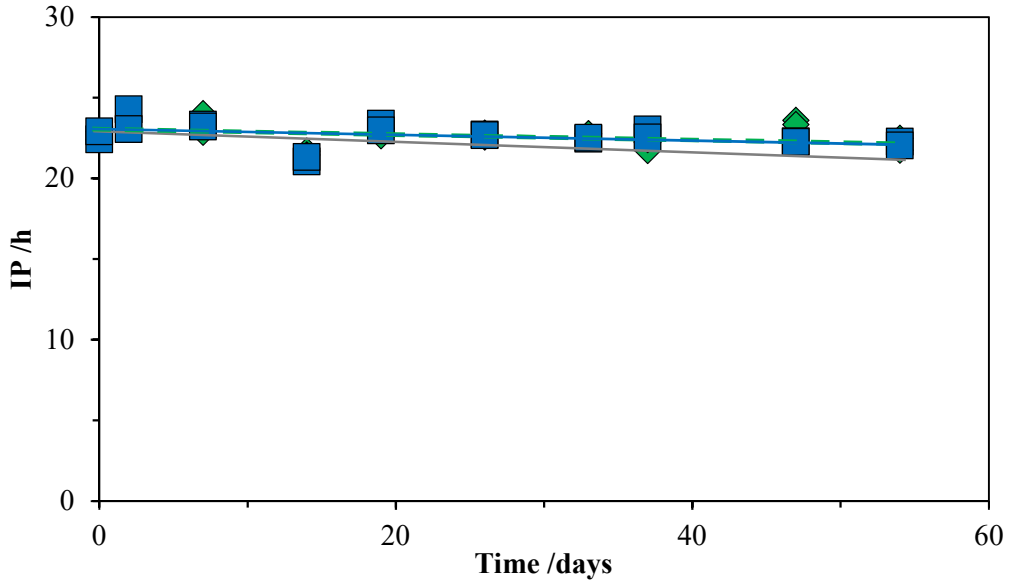

Figure 5.41 - Results for the storage stability of B7 blend study in a presence of water (1 mL) for biodiesel “B” with mineral diesel “X” under nitrogen atmosphere (---♦) and air (—■) measured in a RANCITECH apparatus. (—) results without water under dry air.

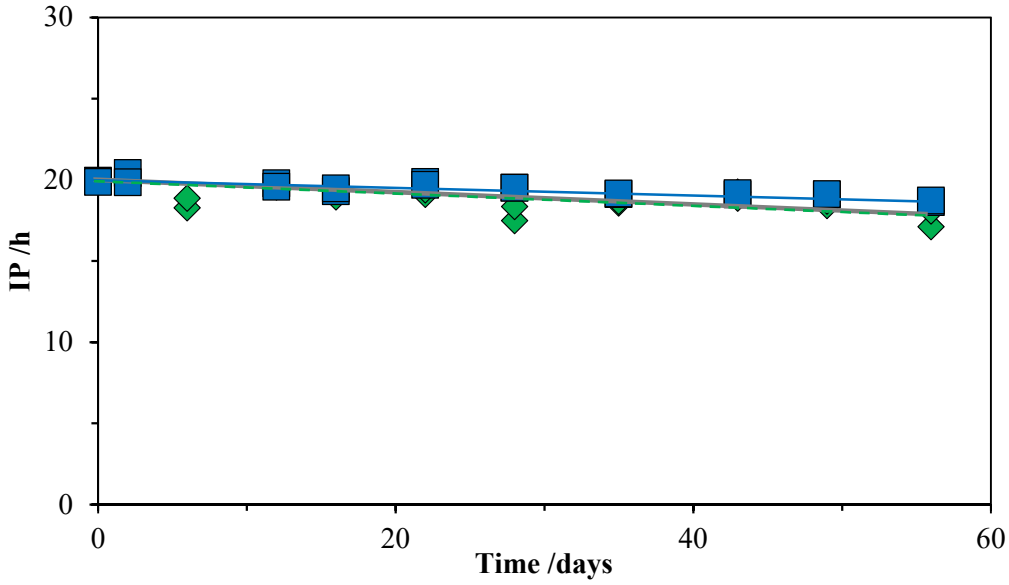

Figure 5.42 - Results for the storage stability of B14 blend study in a presence of water (1 mL) for biodiesel "B" with mineral diesel "X" under nitrogen atmosphere (---♦) and air (—■) measured in a RANCITECH apparatus. (—) results without water under dry air.

In these results is observed again a linear decay of the OS without influence of the different atmospheres. The water did not reduce the OS and, in some cases, it seems to have a stabilizer effect. The absence of effect of water upon the OS is in agreement with the previously reported by Yang *et al* [118]

In this study was also observed the growing of microbiology in the water deposit in the bottom of the sample (Figure 5.43).

Figure 5.43 - Picture of the microbiology formed in the blends with water presence.

5.2.10. Synergistic effect of metal and water in storage stability of biodiesel blends B7 and B14

The last study will regard the synergistic effect of the presence of water and metal in the blends of biodiesel with mineral diesel. The conditions and samples were developed at the same time and in the same apparatus than the mixtures before announced. The blends with biodiesel "A" (Figure 5.44) were evaluated in Rancimat apparatus the results for the blends B7 (Figure 5.45) and B14 (Figure 5.46) are one more time compared with the results obtained for the blends without water or metal.

a b

Figure 5.44 - Pictures of samples B7 (a) and B14 (b) of biodiesel "A" and diesel "X" with water (1 mL) and metal open to atmosphere.

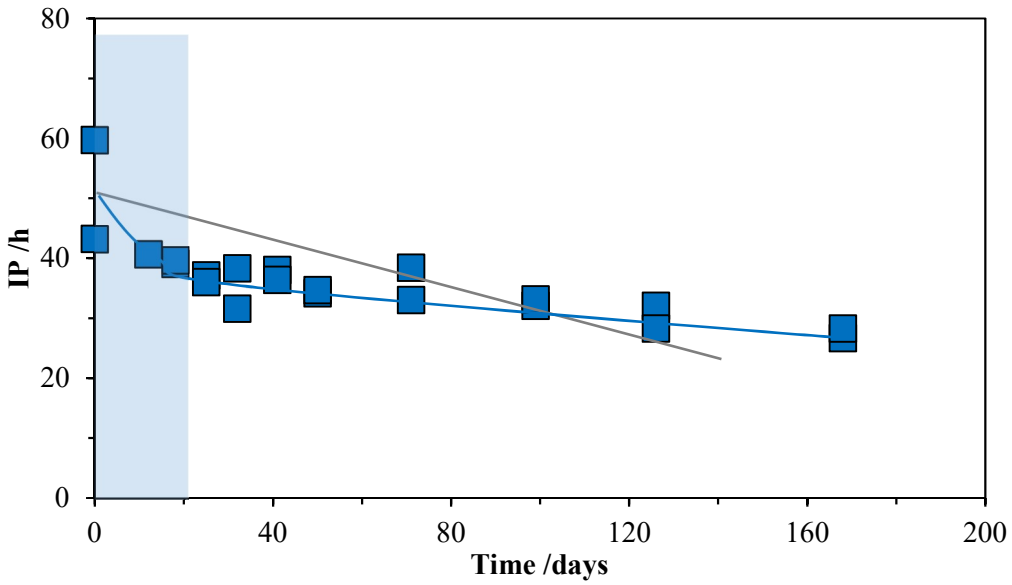

Figure 5.45 - Results for the storage stability of B7 blend study for biodiesel "A" with diesel "X" with water (1 mL) and metal measured in a Rancimat apparatus(—■). (—) results without water and metal under dry air.

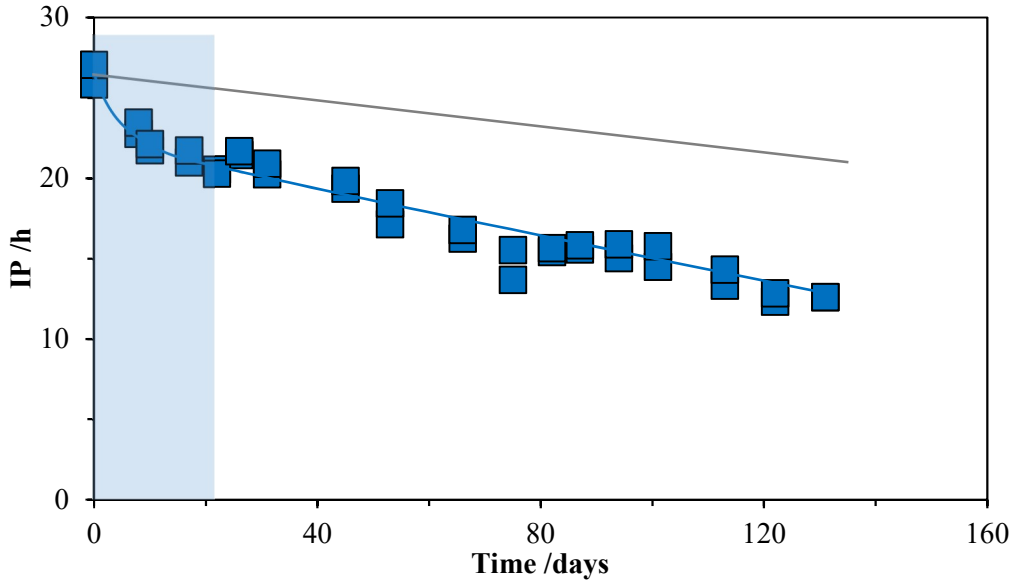

Figure 5.46 - Results for the storage stability of B14 blend study for biodiesel “A” with diesel “X” with water (1 mL) and metal measured in a Rancimat apparatus(—■). (—) results without water and metal under dry air.

These results show that there is not a significant synergistic effect of the water and metal. The results present a similar behaviour to the observed for the samples with metal.

Similarly to the other test was also analysed the storage stability using the biodiesel “B” (Figure 5.47) under nitrogen atmosphere and open to air for blends of B7 (Figure 5.48) and B14 (Figure 5.49) analysed in the RANCITECH apparatus.

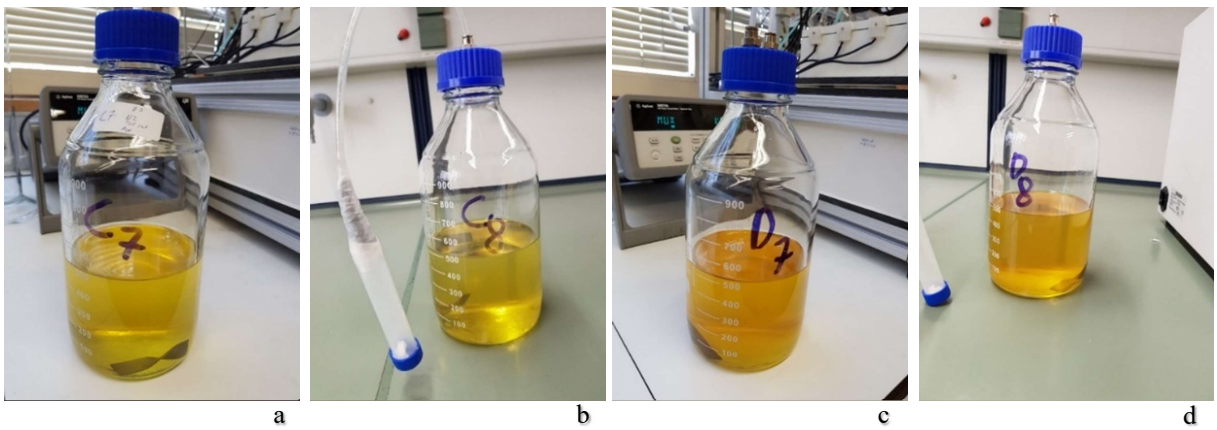

Figure 5.47 - Pictures of samples B7 under nitrogen (a) and dry air (b) and B14 under nitrogen (c) and dry air (d) of biodiesel “B” and diesel “X” with water (1 mL) and metal.

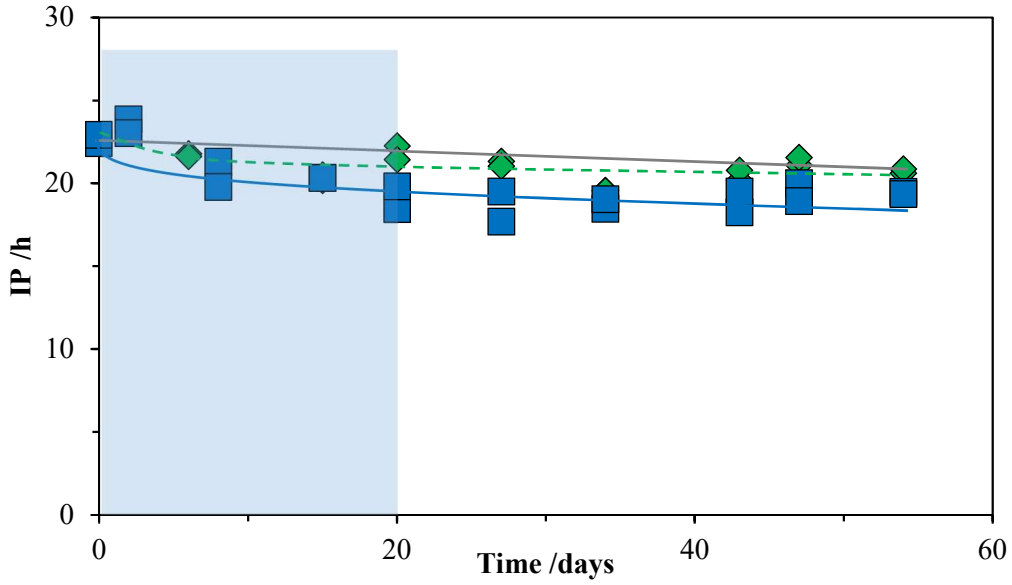

Figure 5.48 - Results for the storage stability of B7 blend study in a presence of water (1 mL) for biodiesel "B" with diesel "X" under nitrogen atmosphere (---◆) and dry air (—■) measured in a RANCITECH apparatus. (—) results without water and metal under dry air.

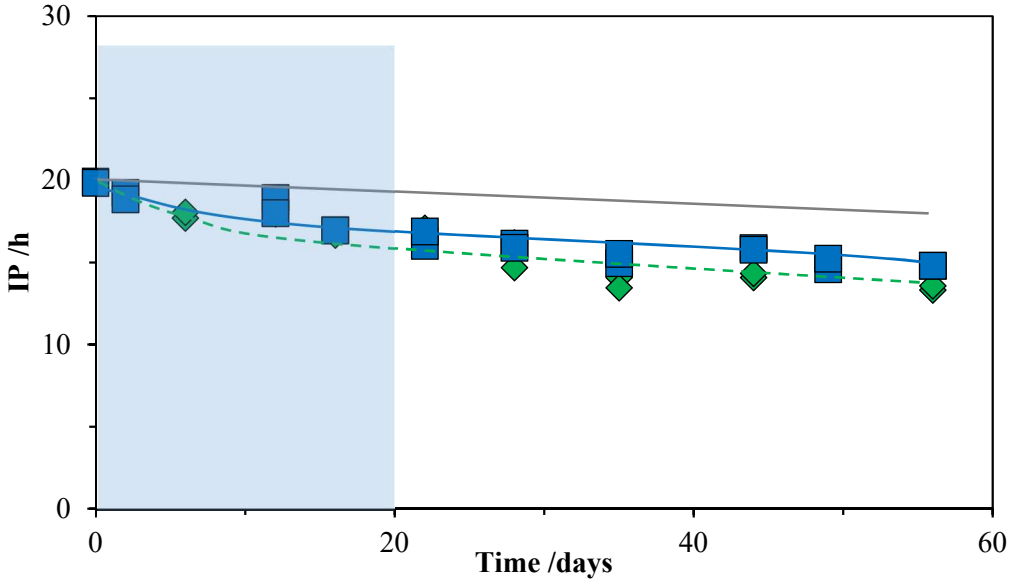

Figure 5.49 - Results for the storage stability of B14 blend study in a presence of water (1 mL) and metal for biodiesel "B" with diesel "X" under nitrogen atmosphere (---◆) and air (—■) measured in a RANCITECH apparatus. (—) results without water and metal under dry air.

It was found that the presence of the metal is the only factor that seem to have a significant effect in the storage stability due to the initial catalytic ability of the metal surface which seem to not increase in the presence of water.

5.3. Conclusions

In this work an exploratory study of the oxidative stability of pure biodiesel and its blends with mineral diesel in different conditions was made.

The results obtained in these studies are summarized in the topics below:

- The OS of the pure biodiesel had a strong effect in blends with mineral diesel;
- The rate of the induction period (1/IP) is linearly dependent of the biodiesel concentration;
- The natural AO (vitamin E) have a higher effectiveness in the distilled biodiesel than non-distilled biodiesel (with natural AO compounds);
- The AO effect is progressively stronger with the dilution of the biodiesel in the blend;
- The AOs (vitamin E and BAYNOX plus)) show a similar effectiveness in biodiesel blends;
- The storage stability of pure biodiesel has a linear time dependence decay;
- A clear effect of a protective atmosphere (N_2(g)) in the pure biodiesel storage stability was found in this work;
- For blends of biodiesel and mineral diesel a protective atmosphere (N_2(g)) seems to not have any effect in the improvement of the storage stability;
- It was found that the presence of the metal has a significant effect the initial period (20 days) of the storage stability due to the initial catalytic ability of the metal surface which seems to be passivated in the biodiesel/mineral diesel blend;
- The water presence didn't show any effect in the storage stability of blends;
- There was not a synergistic effect of metal and water in the blends.

Regarding these results the blends of biodiesel and mineral diesel were strongly influence by the OS of the biodiesel used and the choice of the adequate AO should be made taking in account the biodiesel and its process of production. The activation of the metal surface of the tanks should be avoid reducing the risk of the oxidation of the blends.

6. Final Conclusions and future work

This work explored the biodiesel influence in the OS and in the thermal properties. To improve and minimize the consequences of the use of this fuel. Was explored the effect of the presence of biodiesel and AOs in different concentrations in the OS of blends, the OS along the storage of the blends, pure biodiesel in different conditions and the phase behaviour of six binary mixtures of the most common saturated methyl ester with a saturated alkane.

The results and conclusions derived from the phase behaviour of this set of binary mixtures, between alkanes and methyl esters shown the formation of the solid solution that in a wide range of concentrations, could have important impact on the wax formation as well as in the performance of additives used to improve the low temperatures behaviour of diesel blends. These results can be used as a model for the interpretation of the cloud and pour points increase in biodiesel blends. This studied could be complemented exploring the modifications in the values of CP and CFPP with the addition of controlled quantities of alkanes and FAMEs in a fuel with a well knows composition.

The results of the oxidative stability shown that the main factor affecting the OS of the blends was the OS of the biodiesel. The correct use of AOs could also have an important role since they increase the OS of the pure biodiesel significantly and had a synergistic effect with the mineral diesel in the blends. Regarding the storage of the fuels the OS shows that the presence of metal (steel), water or/and oxygen don't influence significantly the storage stability of blends.

The OS of blends and pure biodiesel should be explored in more detail in the future with other tests. The AO behaviour should be explored in different biodiesels and different AOs to verify what are the most effective AO to the distilled, undistilled or more unsaturated biodiesels. Concerning the storage stability should be made studies to understand and verify the process of passivation of the metal surface and the influence of microbiology when the water is present. Should also be explored the variations in the storage stability of samples under agitation and samples that were previous deaerated with nitrogen. The difference in the storage stability of blends with distilled or undistilled biodiesel should also be explored to understand the dilution/protective effect of the mineral diesel without the AO naturally present in biodiesels.

With the work present in this thesis and the future work enounced should be interesting in the future build a predictive modelling of the effect of the use of biodiesel, with a known composition, in the OS and in the cold flow properties as summarize in Figure 6.1.

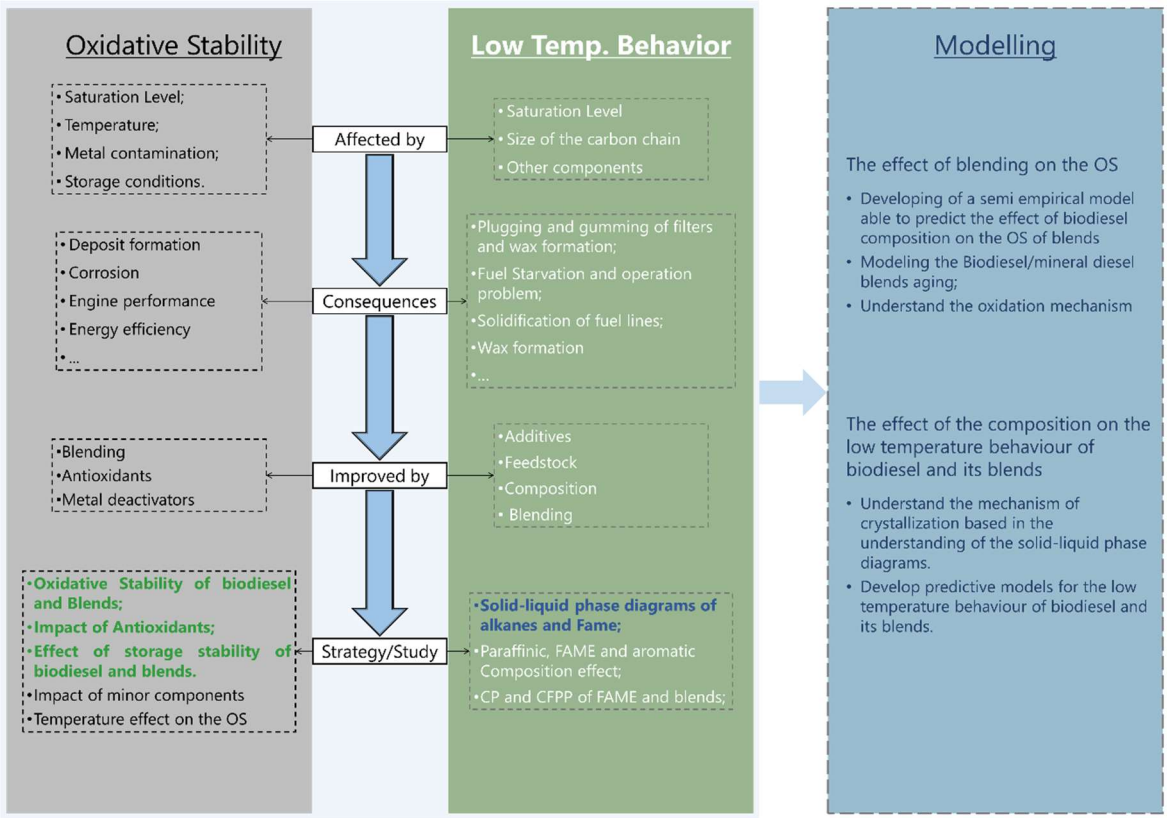

Figure 6.1 - Schematic representation of the work developed and future work for understanding and predict the biodiesel influence in the OS and low temperature properties

References

[1] International Energy Outlook 2017. 2017. doi:10.1016/j.trc.2014.07.001.

[2] World Oil Outlook 2016. 2016. doi:10.1190/1.1439163.

[3] World oil outlook 2017. Organization of the Petroleum Exporting Countries; 2017. doi:10.1190/1.1439163.

[4] U.S. Energy Information Agency. International Energy Outlook 2013. 2013.

[5] United Nations Environment Programme. The Montreal protocol on substances that deplete the ozono layer. 2000. doi:10.1163/15718069620847781.

[6] United Nations. Kyoto Protocol To the United Nations Framework Convention on Climate Change. Rev Eur Community Int Environ Law 1998. doi:10.1111/1467-9388.00150.

[7] Sarin A. Biodiesel: Production and Properties. Royal Society of Chemistry; 2012.

[8] World Oil Outlook 2014. vol. 4. 1985. doi:10.1190/1.1439163.

[9] IEA (International Energy Agency). Renewable Energy Outlook 2013. 2013.

[10] Dwivedi G, Jain S, Sharma MP. Impact analysis of biodiesel on engine performance - A review. Renew Sustain Energy Rev 2011;15:4633–41. doi:10.1016/j.rser.2011.07.089.

[11] Canakci M, Sanli H. Biodiesel production from various feedstocks and their effects on the fuel properties. J Ind Microbiol Biotechnol 2008;35:431–41. doi:10.1007/s10295-008-0337-6.

[12] Hoekman SK, Broch A, Robbins C, Ceniceros E, Natarajan M. Review of biodiesel composition, properties, and specifications. Renew Sustain Energy Rev 2012;16:143–69. doi:10.1016/j.rser.2011.07.143.

[13] Imahara H, Minami E, Saka S. Thermodynamic study on cloud point of biodiesel with its fatty acid composition. Fuel 2006;85:1666–70. doi:10.1016/j.fuel.2006.03.003.

[14] Freitas S. Production of Biodiesel from the Resources Endogeneous of Timor Leste. University of Aveiro, 2013.

[15] Leung DYC, Wu X, Leung MKH. A review on biodiesel production using catalyzed transesterification. Appl Energy 2010;87:1083–95. doi:10.1016/j.apenergy.2009.10.006.

[16] Suresh M, Jawahar CP, Richard A. A review on biodiesel production, combustion, performance, and emission characteristics of non-edible oils in variable compression ratio diesel engine using biodiesel and its blends. Renew Sustain Energy Rev 2018;92:38–49. doi:10.1016/j.rser.2018.04.048.

[17] Kinast JA. Production of biodiesels from multiple feedstocks and properties of biodiesels and

biodiesel/diesel blends. Final report. Report 1 in a series of 6. Subcontractor report. Combustion 2003:57.

[18] Saluja RK, Kumar V, Sham R. Stability of biodiesel – A review. Renew Sustain Energy Rev 2016;62:166–81. doi:10.1016/j.rser.2016.05.001.

[19] Cavalcante T, Melo C De, Moreira MF, Oliveira I, Rocha MI, Clara M, et al. Desempenho de Misturas B7 Quanto a Emissões Veiculares e a estabilidade à Oxidação. Blucher Eng Proc 2015;2.

[20] Fargione J, Hill J, Tilman D, Polasky S, Hawthorne P. Land Clearing and the Biofuel Carbon Debt. Science (80-) 2008;319:1235–8. doi:10.1126/science.1152747.

[21] Tilman D, Hill J, Lehman C. Carbon-Negative Biofuels from Low-Input High-Diversity Grassland Biomass. Science (80-) 2006;314:1598–600. doi:10.1126/science.1133306.

[22] Gebremariam SN, Marchetti JM. Economics of biodiesel production: Review. Energy Convers Manag 2018;168:74–84. doi:10.1016/j.enconman.2018.05.002.

[23] World Oil Outlook 2040. Organization of the Petroleum Exporting Countries; 2018.

[24] Fábrica de Biodiesel 2015. https://www.prio.pt/pt/sobre-nos/fabrica-de-biodiesel_241.html.

[25] Calero J, Luna D, Sancho ED, Luna C, Bautista FM, Romero AA, et al. Development of a new biodiesel that integrates glycerol, by using CaO as heterogeneous catalyst, in the partial methanolysis of sunflower oil. Fuel 2014;122:94–102. doi:10.1016/j.fuel.2014.01.033.

[26] Kinney AJ, Clemente TE. Modifying soybean oil for enhanced performance in biodiesel blends. Fuel Process Technol 2005;86:1137–47. doi:10.1016/j.fuproc.2004.11.008.

[27] Knothe G, Gerpen JH Van, Krahl J. The Biodiesel Handbook. vol. 2. 2005. doi:10.1201/9781439822357.

[28] Sharma YC, Singh B. Development of biodiesel: Current scenario. Renew Sustain Energy Rev 2009;13:1646–51. doi:10.1016/j.rser.2008.08.009.

[29] Verma P, Sharma MP, Dwivedi G. Impact of alcohol on biodiesel production and properties. Renew Sustain Energy Rev 2016;56:319–33. doi:10.1016/j.rser.2015.11.048.

[30] Likozar B, Levec J. Transesterification of canola, palm, peanut, soybean and sunflower oil with methanol, ethanol, isopropanol, butanol and tert-butanol to biodiesel: Modelling of chemical equilibrium reaction kinetics and mass transfer based on fatty acid composition. Fuel Process Technol 2014;122:30–41. doi:10.1016/j.fuproc.2014.01.017.

[31] Oliveira JFG, Lucena IL, Saboya RMA, Rodrigues ML, Torres AEB, Fernandes FAN, et al. Biodiesel production from waste coconut oil by esterification with ethanol: The effect of water removal by adsorption. Renew Energy 2010;35:2581–4. doi:10.1016/j.renene.2010.03.035.

[32] Sánchez M, Bergamin F, Peña E, Martínez M, Aracil J. A comparative study of the production of esters from Jatropha oil using different short-chain alcohols: Optimization and characterization. Fuel 2015;143:183–8. doi:10.1016/j.fuel.2014.11.064.

[33] Knothe G. Dependence of biodiesel fuel properties on the structure of fatty acid alkyl esters. Fuel Process Technol 2005;86:1059–70. doi:10.1016/j.fuproc.2004.11.002.

[34] Malins K, Kampars V, Kampare R, Prilucka J, Brinks J, Murnieks R, et al. Properties of rapeseed oil fatty acid alkyl esters derived from different alcohols. Fuel 2014;137:28–35. doi:10.1016/j.fuel.2014.07.091.

[35] Ambat I, Srivastava V, Sillanpää M. Recent advancement in biodiesel production methodologies using various feedstock: A review. Renew Sustain Energy Rev 2018;90:356–69. doi:10.1016/j.rser.2018.03.069.

[36] Guo F, Fang Z, Tian XF, Long YD, Jiang LQ. Corrigendum to One-step production of biodiesel from Jatropha oil with high-acid value in ionic liquids [Bioresour. Technol. 102 (11) (2011)]. Bioresour Technol 2013;140:447–50. doi:10.1016/j.biortech.2013.03.095.

[37] Jarnefeld J. Integrated Multistage Supercritical Technology To Produce High Quality Vegetable Oil and Biofuels the New York State 2006.

[38] Demirbaş A, Kara H. New options for conversion of vegetable oils to alternative fuels. Energy Sources, Part A Recover Util Environ Eff 2006;28:619–26. doi:10.1080/009083190951357.

[39] Waste Management and Research Center. Feasibility Report: Small Scale Biodiesel Production 2006:20.

[40] Sharma YC, Singh B, Upadhyay SN. Advancements in development and characterization of biodiesel: A review. Fuel 2008;87:2355–73. doi:10.1016/j.fuel.2008.01.014.

[41] Canakci M, Gerpen J Van. Biodiesel production from oils and fats with high free fatty acids. Trans ASAE 2001;44:1429–36. doi:10.1016/j.fuel.2013.09.020.

[42] Parawira W. Biotechnological production of biodiesel fuel using biocatalysed transesterification: A review. Crit Rev Biotechnol 2009;29:82–93. doi:10.1080/07388550902823674.

[43] Schumacher J. Small scale biodiesel production: an overview. Agric Mark Policy Center, Mont State … 2007.

[44] Gerpen J Van, Shanks B, Pruszko R, Clements D. Biodiesel Production Technology 2004;87:3170–5.

[45] Van Gerpen J. Biodiesel processing and production. Fuel Process Technol 2005;86:1097–107. doi:10.1016/j.fuproc.2004.11.005.

[46] Refaat AA. Correlation between the chemical structure of biodiesel and its physical properties. Int J Environ Sci Technol 2009;6:677–94. doi:10.1007/BF03326109.

[47] Ryan TW, Dodge LG, Callahan TJ. The effects of vegetable oil properties on injection and combustion in two different diesel engines. J Am Oil Chem Soc 1984;61:1610–9. doi:10.1007/BF02541645.

[48] Bonazza B, Herman M, Saunders B, Bennett J, Kloss E, da Silva Junior JF. White Paper on Internationally Compatible Biofuel Standards - Tripartite Task Force Brazil, European Union & United States of America 2007:1–95.

[49] Gopinath A, Sairam K, Velraj R, Kumaresan G. Effects of the properties and the structural configurations of fatty acid methyl esters on the properties of biodiesel fuel: A review. Proc Inst Mech Eng Part D J Automob Eng 2015;229:357–90. doi:10.1177/0954407014541103.

[50] Dawoud B, Amer E, Gross D. Production characterization and efficiency of biodiesel A review. Int J Energy Res 2007;31:135–47. doi:10.1002/er.

[51] Standard I. ISO 5165 Petroleum products — Determination of the ignition quality of diesel fuels — Cetane engine method 1998;1998.

[52] Standard AN. ASTM 97-05 Standard Test Method for Pour Point of Petroleum Products. 2005.

[53] Coutinho JAP, Mirante F, Ribeiro JC, Sansot JM, Daridon JL. Cloud and pour points in fuel blends. Fuel 2002;81:963–7. doi:10.1016/S0016-2361(01)00213-7.

[54] Dwivedi G, Sharma MP. Impact of cold flow properties of biodiesel on engine performance. Renew Sustain Energy Rev 2014;31:650–6. doi:10.1016/j.rser.2013.12.035.

[55] Standardization EC for. EN 116:1997 Diesel and domestic heating fuels - Determination of cold filter plugging point 1997.

[56] Standardization IO for. ISO 3015:1992 - Petroleum products - Determination of cloud point. 1992.

[57] Dunn RO, Shockley MW, Bagby MO. Improving the low-temperature properties of alternative diesel fuels: Vegetable oil-derived methyl esters. JAOCS, J Am Oil Chem Soc 1996;73:1719–28. doi:10.1007/BF02517978.

[58] Shahidi F. Bailey ' S Industrial Oil and Fat. vol. 1. 2009. doi:10.1002/047167849X.

[59] Smith PC, Ngothai Y, Dzuy Nguyen Q, O'Neill BK. Improving the low-temperature properties of biodiesel: Methods and consequences. Renew Energy 2010;35:1145–51. doi:10.1016/j.renene.2009.12.007.

[60] Lee I, Johnson LA, Hammond EG. Reducing the crystallization temperature of biodiesel by winterizing methyl soyate. JAOCS, J Am Oil Chem Soc 1996;73:631–6. doi:10.1007/BF02518119.

[61] Gómez MG, Howard-Hildige R, Leahy J. Winterisation of waste cooking oil methyl ester to improve cold temperature fuel properties. Fuel 2002;81:1–7. doi:10.1016/S0016-2361(01)00117-X.

[62] Pérez Á, Casas A, Fernández CM, Ramos MJ, Rodríguez L. Winterization of peanut biodiesel to improve the cold flow properties. Bioresour Technol 2010;101:7375–81. doi:10.1016/j.biortech.2010.04.063.

[63] Stournas S, Lois E, Serdari A. Effects of fatty acid derivatives on the ignition quality and cold flow of diesel fuel. J Am Oil Chem Soc 1995;72:433–7. doi:10.1007/BF02636084.

[64] Serdari A, Lois E, Stournas S. Impact of esters of mono- and dicarboxylic acids on diesel fuel quality. Ind Eng Chem Res 1999;38:3543–8. doi:10.1021/ie9900115.

[65] Sarin A, Arora R, Singh NP, Sarin R, Malhotra RK, Kundu K. Effect of blends of Palm-Jatropha-Pongamia biodiesels on cloud point and pour point. Energy 2009;34:2016–21. doi:10.1016/j.energy.2009.08.017.

[66] Sarin A, Arora R, Singh NP, Sarin R, Malhotra RK, Sarin S. Blends of biodiesels synthesized from non-edible and edible oils: Effects on the cold filter plugging point. Energy and Fuels 2010;24:1996–2001. doi:10.1021/ef901131m.

[67] Park J-Y, Kim D-K, Lee J-P, Park S-C, Kim Y-J, Lee J-S. Blending effects of biodiesels on oxidation stability and low temperature flow properties. Bioresour Technol 2008;99:1196–203. doi:10.1016/j.biortech.2007.02.017.

[68] Yunus R, Fakhru'l-Razi A, Ooi TL, Omar R, Idris A. Synthesis of palm oil based trimethylolpropane esters with improved pour points. Ind Eng Chem Res 2005;44:8178–83. doi:10.1021/ie050530.

[69] Moser BR, Erhan SZ. Synthesis and evaluation of a series of ??-hydroxy ethers derived from isopropyl oleate. JAOCS, J Am Oil Chem Soc 2006;83:959–63. doi:10.1007/s11746-006-5053-7.

[70] Moser BR. Fuel property enhancement of biodiesel fuels from common and alternative feedstocks via complementary blending. Renew Energy 2016;85:819–25. doi:10.1016/j.renene.2015.07.040.

[71] Kraftfahrzeuge K. Automotive fuels — Diesel fuel — Cold operability testing and fuel performance correlation 2015.

[72] Dunn RO, Bagby MO. Low-temperature properties of triglyceride-based diesel fuels: Transesterified methyl esters and petroleum middle distillate/ester blends. J Am Oil Chem Soc 1995;72:895–904. doi:10.1007/BF02542067.

[73] Joshi RM, Pegg MJ. Flow properties of biodiesel fuel blends at low temperatures. Fuel 2007;86:143–51. doi:10.1016/j.fuel.2006.06.005.

[74] Lee I, Pfalzgraf LM, Poppe GB, Powers E, Haines T. The Role of Sterol Glucosides on Filter Plugging. Biodiesel Mag 2007:105.

[75] Pfalzgraf L, Lee I, Forster J, Poppe G. Effect of minor components in soy biodiesel on cloud point and filterability. Inf - Int News Fats, Oils Relat Mater 2007;18:17–21.

[76] Tang H, De Guzman RC, Salley SO, Ng KYS. Formation of insolubles in palm oil-, yellow grease-, and soybean oil-based biodiesel blends after cold soaking at 4 °c. JAOCS, J Am Oil Chem Soc 2008;85:1173–82. doi:10.1007/s11746-008-1303-1.

[77] Tang H, Salley SO, Simon Ng KY. Fuel properties and precipitate formation at low temperature in soy-, cottonseed-, and poultry fat-based biodiesel blends. Fuel 2008;87:3006–17. doi:10.1016/j.fuel.2008.04.030.

[78] Meija J, Coplen TB, Berglund M, Brand WA, De Bièvre P, Gröning M, et al. Atomic weights of the elements 2013 (IUPAC Technical Report). Pure Appl Chem 2016;88:265–91. doi:10.1515/pac-2015-0305.

[79] Knothe G, Dunn RO, Shockley MW, Bagby MO. Synthesis and characterization of some long-chain diesters with branched or bulky moieties. JAOCS, J Am Oil Chem Soc 2000;77:865–71. doi:10.1007/s11746-000-0138-x.

[80] Chiu CW, Schumacher LG, Suppes GJ. Impact of cold flow improvers on soybean biodiesel blend. Biomass and Bioenergy 2004;27:485–91. doi:10.1016/j.biombioe.2004.04.006.

[81] Bhale PV, Deshpande N V., Thombre SB. Improving the low temperature properties of biodiesel fuel. Renew Energy 2009;34:794–800. doi:10.1016/j.renene.2008.04.037.

[82] ASTM International. ASTM Standard D97-05. Stand Test Method Pour Point Pet Prod 2005;2:1–9. doi:10.1520/D0097-17A.

[83] Pullen J, Saeed K. An overview of biodiesel oxidation stability. Renew Sustain Energy Rev 2012;16:5924–50. doi:10.1016/j.rser.2012.06.024.

[84] Yaakob Z, Narayanan BN, Padikkaparambil S, Unni K. S, Akbar P. M. A review on the oxidation stability of biodiesel. Renew Sustain Energy Rev 2014;35:136–53. doi:10.1016/j.rser.2014.03.055.

[85] Urzędowska W, Stępień Z. Prediction of threats caused by high FAME diesel fuel blend stability for engine injector operation. Fuel Process Technol 2016;142:403–10. doi:10.1016/j.fuproc.2015.11.001.

[86] Bondioli P, Gasparoli A, Bella L Della, Giuseppe V. Evaluation of biodiesel storage stability using reference methods. Eur J Lipid Sci Technol 2002;104:777–84.

[87] Rashed MM, Kalam MA, Masjuki HH, Rashedul HK, Ashraful AM, Shancita I, et al. Stability of biodiesel, its improvement and the effect of antioxidant treated blends on engine performance and emission. RSC Adv 2015;5:36240–61. doi:10.1039/C4RA14977G.

[88] Robert O. Dunn. Effect of Temperature on the Oil Stability Index (OSI) of Biodiesel. Energy &

Fuels 2008;22:657–62.

[89] Bouaid A, Martinez M, Aracil J. Production of biodiesel from bioethanol and Brassica carinata oil: Oxidation stability study. Bioresour Technol 2009;100:2234–9. doi:10.1016/j.biortech.2008.10.045.

[90] Obadiah A, Kannan R, Ramasubbu A, Kumar SV. Studies on the effect of antioxidants on the long-term storage and oxidation stability of Pongamia pinnata (L.) Pierre biodiesel. Fuel Process Technol 2012;99:56–63. doi:10.1016/j.fuproc.2012.01.032.

[91] Bouaid A, Martinez M, Aracil J. Long storage stability of biodiesel from vegetable and used frying oils. Fuel 2007;86:2596–602. doi:10.1016/j.fuel.2007.02.014.

[92] Bondioli P, Gasparoli A, Della Bella L, Tagliabue S, Toso G. Biodiesel stability under commercial storage conditions over one year. Eur J Lipid Sci Technol 2003;105:735–41. doi:10.1002/ejlt.200300783.

[93] Geller DP, Adams TT, Goodrum JW, Pendergrass J. Storage stability of poultry fat and diesel fuel mixtures: Specific gravity and viscosity. Fuel 2008;87:92–102. doi:10.1016/j.fuel.2007.03.043.

[94] Gunstone FD. The Chemistry of Olis and Fats Sources, Composition, Properties and Uses. 2004.

[95] McCormick RL, Westbrook SR. Storage stability of biodiesel and biodiesel blends. Energy and Fuels 2010;24:690–8. doi:10.1021/ef900878u.

[96] Jose TK, Anand K. Effects of biodiesel composition on its long term storage stability. Fuel 2016;177:190–6. doi:10.1016/j.fuel.2016.03.007.

[97] Jain S, Sharma MP. Oxidation, Thermal, and Storage Stability Studies of Jatropha Curcas Biodiesel. ISRN Renew Energy 2012;2012:1–15. doi:10.5402/2012/861293.

[98] Knothe G. Some aspects of biodiesel oxidative stability. Fuel Process Technol 2007;88:669–77. doi:10.1016/j.fuproc.2007.01.005.

[99] Knothe G, Dunn RO. Dependence of Oil Stability Index of Fatty Compounds on Their Structure and Concentration and Presence of Metals. JAOCS, J Am Oil Chem Soc 2003;80:1021–6. doi:10.1007/s11746-003-0814-x.

[100] Schober S, Mittelbach M. The impact of antioxidants on biodiesel oxidation stability. Eur J Lipid Sci Technol 2004;106:382–9. doi:10.1002/ejlt.200400954.

[101] Agarwal S, Singhal S, Singh M, Arora S, Tanwer M. Role of Antioxidants in Enhancing Oxidation Stability of Biodiesels. ACS Sustain Chem Eng 2018;6:11036–49. doi:10.1021/acssuschemeng.8b02523.

[102] Bacha K, Ben-Amara A, Vannier A, Alves-Fortunato M, Nardin M. Oxidation stability of diesel/biodiesel fuels measured by a petrooxy device and characterization of oxidation products.

Energy and Fuels 2015;29:4345–55. doi:10.1021/acs.energyfuels.5b00450.

[103] Besser C, Pisarova L, Frauscher M, Hunger H, Litzow U, Orfaniotis A, et al. Oxidation products of biodiesel in diesel fuel generated by artificial alteration and identified by mass spectrometry. Fuel 2017;206:524–33. doi:10.1016/j.fuel.2017.06.038.

[104] De Carvalho AL, Cardoso EA, Da Rocha GO, Teixeira LSG, Pepe IM, Grosjean DM. Carboxylic acid emissions from soybean biodiesel oxidation in the EN14112 (Rancimat) stability test. Fuel 2016;173:29–36. doi:10.1016/j.fuel.2015.12.067.

[105] Arisoy K. Oxidative and thermal instability of biodiesel. Energy Sources, Part A Recover Util Environ Eff 2008;30:1516–22. doi:10.1080/15567030601082845.

[106] Frankel EN. Lipid Oxidation. 2005. doi:9780857097927.

[107] Dunn RO. Antioxidants for improving storage stability of biodiesel. Biofuels, Bioprod Biorefining 2012;6:246–56. doi:10.1002/bbb.

[108] Moser BR. Comparative oxidative stability of fatty acid alkyl esters by accelerated methods. JAOCS, J Am Oil Chem Soc 2009;86:699–706. doi:10.1007/s11746-009-1376-5.

[109] Karavalakis G, Stournas S, Karonis D. Evaluation of the oxidation stability of diesel/biodiesel blends. Fuel 2010;89:2483–9. doi:10.1016/j.fuel.2010.03.041.

[110] Sarin A, Arora R, Singh NP, Sarin R, Malhotra RK. Blends of biodiesels synthesized from non-edible and edible oils: Influence on the OS (oxidation stability). Energy 2010;35:3449–53. doi:10.1016/j.energy.2010.04.039.

[111] Ni H, Chen L, She DQ, Yuan YN. Current Situation of the Study on Oxidative Stability of Biodiesel. Adv Mater Res 2014;887–888:484–7. doi:10.4028/www.scientific.net/AMR.887-888.484.

[112] Knothe G, Steidley KR. The effect of metals and metal oxides on biodiesel oxidative stability from promotion to inhibition. Fuel Process Technol 2018;177:75–80. doi:10.1016/j.fuproc.2018.04.009.

[113] Bondioli P, Gasparoli A, Lanzani A, Fedeli E, Veronese S, Sala M. Storage stability of biodiesel. J Am Oil Chem Soc 1995;72:699–702. doi:10.1007/BF02635658.

[114] Jain S, Sharma MP. Correlation development for effect of metal contaminants on the oxidation stability of Jatropha curcas biodiesel. Fuel 2011;90:2045–50. doi:10.1016/j.fuel.2011.02.002.

[115] Sarin A, Arora R, Singh NP, Sarin R, Sharma M, Malhotra RK. Effect of metal contaminants and antioxidants on the oxidation stability of the methyl ester of pongamia. JAOCS, J Am Oil Chem Soc 2010;87:567–72. doi:10.1007/s11746-009-1530-0.

[116] Sarin A, Arora R, Singh NP, Sharma M, Malhotra RK. Influence of metal contaminants on oxidation stability of Jatropha biodiesel. Energy 2009;34:1271–5.

doi:10.1016/j.energy.2009.05.018.

[117] Sarin A, Arora R, Singh NP, Sarin R, Malhotra RK. Oxidation stability of palm methyl ester: Effect of metal contaminants and antioxidants. Energy and Fuels 2010;24:2652–6. doi:10.1021/ef901172t.

[118] Yang Z, Hollebone BP, Wang Z, Yang C, Brown C, Landriault M. Storage stability of commercially available biodiesels and their blends under different storage conditions. Fuel 2014;115:366–77. doi:10.1016/j.fuel.2013.07.039.

[119] Varatharajan K, Pushparani DS. Screening of antioxidant additives for biodiesel fuels. Renew Sustain Energy Rev 2018;82:2017–28. doi:10.1016/j.rser.2017.07.020.

[120] McCormick RL, Ratcliff M, Moens L, Lawrence R. Several factors affecting the stability of biodiesel in standard accelerated tests. Fuel Process Technol 2007;88:651–7. doi:10.1016/j.fuproc.2007.01.006.

[121] Liang YC, May CY, Foon CS, Ngan MA, Hock CC, Basiron Y. The effect of natural and synthetic antioxidants on the oxidative stability of palm diesel. Fuel 2006;85:867–70. doi:10.1016/j.fuel.2005.09.003.

[122] Mittelbach M, Schober S. The influence of antioxidants on the oxidation stability of biodiesel. JAOCS, J Am Oil Chem Soc 2003;80:62–5. doi:10.1109/CCIENG.2011.6007957.

[123] Christensen ED, Alleman T, McCormick RL. Re-additization of commercial biodiesel blends during long-term storage. Fuel Process Technol 2018;177:56–65. doi:10.1016/j.fuproc.2018.04.011.

[124] Fröhlich A, Schober S. The influence of tocopherols on the oxidation stability of methyl esters. JAOCS, J Am Oil Chem Soc 2007;84:579–85. doi:10.1007/s11746-007-1075-z.

[125] Zhou J, Xiong Y, Liu X. Evaluation of the oxidation stability of biodiesel stabilized with antioxidants using the Rancimat and PDSC methods. Fuel 2017;188:61–8. doi:10.1016/j.fuel.2016.10.026.

[126] Rizwanul Fattah IM, Masjuki HH, Kalam MA, Hazrat MA, Masum BM, Imtenan S, et al. Effect of antioxidants on oxidation stability of biodiesel derived from vegetable and animal based feedstocks. Renew Sustain Energy Rev 2014;30:356–70. doi:10.1016/j.rser.2013.10.026.

[127] Focke WW, Westhuizen I Van Der, Grobler ABL, Nshoane KT, Reddy JK, Luyt AS. The effect of synthetic antioxidants on the oxidative stability of biodiesel. Fuel 2012;94:227–33. doi:10.1016/j.fuel.2011.11.061.

[128] Karavalakis G, Hilari D, Givalou L, Karonis D, Stournas S. Storage stability and ageing effect of biodiesel blends treated with different antioxidants. Energy 2011;36:369–74. doi:10.1016/j.energy.2010.10.029.

[129] Jain S, Sharma MP. Oxidation stability of blends of Jatropha biodiesel with diesel. Fuel 2011;90:3014–20. doi:10.1016/j.fuel.2011.05.003.

[130] Rawat DS, Joshi G, Lamba BY, Tiwari AK, Mallick S. Impact of additives on storage stability of Karanja (Pongamia Pinnata) biodiesel blends with conventional diesel sold at retail outlets. Fuel 2014;120:30–7. doi:10.1016/j.fuel.2013.12.010.

[131] Sendzikiene E, Makareviciene V, Janulis P. Oxidation stability of biodiesel fuel produced from fatty wastes. Polish J Environ Stud 2005;14:335–9.

[132] Yang J, He QS, Corscadden K, Caldwell C. Improvement on oxidation and storage stability of biodiesel derived from an emerging feedstock camelina. Fuel Process Technol 2017;157:90–8. doi:10.1016/j.fuproc.2016.12.005.

[133] Kerkering S, Koch W, Andersson JT. Influence of phenols on the oxidation stability of home heating oils/FAME blends. Energy and Fuels 2015;29:793–9. doi:10.1021/ef502260d.

[134] Moser BR. Efficacy of gossypol as an antioxidant additive in biodiesel. Renew Energy 2012;40:65–70. doi:10.1016/j.renene.2011.09.022.

[135] Sarin A, Singh NP, Sarin R, Malhotra RK. Natural and synthetic antioxidants: Influence on the oxidative stability of biodiesel synthesized from non-edible oil. Energy 2010;35:4645–8. doi:10.1016/j.energy.2010.09.044.

[136] Domingos AK, Saad EB, Vechiatto WWD, Wilhelm HM, Ramos LP. The influence of BHA, BHT and TBHQ on the oxidation stability of soybean oil ethyl esters (biodiesel). J Braz Chem Soc 2007;18:416–23. doi:10.1590/S0103-50532007000200026.

[137] Damasceno SS, Santos NA, Santos IMG, Souza AL, Souza AG, Queiroz N. Caffeic and ferulic acids: An investigation of the effect of antioxidants on the stability of soybean biodiesel during storage. Fuel 2013;107:641–6. doi:10.1016/j.fuel.2012.11.045.

[138] Tang H, Wang A, Salley SO, Ng KYS. The Effect of Natural and Synthetic Antioxidants on the Oxidative Stability o ... Sci York 2008:373–82. doi:10.1007/s11746-008-1208-z.

[139] Borsato D, Cini JRDM, Silva HC Da, Coppo RL, Angilelli KG, Moreira I, et al. Oxidation kinetics of biodiesel from soybean mixed with synthetic antioxidants BHA, BHT and TBHQ: Determination of activation energy. Fuel Process Technol 2014;127:111–6. doi:10.1016/j.fuproc.2014.05.033.

[140] Buosi GM, Da Silva ET, Spacino K, Silva LRC, Ferreira BAD, Borsato D. Oxidative stability of biodiesel from soybean oil: Comparison between synthetic and natural antioxidants. Fuel 2016;181:759–64. doi:10.1016/j.fuel.2016.05.056.

[141] Souza AG, Medeiros ML, Cordeiro AMMT, Queiroz N, Soledade LEB, Souza AL. Efficient antioxidant formulations for use in biodiesel. Energy and Fuels 2014;28:1074–80. doi:10.1021/ef402009e.

[142] Morris SG, Myers JS, Kip ML, Riemenschneider RW. Metal deactivation in lard. J Am Oil Chem Soc 1950;27:105–7. doi:10.1007/BF02634401.

[143] Golubeva IA, Klinaeva E V., Yakovlev VS. Stabilization of blended diesel fuels by combinations of antioxidants and metal deactivators. Chem Technol Fuels Oils 1994;30:119–22. doi:10.1007/BF00723938.

[144] Golubeva IA, Klinaeva E V., Koshelev VN, Kelarev VI, Gol'dsher IA. Stabilization of blended diesel fuel with additive combinations. Chem Technol Fuels Oils 1997;33:23–6. doi:10.1007/BF02768134.

[145] Yang Z, Hollebone BP, Wang Z, Yang C, Landriault M. Factors affecting oxidation stability of commercially available biodiesel products. Fuel Process Technol 2013;106:366–75. doi:10.1016/j.fuproc.2012.09.001.

[146] Jain S, Sharma MP. Effect of metal contents on oxidation stability of biodiesel/diesel blends. Fuel 2014;116:14–8. doi:10.1016/j.fuel.2013.07.104.

[147] Sarin A, Arora R, Singh NP, Sarin R, Malhotra RK, Sharma M, et al. Synergistic effect of metal deactivator and antioxidant on oxidation stability of metal contaminated Jatropha biodiesel. Energy 2010;35:2333–7. doi:10.1016/j.energy.2010.02.032.

[148] Cremonez PA, Feroldi M, de Jesus de Oliveira C, Teleken JG, Meier TW, Dieter J, et al. Oxidative stability of biodiesel blends derived from different fatty materials. Ind Crops Prod 2016;89:135–40. doi:10.1016/j.indcrop.2016.05.004.

[149] Focke WW, Westhuizen I Van Der, Oosthuysen X. Biodiesel oxidative stability from Rancimat data. Thermochim Acta 2016;633:116–21. doi:10.1016/j.tca.2016.03.023.

[150] EN 14112 Fatty Acid Methyl Esters (FAME) — Determination of oxidation stability (accelerated oxidation test). Eur Stand 2005;3.

[151] Engelen B, Baldini L, Cipriano T, Diaz Garcia C, Elliott N, Fiolet G, et al. Laboratory oxidation stability study on B10 biodiesel blends. CONCAWE Reports 2013.

[152] Boros LAD, Batista MLS, Coutinho JAP, Krähenbühl MA, Meirelles AJA, Costa MC. Binary mixtures of fatty acid ethyl esters: Solid-liquid equilibrium. Fluid Phase Equilib 2016;427:1–8. doi:10.1016/j.fluid.2016.06.039.

[153] Maximo GJ, Magalhães AMS, Gonçalves MM, Esperança ES, Costa MC, Meirelles AJA, et al. Improving the cold flow behavior of methyl biodiesel by blending it with ethyl esters. Fuel 2018;226:87–92. doi:10.1016/j.fuel.2018.03.154.

[154] Costa MC, Boros LAD, Batista MLS, Coutinho JAP, Krähenbühl MA, Meirelles AJA. Phase diagrams of mixtures of ethyl palmitate with fatty acid ethyl esters. Fuel 2012;91:177–81. doi:10.1016/j.fuel.2011.07.018.

[155] Costa MC, Boros LAD, Coutinho AP, Krähenbühl MA, Meirelles AJA. Low-Temperature Behavior of Biodiesel: Solid-Liquid Phase Diagrams of Binary Mixtures Composed of Fatty Acid Methyl Esters. Energy Fuels Fuel 2011;25:3244–50.

[156] Benziane M, Khimeche K. Experimental determination and prediction of (solid + liquid) phase equilibria for binary mixtures of aromatic and fatty acids methyl esters. J Therm Anal Calorim 2013:1383–9. doi:10.1007/s10973-013-3147-7.

[157] Benziane M, Khimeche K, Dahmani A, Nezar S, Trache D. Experimental determination and prediction of (Solid + Liquid) phase equilibria for binary mixtures of heavy Alkanes and Fatty acids methyl esters . J Therm Anal Calorim 2013.

[158] Robustillo MD, Meirelles AJ de A, Pessôa Filho P de A. Solid-liquid equilibrium of binary and ternary systems formed by ethyl laurate, ethyl palmitate and dodecylcylohexane: Experimental data and thermodynamic modeling. Fluid Phase Equilib 2016;409:157–70. doi:10.1016/j.fluid.2015.09.038.

[159] Chabane S, Benziane M, Khimeche K, Trache D, Didaoui S, Yagoubi N. Low-temperature behavior of diesel/biodiesel blends: Solid–liquid phase diagrams of binary mixtures composed of fatty acid ethyl esters and alkanes. J Therm Anal Calorim 2018;131:1615–24. doi:10.1007/s10973-017-6614-8.

[160] Lobbia GG, Berchiesi G, Vitali G. Crystallization curve of hexadecane in mixtures with methyl nonadecanoate, methyl octadecanoate, ethyl octadecanoate, and methyl hexadecanoate. A comparison of the experimental and calculated curves. Thermochim Acta 1983;65:29–33. doi:10.1016/0040-6031(83)80004-5.

[161] Baxter R, Hastings N, Law A, Glass EJ. Perry's Chemical Engineers Handbook. vol. 39. 2008.

[162] Poletti L, Lay L. Reference materials for calorimetry and differential thermal analysis. European J Org Chem 2003;331:2999–3024. doi:10.1002/ejoc.200200721.

[163] Victoria M, Temprado M, Chickos JS. Critically Evaluated Thermochemical Properties of Polycyclic Aromatic Hydrocarbons. J Phys Chem 2008;37. doi:10.1063/1.2955570.

[164] Costa MC, Sardo M, Rolemberg MP, Coutinho JAP, Meirelles AJA, Ribeiro-Claro P, et al. The solid-liquid phase diagrams of binary mixtures of consecutive, even saturated fatty acids. Chem Phys Lipids 2009;160:85–97. doi:10.1016/j.chemphyslip.2009.05.004.

[165] Costa JCS, Mendes A, Santos LMNBF. Chain Length Dependence of the Thermodynamic Properties of n-Alkanes and their Monosubstituted Derivatives. J Chem Eng Data 2018;63:1–20. doi:10.1021/acs.jced.7b00837.

[166] Dunn RO. Effects of high-melting methyl esters on crystallization properties of fatty acid methyl ester mixtures. Am Soc Agric Biol Eng 2012;55:637–46.

[167] Chickos JS, Zhao H, Nichols G. The vaporization enthalpies and vapor pressures of fatty acid

methyl esters C18, C21to C23, and C25to C29by correlation - Gas chromatography. Thermochim Acta 2004;424:111–21. doi:10.1016/j.tca.2004.05.020.

[168] Marinovi M. New materials for solar thermal storage — solid / liquid transitions in fatty acid esters 2003;79:285–92.

[169] Höhne GWH, Hemminger WF, Flammersheim H-J. Differential Scanning Calorimetry. 2003. doi:10.1007/978-3-662-06710-9.